PLACE IN RETURN BOX to remove this checkout from your record.
TO AVOID FINES return on or before date due.
MAY BE RECALLED with earlier due date if requested.

DATE DUE	DATE DUE	DATE DUE

6/01 c:/CIRC/DateDue.p65-p.15

THE USE OF EXCITON COUPLED CIRCULAR DICHROISM FOR THE ABSOLUTE STEREOCHEMICAL DETERMINATION OF CHIRAL CARBOXYLIC ACIDS

By

Qifei Yang

A DISSERTATION

Submitted to
Michigan State University
in partial fulfillment of the requirements
for the degree of

DOCTOR OF PHILOSOPHY

Department of Chemistry

2004

ABSTRACT

THE USE OF EXCITON COUPLED CIRCULAR DICHROISM FOR THE ABSOLUTE STEREOCHEMICAL DETERMINATION OF CHIRAL CARBOXYLIC ACIDS

By

Qifei Yang

The Exciton Coupled Circular Dichroic (ECCD) method, a non-empirical method which allows for the determination of the absolute configuration of chiral compounds on a micro-scale, requires the through space coupling of two chromophores on the chiral molecule. This fact limits the use of this method, since the majority of chiral compounds do not fulfill this requirement. To overcome this problem, chromophoric hosts are introduced in the system. As reported before, for the chiral compounds with two sites of attachment, a pentanediol linked bis metal porphyrin tweezer could serve as the chromophoric host for the determination of the absolute stereochemistry. In the case of chiral compounds with only one site of attachment, achiral "carrier" molecules have been designed, which upon derivatization with chiral molecules are capable of binding with bis metal porphyrin to form a 1:1 host/guest complex. The research presented herein is focused on the absolute stereochemical determination of α-chiral carboxylic acids. A series of carrier molecules have been designed, synthesized and derivatized with α-chiral carboxylic acids, and the chiral conjugates were added to zinc porphyrin tweezer in methylcylcohexane to measure their CD. The derivatives with, 1,4-diaminobenzene,

exhibit consistent ECCD spectra, and a mnemonic has been proposed to correlate the observed ECCD sign to the absolute stereochemistry of α-chiral carboxylic acids.

When the same carrier molecule is derivatized with α-chiral halocarboxylic acids, the complexes exhibit consistent ECCD spectra, however, opposite to the predicted sign based on the previous mnemonic. Based on spectroscopic studies, we can explain this behavior by suggesting a novel cooperative binding of the α-halogen and carbonyl oxygen to zinc porphyrin, which only occurs in the case of α-haloamides. This bi-dentate binding leads to a new paradigm of porphyrin binding. In order to prove the above suggestion, a series of α-chiral butyrolactams were synthesized in order to restrict the free rotation of the C_{chiral}-$C_{C=O}$ bond. The spectroscopic study of the new compounds support our suggestion for the most part.

We were also engaged in the synthesis of mono-substituted porphyrin on insoluble and soluble polymers. The synthesis of porphyrins on polymeric backbone provides mono-substituted porphyrins with comparable yields as to the corresponding reaction in solutions, without the troublesome contamination from multiple-substituted products.

Finally, we were interested in designing artificial carbohydrate receptors, which would show selectivity for a specific carbohydrate. For this purpose, we designed boronic porphyrin tweezers and several attempts towards their syntheses were carried out.

Dedicated to my dearest parents and my husband for their love and support.

ACKNOWLEDGEMENT

Although I have a great feeling of accomplishment upon finishing my thesis, there is a stronger feeling of gratitude for all the people who help me reach this point and who helped to make the experience such an intellectually fulfilling and enjoyable one.

I would first like to express my utmost gratitude to my research advisor, Professor Babak Borhan. I have sincerely appreciated his encouragement and his strong support over my graduate career. I will always be grateful for the excellent education I received under his direction.

Not only I learned from Professor Babak Borhan during graduate school, but also from his research group. I will miss the daily interaction with such an interesting and helpful group of people. I want to give special thanks to Chrysoula Vasileiou for her help and patience. She helped me a lot in writing my thesis and she deserves a medal for correcting my thesis and offering great suggestions. A special mention to my good friend, a former lab member Dr. Meenakshi Ramarathnam for being such a warm hearted person and for showing incredible patience with me and the mess I was making in the lab while helping me a lot with my research. I would also like to thank Courtney Olmsted and Marina Tanasova for working together with me. Through our valuable discussions I achieved a better understanding of my research. Thanks especially to the people who helped me so much during my first two years: Dr. Gao Liu, Dr. Chun Wang, Dr. Baoyu Mi, Dr. Chen-yu Yeh and Dr. Jian-yang Cho.

I also want to thank all the lab members that I have ever worked with and all the friends that I made in Michigan State University. When I came to East Lansing six years

ago, this was a brand new place for me, without any family member and friends. Now six years passed by, I have met a lot of people, and they all are very nice to me and have made me feel very comfortable in studying and living in America. In my mind, Babak's lab is the best lab anyone can ever have. We cared about each other and helped each other in every way, just like a big family, and I am very thankful for this. I will miss all the other past and present group members: Jennifer Schomaker, Jun Yan, Montserrat Rabago-Smith, Rachael Crist, Radha Narayan, Tao Zheng, Ben Travis and Kristina Parkanzky. I would like to thank my dear friend Jie Yu and Dr. Shi Jin for their friendship.

Dr. Rui-Huang deserves a lot of thanks for patiently teaching me to use mass spectrometry, and taking a lot of solid probe MS for me. I also should thank the staff of MSU MS facility for taking all the FAB-MS for me.

Finally, I would like to thank my family, my dearest parents and husband, for their unconditional love and support. I would not made it to or through graduate school without them. Thank you all for all you have done and all you have sacrificed for me over the years.

TABLE OF CONTENTS

List of Figures.....xii

List of Schemes.....xix

List of Tables.....xxv

List of Abbreviations.....xxvi

Chapter 1. Introduction

1-1. The Exciton Coupled Circular Dichroism Method (ECCD).....1

1-1.1. Chirality.....1

1-1.2. Optical Rotary Dispersion (ORD) and Circular Dichroism (CD) Spectroscopy....4

1-2. The Exciton Coupled Circular Dichroic (ECCD) method and its applications.....12

1-2.1. The qualitative explanation of Exciton Coupled Circular Dichroic method (ECCD).....13

1-2.2. The explanation of ECCD theory based on Quantum Mechanical theories.....18

1-2.3. The application of ECCD method to determine the absolute stereochemistry of chiral molecules.....21

1-3. Use of chromophoric host such as porphyrins for ECCD studies.....23

1-3.1. Use of chromophoric host.....24

1-3.2. Use of porphyrins as chromophoric host.....26

Chapter 2. Polymer-supported synthesis of mono-substituted porphyrins

2-1. The synthesis of the zinc porphyrin tweezer.....43

2-2. The synthesis of mono-substituted porphyrins on polymers.....48

2-2.1. Synthesis of mono-substituted porphyrin on insoluble polymer.....50

2-2.2. Synthesis of mono-substituted porphyrin with soluble polymer.....52

Experimental materials and general procedures.....58

Reference.....67

Chapter 3. Absolute stereochemical determination of α-chiral carboxylic acids

3-1. Stereochemical determination of α-chiral carboxylic acids with carrier **A**.....74

3-2. Stereochemical determination of α-chiral carboxylic acids with carrier **B**.....81

3-3. Carrier **C** for the stereochemical study of chiral carboxylic acids.....97

3-4. Carrier **D** for the stereochemical study of chiral carboxylic acids.....104

3-5. Carrier **E** and **F** for the stereochemical study of α-chiral carboxylic acids.....108

3-6. Use of 2-aminopyrazine as the new carrier **G**.....116

3-7. Design of a new carrier **H** for chiral carboxylic acids.....118

3-8. Conclusion.....119

3-9. Another approach towards the same goal.....121

Experimental materials and general procedures.....124

Reference.....149

Chapter 4. The stereochemical determination of α-chiral halocarboxylic acids

4-1. Synthesis of α-chiral halocarboxylic acids derivatives and the ECCD data of carrier **B** derivatives.....153

4-2. Explanations for the unexpected ECCD of carrier **B** derivatized α-chiral halocarboxylic acids.....159

4-2.1. Determining the rotation of C_{α}-$C_{c=o}$ bond by NMR study.....160

4-2.2. The study with carrier B derivative of 2-trifluoromethylpropionic acid.....162

4-2.3. The possibility of $\sigma^*-\pi$ interaction.....169

4-2.4. The NMR study to determine the interaction between zinc porphyrin tweezer and carrier B derivatized α-chiral halocarboxylic acids.....173

4-3. The study of the interaction between the zinc porphyrin tweezer and carrier **B** derivatized α-chiral halocarboxylic acids by forming five-membered α-halolactams.....178

4-3.1. The synthesis of chiral α-substituted-γ-butyrolactams.....179

4-3.2. The synthesis of chiral α-alkyl-γ-butyrolactams.....191

Experimental materials and general procedures.....210

Reference.....240

Chapter 5. The chiral aggregation of porphyrin acids

5-1. Determination of extinction coefficient (ε) of zinc porphyrin acid.....245

5-1.1. Determination of extinction coefficient (ε) by Lambert-Beer's Law.....245

5-1.2. Determination of extinction coefficient (ε) of zinc porphyrin acid based on that of zinc porphyrin methyl ester.....246

5-2. The zinc porphyrin acid aggregate with carrier **F** derivatized (*S*)-*O*-acetylmandelic acid **9F**.....248

5-3. Other chiral substrates for the zinc porphyrin acid aggregates.....254

5-4. Porphyrin aggregates with other porphyrin compounds.....255

Conclusion.....257

Experimental materials and general procedures.....259

Reference.....261

Chapter 6. The attempted synthesis of boronic porphyrin tweezer

6-1. Synthesis of porphyrin tweezer **1**.....266

6-2. Synthesis of boronic porphyrin tweezer **2**.....270

6-2.1. Synthesis of boronic porphyrin tweezer **2** by MacDonald "2+2" cyclization...270

6-2.2. Synthesis of boronic porphyrin tweezer **2** by Pd catalyzed coupling reaction....284

6-2.3. Hydrolysis of pinacolborane.....298

6-3. Transmetallation to introduce boronic acid.....304

6-4. Synthesis of water soluble boron containing porphyrin **45**.....305

Experimental materials and general procedures.....310

Reference.....332

APPENDIX.....335

Change in proton chemical of compound **21** upon addition to ZnTPP.....336

Change in proton chemical of compound **26** upon addition to ZnTPP.....337

Change in proton chemical of compound **27** upon addition to ZnTPP.....338

Change in proton chemical of compound **28** upon addition to ZnTPP.....339

ECCD spectrum of compound **B-1-Br**.....340

ECCD spectrum of compound **B-2-Br**.....341

ECCD spectrum of compound **B-3-Br**.....342

ECCD spectrum of compound **B-4-Br**.....343

ECCD spectrum of compound **B-5-Br**.....344

ECCD spectrum of compound **B-1-Cl**.....345

ECCD spectrum of compound **B-2-Cl**.....346

ECCD spectrum of compound **B-3-Cl**.....347

ECCD spectrum of compound **B-4-Cl**.....348

ECCD spectrum of compound **B-5-Cl**.....349

ECCD spectrum of compound **B-1-F**.....350

ECCD spectrum of compound **B-2-F**.....351

ECCD spectrum of compound **B-3-F**.....352

ECCD spectrum of compound **B-4-F**.....353

ECCD spectrum of compound **B-5-F**.....354

ECCD spectrum of compound **B-1-I**.....355

ECCD spectrum of compound **37**.....356

ECCD spectrum of compound **38**.....357

ECCD spectrum of compound **50**.....358

ECCD spectrum of compound **51**.....359

ECCD spectrum of compound **52**.....360

ECCD spectrum of compound **53**.....361

ECCD spectrum of compound **54**.....362

ECCD spectrum of compound **55**.....363

ECCD spectrum of compound **75**.....364

ECCD spectrum of compound **77**.....365

ECCD spectrum of compound **78**.....366

Addition of L-lysine to zinc porphyrin alcohol **2**.....367

LIST OF FIGURES

Note: Images in this dissertation are presented in color.

Figure 1-1. Examples of some chiral molecules and their mirror images.....1

Figure 1-2. The structures of (*S*)- and (*R*)-Carvone.....2

Figure 1-3. The structures of (*R*)- and (*S*)-Thalidomide.....3

Figure 1-4. The linearly polarized light and circularly polarized light.....4

Figure 1-5. (***a***) Positive and (***b***) negative CD Cotton effects.....7

Figure 1-6. The "right hand rule" to determine the direction of magnetic transition dipole moment *m*.....8

Figure 1-7. The transition moments for hexahelicene. Antiparallel moments for (M) and parallel moments for (P) helicities.....9

Figure 1-8. The CD spectropolarimeter.....10

Figure 1-9. Exciton Coupled Circular Dichroism (ECCD) of steroidal 2,3-bisbenzoate.....12

Figure 1-10. The qualitative explanation of ECCD based on a dibenzoate ester.....14

Figure 1-11. The ECCD couplet for the configuration shown in Figure 11-10*b*.....17

Figure 1-12. The screw sense of the chromophores and its corresponding ECCD sign.....17

Figure 1-13. Splitting of the excited states of isolated chromophores i and j by exciton interaction. The energy gap $2V_{ij}$ is called Davydov splitting.....17

Figure 1-14. The stereochemical determination of abscisic acid by ECCD method.....22

Figure 1-15. Examples of exciton chirality CD method in absolute configurational assignment.....23

Figure 1-16. The induced chirality of biphenol upon binding to chiral diamine.....24

Figure 1-17. Achiral porphyrins and inherently achiral porphyrins.....27

Figure 1-18. UV-vis spectra of porphyrin methyl ester and zinc porphyrin methyl ester.....29

Figure 1-19. Structure of zinc porphyrin tweezer **4**.....30

Figure 1-20. Assignment of absolute configuration of acyclic chiral diamines by Exciton Coupled Circular Dichroism (ECCD).....31

Figure 1-21. The chiral complex and its most stable conformation.....34

Figure 1-22. Use of carrier **5** to determine the absolute stereochemistry of chiral monoamine by Exciton Coupling Circular Dichroism.....36

Figure 3-1. Stereochemical determination of chiral monoamine with carrier **1**.....70

Figure 3-2. The absolute stereochemical assignment of α-chiral carboxylic acids by NMR.....71

Figure 3-3. Chiral auxiliary reagents.....71

Figure 3-4. The derivatization of PGME with chiral acids.....71

Figure 3-5. Two-step derivatization of α-hydroxy carboxylic acids.....72

Figure 3-6. The structure of 1-carboxyethyl substituted monosaccharides.....73

Figure 3-7. The structures of carrier **1** and carrier **A**.....74

Figure 3-8. Comparison of chiral complexes of carrier **1** and carrier **A**: carrier **1** complexes are locked in a conformation, while carrier **A** complexes are not so rigid.....76

Figure 3-9. The ECCD spectra of carrier **A** derivatized (*R*)- and (*S*)-phenoxypropionic acid with zinc porphyrin tweezer **2**.....77

Figure 3-10. Lowest energy conformations of carrier **A** derivatized complexes based on modeling without binding to zinc porphyrin.....79

Figure 3-11. Based on modeling, binding of the Zn porphyrin to carrier **A** conjugates forces the rotation of the C_{aryl}-N_{amide} bond.....80

Figure 3-12. The possible binding of carrier **B** derivatives to zinc porphyrin tweezer..83

Figure 3-13. UV-vis spectra of adding two amides to ZnTPP 84

Figure 3-14. The secondary derivative of UV spectrum of ZnTPP with *t*-butylformamide (200 eq.).....85

Figure 3-15. The binding study of the chiral conjugates**14B** with zinc porphyrin tweezer **2** by NMR.....86

Figure 3-16. The structure of N-methyl-1,4-phenylenediamine.....87

Figure 3-17. The binding of carrier **B** derivatives and zinc porphyrin tweezer based on UV-vis, IR and NMR study.....88

Figure 3-18. Minimized structure of Zn-TPP bound to **9B** (most of the hydrogen atoms deleted for clarity) in which the chiral center has adopted a conformation to minimize steric strain.....89

Figure 3-19. Proposed mnemonic for carrier **B** derivatized chiral acids.....90

Figure 3-20. The CD spectra of (*S*)-methoxyphenylacetic acid **8B** at 0 °C.....93

Figure 3-21. The ECCD spectra of compound **13B** and **Me-13B**.....95

Figure 3-22. The structure of carrier **B** and **C**.....98

Figure 3-23. The structure of **13B** and **13C**.....101

Figure 3-24. The structure of **13C** and **13C'**.....102

Figure 3-25. The conformations and ECCD of **13B**, **13C** and **13C'**.....103

Figure 3-26. Structure of carrier **D**.....104

Figure 3-27. Structures of carrier **B** and **E**.....108

Figure 3-28. The ECCD of carrier **E** derivatized methylbutyric acid **14E**.....109

Figure 3-29. Carrier **B** and **E** derivatized amides bind to zinc porphyrin tweezer.....110

Figure 3-30. Structure of carrier **F** and its derivatized binds to zinc porphyrin tweezer.....111

Figure 3-31. The ECCD of compound **8F** at different temperatures.....114

Figure 3-32. Hydrogen bonding vs. hydrogen-π interaction.....115

Figure 3-33. The different interactions between the zinc porphyrin tweezer and carrier **B** and carrier **F** derivatives.....116

Figure 3-34. The binding between carrier **G** derivatives **12G** and zinc porphyrin tweezer.....117

Figure 3-35. Carrier **A-H**.....120

Figure 3-36. The stereochemical study of carrier **B** derivatized α-chiral carboxylic acids with zinc porphyrin tweezer **2**.....121

Figure 3-37. The binding of chiral conjugate to zinc porphyrin tweezer.....122

Figure 3-38. Opposite ECCD spectra with the two carriers **B** and **X**.....123

Figure 4-1. The contradiction of the observed ECCD sign vs. the predicted sign based on the mnemonic.....153

Figure 4-2. The observed and predicted ECCD of **B-2-Br**.....159

Figure 4-3. Possible conformations leading to the observed ECCD signs.....160

Figure 4-4. The conformation of the amide part in the derivatives.....161

Figure 4-5. NMR of compounds **6R** and **6S**.....161

Figure 4-6. The structures of 2-trifluoromethylpropionic acid **9** and 2-trifluoromethylbutyric acid **10**.....165

Figure 4-7. The two possible conformations for compound **18** and its ECCD spectrum.....170

Figure 4-8. The conformations dictated by $\sigma^*-\pi$ interaction and hydrogen bonding.....171

Figure 4-9. The conformations of **11B** and **Me-11B**.....172

Figure 4-10. The change of chemical shift of bromoamide **28** upon addition of ZnTPP.....176

Figure 4-11. The interaction of carrier **B** derivatized α-chiral halocarboxylic acids with zinc porphyrin tweezer.....177

Figure 4-12. The carrier **B** derivatives versus the five-membered chiral α-lactams....178

Figure 4-13. The comparison of interaction of five-membered lactam and an α-halolactam interacting with zinc porphyrin tweezer.....179

Figure 4-14. The synthesis five-membered α-chiral lactams from α–chiral–γ–butyrolactones.....179

Figure 4-15. The conformation of (*R*)-α-alkoxy-γ-butyrolactams **50-53** binding to zinc porphyrin tweezer.....190

Figure 4-16. The conformation of (*R*)-α-chloro-γ-butyrolactam **37** binding to zinc porphyrin tweezer.....190

Figure 4-17. The conformation of chiral α-alkoxy-γ-butyrolactams **38**, **54** and **55** binding to zinc porphyrin tweezer.....191

Figure 4-18. The observed ECCD sign is opposite to the predicted sign based on model.....208

Figure 5-1. The self-assembly of porphyrins.....243

Figure 5-2. Porphyrin acid aggregate as a chromophoric host to determine the stereochemistry of chiral substrates.....244

Figure 5-3. The structure of the carrier **F** derivatized (*S*)-*O*-acetylmandelic acid **9F** and zinc porphyrin acid.....248

Figure 5-4. The addition of chiral substrate **9F** to zinc porphyrin acid in methylcyclohexane leads to a positive ECCD.....249

Figure 5-5. The time study of zinc porphyrin acid aggregate with **9F**.....249

Figure 5-6. The photo bleaching study.....250

Figure 5-7. The titration of zinc porphyrin acid with **9F**.....251

Figure 5-8. The ECCD of **9F** in zinc porphyrin methyl ester.....252

Figure 5-9. The addition of sodium carbonate to zinc porphyrin tweezer.....253

Figure 5-10. The CD spectrum of **9F** to pre-treated zinc porphyrin acid.....253

Figure 5-11. Adding diisopropylmethylamine (1eq.) to the zinc porphyrin acid with **9F**.....254

Figure 5-12. Structures of (*S*)-methoxyphenylpropionic acid derivative **8F** and L-lysine methyl ester.....255

Figure 5-13. The time study of zinc porphyrin mono-alcohol with carrier **F** derivatized (*S*)-O-phenylmandelic acid **9F**.....257

Figure 6-1. A receptor for glucopyranose and its glucose complex.....263

Figure 6-2. The boronic porphyrin and its binding to sugars.....264

Figure 6-3. The structure of boronic porphyrin tweezer **1** and **2**.....264

Figure 6-4. The structure of a new porphyrin tweezer **45**.....306

LIST OF SCHEMES

Scheme 1-1. The derivatization of binaphthalene **3** with chiral alcohols.....25

Scheme 1-2. Converting the amino acids and amino alcohols to diamines.....32

Scheme 2-1. Synthesis of zinc porphyrin tweezer **1** from porphyrin carboxylic acid...43

Scheme 2-2. Synthesis of mono-substituted porphyrin methyl ester **2**.....44

Scheme 2-3. Hydrolysis of porphyrin methyl ester **2** to carboxylic acid **3**.....44

Scheme 2-4. EDC coupling of porphyrin carboxylic acid **3** with 1,5-pentanediol.....46

Scheme 2-5. The synthesis of mono-substituted porphyrin **2** in $BF_3{\cdot}Et_2O$ condition....48

Scheme 2-6. Synthesis of mono-substituted porphyrins on insoluble polymer.....51

Scheme 2-7. Copolymerization to synthesize NCPS polymer.....54

Scheme 2-8. Synthesis of mono-substituted porphyrin on soluble polymer.....56

Scheme 3-1. The synthesis of Boc-protected carrier **A**.....75

Scheme 3-2. The synthesis of chiral complexes from **Boc-A**.....75

Scheme 3-3. The synthesis of carrier **B** derivatized chiral complexes.....81

Scheme 3-4. The synthesis of methylated carrier **B** derivative **Me-13B**.....94

Scheme 3-5. The synthesis of carrier **C** derivatized chiral acids.....98

Scheme 3-6. The coupling of carrier **C** with acids to form amide bond.....102

Scheme 3-7. The structure of zinc porphyrin tweezer **2'**, in which 1,3-propanediol serves as the linkage.....118

Scheme 3-8. The synthesis of chiral benzimidazole.....119

Scheme 4-1. The derivitization of (*R*)-2-bromopropionic acid **1-Br** to carrier **A** and **B**.....152

Scheme 4-2. The synthesis of α-chiral halocarboxylic acids.....153

Scheme 4-3. The mechanism of the α-chiral halocarboxylic acids synthesis.....154

Scheme 4-4. The attempted synthesis of carrier **B** derivatized iodocarboxylic acid **B-1-I**.....157

Scheme 4-5. The synthesis of carrier **B** derivatized (*S*)-2-iodopropionic acid **B-1-I**...158

Scheme 4-6. The proposed synthesis of chiral 2-trifluoromethyl carboxylic acids.....163

Scheme 4-7. The synthesis of triethylborane **8**.....164

Scheme 4-8. The synthesis of trifluoromethyl iodide **7**.....164

Scheme 4-9. The amidation with Evans' chiral auxiliary.....165

Scheme 4-10. The introduction of trifluoromethyl group to the α position.....166

Scheme 4-11. The synthesis of carrier **B** derivatized 2-methyltrifluoropropionic acid **18**.....167

Scheme 4-12. The synthesis of methylated carrier **B** derivative **Me-11B**.....171

Scheme 4-13. The synthesis of modified carrier **B** derivative **MeB-1-Br**.....173

Scheme 4-14. The synthesis of chiral α–chloro–γ–butyrolactone **32**.....180

Scheme 4-15. The synthesis of α–chloro–γ–butyrolactone **32**.....181

Scheme 4-16. The synthesis of α-phenoxy-γ-butyrolactone **36**.....181

Scheme 4-17. Converting butyrolactone to butyrolactam.....182

Scheme 4-18. Second route for the synthesis of (*S*)-α-phenoxy-γ-butyrolactam **38**.....183

Scheme 4-19. Third route for the synthesis of (*S*)-α-phenoxy-γ-butyrolactam **38**.....184

Scheme 4-20. The synthesis (*R*)-α-methoxy-γ-butyrolactam **43**.....185

Scheme 4-21. The attempted synthesis of α-alkoxy-γ-butyrolactones.....185

Scheme 4-22. The synthesis of chiral benzoxy and allyoxy lactones.....187

Scheme 4-23. The synthesis of (*S*)-α-naphthyloxy-γ-butyrolactone **48** and (*S*)-α-*p*-*tert*-butylphenoxy-γ-butyrolactone **49**.....187

Scheme 4-24. The hydrogenation of lactam **50** to **51**.....188

Scheme 4-25. The synthesis of chiral α-alkyl-γ-butyrolactams using cuprates.....192

Scheme 4-26. The synthesis of (*R*)-α-tosyl-γ-butyrolactone **56**.....192

Scheme 4-27. Second route for the synthesis of (*R*)-α-tosyl-γ-butyrolactone **56**.....193

Scheme 4-28. The first reaction of (*R*)-α-tosyl-γ-butyrolactone **56** with dimethylcuprate.....193

Scheme 4-29. The second reaction of compound **56** with dimethylcuprate.....194

Scheme 4-30. The reaction of (*R*)-α-tosyl-γ-butyrolactone **56** with dibutylcuprate.....195

Scheme 4-31. A palladium catalyzed coupling reaction of Reformatsky reagent with allylic acetates.....196

Scheme 4-32. The proposed synthesis of chiral α-allyl-γ-butyrolactones by palladium catalyzed Reformatsky reagent utilizing zinc on graphite.....196

Scheme 4-33. The palladium coupling reaction of Reformatsky reagent with allylacetate.....197

Scheme 4-34. The proposed synthesis of chiral α-alkyl-γ-butyrolactones with chiral auxiliary.....198

Scheme 4-35. The synthesis of benzyl protected γ-hydroxy-carboxylic acid **58**.....198

Scheme 4-36. The attempted conversion of the acid **58** to acyl chloride.....199

Scheme 4-37. The unsuccessful reaction between chiral auxiliary **60** with butyrolactone **57**.....199

Scheme 4-38. The coupling of chiral auxiliary **60** with acid **58** by generating mixture anhydride.....200

Scheme 4-39. The synthesis of chiral butyrolactones with chiral 2-methyloxazoline **62**.....201

Scheme 4-40. Rationale for the absolute configuration of chiral butyrolactones.....202

Scheme 4-41. The published synthesis of 2-(trimethylsilyloxy)ethyl iodide **64**.....202

Scheme 4-42. The reactions for the synthesis of benzophenone ethylene acetal **69**.....203

Scheme 4-43. The synthesis of 2-(OTBS)ethyl iodide **68**.....204

Scheme 4-44. The synthesis of (*S*)-2-allyl-γ-butyrolactone **67**.....204

Scheme 4-45. The synthesis of (*S*)-2-allyl-γ-butyrolactam **75**.....205

Scheme 4-46. The synthesis of (*S*)-2-propyl-γ-butyrolactam **77**.....207

Scheme 5-1. The synthesis of porphyrin mono-alcohols **1** and **2**.....256

Scheme 6-1. Proposed synthesis of porphyrin tweezer **1** by MacDonald "2+2" cyclization.....265

Scheme 6-2. Proposed synthesis of porphyrin tweezer **2** by MacDonald "2+2" cyclization.....266

Scheme 6-3. Synthesis of dipyrromethane **5**.....267

Scheme 6-4. The proposed synthesis of dipyrromethane-dialdehyde **6** from 2-pyrrole-carboxylic acid **8**.....268

Scheme 6-5. The esterification of 2-pyrrol-carboxylic acid **8**.....268

Scheme 6-6. The condensation of ethyl ester **12** with aldehyde **9**.....269

Scheme 6-7. Unsuccessful synthesis of dipyrromethane-dialdehydes **6a and 6b** from pyrrole.....269

Scheme 6-8. Proposed synthesis of boronic porphyrin acid **4**.....271

Scheme 6-9. Synthesis of dipyrromethane-dicarbinol **17**.....272

Scheme 6-10. Two pathways for the synthesis of porphyrin tweezer **2**.....274

Scheme 6-11. The unsuccessful EDC coupling of compound **16** and 1,5-pentanediol..275

Scheme 6-12. The unsuccessful hydrolysis of methyl ester **17** to acid **16**.....275

Scheme 6-13. Alternate way to synthesize dimer **19**.....276

Scheme 6-14. The synthesis of dimer **20**.....276

Scheme 6-15. The unsuccessful Freidel-Crafts reaction to synthesize dimer **19**.....277

Scheme 6-16. The first attempt to synthesize compound **19** from methyl ester **17**.....277

Scheme 6-17. Directly synthesis of diester **19** from methyl ester **17**.....278

Scheme 6-18. The MacDonald "2+2" cyclization of compound **5** and **17**.....279

Scheme 6-19. The attempted synthesis of boronic porphyrin tweezer **2**.....281

Scheme 6-20. The synthesis of boronic methyl ester **24**.....282

Scheme 6-21. The unsuccessful removal of methyl ester of compound **24**.....283

Scheme 6-22. The attempted synthesis of porphyrin tweezer **2**.....284

Scheme 6-23. Pd catalyzed coupling of pinacolborane with aryl halides.....284

Scheme 6-24. The synthesis of porphyrin tweezer **2** by Pd coupling reaction.....285

Scheme 6-25. The synthesis of *p*-bromoporphyrin alcohol **29**.....285

Scheme 6-26. The attempted synthesis of dibromo tweezer **31**.....286

Scheme 6-27. The unsuccessful synthesis of bromoporphyrin carboxylic acid **32**.....287

Scheme 6-28. The synthesis of porphyrin methyl ester **33**.....287

Scheme 6-29. Hydrolysis of methyl ester **33** to acid **32**.....288

Scheme 6-30. EDC coupling of acid **32** with 1,5-pentanediol.....289

Scheme 6-31. The Pd catalyzed coupling of dibromo tweezer.....290

Scheme 6-32. The coupling reaction of porphyrin methyl ester **33**.....291

Scheme 6-33. The unsuccessful coupling with bis(pinacolato)diboron.....292

Scheme 6-34. Synthesis of triflate porphyrin methyl ester **39**.....293

Scheme 6-35. The unsuccessful Pd coupling of triflate **39**.....294

Scheme 6-36. Synthesis of iodoporphyrin methyl ester **41**.....295

Scheme 6-37. The synthesis of diiodoporphyrin tweezer **42**.....297

Scheme 6-38. The Pd coupling of diiodoporphyrin tweezer **42** to synthesize porphyrin tweezer **pinacol-2**.....298

Scheme 6-39. The unsuccessful hydrolysis of boronic porphyrin **36**.....299

Scheme 6-40. The cleavage of pinanediol boronate to boronic acids.....300

Scheme 6-41. The attempted oxidation of porphyrin methyl ester **36**.....301

Scheme 6-42. The oxidation studies on model molecule **44**.....302

Scheme 6-43. The attempted reduction of methyl ester **36**.....303

Scheme 6-44. The transmetallation with bromobenzene.....304

Scheme 6-45. The attempted transmetallation with bromoporphyrin **33**.....305

Scheme 6-46. The synthesis of boronic porphyrin methyl ester **46**.....306

Scheme 6-47. The synthesis of pyridine porphyrin **47**.....307

Scheme 6-48. The bromination of compound **48**.....307

Scheme 6-49. The reaction between pyridine and primary bromide **48**.....308

Scheme 6-50. The synthesis of water soluble porphyrin methyl ester **46**.....309

LIST OF TABLES

Table 1-1. Definition of exciton chirality for a binary system.....19

Table 2-1. Synthesis of soluble polymer supported aldehyde **10**.....55

Table 3-1. CD predictions and amplitudes of carrier **A** derivatized chiral carboxylic acids bound to porphyrin tweezer **2**.....78

Table 3-2. CD predictions and amplitudes of carrier **B** derivatived chiral carboxylic acids bound to porphyrin tweezer **2**.....91

Table 3-3. CD amplitudes of carrier **C** derivatized chiral carboxylic acids bound to zinc porphyrin tweezer **2**.....100

Table 3-4. The extinction coefficient ε of Mg porphyrin tweezer in different solvents.....106

Table 3-5. The CD data of carrier **D** derivatized chiral acids with magnesium porphyrin tweezer.....107

Table 3-6. Comparison of the CD data of carrier **B** and **F** derivatives.....112

Table 4-1. The enatiomeric ratio for chiral α-halogen carboxylic acids.....155

Table 4-2. The CD data of carrier **B** derivatives of α-chiral halocarboxylic acids...156

Table 4-3. Change in proton chemical shift upon addition to ZnTPP.....174

Table 4-4. The change in chemical shifts of haloamides upon addition of ZnTPP..176

Table 4-5. The CD data of chiral butyrolactams.....189

Table 4-6. The ECCD data of (*S*)-2-alkyl-γ-butyrolactams.....207

Table 6-1. The palladium catalyzed coupling of iodoporphyrin **41** with pinacolborane.....295

LIST OF ABBREVIATIONS

α	angle of rotation
$[\alpha]$	specific rotation
A	CD amplitude
9-AHA	9-anthrylhydroxyacetic acid
AIBN	2,2'-azobis(isobutyronitrile)
Ar	aromatic
$BF_3 \cdot Et_2O$	boron trifluoride diethyl etherate
Boc	*tert*-butoxycarbonyl
BOP	benxotriaoyl-1-yloxytris(dimethylamino)phosphonium hexafluorophosphate
Bu_2CuLi	lithium dibutylcuprate
Bu_3P	tributylphosphine
C_8K	potassium-graphite
CD	circular dichroism
CE	Cotton effect
CF_3I	trifluoromethyl iodide
$(COCl_2)_2$	oxalyl chloride
p-chloranil	tetrachloro-1,4-benzoquinone
cm	centimeter
d	doublet
DDQ	2,3-dichloro-5,6-dicyano-1,4-Benzoquinone

DIAD	diisopropylazodicarboxylate
DMAP	4-dimethylaminopyridine
DMF	N,N-dimethylformamide
DMSO	dimethyl sulphoxide
Et_3N	triethylamine
ε	molar absorption coefficient
ECCD	exciton coupled circular dichroism
EDC	1-(3-dimethylaminopropyl)-3-ethylcarbodiimide
EtOAc	ethyl acetate
eq	equivalents
Et_3B	triethylborane
FAB-MS	fast atom bombardment mass spectroscopy
g	gram
GPC	gel permeation chromatography
HPLC	high pressure liquid chromatography
h	hour
IR	infrared
J	NMR coupling constant
KH	potassium hydride
KI	potassium iodide
LDA	lithium diisopropylamide
m	magnetic transition dipole moment

*m*CPBA	3-chloroperoxybenzoic acid
Me_2CuLi	lithium dimethylcuprate
min	minute
mg	milligram
MHz	megahertz
MS	mass spectroscopy
n	refractive index
$NaBH_4$	sodium borohydrate
NaH	sodium hydride
NaHMDS	sodium hexamethyldisilazane
$NaIO_4$	sodium periodate
$NaNO_2$	sodium nitrite
NBS	N-bromosuccinimide
NCPS	non-cross-linked chloromethylated polystyrene
NIS	N-iodosuccinimide
nm	nanometer
NMR	nuclear magnetic resonance
ORD	optical rotatory dispersion
PGME	phenylglycine methyl ester
PPh_3	triphenylphosphine
i-Pr_2Net	diisopropylethylamine
PDI	polydispersity index
$Pd(PPh_3)_4$	tetrakis(triphenylphosphine)palladium

Chapter 1

Introduction

1-1. The Exciton Coupled Circular Dichroic Method

1-1.1. Chirality

Chirality, based on the Greek word of "hand" (cheir) means "handness", in reference to that pair of non-superimposable mirror images constantly presented before us: our two hands.[1] In chemistry, chirality is an important property of organic compounds, which arises from asymmetric disposition of atoms. Molecules that are not identical with their mirror image are defined to be "chiral". The simplest example of a chiral compound is a molecule containing a chiral center, which is a tetrahedral carbon bound to four different substituents, such as 2-methylbutyric acid. Chemists use the letters *R* and *S* to indicate the configuration (arrangement of groups) of the chiral center, based on defined priorities.[1]

Molecules devoid of a chiral center can also be chiral, as long as they lack a plane of symmetry. Examples of this type of chirality are allenes,[2] helicenes[3] and atropisomers.[4] Figure 1-1 shows examples of chiral molecules and their mirror images.

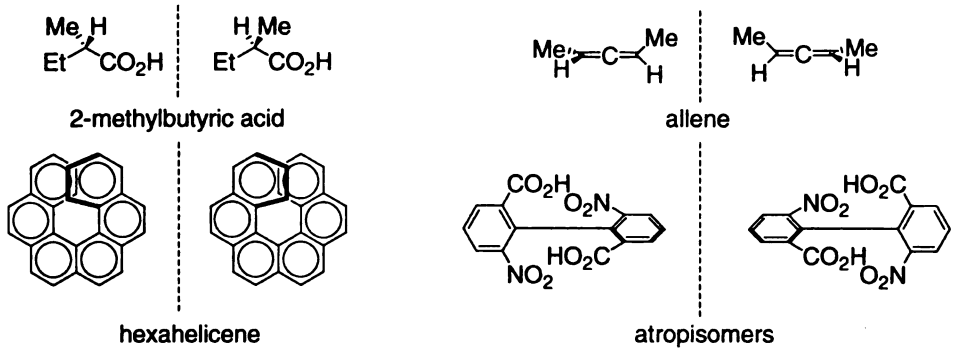

Figure 1-1. Examples of some chiral molecules and their mirror images.

Allenes are chiral because they lack a plane of symmetry. Since the two π bonds in allenes are perpendicular to each other, the plane containing one H-C-Me group is perpendicular to the plane containing the other H-C-Me group. Therefore, allenes are not superimposable, and these compounds are chiral.[2] The polycyclic hexahelicene is the classic example of an inherently chiral chromophore.[3] Because hexahelicene is not a planar molecule but a helix, it lacks a plane of symmetry. (+)-Hexahelicene has right handed helicity or the P configuration, and correspondingly, (-)-hexahelicene has left handed helicity or the M configuration. Atropiosmerism is isomerism caused by "freezing" the internal rotation about a single bond in a molecule. In the example shown in Figure 1-1, because of the steric interactions of the substituents at *ortho-* position, the biphenyls with *o*-substituents are chiral.[5]

The stereochemistry of natural compounds has a large impact on their chemical and biological properties. For example, the (*S*) enantiomer of Carvone has the odor of caraway seeds, while the (*R*) enantiomer has the odor of spearmint (Figure 1-2).[1]

(*S*)-Carvone (in caraway seeds) (*R*)-Carvone (in spearmint oil)

Figure 1-2. The structures of (*S*)- and (*R*)-Carvone.

A dramatic example of how a simple change in stereochemistry can affect the biological property of a molecule is found in the compound, Thalidomide, which was a commercially available drug about half a century ago for morning sickness during pregnancy. As shown in Figure 1-3, Thalidomide has a single stereogenic center and can thus exist in two stereoisomeric forms.[1] One of the enatiomers, (*R*)-Thalidomide, has

strong sedative properties, while other enantiomer, (*S*)-Thalidomide, is highly teratogenic. Since the drug at that time was produced in racemic form, women who were given the drug during the first three months of pregnancy had babies with a wide variety of birth defects.

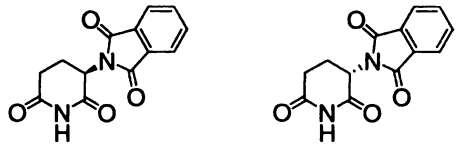

Figure 1-3. The structures of (*R*)- and (*S*)-Thalidomide.

It is, therefore, of great importance to determine the absolute stereochemistry of chiral compounds for natural product chemistry, pharmaceutics, and biochemistry. However, despite the extensive research currently underway in this field, determination of absolute stereochemistry is not a trivial task. The general techniques used include: (1) X-ray crystallography; (2) chiroptical methods such as optical rotatory dispersion (ORD) and circular dichroism (CD);[6] (3) nuclear magnetic resonance (NMR) spectroscopy of Mosher esters and related derivatives;[7] and (4) chemical correlation with known chiral compounds.[8]

Up to date, the most dependable method for absolute stereochemical determination of chiral molecules is X-ray crystallography. The crystal structure of any compound can unambiguously determine the absolute stereochemistry of all chiral centers in a single experiment, and so far, has been the method of choice for most systems. However, there are significant drawbacks associated with this method. First of all, not all compounds can easily crystallize to give single crystals of the quality required for X-ray crystallography. This is part of the reason crystallography can be a very time

consuming technique that requires special training. At the same time, it requires significant amount of material that might not always be available. That is why easier and more accessible methods are needed and several spectroscopic methods have been developed.

The goal of our research is to develop general and sensitive circular dichroic (CD) methods for absolute stereochemical determination of chiral compounds.

1-1.2. Optical Rotatory Dispersion (ORD) and Circular Dichroism (CD) Spectroscopy

Light, which is electromagnetic radiation, has an electric and a magnetic field. These two fields oscillate perpendicular to one another and to the direction of the propagation of light. The polarization of light is defined by the direction of its electric field vector.[9]

Light from ordinary light sources, such as sun and a light bulb, is unpolarized, since it consists of light vibrating in all directions. However, if unpolarized light passes through a polarizing filter, only the subset with parallel oscillation with the direction of the filter survives, and is referred to as linearly polarized light. Linearly polarized light can be decomposed into a pair of circularly polarized light beams: left and right circularly polarized light. In a circularly polarized light beam, the electric field remains constant in magnitude, but traces out a helix as a function of time. Figure 1-4 shows the linearly polarized and circularly polarized light.[10]

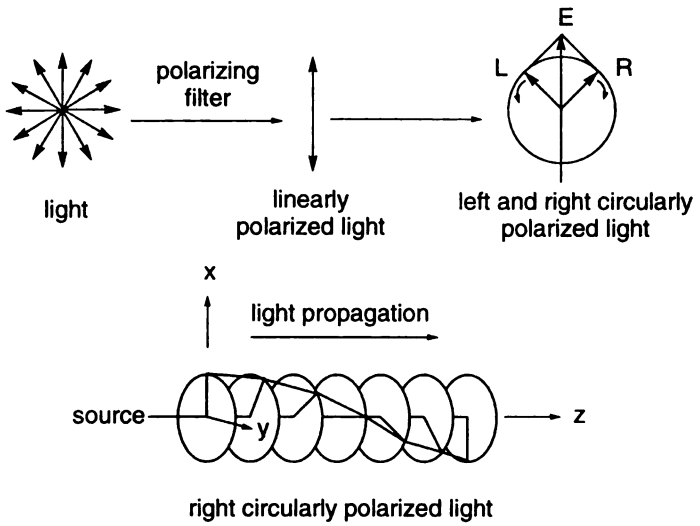

Figure 1-4. The linearly polarized light and circularly polarized light.

When circularly polarized light passes through an achiral compound or a racemic mixture, the velocity and absorbance of the left and right circularly polarized light is affected similarly. On the other hand, if it passes through an optically active medium, the velocity and absorbance of one circularly polarized component is altered to a greater extent as compared to the other opposing circularly polarized component.[11] This is referred to as a Cotton effect (CE, in honor of French physicist Aimé Cotton, who observed both ORD and CD phenomena, beginning in 1896).

$$\Delta n = n_L - n_R \neq 0 \qquad (1\text{-}1)$$

In equation (1-1),[9] n_L and n_R are the refractive indices for left and right circularly polarized light. Differences in refractive indices correspond to the differences in the velocity of light. The difference in velocity of left and right circularly polarized light results in Optical Rotatory Dispersion (ORD) spectroscopy. Since the left and right circularly polarized light travels in the optically active medium with different speed, the two components are no longer in phase and the resultant vector has been rotated by the

angle α relative to the original plane of polarization. Optical Rotatory Dispersion (ORD) spectroscopy is the measurement of specific rotation, [α], as a function of wavelength.

The difference in refractive indices for left and right circularly polarized light is related to the angle of rotation, α, as shown in equation 1-2:[9]

$$\alpha = (n_L - n_R)1800l / \lambda_0 \qquad (1\text{-}2)$$

where α is the angle of rotation, with the unit in degrees, n_L and n_R are the refractive indices for left and right circularly polarized light, l is the path length in decimeters, and λ_0 is the wavelength in vacuum of the light beams in centimeters.

The specific rotation, [α], can be calculated from the observed angle of rotation, α, as expressed by equation 1-3:[9]

$$[\alpha] = \frac{\alpha}{cl} \qquad (1\text{-}3)$$

where α is the angle of rotation, with the unit in degrees, c is the concentration of the sample in g mL^{-1}, and l is the path length in decimeters.

Theoretically, ORD may be detected over all wavelengths, since it is based on the unequal refractive indices for left and right circularly polarized light. All chiral substances exhibit a molecular refraction at almost any wavelength of incident irradiation. Optical rotation at a single wavelength, such as 589 nm (sodium D-line), has been used to detect and quantitate optical activity.

When circularly polarized light passes through an optically active medium, not only is there a difference in the velocity of the left and right circularly polarized light, but also the absorbance of these two components is different (equation 1-4).[9] The difference

in molar absorptivity, $\Delta\varepsilon$, is termed Circular Dichroism (CD). ε_L and ε_R are the molar absorption coefficients for left and right circularly polarized light.

$$\Delta\varepsilon = \varepsilon_L - \varepsilon_R \neq 0 \tag{1-4}$$

CD is an absorptive process, namely the different absorption of left and right circularly polarized light, and therefore, CD only occurs in the vicinity of an absorption band. Thus, in order to observe a CD spectrum, the chiral substances need to contain a chromophore. The shape and appearance of a CD curve closely resembles that of the ordinary UV-vis absorption curve of the electronic transition to which it corresponds. However, unlike the ordinary UV-vis absorption curves, CD curves may be positive or negative, as in Figure 1-5. CD curves plot $\Delta\varepsilon$ vs. wavelength.[9]

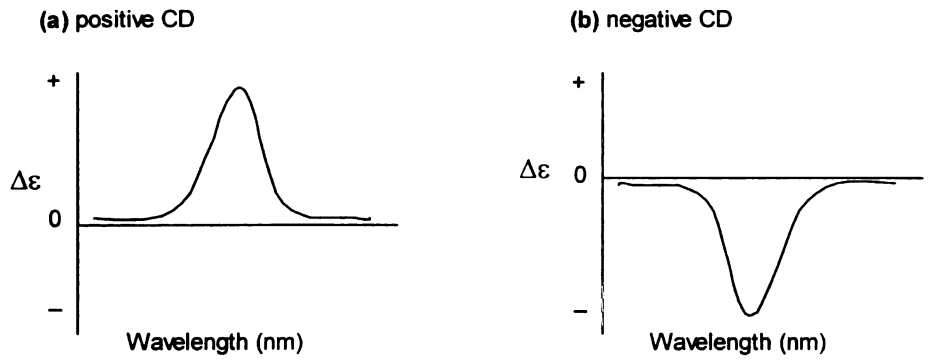

Figure 1-5. (*a*) Positive and (*b*) negative CD Cotton effects.

Circular Dichroism (CD) and Optical Rotatory Dispersion (ORD) are two manifestations of one and the same phenomenon. The molar amplitude a of an ORD can be related to the intensity of the CD curve, $\Delta\varepsilon$, by equation 1-5:[12]

$$a \approx 40.28\Delta\varepsilon \tag{1-5}$$

In a molecule, the absorption of light promotes an electron from its ground state to an excited state, which creates a momentary dipole, commonly referred to as the

electric transition dipole moment and is denoted by the vector μ. In an achiral molecule, the net electron redistribution during the process is always planar, while in a chiral molecule the electron rearrangement during the transition is always helical. In the latter case, not only the charge displacement takes place during the electronic transition, which generates the electric transition dipole moment μ, but also the rotation of electric charge creates a magnetic field whose strength and direction may be described by the magnetic transition dipole moment and which is denoted by the vector m.[8]

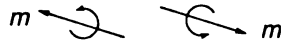

Figure 1-6. The "right hand rule" to determine the direction of magnetic transition dipole moment m.

As shown in Figure 1-6, the direction of magnetic transition dipole moment m can be determined by the application of the "right hand rule" to the rotation of the charge (circular current): If the current flows in the direction of the curved fingers of the right hand, then the outstretched thumb points the direction of m.[13]

The rotational strength, R, which is a theoretical parameter representing the sign and strength of a CD Cotton effect (CE), is given by the scalar product of the electric and magnetic transition moments (equation 1-6):[8]

$$R = \mu \bullet m = |\mu||m|\cos\beta \qquad (1\text{-}6)$$

where μ and m are the electric and magnetic transition dipole moments, respectively, and β is the angle between the two transition moments.

The sign of CE is positive when the angle is acute ($0<\beta<90^{\circ}$) or, in the limiting case, parallel, and it is negative when the angle is obtuse ($90^{\circ}<\beta<180^{\circ}$) or, in the limiting case, antiparallel. Dextrorotation results when $R>0$, together with positive CD curve, and

levorotation is generated when $R<0$, together with negative CD curve. There is no CE when the electric and magnetic transition dipole moments are perpendicular to each other.

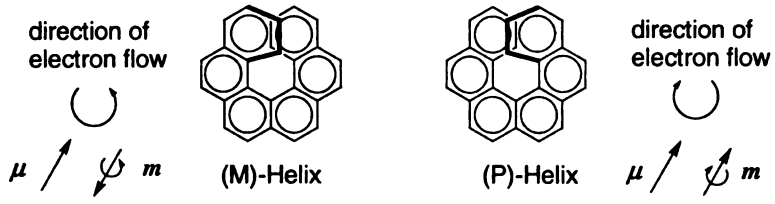

Figure 1-7. The transition moments for hexahelicene. Antiparallel moments for (M) and parallel moments for (P) helicities.

The electron helical motion of chiral compounds during excitation can be easily demonstrated with hexahelicene, as shown in Figure 1-7.[14] The direction of electron flow traces the helicity of the hexahelicene. The electric transition dipole moment μ is identical for either enantiomer, whereas the magnetic transition dipole moment direction m is reversed. According to equation (1-6), in (M)-helix, the antiparallel alignment of the transition moments leads to a negative Cotton effect. So it is defined as being levorotation, and has a negative CD spectrum. On the other hand, the (P)-helix, the parallel alignment of the transition moments leads to a positive Cotton effect. So it is defined as being dextrorotation, and has a positive CD spectrum.

The absorption of light promotes the electron from its ground state to an excited state, and in a chiral molecule the electron rearrangement during the transition is always helical. That the electron with helical movement interacts differently with the left and right circularly polarized light is the cause of the Cotton effect (CE), which states that the velocity and absorbance of one circularly polarized component is different from those for the other one.[11]

Both ORD and CD spectroscopy can be recorded by Circular Dichrometers (spectropolarimeters). The essential features of a CD spectropolarimeter are a source of monochromatic left and right circularly polarized light and a means of detecting the difference in absorbance of the two polarized light.

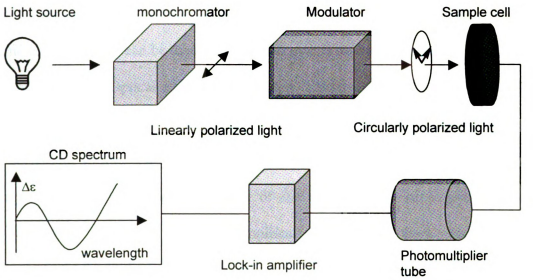

Figure 1-8. The CD spectropolarimeter.

As shown in Figure 1-8,[15] the light typically from a Xenon lamp passes through monochromators, which are crystal prisms, to achieve linearly polarized light. In the CD spectropolarimeter, the optical system comprises of two monochromators, and is known as double monochromator. The ability of a double monochromator in reducing stray light makes it indispensable in CD measurement. The linearly polarized light is then modulated into left and right circularly polarized light before it passes through the sample chamber. The transmission of light through the sample is measured by a photomultiplier tube, which produces a current whose magnitude depends on the number of incident photons. This current is then detected by a lock-in amplifier and recorded.

Most CD spectropolarimeters measure differential absorbance, ΔA, which is converted to $\Delta\varepsilon$ based on the Lambert-Beer's Law (equation 1-7):[8]

$$\Delta A = \Delta\varepsilon cl \tag{1-7}$$

Since Optical Rotatory Dispersion (ORD) and Circular Dichroism (CD) are manifestations of chiral substances and are not observed for achiral compounds or racemic mixtures, they can be used to detect and quantitate optical activity. But it should be emphasized that Optical Rotatory Dispersion (ORD) and Circular Dichroism (CD) themselves do not allow the configuration of a given product to be defined. Attempts have been made to find empirical rules[16] and semi-empirical rules,[17] such as sector rules, which would permit *a-priori* calculation of the ORD or CD of a given structure. However, these empirical and semi-empirical rules suffer from one significant shortcoming, which is that they are not valid in all cases. These rules are to be applied with great caution, and simple application of the rules does not permit the determination of absolute configuration.

Recent developments on this field allow for a quantitatively reliable quantum chemical calculation of the rotation angle of chiral molecules.[18, 19] Accordingly, the absolute stereochemistry of the chiral molecule can be assigned upon comparison of the calculated rotation angle and the experimental result. The computation of the specific rotation angle is based on the calculation of the electric-dipole magnetic-dipole polarization (G'),[20, 21] a measure of the overlap of the electronic polarization induced by the electric and the magnetic field of the incident light, which can be computed routinely using the coupled-perturbed Hartree-Fock method[22] on standard desktop workstation.[18, 19]

In the method developed by Peter Wipf and his coworkers, the individual contributions of all the atoms and functional groups are calculated and summed up to obtain the specific rotation angle of the chiral molecule.[23, 24] In this way, the structure of the chiral compound is linked to the sign and magnitude of the optical rotation angle.[25] This method is of special importance in assigning the absolute stereochemistry of large, flexible molecules with multiple chiral centers, and it has been successfully applied to determine the absolute stereochemistry of several natural products.[26-28] However, more work remains to be done to establish a better understanding of this protocol and determine the possible limitations of this fundamental approach for structural analysis.

1-2. The Exciton Coupled Circular Dichroic (ECCD) method and its applications The Exciton Coupled Circular Dichroic (ECCD) method[29] is a non-empirical method to establish the absolute configuration of chiral compounds on a microscale. The ECCD method, developed from the coupled oscillator theory[30] and group polarizability theory,[31] is based on the through space exciton coupling between two or more chirally oriented chromophores, which are not conjugated to each other. The coupling of the chromophores' electric transition dipole moment leads to the observed bisignate CD spectrum and the non-empirical determination of their orientation. Figure 1-9 is an example of exciton coupling between the two benzoates in steroidal 2,3-bisbenzoate.[29]

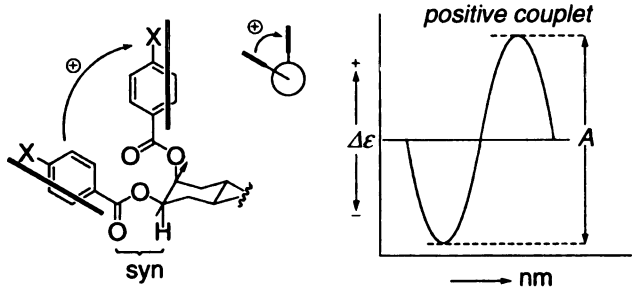

Figure 1-9. Exciton Coupled Circular Dichroism (ECCD) of steroidal 2,3-bisbenzoate.

As shown in Figure 1-9, a typical ECCD spectrum is a bisignate curve. The extremum at longer wavelength is called the first Cotton effect, and correspondingly, the extremum at shorter wavelength is called the second Cotton effect. If the sign of the first Cotton effect is positive, the ECCD spectrum is defined as positive, and if the sign of the first Cotton effect is negative, then the sign of the ECCD spectrum is negative. The amplitude (A) of the ECCD spectrum is defined as: $A = \Delta\varepsilon_1 - \Delta\varepsilon_2$ where $\Delta\varepsilon_1$ and $\Delta\varepsilon_2$ are the intensities of the first and second Cotton effect, respectively.

Based on the ECCD method, the sign of the ECCD spectrum is dictated by the relative orientation of the chromophores in the chiral molecule. As the steroidal 2,3-bisbenzoate system in Figure 1-9 indicates, the clockwise orientation of the two chromophores results in a positive ECCD curve, and counterclockwise orientation will result in a negative ECCD curve.[29]

What follows is an attempt to understand the Exciton Coupled Circular Dichroic (ECCD) method based on qualitative explanation and Quantum Mechanical theories.

1-2.1. The qualitative explanation of Exciton Coupled Circular Dichroic method (ECCD)

As it has been mentioned before, the absorption of light promotes the electron from its ground state to an excited state. The redistribution of electron during the process creates a momentary dipole, called the electric transition dipole moment (μ), and the rotation of electric charge creates a magnetic field whose strength and direction can be described by the magnetic transition dipole moment (m).

When the molecule contains two identical chromophores, which are not conjugated with each other, the most significant coupling takes place between the

transitions occurring at the same energy, *E*. The through space coupling of the electric transition dipole moments of these two chromophores generates one of the two helices, depending upon whether they are in-phase (symmetric) or out-of-phase (anti-symmetry)-so we expect to see a CD spectrum with two peaks. This can be explained by examining a dibenzoate ester in Figure 1-10.[13]

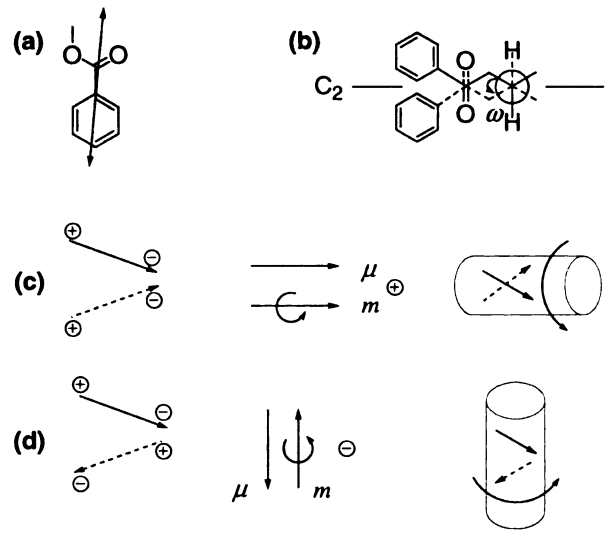

Figure 1-10. The qualitative explanation of ECCD based on a dibenzoate ester. (***a***) Orientation of the electric transition dipole moment in benzoates, λ_{max}=230 nm; (***b***) Preferred configuration of a *vic*-dibenzoate with negative dihedral angle; (***c***) and (***d***) combination of the individual electric transition dipole moments and resultant magnetic transition dipole moment.[13]

In the benzoate esters, there is a strong UV absorption band at about 230 nm, and it arise from the $\pi \rightarrow \pi^*$ transition involving the benzene ring and CO_2R.[32] The large electric transition dipole moment μ of each benzoate group is oriented approximately collinearly with the long axis of the benzoate group and almost parallel to the direction of the C-O ester bond (Figure 1-10*a*).

The conformations of benzoates are well known and are approximated in Figure 1-10*b*. In Figure 1-10*b*, the two benzoate groups are oriented in a counterclockwise manner, and correspondingly, the dihedral angle ω between the C-O bonds is negative. As it has been mentioned above, since the individual electric transition dipole moment μ aligns almost parallel to the C-O ester bonds, the dihedral angle ω between the C-O bonds thus corresponds roughly to that between the two electric transition dipole moment μ.

The individual electric transition dipole moment μ of an electronic transition couples in-phase (symmetric) or out-of-phase (anti-symmetric) (Figure 1-10*c* and *d*, respectively). In case *c*, where the two electric transition dipole moments couple in-phase, the "total" electric transition dipole moments are oriented along the chromophoric C_2 axis, and in case *d*, where the two electric transition dipole moments couple out-of-phase, the "total" electric transition dipole moments are oriented perpendicular to the chromophoric C_2 axis.

The charge rotation associated with the transition may be visualized by placing the partial moments tangent to a cylinder with the latter aligned along the axis of the "total" electric transition dipole moment μ. In case *c*, the electric transition dipole moment μ and the resultant magnetic transition dipole moment *m* are arranged parallel, and according to equation 1-6, $R = \mu \bullet m = |\mu||m|\cos\beta$, leads to a positive Cotton effect and thus a positive CD band. In case *d*, the electric transition dipole moment μ and the resultant magnetic transition dipole moment *m* are arranged anti-parallel, and correspondingly, that leads to a negative Cotton effect and a negative CD band.[13]

So the two resulting CD bands generated from the through space coupling of the electric transition dipole moments of the dibenzoate have equal magnitude and opposite sign, based on if the coupling of the electric transition dipole moments follows mode *c* or *d* in Figure 1-10. Since the energies of the two CD signals are close to the localized energy *E*, the observed CD spectrum is actually the overlapping of these two CD signals with equal magnitude and opposite sign, and this leads to the adjacent bisignate CD bands that are characteristic of Exciton Coupled Circular Dichroism (ECCD).

Repulsion between poles of the same sign in the *c* mode indicates that in-phase coupling is of higher energy than the out-of-phase mode *d*, where the poles of unlike sign are closest together. Consequently, the positive CD band associated with the *c* mode is at shorter wavelengths than the negative CD band resulting from the *d* mode; the energy gap between these two CD bands is defined as Davydov splitting. Since the negative CD band is at the longer wavelength than the positive CD band, for the absolute configuration shown in Figure 1-10*b*, the bisignate couplet is negative overall as in Figure 1-11.

As shown in Figure 1-11, in the case of the CD spectrum, the *c* and *d* modes (Figure 1-10) have opposite signs and the summation peak is a bisignate couplet. On the other hand, in the case of the UV spectrum, the *c* and *d* mode, which are real absorptions observable in UV, are always positive, and therefore, summation of the two component spectra always leads to an unsplit absorption band of double intensity.[29]

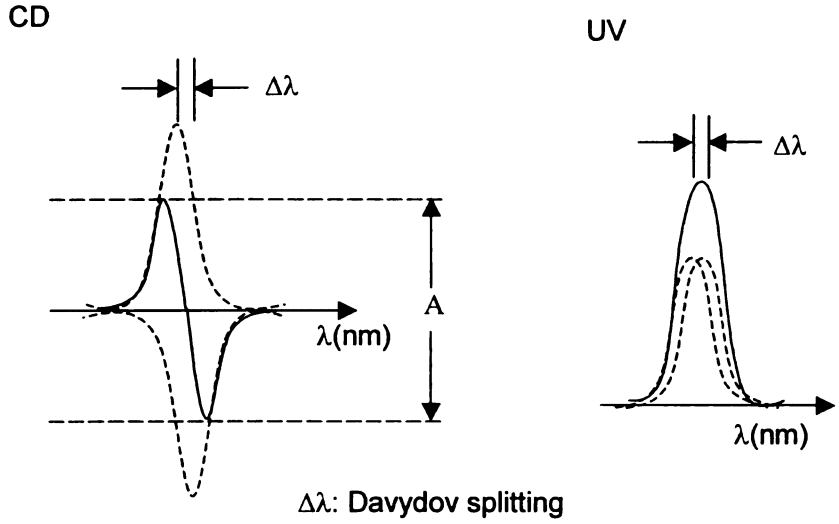

Figure 1-11. The ECCD couplet for the configuration shown in Figure 11-10*b*. The summation curves (the observed ECCD curve, shown in solid line) of two Cotton effects (dashed line) of opposite signs separated by Davydov splitting Δλ.

In conclusion, the ECCD spectrum is a bisignate spectrum because of the through space coupling of the electric transition dipole moments of the non-conjugated chromophores, with the in-phase (symmetric) and out-of-phase (anti-symmetric) coupling yielding opposite Cotton effect. Moreover, as shown in Figure 1-12, the sign of the resulting ECCD spectrum is dictated by the orientation of the interacting chromophore: the counterclockwise orientation of the chromophores, when the nearest chromophores can be made to eclipse the farther chromophore by rotating along the shortest path in a counterclockwise direction, leads to a negative ECCD spectrum, and correspondingly, the clockwise orientation leads to a positive ECCD spectrum.[33]

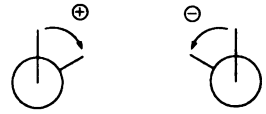

Figure 1-12. The screw sense of the chromophores and its corresponding ECCD sign.

1-2.2. The explanation of ECCD theory based on Quantum Mechanical theories

The ECCD theory can also be explained by Quantum Mechanical theories. When a molecule contains two identical non-conjugated chromophores, because of the through space interactions, excitation is delocalized between the two chromophores and the excited state (exciton)[34] is split into two states, α and β, by resonance interaction of the local excitations (Figure 1-13), just as in the case of electron delocalization of an ethylene double bond.

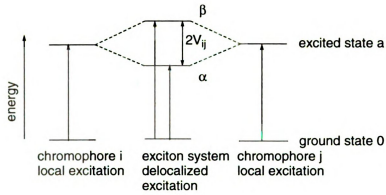

Figure 1-13. Splitting of the excited states of isolated chromophores i and j by exciton interaction. The energy gap $2V_{ij}$ is called Davydov splitting.

Based on theoretical calculation on the binary system, the rotational strength, *R*, which is a theoretical parameter representing the sign and strength of a CD Cotton effect, can be approximated as equation 1-8:[29]

$$R_{\alpha,\beta} = \pm(1/2)\pi\sigma_0\vec{R}_{ij} \bullet (\vec{\mu}_{i0a} \times \vec{\mu}_{j0a}) \qquad (1\text{-}8)$$

where the positive and negative signs correspond to α- and β- state, respectively.

In equation 1-8, $\vec{R}_{ij}$ is the distance vector from chromophore i to j, $\vec{\mu}_{i0a}$ and $\vec{\mu}_{j0a}$ are electric transition dipole moments for excitation 0→a of group i and j, respectively, and σ_0 is the excitation number of transition from ground state 0 to excited

state a, which can be expressed as: $\sigma_0 = \nu_0 / c = (E_a - E_0)/(hc)$, h is the Planck constant and c is the speed of light in vacuum. The equation 1-8 indicates that the Cotton effect of α- and β- state have identical rotational strength of opposite sign. As shown in Figure 1-11, this leads to a bisignate CD spectrum with two Cotton effect peaks of opposite signs, which are separated by the energy gap $\Delta\lambda$ (Davydov splitting).

The sign and amplitude of the bisignate ECCD spectrum is theoretically defined in equation 1-9 as:[29]

$$\vec{R}_{ij} \bullet (\vec{\mu}_{ioa} \times \vec{\mu}_{joa}) V_{ij} \qquad (1\text{-}9)$$

Where $\vec{R}_{ij}$ is the distance vector from chromophore i to j, $\vec{\mu}_{ioa}$ and $\vec{\mu}_{joa}$ are electric transition dipole moments for excitation 0→a of group i and j, respectively, and V_{ij} is interaction energy between the two group i and j.

If the equation 1-9 is positive, the observed ECCD spectrum is positive, and if it is negative, then the observed ECCD spectrum is negative. From the equation above, the sign of the bisignate curve completely depends on the spatial orientation of the two chromophores.[35] The definition of exciton chirality for a binary system is shown in Table 1-1.[33]

Table 1-1. Definition of exciton chirality for a binary system

	Qualitative Definition	Quantitative Definition	Cotton effects
Positive Chirality	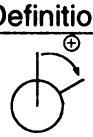	$\vec{R}_{ij} \bullet (\vec{\mu}_{ioa} \times \vec{\mu}_{joa}) V_{ij} > 0$	positive first and negative second Cotton effects
Negative Chirality		$\vec{R}_{ij} \bullet (\vec{\mu}_{ioa} \times \vec{\mu}_{joa}) V_{ij} < 0$	negative first and positive second Cotton effects

If the electric transition dipole moments of the two chromophores from front to back constitute a clockwise orientation, then according to the equation above, it will give a positive ECCD spectrum, and *vice versa*.[36, 37] Therefore, as long as the orientation of two chromophores in space is known, the sign of its ECCD spectrum can be predicted. On the other hand, the sign of the bisignate ECCD spectrum enables one to determine the relative orientation of the two chromophores in space in a non-empirical manner.

The amplitude (A) of the ECCD couplet, defined as the difference in $\Delta\varepsilon$ between the first and second Cotton effect of the couplet, is affected by the following factors:[38]

(1) **Molar absorptivity coefficient (ε value) of the chromophores:** A is proportional to ε^2. Therefore, chromophores with strong absorption are preferred for higher sensitivities of the ECCD method. If highly sensitive chromophores are employed, both the chromophoric derivatization and CD measurements can be performed at the microgram or nanogram level;

(2) **Interchromophore distance (R):** A is sensitive to the distance between the interacting chromophores, since it is inversely proportional to R^2. To achieve high amplitude, the coupling chromophores should be close to each other in space;

(3) **Projection angle between the interacting chromophores:** A value is maximal when the projection angle is around 70°, while there is no exciton coupling when the projection angle is 0° or 180°;

(4) **Number of interacting chromophores (X, Y, Z):** the A value of the whole molecule is the summation of the A value of each pair of interacting chromophores,

i.e. $A_{total} = A_{xy} + A_{xz} + A_{yz}$. The additivity rule has been proven by experiments and theoretical calculation of multichromophoric systems.[39-41]

Not only can exciton coupling take place between identical chromophores but also it can occur between different chromophores, however it is less effective.[42-44] For example, when different benzoates are used as the chromophores with λ_{max} between 200 nm to 300 nm, as long as the absorption maxima of the chromophores are not separated by more than 80 nm, exciton coupling can happen between them.[29]

The interacting chromophores do not even have to be within one molecule, as long as they are in close proximity to each other in space. For example, stacking of anthocyanins[45] and porphyrin containing brevetoxins[46] give rise to exciton coupled CD bands.

1-2.3. The application of ECCD method to determine the absolute stereochemistry of chiral molecules

Since the Exciton Coupled Circular Dichroic (ECCD) method is based on sound theoretical calculation, the absolute stereochemistry of organic compound exhibiting typical bisignate ECCD spectrum is assignable in a non-empirical manner. The Exciton Coupled Circular Dichroic (ECCD) method is a sensitive and general method requiring only microgram scale samples. It has been successfully applied in determining absolute stereochemistry of wide variety of compounds, including polyols,[47] carbohydrates,[48] quinuclidines[49] and hydroxy acids,[50] etc.[51]

Figure 1-14 is a simple example of determining the absolute stereochemistry of (+)-abscisic acid by ECCD method.[52, 53] Abscisic, a plant hormone, contains only one chiral center in the molecule, and two non-conjugated chromophores: enone and dienoic

acid. The enone and dienoic acid chromophores interact with each other through space resulting in a positive ECCD couplet. Based on the sign of the ECCD spectrum, the two chromophores must be oriented in a clockwise manner in space, which directly indicates the α- configuration of the tertiary hydroxyl group.

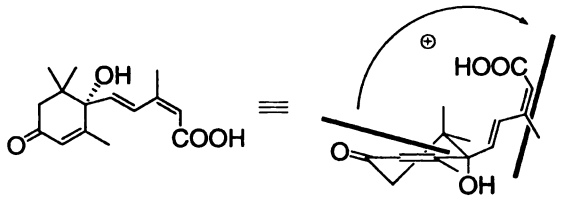

Figure 1-14. The stereochemical determination of abscisic acid by ECCD method.

More examples of determining absolute stereochemistry of chiral compounds with ECCD are shown in Figure 1-15. (i) The configuration of the 15-glcNAc group in pavoninin-4, a shark repellent, is determined from the sign of the ECCD between the enone and bromobenzoate.[54] (ii) The absolute configuration of the potent cockroach sex excitant periplanone B is established by carbonyl reduction, benzoylation, and measurement of the ECCD arising from interactions between the benzoate and diene chromophores.[55] (iii) The absolute configuration of the polyol side chain of ahopanoid from Nostoc PCC 6720 is assigned from the bichromophoric excition coupled CD spectra. This is a case of heterochromophoric coupling, which can provide fingerprint spectra for the molecules.[49]

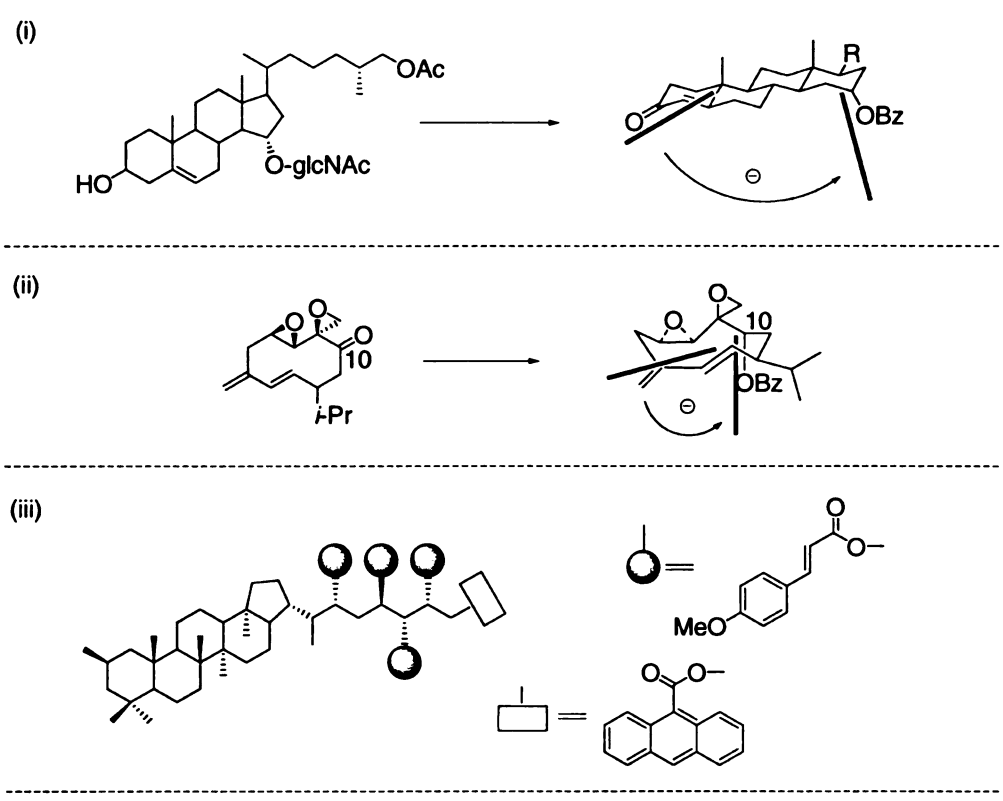

Figure 1-15. Examples of exciton chirality CD method in absolute configurational assignment.

1-3. Use of chromophoric host such as porphyrins for ECCD studies

As mentioned above, the Exciton Coupled Circular Dichroic (ECCD) method is a strong tool for assigning the absolute stereochemistry of chiral compounds in a non-empirical fashion. However, use of the ECCD method to determine the absolute stereochemistry of any chiral compound requires the presence of at least two interacting chromophores in the chiral molecule. This fact could limit the use of this method, since majority of chiral compounds do not fulfill this requirement. In order to address the above issue, chromophoric receptors have been designed to act as hosts for the non-chromophoric chiral molecule. Upon binding of the chiral substrate, either covalently or

non-covalently, the host will adopt a preferred chiral conformation, induced by the chiral guest, which can be observed as ECCD couplet.

1-3.1. Use of chromophoric hosts

Chiral induction, where a chiral molecule induces chirality in an achiral molecule by intermolecular forces, was apparently first demonstrated on dyes bound to polypeptides in their helical conformations.[56] It remains a tool for probing the conformations of macromolecules.[57] The process for transmission of configurational information comprise of, at least, two elementary processes: (1) complex formation and (2) some dynamic processes associated with it, such as conformational changes of interacting molecules.[58-60] If the interactions between two molecules are strong enough, they will lead to efficient transmission of information.

The chromophoric hosts used for ECCD studies are achiral themselves, however, upon binding to the chiral substrate, the chromophoric host will adopt an induced chirality dictated by the chirality of the substrate through chiral induction. The induced helicity of the chromophoric hosts could be observed and determined by ECCD, which in turn will lead to the stereochemical determination of the bound chiral substrate. An example of the induced chirality in chromophoric host with chiral substrates is shown in Figure 1-16.[61]

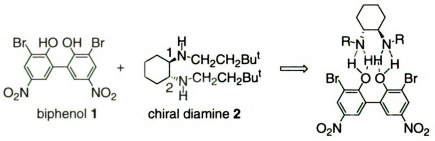

Figure 1-16. The induced chirality of biphenol upon binding to chiral diamine.

In Figure 1-16, the biphenol compound **1** serves as the chromophoric host to bind with the chiral diamine **2**. The two phenyl rings in biphenol **1** are not in the same plane, because of the steric interactions between the two hydroxyl group, thus they are not conjugated with each other, and therefore, meet the criteria of chromophores that could undergo exciton coupling.

Biphenol **1** and diamine **2** form a complex in solution through hydrogen bonding. The hydrogen bonding between phenolic OH and aliphatic amines has been well studied.[62-64] Without chiral diamine **2**, biphenol **1** has two chiral conformations, which can rapidly convert to each other at room temperature. Biphenol **1** has no CD at room temperature, but upon the addition of chiral diamine **2**, an ECCD spectrum is observed. The observed ECCD is due to the through space coupling of the two phenol groups and indicates that chirality has been induced in biphenol **1** by complexation with chiral diamine **2**. The chirality adopted by biphenol **1** is dictated by the absolute stereochemistry of the bound chiral diamine **2**.

In a similar manner, the same has been applied to determine the absolute stereochemistry of chiral secondary alcohols.[65] As shown in Scheme 1-1, the chromophoric reagent, 3-cyanocarbonyl-3'-methoxycarbonyl-2,2'-binaphthalene **3** can be esterified with chiral secondary alcohols and the resultant complex exhibits induced ECCD as a result of favoring one atropisomer.

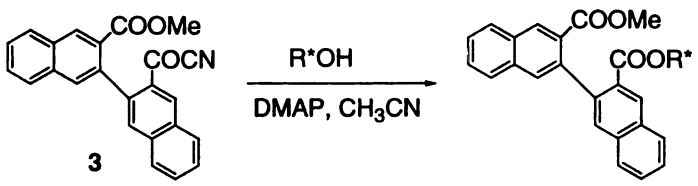

Scheme 1-1. The derivatization of binaphthalene **3** with chiral alcohols.

The chirality has been transmitted from the chiral alcohols to the binaphthylene system by minimizing the steric interaction between the substituents on the chiral alcohols with the methyl ester group in the binaphthylene. This conclusion has been verified by molecular mechanics calculations, and it suggests that the transmission of the chirality occurred in a thermodynamically controlled fashion.[65]

1-3.2. Use of zinc porphyrin as chromophoric host

Porphyrins have received a great deal of attention as receptors for chiral recognition due to several unique features:[66]

(1) Their planar structures provide a well-defined binding pocket that is accentuated by substitutions on the ring. There are many sites that can be derivatized such as the meso and β-positions, the central metal and the inner nitrogen atoms. By varying substituents on the periphery of porphyrins the solubility of the porphyrin containing compounds in non-polar and polar solvents can be easily modified;

(2) They are good chromophores, with absorption maximum around 418 nm for the main absorption band (Soret band). The absorption of the porphyrins is far red-shifted than most chromophores that likely preexist in the system, such as carbonyl and alkenes. This prevents the unwanted interaction between the introduced chromophore and the preexisting chromophores, which can complicate the analysis of the resulting ECCD spectrum;

(3) They are highly chromophoric with ε (molar absorption coefficient) higher than 400,000. As it has been mentioned before, the amplitude (A) of the ECCD couplet is proportional to the ε^2, so the sensitivity of CD will be greatly enhanced with the strong absorbing chromophores. Therefore, porphyrins are ideal chromophores for detecting

subtle changes in their close environment such as binding of chiral ligands. These intermolecular interactions can be easily followed by UV-vis, fluorescence, NMR, and resonance Raman;[66]

(4) Metal incorporation into the porphyrin ring can be easily achieved. Metalloporphyrins, such as zinc porphyrins and magnesium porphyrins, can provide extra stereodifferentiation with their Lewis base binding sites.

There are two types of porphyrin chromophores: achiral porphyrins and inherently chiral porphyrins;[67] examples of each is shown in Figure 1-17. The achiral porphyrins are planar molecules, while the chiral porphyrins are "saddle" shaped.

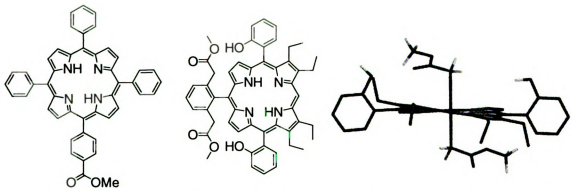

achiral porphyrin inherently chiral porphyrin side-view of the chiral porphyrin

Figure 1-17. Achiral porphyrins and inherently achiral porphyrins.

Achiral porphyrins have been widely utilized in stereochemical studies by CD. These include absolute configurational assignments,[46, 68, 69] stereochemical differentiations of sugars and amino acids,[70, 71] and interactions with bio-macromolecules.[72, 73]

Porphyrins have been used broadly in UV-vis and CD study because of their far red-shift absorption band and their high absorption. The porphyrin free base generally has four absorption bands (Q band) in the visible region. The very intense band

appearing around 415 nm in the near ultraviolet is the B band, and more commonly referred to as Soret band. Generally, the concentration of the porphyrin solution can be determined by the intensity of the Soret band based on the Lambert-Beer's Law: $A = \varepsilon cl$. There are also additional bands (N, L, M bands) at the ultraviolet regions but these bands are usually much weaker. For porphyrins with different substituents on the periphery, the positions of the Soret band and the other bands vary a little.

Upon formation of metalloporphyrins, such as zinc porphyrins, the four Q bands in the visible region collapse into essentially two bands due to higher symmetry, while the Soret band may remain in the usual range or shifted to higher or lower energy. The molar absorption coefficient (ε) of the Soret band changes with the insertion of metals in the porphyrin ring. As shown in Figure 1-18, zinc porphyrin methyl ester (ε=550,000)[74] has higher molar absorption coefficient in the Soret band than the porphyrin free base (ε=440,000),[75] and the position of this band is also slightly red shifted.

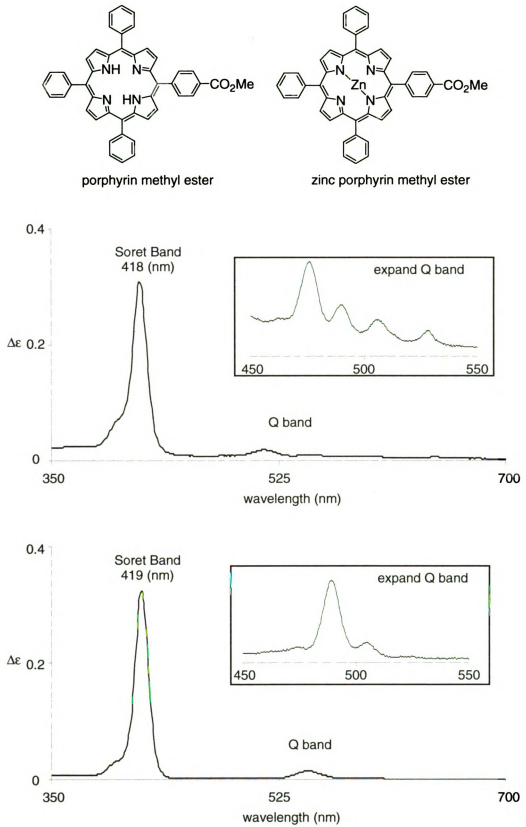

Figure 1-18. UV-vis spectra of porphyrin methyl ester and zinc porphyrin methyl ester.

Porphyrins, as the alkyl connected bis-metalloporphyrins **4** shown in Figure 1-19, can be used as host systems for stereochemical determination of chiral compounds because of their ability to bind to the chiral compounds and report the chirality of bound guests based on Exciton Coupled Circular Dichroic spectroscopy (ECCD).[76-81]

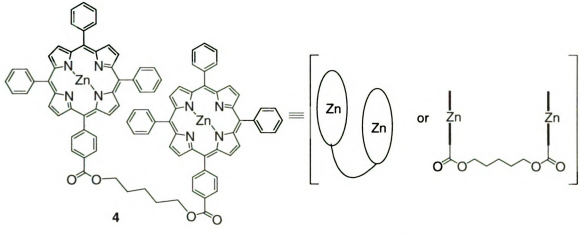

Figure 1-19. Structure of zinc porphyrin tweezer **4**.

Zinc porphyrin tweezer **4**, as shown in Figure 1-19, can undergo host-guest complexation with chiral diamines and adopt a chirally oriented conformation (helicity) leading to a bisignate ECCD spectrum. The helicity of the interacting chromophores can be observed by CD and is exhibited as bisignate ECCD spectrum. The helicity of the receptor in turn reflects the chirality of the bound compound.

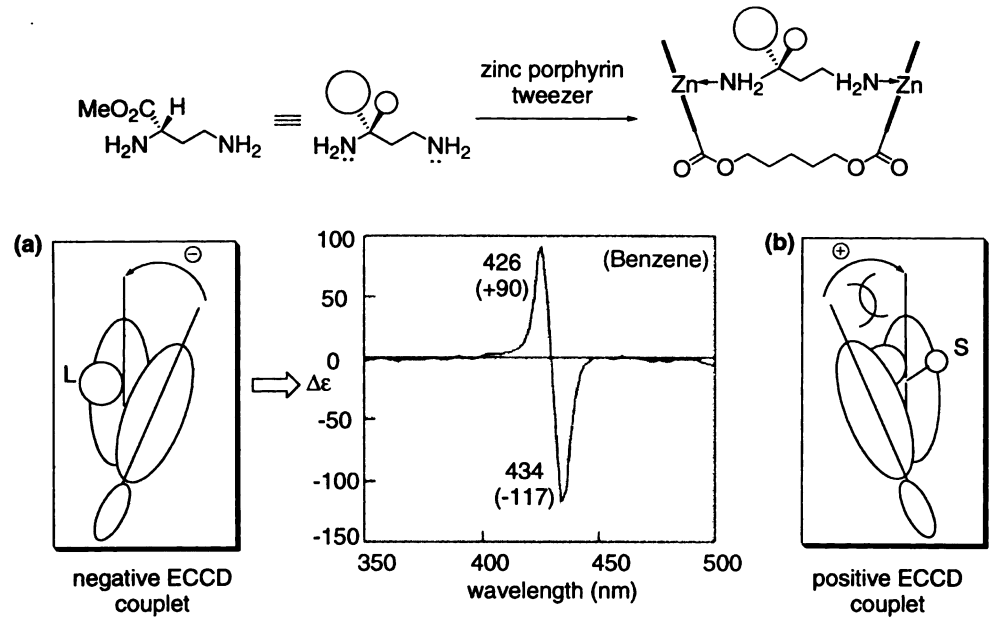

Figure 1-20. Assignment of absolute configuration of acyclic chiral diamines by Exciton Coupled Circular Dichroism (ECCD).

As shown in Figure 1-20, when zinc porphyrin tweezer **4** is added to the solution of chiral diamine (*S*)-methyl-2,4-diaminobutyrate, the porphyrin tweezer binds to the chiral diamine via Zn-N coordination to form a "sandwich" structure.[81]

The porphyrin, which is far away from the chiral center, does not interact with the chiral center. However, the porphyrin, coordinated to the end which is close to the chiral center, will interact with the groups on the chiral center in a way to minimize the steric interactions between the porphyrin ring and the chiral substituents. In order to minimize the steric interaction, the porphyrin ring 'slides away' from the large group on the chiral center and covers the small group (Figure 1-20*a*). This conformation is more stable than the alternate (Figure 1-20*b*), in which the porphyrin ring 'slides away' from the small group and interacts with the large group instead. The more stable conformation (*a*), leads

to the two porphyrin planes adopting a counterclockwise orientation and a negative ECCD couplet is predicted. This prediction matches the CD observation.

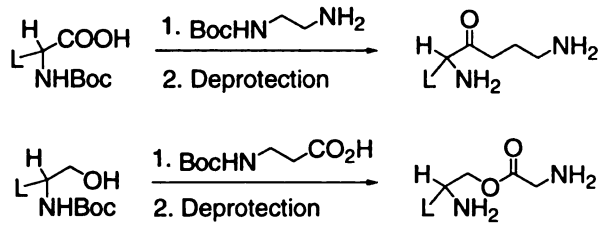

Scheme 1-2. Converting the amino acids and amino alcohols to diamines.

This approach has been extended to determine the absolute stereochemistry of chiral amino acids and amino alcohols, which have a primary amino group directly attached to the stereogenic center.[81] After simple chemical modifications as shown in Scheme 1-2, the amino acid and amino alcohols can be converted to diamines, whose stereochemistry can be determined by the method mentioned above.

Zinc porphyrin tweezer **4** cannot be used directly to determine the absolute stereochemistry of chiral compounds that have only one site of attachment, since two chromophores need to be bound and interact through space in order to observe ECCD. To overcome this problem, carrier molecules have been designed to convert compounds with only one site of attachment to molecules possessing two sites of attachment. Carriers are achiral molecules, which can be derivatized with the chiral substrates to provide the requisite two sites of attachment for binding to zinc porphyrin tweezer.

The carrier molecules need to possess the following characteristics:[78]

(1) They should have a functional group that can be derivatized with the chiral compounds. For example, a carboxylic acid will serve well when a chiral amine is to be analyzed;

(2) The derivatized carriers should be able to bind to the zinc porphyrin tweezer **4** or a comparable host at 1:1 ratio;

(3) The carrier derivatized conjugates should be rigid, since flexible structures will give multiple conformations leading to weak or even complex CD spectra;

(4) The carriers should be achiral, since the introduction of the extra chiral center into the system will result in diastereomers, which will complicate interpretation of the ECCD spectrum.

Ultimately, the success of this carrier method relies on identifying the most energetically favored conformation of the derivatized carrier. This is imperative because the conformation of the derivatized carrier dictates the position of the substituents at the chiral center in space relative to the porphyrins, and therefore, will dictate the spacial orientation adopted by the two porphyrin planes. The ideal carrier, upon derivatization with chiral compounds, exhibits a rigid and predictable conformation about the free rotating single bonds. Rotation along any of the single bond can dramatically alter the position of the large, medium, and small group with respect to the porphyrins.

Following these guidelines, carrier **5** has been designed and synthesized in order to determine the absolute stereochemistry of chiral monoamine in conjunction with zinc porphyrin tweezer.[78] It can be derivatized with chiral monoamines by the carboxylic acid functionality to form an amide bond. After the Boc protecting group is removed, it provides two binding sites to coordinate with zinc porphyrin tweezer. This conjugate can bind to the zinc porphyrin tweezer to form a complex, the stereochemistry of which can be assigned based on the Exciton Coupled Circular Dichroic method.

As Figure 1-21 shows, derivatization of (*R*)-1-cyclohexylethylamine with carrier **5**, followed by deprotection, leads to conjugate **6** with two nitrogen atoms, the pyridine nitrogen and the free amino nitrogen, serving as the binding handle for both zinc sites of porphyrin tweezer **4**. The complexation leads to a unique helical arrangement of the two porphyrin planes with respect to each other, and can be observed by ECCD spectrum. The correlation between the sign of the ECCD spectrum and the absolute stereochemistry of the chiral conjugate **6** can be deduced by the following reasoning.

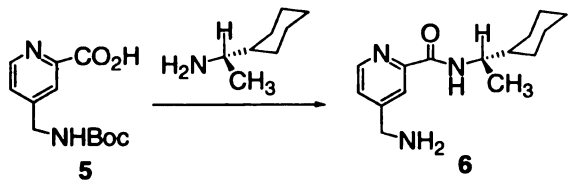

In the most stable conformation:

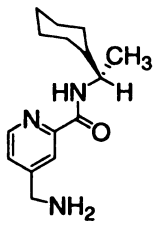

- The carbonyl oxygen is *anti* to the pyridine ring due the electrostatic repulsion.
- The carbonyl oxygen is *syn* to the small group (H) on the chiral center to reduce the pseudo $A_{1,3}$ strain.

Figure 1-21. The chiral complex and its most stable conformation.

Molecular modeling of the conjugate **6** suggests that it is a rigid molecule and it has a predictable energetically favored conformation.[78] In this most favorable conformation, the free rotations around the single bonds: C_{Ar}-$C_{C=O}$, $C_{C=O}$-NH, and NH-C_{chiral} are restricted. Molecular modeling of the conjugate has shown that the conjugate **6** favors a coplanar orientation of the carbonyl group to the pyridine ring. Moreover, due to electrostatic repulsion, the *anti* carbonyl oxygen/pyridine nitrogen disposition is preferred by ~30 kJ/mol. Finally, it has been well understood that in an amide, due to the pseudo

$A_{1,3}$ interaction, the small group on the chiral center (hydrogen) is *syn* to the carbonyl oxygen.

Since the spacial arrangement of the substituents of the chiral center can be deduced from this favored conformation, the orientation of the porphyrin planes can be predicted based on the interaction between the chiral compound and the porphyrin planes.

The three substituent groups at the chiral center are assigned S (small), M (medium), and L (large) according to their size,[8] with hydrogen being the S group, methyl being M group and cyclohexyl being L group. As shown in Figure 1-22, upon binding to zinc porphyrin tweezer **4**, the chiral substrate will adopt a conformation such that L points out of the plane formed by the amide and the pyridine ring, while M points into the plane. The zinc porphyrin's approach of the pyridine nitrogen will bias the side of M group in order to avoid the unfavorable steric interaction with L. Thus, the two porphyrin planes of the tweezer orient in a clockwise way, and dictate a positive ECCD spectrum. This prediction matches with the experimental observation.

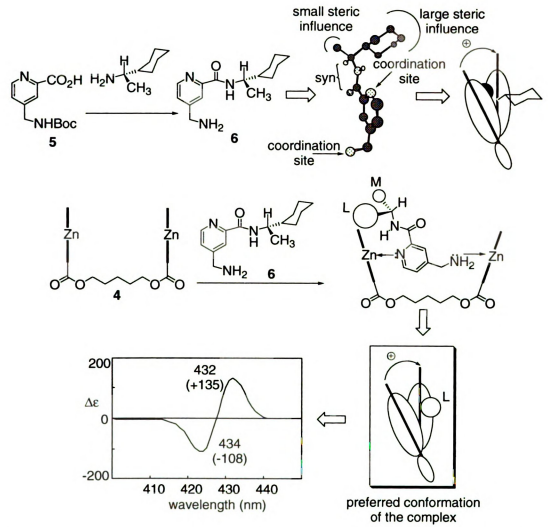

Figure 1-22. Use of carrier **5** to determine the absolute stereochemistry of chiral monoamine by Exciton Coupling Circular Dichroism.

The goal of our research is to further the above studies by determining the absolute stereochemistry of chiral compounds with different functional group, namely α-chiral carboxylic acids, by using the stated Exciton Coupled Circular Dichroic (ECCD) method. In order to achieve that goal, we have studied the synthesis of zinc porphyrin tweezers, the design and synthesis of different carriers for α-chiral carboxylic acids, and their spectroscopic studies.

Reference:

1. Bruice, P. Y. *Organic chemistry*, 3rd ed.; Prentice-Hall, Inc.: Upper Saddle River, New Jersey, **2001**.

2. Rossi, R.; Diversi, L. *Synthesis* **1973**, 25.

3. Laarhoven, W. H.; Prinsen, W. J. C. *Top. Curr. Chem.* **1984**, *125*, 63.

4. Eliel, E. L. *Stereochemistry of Carbon Compounds*; McGraw-Hill: New York, **1962**.

5. Oki, M. Recent Advances in Atropisomerism. In *Topics in Stereochemistry*; Allinger, N. L., Eliel, E. L., Wilen, S. W., Eds.; An Interscience Publication: New York, 1983.

6. Humpf, H. -U.; Berova, N.; Nakanishi, K.; Jarstfer, M. B.; Poulter, C. D. *J. Org. Chem.* **1995**, *60*, 3539.

7. Dale, J. A.; Moser, H. S. *J. Am. Chem. Soc.* **1973**, *95*, 512.

8. Eliel, E. L.; Wilen, S. W.; Mander, L. N. *Stereochemistry of Organic Compounds*; Wiley: New York, **1994**.

9. Lambert, J. B.; Shurvell, J. F.; Lightner, D. A.; Cooks, R. G. *Organic Structural Spectroscopy*; Prentice Hall: Upper Saddle River, **1998**.

10. Solomons, T. W. G. *Organic Chemistry*; John Wiley & Sons. Inc.: New York, **1978**.

11. Velluz, L.; LeGrand, M.; Grosjean, M. *Optical Circular Dichroism*; Academic Press Inc.: New York, **1965**.

12. Mislow, K.; Glass, M. A. W.; O'Brien, R. E.; Rutkin, P.; Steinberg, D. H.; Weiss, J.; Djerassi, C. *J. Am. Chem. Soc.* **1962**, *84*, 1455.

13. Snatzke, G. *Angew. Chem. Int. Ed. Engl.* **1979**, *18*, 363.

14. Nogrady, M. *Stereochemistry*; Pergamon Press Ltd.: Oxford, **1981**.

15. Berova, N.; Nakanishi, K.; Woody, R. W. *Circular Dichroism: Principles and Applications*; Wiley-VCH: New York, **2000**.

16. Moffitt, W.; Woodward, W. B.; Moscowitz, A.; Klyne, W.; Djerassi, C., *J. Am. Chem. Soc.* **1961**, 83.

17. Snatzke, G. *Optical Activity and Chiral Discrimination*; Reidel, Dordrecht, and Neatherlands: 1979.

18. Polavarapu, P. L. *Molec. Phys.* **1997**, *91*, 551.

19. Polavarapu, P. L.; Chakraborty, D. K. *J. Am. Chem. Soc.* **1998**, *120*, 6160.

20. Amos, R. D. *Chem. Phys. Lett.* **1982**, *87*, 23.

21. Kondru, R. K.; Wipf, P.; Beratan, D. N. *J. Am. Chem. Soc.* **1998**, *120*, 2204.

22. Amos, T. D.; Rice, J. E.; Cdwell S. M. *J. Chem. Phys.* **1990**, *93*, 8828.

23. Kondru, R. K.; Wipf, P.; Beratan, D. N. *Science* **1998**, *282*, 2247.

24. Kondru, R. K.; Lim, S.; Wipf, P.; Beratan, D. N. *Chirality* **1997**, *9*, 469.

25. Kondru, R. K.; Wipf, P.; Beratan, D. N. *J. Phys. Chem. A* **1999**, *103*, 6603.

26. Ribe, S.; Kondru, R. K.; Beratan, D. N.; Wipf, P. *J. Am. Chem. Soc.* **2000**, *122*, 4608.

27. Kondru, R. K.; Beratan, D. N.; Friestad, G. K.; Smith, I., A. B.; Wipf, P. *Org. Lett.* **2000**, *2*, 1509.

28. Kondru, R. K.; Chen, C. H.; Curran, D. P.; Beratan, D. N.; Wipf, P. *Tetrahedron: Asymmetry* **1999**, *10*, 4143.

29. Harada, N.; Nakanishi, K. *Circular Dichroic Spectroscopy: Exciton Coupling in Orgainc Stereochemistry*; University Science Books: Mill Valley, **1983**.

30. Kuhn, W. *Trans. Faraday Soc.* **1930**, *26*, 293.

31. Kirkwood, J. G. *J. Chem. Soc.* **1937**, *5*, 479.

32. Wiesler, W. T.; Vazquez, J. T.; Nakanishi, K. *J. Am. Chem. Soc.* **1987**, *109*, 5586.

33. Harada, N.; Chen, S. -M. L.; Nakanishi, K. *J. Am. Chem. Soc.* **1975**, *97*, 5345.

34. Chen, S. -M. L.; Harada, N.; Nakanishi, K., *J. Am. Chem. Soc.* **1974**, *96*, 7352.

35. Harada, N.; Nakanishi, K. *Acc. Chem. Res.* **1972**, *5*, 257.

36. Wagniere, G.; Hug, W, *Tetrahedron Lett.* **1970**, *11*, 4765.

37. Hug, W.; Wagniere, G. *Tetrahedron* **1972**, *28*, 1972.

38. Weckerle, B.; Schreiber, P.; Humpf, H. -U. *J. Org. Chem.* **2001**, *68*, 8160.

39. Lichtenthaler, F. W.; Sakakibara, T. *Carbohydr. Res.* **1977**, *59*, 47.

40. Liu, H. W.; Nakanishi, K. *J. Am. Chem. Soc.* **1981**, *103*, 7005.

41. Dong, J. -G.; Akritopoulou-Aanae, I.; Guo, J.; Berova, N.; Nakanishi, K.; Harada, N. *Enantiomer* **1997**, *2*, 397.

42. Harada, N.; Iwabuchi, J.; Yokota, Y.; Uda, H.; Nakanishi, K. *J. Am. Chem. Soc.* **1981**, *103*, 5590.

43. Gonnella, N. C.; Nakanishi, K.; Martin, V. S.; Sharpless, K. B., *J. Am. Chem. Soc.* **1974**, *104*, 3775.

44. Mori, Y.; Kohchi, Y.; Suzuki, M.; Furukawa, H. *J. Am. Chem. Soc.* **1992**, *114*, 3557.

45. Goto, T.; Kondo, T. *Angew. Chem. Int. Ed. Engl.* **1991**, *30*, 17.

46. Matile, S.; Berova, N.; Nakanishi, K. *Chem. & Biol.* **1996**, *3*, 379.

47. Rele, D.; Zhao, N.; Nakanishi, K.; Berova, N. *Tetrahedron* **1996**, *52*, 2795.

48. Wiesler, W. T.; Nakanishi, K. *J. Am. Chem. Soc.* **1989**, *111*, 9205.

49. Zhao, N.; Berova, N.; Nakanishi, K.; Rohmer, M.; Mougenot, P.; Jurgnes, U. J. *Tetrahedron* **1996**, *52*, 2777.

50. Gimple, O.; Schreiber, P.; Humpf, H. -U. *Tetrahedron: Asymmetry* **1997**, *8*, 11.

51. Nakanishi, K.; Berova, N. *Circular Dichroism. Principles and Applications*; VCH Publishers: New York, **1994**.

52. Harada, N. *J. Am. Chem. Soc.* **1973**, *95*, 240.

53. Koreeda, M.; Weiss, G.; Nakanishi, K. *J. Am. Chem. Soc.* **1973**, *95*, 239.

54. Tachibana, K.; Sakaitani, M.; Nakanishi, K. *Science* **1973**, *226*, 703.

55. Adams, M.; Nakanishi, K.; Still, W. C.; Arnold, E. V.; Clardy, J.; Presoons, C. J. *J. Am. Chem. Soc.* **1979**, *101*, 2495.

56. Blout, E. R.; Stryer, L. *Proc. Natl. Acad. USA* **1959**, *45*, 1591.

57. Stryer, L.; Blout, E. R. *J. Am. Chem. Soc.* **1961**, *83*, 1411.

58. Beer, P. D.; Rothin, A. S. *J. Chem. Soc., Chem. Commun.* **1988**, 52.

59. Mizutani, T.; Yagi, S.; Honmaru, A.; Ogoshi, H. *J. Am. Chem. Soc.* **1996**, *118*, 5318.

60. Hayashi, T.; Asai, T.; HoKazono, H.; Ogoshi, H. *J. Am. Chem. Soc.* **1993**, *115*, 12210.

61. Mizutani, T.; Takagi, H.; Hara, O. *Tetrahedron Lett.* **1997**, *38*, 1991.

62. Hanessian, S.; Gomtsyan, A.; Simard, M.; Roelens, S. *J. Am. Chem. Soc.* **1995**, *117*, 7630.

63. Kramer, R.; Zundel, G. *J. Chem. Soc., Faraday Trans.* **1990**, *86*, 301.

64. Bell, C. L.; Barrow, G. M. *J. Chem. Phys.* **1959**, *36*, 5.

65. Hosoi, S.; Kamiya, M.; Ohta, T. *Org. Lett.* **2001**, *3*, 3659.

66. Ogoshi, H.; Mizutani, T. *Acc. Chem. Res.* **1998**, *31*, 81.

67. Mizutani, T.; Ema, T. *J. Am. Chem. Soc.* **1994**, *116*, 4240.

68. Matile, S.; Berova, N.; Nakanishi, K. *J. Am. Chem. Soc.* **1995**, *117*, 7021.

69. Arimori, S.; Takeuchi, M.; Ahinkai, S. *J. Am. Chem. Soc.* **1996**, *118*, 245.

70. Crossley, M. J.; Mackay, L. G.; Try, A. C., *J. Chem. Soc., Chem. Commun.* **1995**, 1925.

71. Crossley, M. J.; Hambley, T. W.; Mackay, L. G.; Try, A. C.; Walton, R. *J., Chem. Soc., Chem. Commun.* **1995**, 1077.

72. Suenaga, H.; Arimori, S.; Shinkai, S. *J. Chem. Soc., Perkin Trans. 2* **1996**, 607.

73. Foster, N.; Singhal, A. K.; Smith, M. W.; Marcos, N. G.; Schra, K. J. *Biochim. Biophys. Acta.* **1988**, *950*, 118.

74. Matile, S.; Berova, N.; Nakanishi, K.; Fleischhuer, J.; Woody, R. W. *J. Am. Chem. Soc.* **1996**, *118*, 5198.

75. Rickman, B. H.; Matile, S.; Nakanishi, K.; Berova, N. *Tetrahedron* **1998**, *54*, 5041.

76. Huang, X.; Fujioka, N.; Pescitelli, G.; Koehn, F. E.; Williamson, R. T.; Nakanishi, K.; Berova, N. *J. Am. Chem. Soc.* **2002**, *124*, 10320.

77. Huang, X. F.; Nakanishi, K.; Berova, N. *Chirality* **2000**, *12*, 237.

78. Huang, X.; Borhan, B.; Rickman, B. H.; Nakanishi, K.; Berova, N. *Chem. Eur. J.* **2000**, *6*, 216.

79. Kurtan, T.; Nesnas, N.; Li, Y. Q.; Huang, X. F.; Nakanishi, K.; Berova, N. *J. Am. Chem. Soc.* **2001**, *123*, 5962.

80. Proni, G.; Pescitelli, G.; Huang, X. F.; Quraishi, N. Q.; Nakanishi, K.; Berova, N. *Chem. Commun.* **2002**, 1590.

81. Huang, X. F.; Rickman, B. H.; Borhan, B.; Berova, N.; Nakanishi, K. *J. Am. Chem. Soc.* **1998**, *120*, 6185.

Chapter 2

Polymer-supported synthesis of mono-substituted porphyrins

Porphyrins have received a great deal of attention as receptors for chiral recognition due to several unique features:[1]

(1) Their planar structures provide a well-defined binding pocket that is accentuated by substitutions on the ring. There are many sites that can be derivatized such as the *meso* and β-positions, the central metal and the inner nitrogen atoms. By varying substituents on the periphery of porphyrins, the solubility of the porphyrin containing compounds in non-polar and polar solvents can be easily modified;

(2) They are good chromophores, with absorption maximum around 418 nm for the main absorption band (Soret band).[2] The absorption of the porphyrins is far red-shifted than most chromophores that likely preexist in the system, such as carbonyl and alkenes. This prevents the unwanted interaction between the introduced chromophore and the preexisting chromophores, which can complicate the analysis of the resulting ECCD spectrum;

(3) They are highly chromophoric with ε (molar absorptivity coefficient) higher than 400,000.[3] As it has been mentioned before, since the amplitude (A) of the ECCD couplet is proportional to the ε^2, the sensitivity of CD will be greatly enhanced when a strong absorbing chromophore is used. So porphyrins are ideal chromophores for detecting subtle changes in their close environment such as binding of chiral ligands. These intermolecular interactions can be easily followed by UV-vis, fluorescence, NMR, and resonance Raman;[1]

(4) Metal incorporation into the porphyrin ring can be easily achieved. Metalloporphyrins, such as zinc porphyrins and magnesium porphyrins, can provide extra stereodifferentiation with their Lewis base binding sites.

2-1. The synthesis of the zinc porphyrin tweezer

The zinc porphyrin tweezer has been demonstrated to be successful in determining the stereochemistry of chiral compounds, such as chiral diamines, amino acids, and amino alcohols through host-guest complexes.[4] The porphyrin tweezer can be easily synthesized from mono-substituted porphyrins, such as porphyrin carboxylic acids and alcohols. The carboxylic acid or alcohol functionality at the *meso* position of the mono-substituted porphyrin is used to connect with an alkyl chain to form the porphyrin tweezer (Scheme 2-1).

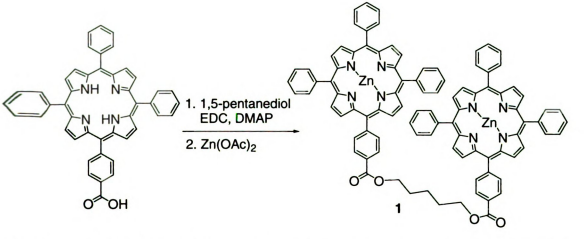

Scheme 2-1. Synthesis of zinc porphyrin tweezer **1** from porphyrin carboxylic acid.

The synthesis of the zinc porphyrin tweezer **1** depends heavily on the synthesis of mono-substituted porphyrins. As shown in Scheme 2-2, the mono-substituted porphyrin methyl ester **2** could be synthesized by condensing pyrrole, benzaldehyde and 4-carboxymethylbenzaldehyde in refluxed propionic acid at 4:3:1 ratio.[4] Zinc acetate was used to serve as a template to help the assembly of the porphyrin rings. After the reaction

mixture was refluxed in propionic acid for several hours, DDQ was added to the reaction mixture as an oxidation reagent to finish the synthesis of porphyrin compounds. The zinc was removed from the porphyrins by washing it with 6 N hydrochloric acid.

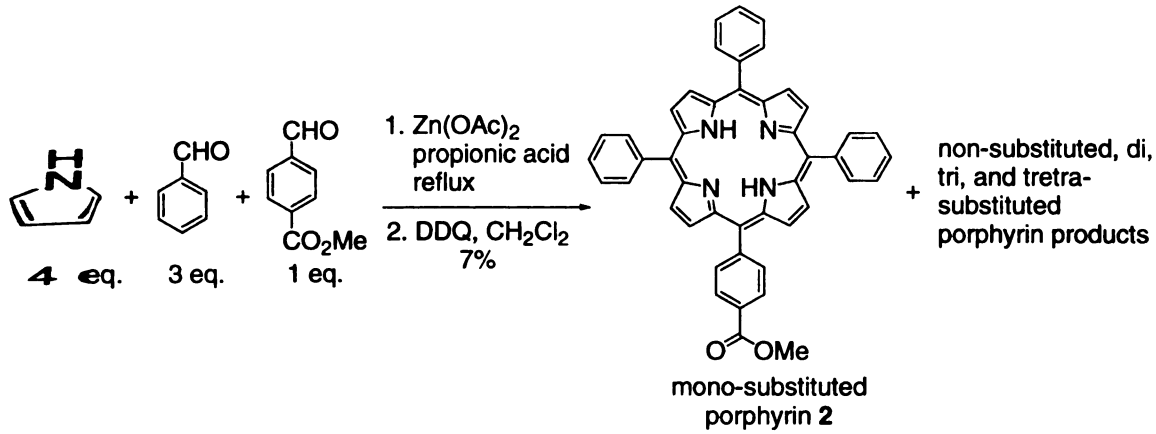

Scheme 2-2. Synthesis of mono-substituted porphyrin methyl ester **2**.

This synthesis leads to the formation of the desired mono-substituted porphyrin **2** along with a mixture of tetraphenylporphyrin, and di-, tri-, and tetra-substituted porphyrins. The separation of the desired mono-substituted porphyrin from all the byproduct is tedious, however, it can be achieved by multiple column chromatographies.

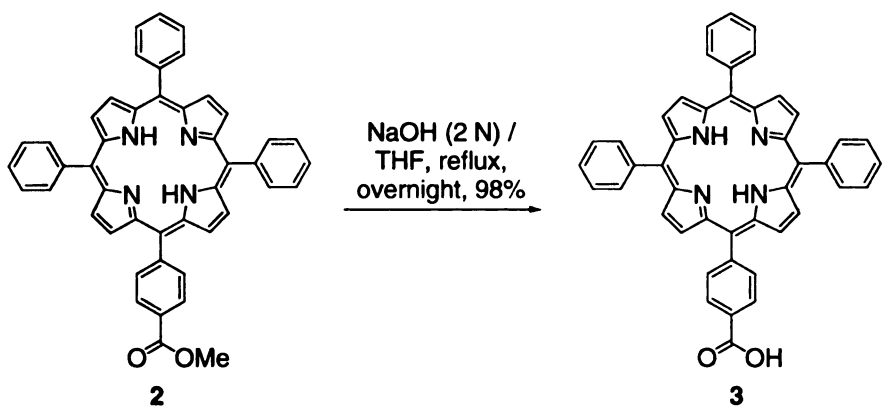

Scheme 2-3. Hydrolysis of porphyrin methyl ester **2** to carboxylic acid **3**.

After the separation of the mono-substituted porphyrin methyl ester **2**, it was subsequently hydrolyzed under basic condition to yield the corresponding porphyrin

carboxylic acid **3** (Scheme 2-3). Since porphyrin methyl ester **2** does not dissolve in water, THF was used in the hydrolysis step as a co-solvent for better solubility. After the reaction mixture was refluxed overnight, it was acidified with 6 N hydrochloric acid and extracted with CH_2Cl_2. The porphyrins are purple red in basic solutions, and when the solution is acidified, a color change from purple red to green can be clearly observed.

The extraction of porphyrin acid **3** with CH_2Cl_2 is tricky. Before extracting, THF has to be removed. The porphyrin carboxylic acid **3** dissolves much better in THF than in CH_2Cl_2 because of its high polarity. Since THF is partially soluble in water, its presence would make the extraction of porphyrin acid **3** harder. Small amount of methanol needs to be added into CH_2Cl_2 to help the extraction of the porphyrin acid **3**, however, since the porphyrin acid does not dissolve in MeOH, too much methanol will reduce the solubility of porphyrin acid. The optimal ratio of methanol and CH_2Cl_2 for porphyrin acid extraction is about 1:100.

After the extraction of the acidified porphyrin with the mixture of methanol and CH_2Cl_2, the organic layer was neutralized. Instead of using a basic solution, water was used to wash away the acid, since the base was likely to form the carboxylate salt of the porphyrin carboxylic acid **3**. The porphyrin acid **3** separated in this way is pure enough for further reactions.

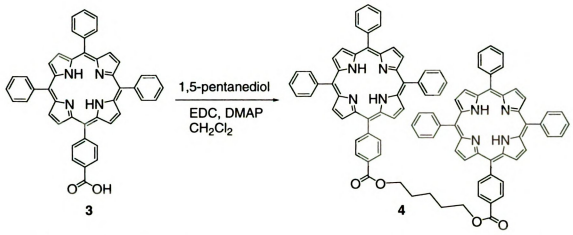

Scheme 2-4. EDC coupling of porphyrin carboxylic acid **3** with 1,5-pentanediol.

After securing porphyrin carboxylic acid **3**, a simple esterification with 1,5-pentanediol, as shown in Scheme 2-4, could provide the porphyrin tweezer **4**. However, the reaction under standard ECD coupling condition did not proceed as expected. TLC analysis indicated the presence of many porphyrin spots with very close polarity, and it was impossible to isolate any pure product by column chromatography. The reaction had been repeated many times and each time the same result was observed. Finally, it was realized that the reaction did not work because the porphyrin carboxylic acid **3** was not pure. It contained both the free-base porphyrin acid and zinc porphyrin acid. Not only could the zinc porphyrin acid interact with the coupling reagent EDC to reduce the yield of the coupling product, but also the presence of both the free-base porphyrin acid and zinc porphyrin acid in the EDC coupling reaction resulted in three porphyrin tweezer products: porphyrin tweezer free base **4**, di-zinc porphyrin tweezer **1** and mono-zinc porphyrin tweezer. The polarities of the three tweezers were very close to each other, and it was impossible to isolate them by column chromatography.

The procedure was altered to remove zinc from the first step of synthesizing porphyrin methyl ester **2**. Zinc acetate was used to aid in the synthesis of porphyrins, and

was to be removed by washing with 6 N hydrochloric acid. In our case, because of the scale of the reaction, not all the zinc was removed from the porphyrin. In order not to introduce zinc, the porphyrin methyl ester **2** was synthesized again by the same propionic acid method but without the addition of zinc acetate. The separated yield of the desired mono-substituted porphyrin methyl ester **2** was 7%, comparable to that of the reactions with the addition of zinc acetate.

After the isolation of the pure porphyrin methyl ester **2**, it was hydrolyzed to porphyrin carboxylic acid **3** as described above. The EDC coupling of porphyrin acid **3** with 1,5-pentanediol proceeded very smoothly, and provided the desired porphyrin tweezer **4** in good yield. Depending on the ratio between the porphyrin acid **3** and 1,5-pentanediol, the synthesis of porphyrin tweezer **4** can be finished in a single step or step-wise, i.e., synthesize the monoester, isolate and submit the product to another round of esterification for yield the diester, or formation of the diester in one pot. The yield of the step-wise synthesis was higher than the single step synthesis.

Excess zinc acetate was then added to the porphyrin tweezer free-base **4** to yield the zinc porphyrin tweezer **1**. The excess zinc acetate could be easily removed by simple filtration. However, even starting with a pure porphyrin tweezer free base **4**, flash column chromatography was required to secure the pure zinc porphyrin tweezer **1** due to the decomposition of porphyrins.

A much milder condition was also used to synthesize porphyrin methyl ester **2**. As shown in Scheme 2-5, the porphyrin was synthesized in CH_2Cl_2 with boron trifluoride diethyl etherate ($BF_3{\cdot}Et_2O$) as the acidic catalyst.[5, 6] Under these conditions, the reaction can be carried out at room temperature instead of refluxing at 160 °C.

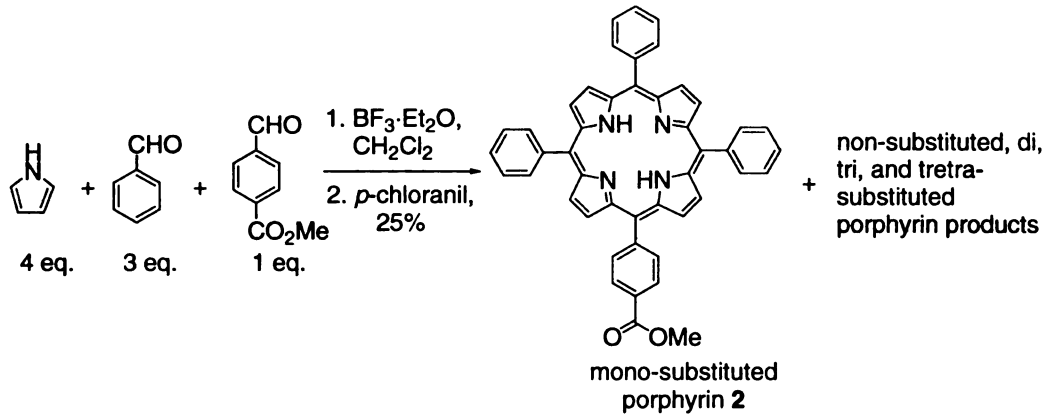

Scheme 2-5. The synthesis of mono-substituted porphyrin **2** in BF_3·Et_2O condition.

Pyrrole, benzaldehyde and 4-carboxymethylbenzaldehyde were dissolved in CH_2Cl_2 at 4:3:1 ratio for the optimal yield of the mono-substituted product. Catalytic amount of BF_3·Et_2O was added into the reaction, and after two-hour stirring at room temperature, *p*-chloranil was added to finish the synthesis. The isolated yield of the desired mono-substituted porphyrin **2** was improves from 7% (propionic acid condition) to 25%.

Using BF_3·Et_2O as the catalyst, one has to be very careful about removing all the air from the reaction. BF_3·Et_2O is very sensitive to moisture, and since only catalytic amount of BF_3·Et_2O is used, small amounts of moisture could derail the reaction. Therefore, the reaction solution was purged with nitrogen for at least 15 minutes before BF_3·Et_2O was added.

2-2. The synthesis of mono-substituted porphyrins on polymers

As shown above, the synthesis of zinc porphyrin tweezer **1** depends heavily on procuring mono-substituted porphyrins efficiently. The synthesis of structurally complex porphyrins has seen tremendous progress in the last 30 years,[7-10] and as such the synthesis of mono-substituted porphyrins methyl ester **2** can be achieved by utilizing many of the

methods that have been developed.[11] However, the most common and direct methodology to synthesize these mono-substituted porphyrins is to condense a mixture of pyrrole, benzaldehyde, and the appropriately substituted benzaldehyde in a 4:3:1 ratio in acidic condition. This leads to the synthesis of the desired mono-substituted porphyrin together with a mixture of tetraphenylporphyrin, and di-, tri-, and tetra-substituted compounds, which makes the chromatographic separation of these compounds tedious and time consuming. In most cases, multiple flash column chromatographies are required to isolate the pure desired porphyrin product.

As Scheme 2-2 and 2-5 shows, propionic acid and $BF_3 \cdot Et_2O$ are two commonly used catalysts for the synthesis of mono-substituted porphyrins.[4, 6] The $BF_3 \cdot Et_2O$ is much milder than using propionic acid and the yield has also been improved, but it still generates the unwanted byproducts. The propionic acid condition yield ratio between the non-, mono-, and di-substituted compounds of 1:3:1, and for the $BF_3 \cdot Et_2O$ condition, the ratio between non-, mono- and di-substituted compounds is 1:2.6:1.3. The generation of porphyrin byproducts not only leads to tedious and time consuming chromatographic separations, but also, depending on the substituted benzaldehyde utilized in the reaction, wasting of this compound by synthesizing undesired porphyrin can be synthetically limiting. In order to simplify the isolation of desired mono-substituted porphyrin and also improve the yield, we have modified the synthesis of mono-substituted porphyrins by using insoluble and soluble polymers.

The method of utilizing insoluble polymer for the synthesis of mono-substituted porphyrins was first developed by Leznoff and Svirskaya.[12] There are several advantages in synthesizing mono-substituted porphyrins on polymer supports.[13] First, it is easy to

separate the polymer-supported species from the small molecules present in the reaction medium by simple filtration. The easy isolation of the polymer bound species in turn allows for the use of excess soluble starting material to achieve higher yields. Second, the size of the polymer renders the resin-bound species inaccessible to each other, and therefore, cross-reactions are avoided. In the porphyrin synthesis, since the substituted aldehyde is anchored onto the polymer, this advantage excludes the formation of di-, tri- and tetra-substituted porphyrins. Finally, the use of polymers in the synthesis of mono-substituted porphyrins eases the purification of the desired product.

In the strategy presented here, the substituted aromatic aldehyde that will eventually become the mono-substituted portion of the final porphyrin is anchored onto a polymeric backbone. This allows for the construction of the porphyrin on the polymeric support with pyrrole and an aldehyde in solution. In this manner free mono-substituted aldehyde is not utilized and thus di, tri, and tetra-substituted porphyrins are not synthesized. Therefore, on the insoluble polymer, there is only mono-substituted porphyrin, and there is only non-substituted porphyrin (tetraphenylporphyrin) in the reaction solution.

2-2.1. Synthesis of mono-substituted porphyrin on insoluble polymer

The synthesis of mono-substituted porphyrin carboxylic acid **3** on insoluble polymer is illustrated in Scheme 2-6. 4-Carboxybenzaldehyde **5** was attached to a 2% crosslinked divinylbezene/polystyrene beads **6**, containing 1 mmole/eq. of benzyl chloride by reported procedures,[14] which results in 85% conversions from the chloride to the attached aldehyde. The conversion was determined by releasing the aldehyde from the polymer support by refluxing in sodium hydroxide. The functionalized polymer

support with the bound aldehyde **7** was used in the synthesis of the mono-substituted porphyrins. Addition of excess of pyrrole and benzaldehyde to the polymer **7** in refluxing propionic acid followed by DDQ oxidation yielded the mono-substituted product **8** on the resin and only tetraphenylporphyrin (TPP) in the solution phase. Since benzaldehyde and pyrrole are inexpensive reagents, the sacrifice in making tetraphenylporphyrin in solution was well compensated by the fact that only the mono-substituted porphyrin was synthesized on the polymer.

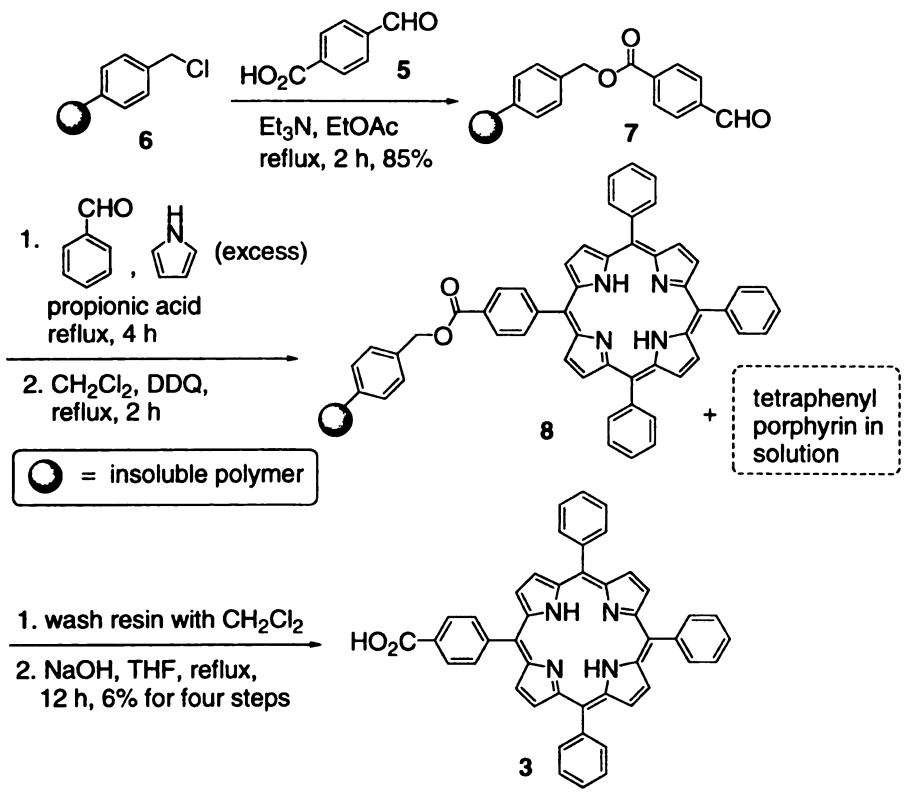

Scheme 2-6. Synthesis of mono-substituted porphyrins on insoluble polymer.

The tetraphenylporphyrin generated in solution could be easily removed from the polymer-supported porphyrins by washing the polymer resin with CH_2Cl_2 (Soxhlet extraction). Cleavage of the covalently attached porphyrin from the beads in refluxing aqueous NaOH solution led to the isolation of the desired porphyrin carboxylic acid **3** in

good purity and 6% overall yield. The yield is comparable to solution phase synthesis of **3** in refluxing propionic acid,[4] however, the crude isolation is not complicated with mixtures of multi-substituted porphyrins, and thus the purification proves to be straightforward from the polymer beads.

The porphyrin synthesis on insoluble polymer had also been tried by using $BF_3 \cdot Et_2O$ as the acidic catalyst instead. Unfortunately, it was found that $BF_3 \cdot Et_2O$ was not compatible with the insoluble polymer, since not only there was no porphyrin carboxylic acid isolated, but also there was no tetraphenylporphyrin (TPP) forming in the solution. The lack of the tetraphenylporphyrin generation in the reaction indicated that the $BF_3 \cdot Et_2O$ failed to serves as the acidic catalyst to generate porphyrins. This reaction was repeated several times, and every time the result was the same. So the porphyrin synthesis on insoluble polymer can only be carried out in refluxing propionic acid condition.

2-2.2. Synthesis of mono-substituted porphyrin with soluble polymer

Limitations in the use of solid polymers in synthetic chemistry are pronounced by the difficulty in using NMR to characterize intermediates, and the heterogeneous nature of the chemistry that could result in low yields. However, soluble polymers can be used as an alternative matrix for organic synthesis.[15] These polymers are non-cross-linked long chains, and exhibit both soluble and insoluble characteristics depending on the solvent used in the reaction. Synthetic approaches that utilize soluble polymers couple the advantages of homogeneous solution chemistry (high reactivity, lack of diffusion phenomena and ease of analysis) with those of solid phase methods (use of excess reagents and easy isolation and purification of products).[16]

Non-cross-linked chloromethylate polystyrene (NCPS) polymer is a soluble polymer used in the porphyrin synthesis.[17] This copolymer is readily prepared, and the functional group content easily controlled and quantified via NMR by varying ratios of starting monomers. NCPS polymer has remarkable solubility properties that are amenable to organic chemistry. It is soluble in THF, CH_2Cl_2, $CHCl_3$, and ethyl acetate even at low temperatures, and is insoluble in water and alcohols. Consequently, after the homogeneous reaction of supported intermediates, the polymer and its uniquely bound product can be easily separated from excess reactants and byproducts by treating with cold methanol, in which the soluble polymer precipitates as a solid polymer, and the soluble reagents and byproducts are filtered away. Because the polymer is soluble in $CHCl_3$, NMR analysis of all intermediates may be accomplished in a non-destructive manner without the need for any specialized NMR techniques.[18] All the reaction with the soluble polymer can be monitored with NMR, and the porphyrin peaks are observable in NMR spectrum.

As illustrated in Scheme 2-7, the non-cross-linked chloromethylate polystyrene (NCPS, **9**) was prepared as reported by Janda and coworkers by the copolymerization of styrene with 3 mol% of 4-(chloromethyl) styrene in the presence of 2, 2'-azobis(isobutyronitrile) (AIBN) in benzene at 70 °C for 40 h.[17] After the reaction was over, most of the solvent was removed under reduced pressure, and the residue was added to chilled methanol (-30 °C). The soluble polymer precipitated in the methanol as a white powder, which could be separated from the remaining starting material by suction filtration.

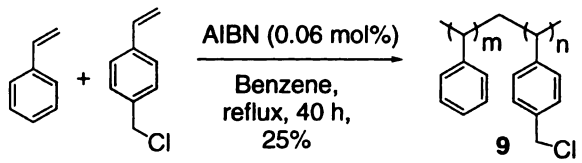

Scheme 2-7. Copolymerization to synthesize NCPS polymer.

Having the correct particle size for the precipitated polymer is important for successful and efficient suction filtration. If the polymer size is too small, the polymer is likely to go through the filter paper, which can clog the funnel and make the filtration take several hours to finish. The size of the polymer powder depends on both the amount of solvent it is dissolved in before it is precipitated with cold methanol (the larger amount of solvent used, the finer the powder is), and more importantly, on the average molecular weight of the polymer itself. The molecular weight of the soluble polymer is controlled by the amount of radical initiator (AIBN) used in the copolymerization reaction. The smaller amount of initiator, the higher average molecular weight, but at the same time, the yield of the copolymer decreases. When 0.5 mol% of AIBN was used, the MW_{avg} of the copolymer isolated was 15,000, and the yield was 50%. The filtration of this polymer was tedious. By decreasing the initiator to 0.06 mol%, the MW_{avg} of the polymer increased to 60,000 and a PDI of 2.14 was measured by GPC.[19] The yield of polymerization was 25%.

Table 2-1. Synthesis of soluble polymer supported aldehyde **10**

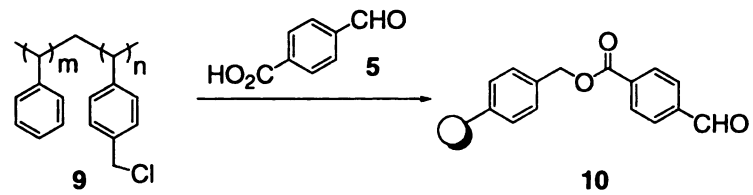

Base	Solvent	Temp (°C)	Period (day)	Yield (%)
NaH	DMF	90	1	---
KH	DMF	90	1	80
NaHMDS	THF	66	2	---
i-Pr_2NEt	EtOAc	77	5	25
Et_3N	EtOAc	77	2	60
Et_3N	EtOAc	90 (sealed tube)	3	>95

A variety of conditions had been probed to attach 4-carboxybenzaldehyde **5** to the soluble polymer **9**, and the results are outlined in Table 2-1. The best result was obtained by using triethylamine as the base and heating the reaction mixture in ethyl acetate to 90 °C in a sealed tube. The loading of the aryl aldehyde in **10** was calculated from NMR integrations of the latter moiety vs. the polymer backbone signals. The conversion was higher than 95%.

The synthesis of mono-substituted porphyrin on soluble polymer **10** is shown in Scheme 2-8. Boron trifluoride diethyl etherate ($BF_3 \cdot Et_2O$) was used as the acidic catalyst in the porphyrin synthesis on soluble polymer, since this condition was much milder and the yield was higher. The results were quite satisfactory; thus the synthesis was not attempted with propionic acid condition.

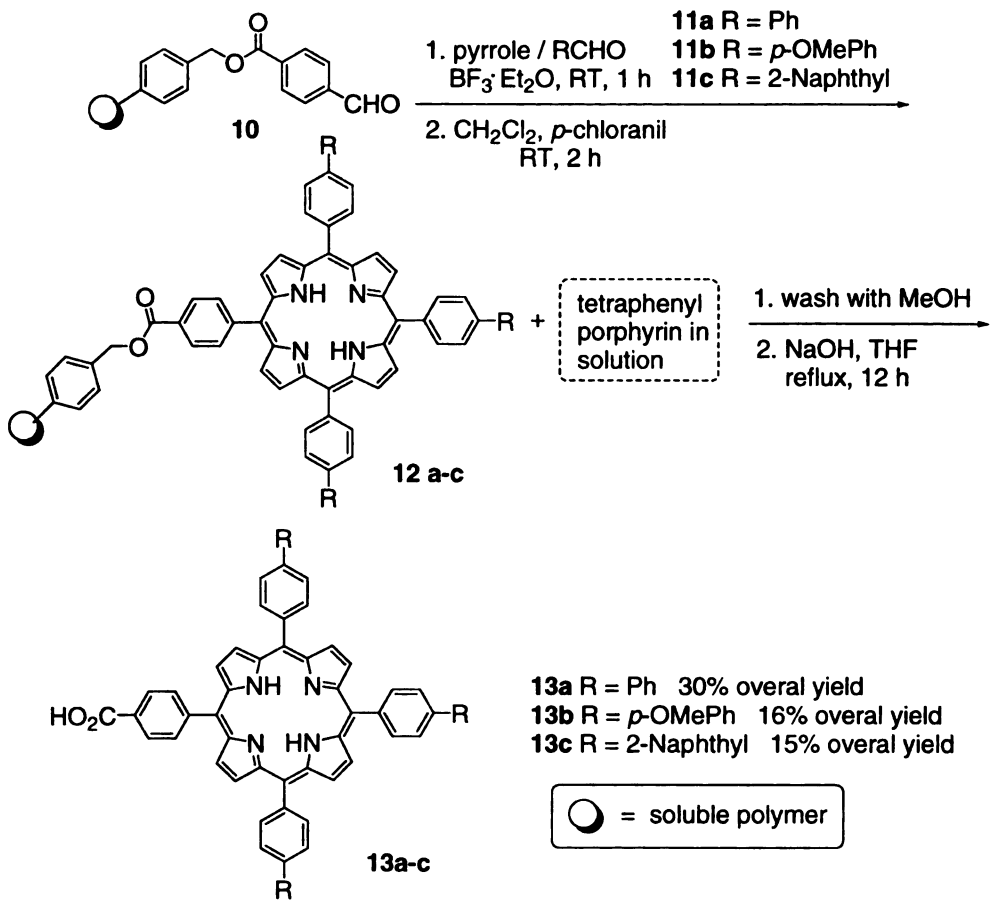

Scheme 2-8. Synthesis of mono-substituted porphyrin on soluble polymer.

Condensation of polymer supported aldehyde **10** and pyrrole with excess of either benzaldehyde **11a**, *p*-methoxybenzaldehyde **11b**, or 2-naphthylaldehyde **11c** with $BF_3 \cdot Et_2O$ in CH_2Cl_2 (similar to reported procedures for normal porphyrin synthesis in solution[6]) and subsequent oxidation with *p*-chloranil led to the formation of the corresponding soluble polymer bound porphyrins **12a-c**. The product in each case was isolated and by basic hydrolysis of the ester functionality (2 N NaOH) to yield the porphyrin acids **13a-c** in yields comparable to solution phase synthesis. However, in comparison to non-polymer supported solution phase synthesis, the purity of the crude product is substantially improved, and each product is easily purified by a simple silica

chromatography. The yield of each porphyrin was calculated based on the amount of bound aldehyde **10** used in the reaction. The mono-substituted porphyrin acids were purified by silica column chromatography and eluted with 3% methanol in CH_2Cl_2. Non-aromatic aldehydes such as *i*-butyl aldehyde, propanal, and acetaldehyde did not yield any product, presumably due to the polymerization of these reagents under the reaction conditions.

In conclusion, synthesis of porphyrins on polymeric backbone can be used as a strategy to selectively synthesize mono-substituted porphyrins without the troublesome contamination from multiple-substituted products.

Experimental materials and general procedures:

Anhydrous CH_2Cl_2 was dried over CaH_2 and distilled. Unless otherwise noted, materials were obtained from commercial suppliers and were used without further purification. All reactions were performed in dried glassware under nitrogen. Column chromatography was performed using SiliCycle silica gel (230-400 mesh). ^{1}H-NMR spectra were obtained on Varian Inova 300 MHz instrument and are reported in parts per million (ppm) relative to the solvent resonances (δ), with coupling constants (J) in Hertz (Hz).

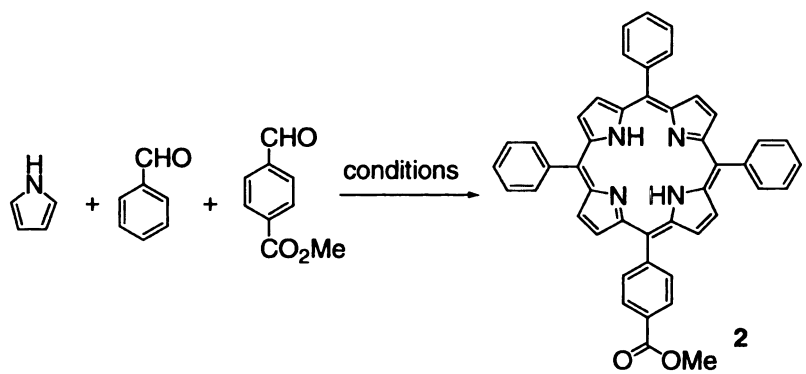

5-(4-Methylcarboxy-phenyl)-10,15,20-triphenylporphyrin 2:

Method 1. To a mixture of 4-carboxymethylbenzaldehyde (0.83 g, 5 mmol), benzaldehyde (1.62 g, 15 mmol, and $Zn(OAc)_2$ (1.09 g, 5 mmol) in propionic acid (100 mL) was added pyrrole (1.32 g, 20 mmol) when the temperature reached 120 °C. The solution was refluxed for 4 h with vigorous stirring. The solvent was removed under reduced pressure, and the dark solid residue was dissolved in CH_2Cl_2, and excess amount of DDQ (0.42 g) was added to the solution. The mixture was refluxed for another 2 h. The mixture was then cooled to room temperature, and the solution was washed with 6 N HCl (3 × 40 mL), neutralized with saturated $NaHCO_3$ aqueous solution (3 × 40 mL), followed by brine (1 × 50 mL), and dried with anhydrous Na_2SO_4. The solvent was

removed under reduced pressure. Product was purified by multiple column chromatographies (CH_2Cl_2) to yield pure **2** (0.26 g, 7%) as deep purple crystals.

Method 2. To a mixture of 4-carboxymethylbenzaldehyde (0.83 g, 5 mmol) and benzaldehyde (1.62 g, 15 mmol) in propionic acid (100 mL) was added pyrrole (1.32 g, 20 mmol) when the temperature reached 120 °C. The solution was refluxed for 4 h with vigorous stirring. The solvent was removed under reduced pressure, and the dark solid residue was dissolved in CH_2Cl_2, and excess amount of DDQ (0.42 g) was added to the solution. The mixture was refluxed for another 2 h. The solution was then cooled to room temperature, and the solvent was removed under reduced pressure. Purification by multiple column chromatographies (CH_2Cl_2) yielded pure **2** (0.24 g, 7%) as deep purple crystals.

Method 3. To a mixture of 4-carboxymethylbenzaldehyde (0.83 g, 5 mmol) and benzaldehyde (1.62 g, 15 mmol) in freshly distilled CH_2Cl_2 (100 mL) was added pyrrole (1.32 g, 20 mmol). Nitrogen gas was purged into the solution with vigorous stirring, and after 15 min catalytic amount of $BF_3 \cdot Et_2O$ (0.1 mL) was added. After 10 min, the solution turned from colorless to amber. The reaction flask was shielded from light by aluminum foil, and the reaction was stirred at room temperature for another 2 h. Excess amount of *p*-chloranil (3 g) was added to the solution, and it was stirred for an additional 2 h. The solvent was then removed under reduced pressure, and the residue was purified as described above to yield pure **2** (0.81 g, 25%). ^{1}H NMR ($CDCl_3$, 300 MHz) δ 8.76-8.85 (m, 8H), 8.42 (d, *J*=8.3 Hz, 2H), 8.29 (d, *J*=8.3 Hz, 2H), 8.19-8.21 (m, 6H), 7.71-7.79 (m, 9H), 4.09 (s, 3H), -2.81 (s, 2H).

2 3

5-(4-Carboxyphenyl)-10,15,20-triphenylporphyrin 3:

To the solution of **2** (75 mg, 0.1 mmol) in THF (5 mL) was added 2 N NaOH aqueous solution (1.5 mL), and the solution was refluxed overnight. After the reaction was cooled down to room temperature, the pH of the reaction solution was adjusted to 4 with 6 N HCl. THF was removed under reduced pressure, and the aqueous layer was extracted with MeOH/CH_2Cl_2 (1:100, 3 × 20 mL) until there was no purple color left in the aqueous layer. The organic layers were combined and washed with DI water (2 × 20 mL). The organic layer was then dried with anhydrous Na_2SO_4, and removed under reduced pressure to afford the acid **3** in 98% yield. ^{1}H NMR ($CDCl_3$, 300 MHz) δ 8.76-8.85 (m, 8H), 8.42 (d, *J*=8.3 Hz, 2H), 8.29 (d, *J*=8.3 Hz, 2H), 8.19-8.21 (m, 6H), 7.71-7.79 (m, 9H), -2.81 (s, 2H).

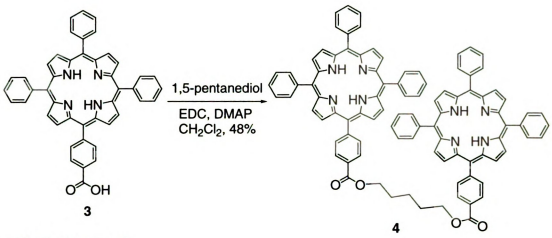

Porphyrin tweezer 4:

To a solution of acid **3** (90 mg, 0.14 mmol) and 1,5-pentanediol (5 mg, 0.05 mmol) in anhydrous CH_2Cl_2 (4 mL) was added EDC (27 mg, 0.14 mmol) and DMAP (18 mg, 0.14 mmol). The reaction mixture was stirred at room temperature overnight, and it was applied directly to silica gel column and purified (CH_2Cl_2) to afford the title compound 4 (34 mg, 48%). ^{1}H NMR ($CDCl_3$, 300 MHz) δ 8.94-9.04 (m, 16H), 8.48 (d, *J*=8.0 Hz, 4H), 8.17-8.23 (m, 16H), 7.46-7.54 (m, 18H), 4.28 (t, *J*=6. 6 Hz, 4H), 1.65 (m, 4H), 1.48 (m, 2H), -2.81 (s, 2H).

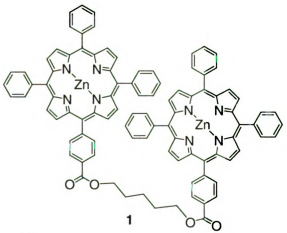

Zinc porphyrin tweezer 1:

To a solution of porphyrin tweezer free base **4** (10 mg) in CH_2Cl_2 (3 mL) was added $Zn(OAc)_2$ (30 mg, 0.16 mmol). The reaction mixture was stirred at room

temperature overnight. The solution was applied directly to silica gel column (CH_2Cl_2) to afford the pure zinc porphyrin tweezer **1** (96 mg, 95%) as a deep purple powder. ^1H NMR ($CDCl_3$, 300 MHz) δ 8.94-9.04 (m, 16H), 8.48 (d, *J*=8.0 Hz, 4H), 8.17-8.23 (m, 16H), 7.46-7.54 (m, 18H), 4.28 (t, *J*=6. 6 Hz, 4H), 1.65 (m, 4H), 1.48 (m, 2H).

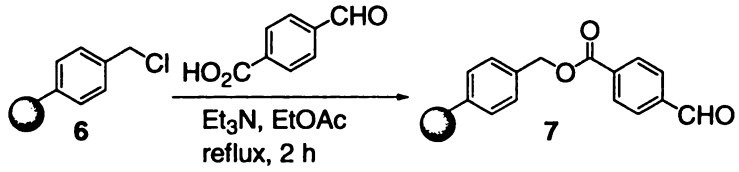

Insoluble polymer anchored substituted aldehyde 7:

2% cross-linked divinylbenzene/polystyrene beads **6** (3 g), containing 1 mmole/eq. of benzyl chloride, 4-carboxybenzaldehyde (0.9 g, 6 mmol) and Et_3N (1 mL) were added to EtOAc (20 mL), and the reaction mixture was refluxed for 2 h. The reaction was then cooled down, and the polymer was washed with ethyl acetate, benzene, water and acetone, and then dried under vacuum. Since the polymer does not dissolve in any solvent, the conversion could not be monitored with NMR.

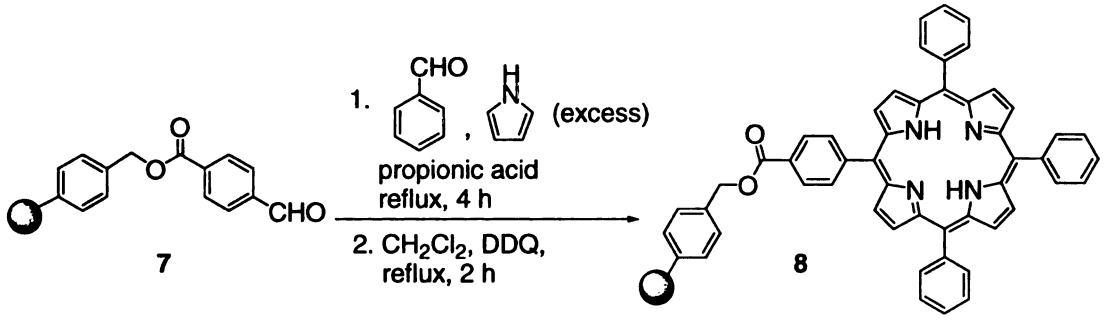

Insoluble polymer supported porphyrin 8:

Polymer anchored aldehyde **7** (0.5 g, 0.29 mmol), benzaldehyde (190 mg, 1.8 mmol) and pyrrole (155 mg, 2.3 mmol) were added into propionic acid (20 mL), and the mixture was refluxed for 4 h. The solvent was removed under reduced pressure, and the dark solid residue was dissolved in CH_2Cl_2, and excess amount of DDQ (0.42 g) was

added to the solution. The mixture was refluxed for another 2 h. The mixture was then cooled to room temperature, and the polymer supported porphyrin was separated from non-substituted porphyrin (tetraphenylporphyrin) by Soxhlet extraction with CH_2Cl_2 as solvent.

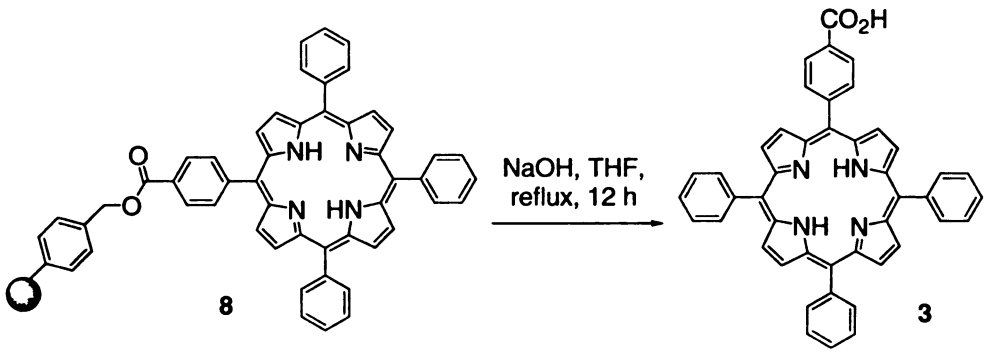

8 3

Hydrolysis of insoluble polymer supported porphyrin 8 to acid 3:

To the solution of polymer supported porphyrin **8** (0.5 g) in THF (5 mL) was added 2 N NaOH (1.5 mL), and the solution was refluxed overnight. After cooling the solution to room temperature, the polymer was filtered, and washed with THF until all the purple color was removed. The pH of the filtrate was adjusted to 4 with 6 N HCl. The THF was removed under reduced pressure, and the aqueous layer was extracted with MeOH/CH_2Cl_2 (1:100, 3 × 20 mL) until there was no purple color left in the aqueous layer. The organic layers were combined and washed with DI water (2 × 20 mL). The organic layer was then dried with anhydrous Na_2SO_4, and removed under reduced pressure to afford the acid **3**. The yield for the two steps, from **7** to **3**, was 6%.

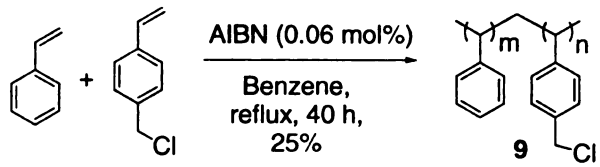

Synthesis of soluble polymer NCPS 9:

Styrene with 3 mol% of 4-(chloromethyl)styrene were dissolved in benzene. 2, 2'-azobis(isobutyronitrile) (AIBN) was added into the reaction mixture, and it was stirred at 70 °C for 40 h. The solvent was removed under reduced pressure to yield an oil like residue, and it was then added to cold methanol (-30 °C) dropwise with vigorous stirring to remove the unreacted styrene and 4-(chloromethyl)styrene. The oil like residue became white powder as soon as cold methanol was added. The precipitate was filtered, and redissolved with benzene and re-precipitated in cold methanol again. This cycle was repeated three times until no styrene and 4-(chloromethyl)styrene could be observed by NMR.

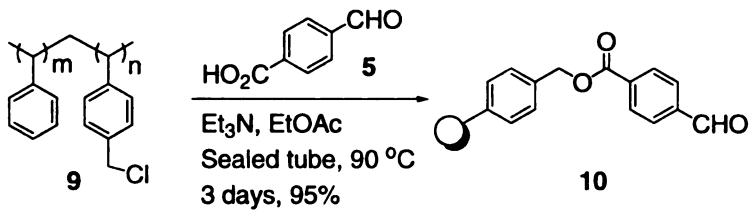

Soluble polymer supported benzaldehyde aldehyde 10

Soluble polymer NCPS **9** (2 g), 4-carboxybenzaldehyde (0.9 g, 6 mmol) and Et_3N (1 mL) were added to EtOAc (20 mL). The reaction mixture was refluxed for 3 days. The reaction was then cooled down, and the solvent was removed by reducing pressure. The oil like residue became white powder as soon as it was added to cold methanol. The precipitate was filtered, and redissolved with acetyl acetate to precipitated in cold

methanol again. This cycle was repeated until all the 4-carboxybenzaldehyde was removed.

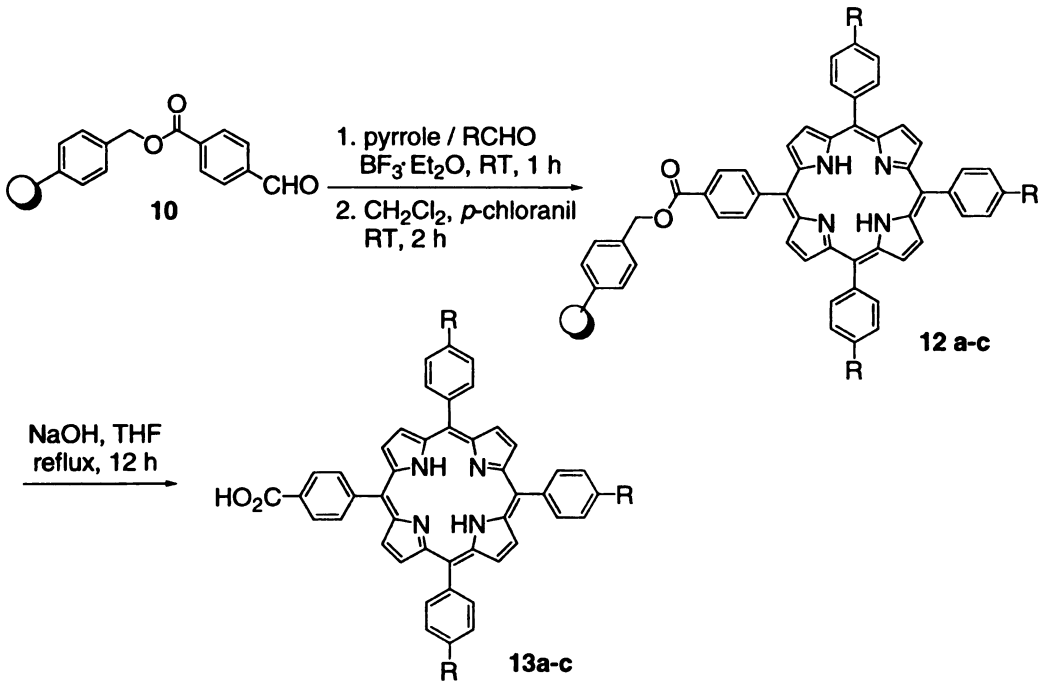

The general procedure for syntheses of mono-substituted porphyrins 13a-13c on soluble polymer:

To a mixture of the soluble polymer supported benzaldehyde aldehyde **10** (1 g) and aldehyde (15 mmol) in freshly distilled CH_2Cl_2 (30 mL) was added pyrrole (1.32 g, 20 mmol). Nitrogen gas was purged into the solution with vigorous stirring, and after 15 min, catalytic amount of $BF_3{\cdot}Et_2O$ (0.1 mL) was added. After 10 min, the solution turned from colorless to amber. The reaction flask was shielded from light by aluminum foil, and the reaction was stirred at room temperature for another 1 h. Excess amount of *p*-chloranil (3 g) was added to the solution, and it was stirred for additional 2 h. Then the reaction mixture was condensed and the residue was precipitated in cold methanol to remove the tetraphenylporphyrin.

To the solution of polymer supported porphyrin **12a-c** (0.6 g) in THF (10 mL) was added 2 N NaOH aqueous solution (5 mL), and the solution was refluxed overnight. After cooled down to room temperature, the pH of the mixture was adjusted to 4 with 6 N HCl solution. The THF was removed by reduced pressure, and the aqueous layer was extracted with MeOH/CH_2Cl_2 (1:100, 3 × 20 mL) until there was no purple color left in the aqueous layer. The organic layer was combined and condensed by reducing pressure. The residue was dissolved in CH_2Cl_2 (5 mL), and precipitated in cold methanol/THF (10:1). This cycle was repeated three times, and all the organic solvents were combined. The solvents were removed under reduced pressure, and the residue was purified by column chromatography (3% MeOH in CH_2Cl_2) to afford the pure porphyrin acids **13a-c**.

Reference:

1. Ogoshi, H.; Mizutani, T. *Acc. Chem. Res.* **1998**, *31*, 81.

2. Berova, N.; Nakanishi, K.; Woody, R. W. *Circular Dichroism: Principles and Applications*; Wiley-VCH: New York, **2000**.

3. Matile, S.; Berova, N.; Nakanishi, K.; Fleischhuer, J.; Woody, R. W. *J. Am. Chem. Soc.* **1996**, *118*, 5198.

4. Huang, X. F.; Rickman, B. H.; Borhan, B.; Berova, N.; Nakanishi, K. *J. Am. Chem. Soc.* **1998**, *120*, 6185.

5. Littler, B. J.; Miller, M. A.; Hung, C. -H.; Lindsey, J. S. *J. Org. Chem.* **1999**, *64*, 1391.

6. Lindsey, J. S.; Schreiman, I. C.; Hsu, H. C.; Kearney, P. C.; Marguerettaz, A. M. *J. Org. Chem.* **1987**, *52*, 827.

7. Smith, K. M. *Porphyrins and Metalloporphyrins*; Elsevier Scientific Pub. Co.: New York, **1975**.

8. Lavallee, D. K. *The Chemistry and Biochemistry of N-Substituted Porphyrins*; VCH Publishers: New York, **1987**.

9. Kadish, K. M.; Smith, K. M.; Guilard, R. *Synthesis and Organic Chemistry*; Academic Press: San Diego, CA, **2000**.

10. Dolphin, D. *The Porphyrins: Structure and Synthesis*; Academic Press: New York, **1979**.

11. Lindsey, J. S., Synthesis of *meso*-Substituted Porphyrins. In *The Porphyrin Handbook*; Kadish, K. M., Smith, K. M., Guilard, R., Eds.; Academic Press: San Diego, CA, **2000**.

12. Leznoff, C. C.; Svirskaya, P. I. *Angew. Chem. Int. Ed. Engl.* **1978**, *17*, 947.

13. Lorsbach, B. A.; Kurth, M. J. *Chem. Rev.* **1999**, *99*, 1549.

14. Merrifield, R. B. *J. Am. Chem. Soc.* **1963**, *85*, 2149.

15. Gravert, D. J.; Janda, K. D. *Chem. Rev.* **1997**, *97*, 489.

16. Wentworth, P.; Janda, K. D. *Chem. Commun.* **1999**, 1917.

17. Chen, S. Q.; Janda, K. D. *J. Am. Chem. Soc.* **1997**, *119*, 11355.

18. Fitch, W. L.; Detre, G.; Holmes, C. P.; Keifer, P. A. *J. Org. Chem.* **1994**, *59*, 7955.

19. Yin, M.; Baker, G. L. *Macromol.* **1999**, *32*, 7711.

Chapter 3

Absolute stereochemical determination of α-chiral carboxylic acids

Developing methodologies that can be used to determine the absolute stereochemistry of chiral compounds is the goal of our research. Our approach entails designing and synthesizing chromophoric receptors, which can bind to the chiral compounds and adopt a helicity through an induced chirality. The host-guest interactions between the chiral compounds and the receptors can be observed by CD. In particular, the Exciton Coupling Circular Dichroic (ECCD) method[1] will be used to assign the stereochemistry of the asymmetric center non-empirically.

According to the number of sites of attachment the chiral molecules possess, the chiral compounds can be divided into two categories:

- Chiral compounds with two sites of attachment: Porphyrin tweezer has been designed to serve as the receptor, which can interact with the binding molecule and adopt a chiral conformation as a result of induced chirality.[2]
- Chiral compounds with only one site of attachment: The stereochemistry of these compounds is more difficult to determine as compared to the ones with two sites of attachment. Porphyrin tweezer method cannot be applied directly to these compounds since the two porphyrin groups cannot be oriented relative to each other when there is only one attachment instead of two. To overcome this problem, "carrier" molecules have been designed, which upon derivatization with chiral molecules, provide two sites of attachment.[3]

As has been discussed in detail (see Section 1-3.2), the carrier method has been successfully applied to chiral monoamines to determine their absolute stereochemistry,

by using carrier molecule **1** and zinc porphyrin tweezer **2** (Figure 3-1).[3] Now, we are interested in exploring the possibility of extending the same methodology to chiral compounds with other functional groups, especially α-chiral carboxylic acids.

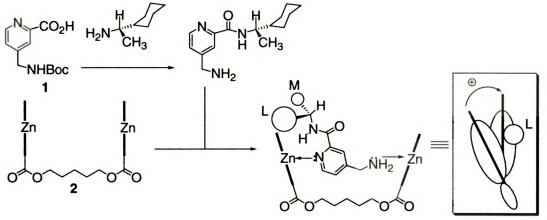

Figure 3-1. Stereochemical determination of chiral monoamine with carrier **1**.

The most widely employed approach for absolute stereochemical assignment of α-chiral carboxylic acids is NMR, by using Mosher's method and its modified versions.[4-7] According to this protocol the chiral carboxylic acids are derivatized to either amides or esters by using both the (*R*)- and (*S*)-enantiomers of a chiral auxiliary reagent. This auxiliary, such as 9-AHA (9-anthrylhydroxyacetic acid ethyl ester), usually contains an aryl ring that directs its anisotropic cone selectively towards one of the substituents of the asymmetric center of the chiral acid. The chemical shifts observed for each of the groups of the chiral acid (L_1, L_2 in Figure 3-1) reflect their spatial relationship with respect to the aryl ring. Therefore, the absolute configuration of the chiral center can be obtained from the difference in the chemical shifts ($\Delta\delta^{RS}$) measured (Figure 3-2).[8] Some of the commonly used chiral auxiliary reagents are shown in Figure 3-3.[4-7]

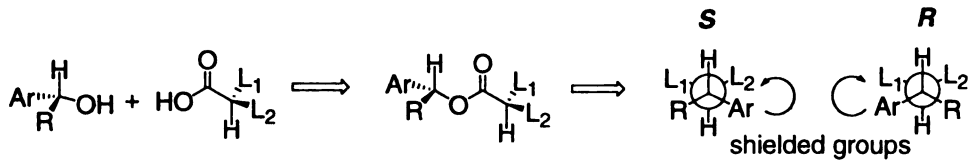

Figure 3-2. The absolute stereochemical assignment of α-chiral carboxylic acids by NMR.

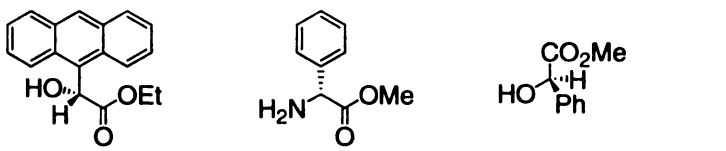

Figure 3-3. Chiral auxiliary reagents.

When using auxiliary reagents for the stereochemical determination of α-chiral carboxylic acids, the conformation of the chiral conjugate has to be well understood. Figure 3-4 is an example of using PGME (phenylglycine methyl ester) as the auxiliary reagent.[5, 6] In order for the phenyl group to exert its diamagnetic field effect upon L_1 and L_2, coplanarity of C1 to C5 is necessary. Coplanarity of the atoms from position 1 to 4 is guaranteed due to the *s-trans* amide linkage, which is well established in peptide chemistry.[9] The planarity can be extended to the methoxycarbonyl group at 5-position, because of the electrostatic repulsion between carbonyl groups at 2- and 5-position, which has been verified by X-ray crystallography and NOE studies.[5]

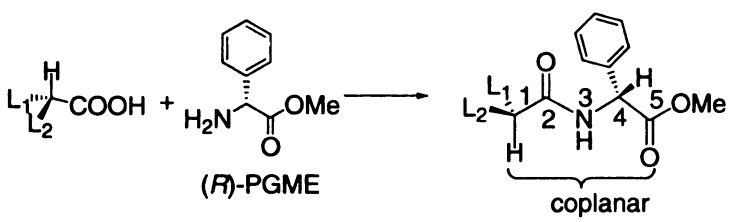

Figure 3-4. The derivatization of PGME with chiral acids.

However, very few of the chiral auxiliary reagents have been subject to detailed theoretical or experimental studies.[10] From a practical point of view, selecting the most suitable reagent for a certain substrate is still problematic, and sometimes, the signals in the NMR spectra of the diastereoisomeric derivatives can be too close for drawing any safe conclusion.

Another approach for the absolute stereochemical determination of α-chiral carboxylic acids is by using circular dichroism (CD), in particular, the exciton coupled circular dichroism (ECCD).[11] Although the ECCD method has been applied to several classes of molecules to determine their absolute stereochemistry, in the case of chiral carboxylic acids, it can only be applied to α-hydroxy carboxylic acids with free hydroxyl group[12, 13] or chiral acids carrying an additional chromophore in the molecule. Figure 3-5 is an example of applying the ECCD method for the absolute stereochemical determination of α-hydroxy carboxylic acids.

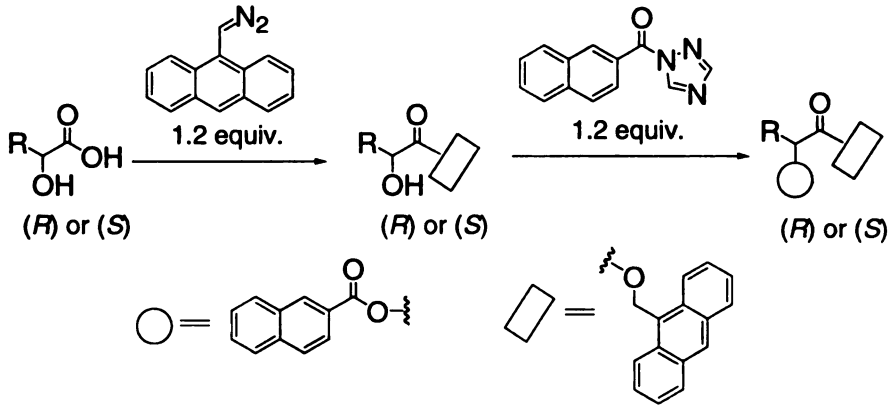

Figure 3-5. Two-step derivatization of α-hydroxy carboxylic acids.

After a two-step derivatization with 9-anthryldiazomethane and 2-naphthoyltriazole, the α-hydroxy carboxylic acid can be converted to a bichromophoric system.[14] The absolute stereochemistry of the chiral center determines the orientation of

the two chromophores in space, which in turn dictates the observed ECCD spectrum. All the (*R*) acids exhibit positive ECCD, while (*S*) acids exhibit negative ECCD.[13]

However, in cases where the substrate has no site other than the carboxyl group for derivatization, application of the ECCD protocol is not straightforward. The 210 nm n-π* transition of the carboxyl chromophore has been used in the past for configurational assignment of the carboxylates.[15] As structures shown in Figure 3-6, the CD of a series of 1-carboxyethyl substituted monosaccharides have been measured, and the results indicated that the absolute stereochemistry of the 1-carboxyethyl substituents can be correlated to the sign of the CD for the carboxyl chromophore with absorption at 210 nm, with (*R*) carboxylates having negative CD, while (*S*) carboxylates exhibit positive CD.[15, 16] The absorption bands are weak, and this empirical method can only be applied to 1-carboxylethyl substituted hexoses.

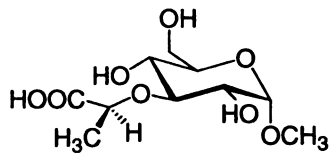

Figure 3-6. The structure of 1-carboxyethyl substituted monosaccharides.

We are interested in developing a general protocol for the non-empirical determination of the absolute stereochemistry of α-chiral carboxylic acids. In order to achieve this goal, we are relying heavily on the Exciton Coupling Circular Dichroic (ECCD)[1] method by using different carriers in conjunction with porphyrin tweezer. Nearly at the same time, Nakanishi's lab has also developed with a very similar methodology in determining the absolute stereochemistry of α-chiral carboxylic acids.[17, 18] Their system will be discussed later in this chapter.

3-1. Stereochemical determination of α-chiral carboxylic acids with carrier A

Carrier **1** has been used by Nakanishi and his coworkers to determine the absolute stereochemistry of chiral monoamines.[3] It contains a carboxylic acid functionality to derivatize with chiral amines, and the resulting chiral conjugate provides two nitrogen binding sites to coordinate with zinc porphyrin tweezer **2**. We are interested in stereochemical determination of α-chiral carboxylic acids, thus it is reasonable to design a carrier **A** with similar structure to that of carrier **1**, but having changed the carboxylic acid functionality in carrier **1** to an amino group, so it can form derivatives with carboxylic acids (Figure 3-7).

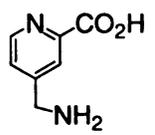

carrier **1** for chiral monoamines

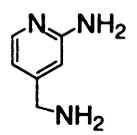

carrier **A** for α-chiral carboxylic acids

Figure 3-7. The structures of carrier **1** and carrier **A**.

The synthesis of Boc-protected carrier **Boc-A** is shown in Scheme 3-1. The synthesis is straightforward, starting with the commercially available 4-aminomethylpyridine **3**. The free amino group in **3** was protected with the Boc protecting group, and the pyridine nitrogen of compound **4** was oxidized by *m*CPBA to form pyridine oxide **5**. The cyano functionality was introduced at the *ortho* position by treating the pyridine oxide **5** with TMSCN and dimethylcarbamyl chloride in CH_2Cl_2 at room temperature for two days. The cyano group was then hydrolyzed to amide **6** by refluxing in KOH/*t*-BuOH mixture for half an hour.[19] Finally, the amide functionality in compound **7** was converted to the amino group via Hofmann rearrangement to form the desired Boc-protected carrier **Boc-A**. Two reaction conditions were tested for the

Hofmann rearrangement. First was heating the amide **7** with bromine in a solution of sodium methoxide and methanol, however, no conversion was observed. Second method entailed heating the amide **7** with bromine and aqueous sodium hydroxide solution. The second reaction condition worked smoothly and provided the desired amine **Boc-A** in 75% yield.

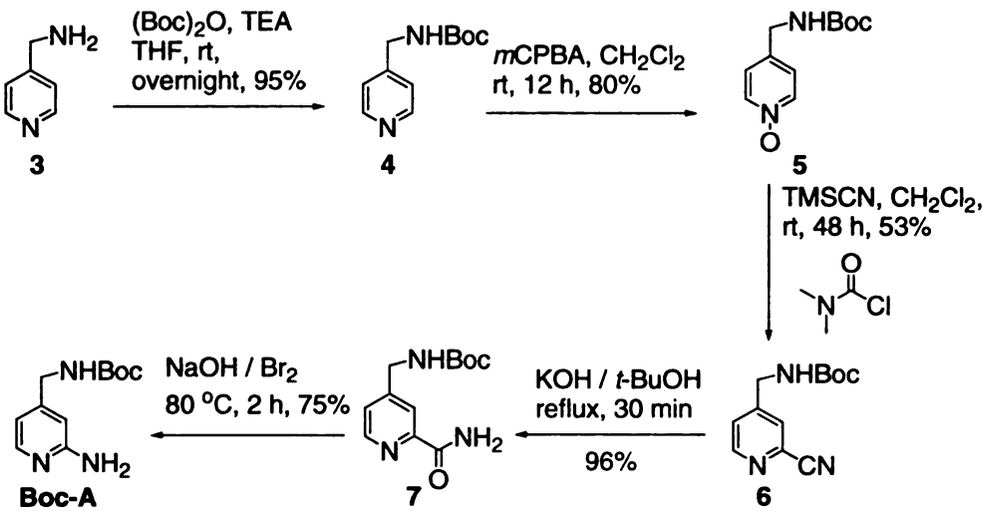

Scheme 3-1. The synthesis of Boc-protected carrier **A**.

The protected carrier **Boc-A** was then coupled with chiral carboxylic acids by BOP coupling to generate the chiral conjugates.[20] This amide formation reaction was also examined by using EDC as the coupling reagent; however, EDC did not lead to high yield of the desired amide. After the formation of the chiral conjugate, the Boc group was removed by stirring in a mixture of trifluoroacetic acid and CH_2Cl_2 to provide the final chiral complex, which was ready for CD analysis.

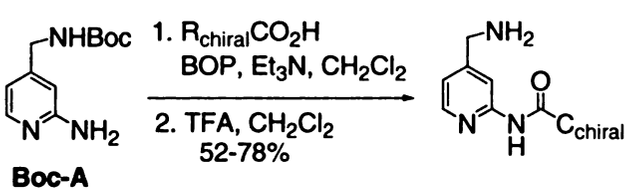

Scheme 3-2. The synthesis of chiral complexes from **Boc-A**.

Compared to carrier **1** derivatized chiral monoamines, the carrier **A** derivatized α-chiral carboxylic acid complexes are not as rigid in structure. As shown in Figure 3-8, when carrier **1** is derivatized with a chiral monoamine, the resulting chiral complex is very rigid. There is no free rotation around the C_{Ar}-$C_{C=O}$, $C_{C=O}$-NH, and NH-C_{chiral} bonds, since all the free rotations around the single bonds are restricted: the *anti* pyridine nitrogen/carbonyl oxygen disposition is preferred by 30 kJ/mol, due to electrostatic repulsion, and the small group (hydrogen) at the chiral center is *syn* to the carbonyl oxygen because of pseudo $A_{1,3}$ steric interaction.

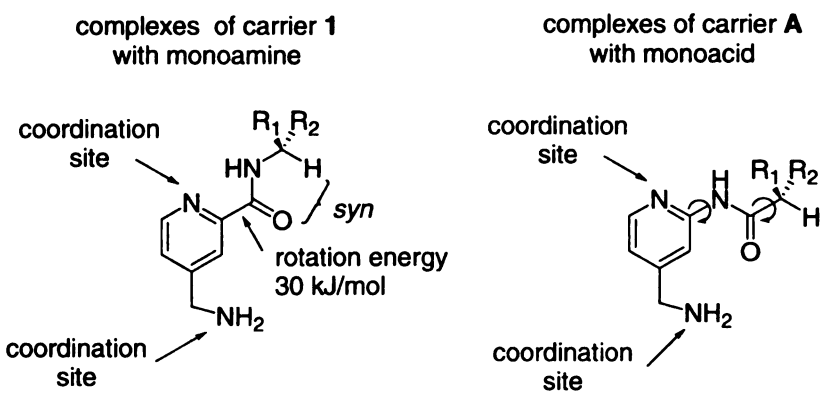

Figure 3-8. Comparison of chiral complexes of carrier **1** and carrier **A**: carrier **1** complexes are locked in a conformation, while carrier **A** complexes are not so rigid.

However, the complexes formed by carrier **A** with mono-carboxylic acid are not as rigid. The orientation of the pyridine nitrogen with respect to the carbonyl oxygen is not as certain, since the carbonyl is not directly attached to the pyridine ring and the electrostatic repulsion is not as strong. More importantly, the free rotation around the C_{chiral}-$C_{C=O}$ bond is hard to predict. The pseudo $A_{1,2}$ interaction present in carrier **A** complexes is not as determinant as the pseudo $A_{1,3}$ steric interaction in the carrier **1** complex to freeze the rotation around the C_{chiral}-$C_{C=O}$ bond. The flexibility of this

conjugate may cause problems in correlating the absolute stereochemistry of the chiral complexes to the observed ECCD signs.

As shown in Scheme 3-2, the carrier **A** derivatized α-chiral carboxylic acids were synthesized by coupling **Boc-A** with different α-chiral carboxylic acids by standard BOP coupling, followed by Boc deprotection. A pinch of Na_2CO_3 was added into the solution of the carrier **A** derivatives to keep the free amino group of the chiral complex from being protonated. The solution was then added to the zinc porphyrin tweezer in methylcyclohexane for spectroscopic evaluation. As an example, the ECCD spectra of a pair of carrier **A** derivatized enantiomers are shown in Figure 3-9.

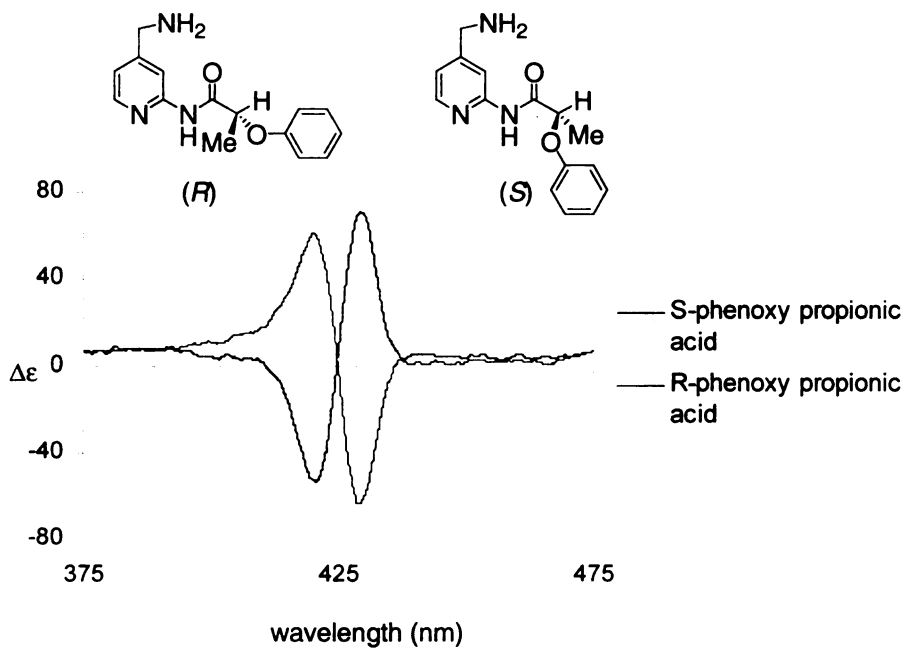

Figure 3-9. The ECCD spectra of carrier **A** derivatized (*R*)- and (*S*)-phenoxypropionic acid with zinc porphyrin tweezer **2**.

The observed ECCD signs and amplitudes of the carrier **A** derivatized chiral carboxylic acids upon addition to zinc porphyrin tweezer **2** in methylcyclohexane are recorded in Table 3-1. The signs of the predicted CD spectrum based on the

computational modeling studies are also compared to the observed CD signs. All the CD measurements listed in Table 3-1 were carried out at room temperature, except for the conjugate **14A**, which was measured at 0 °C. This conjugate exhibited no ECCD peak at room temperature, and the ECCD peak could only be observed at 0 °C.

Table 3-1. CD predictions and amplitudes of carrier **A** derivatized chiral carboxylic acids bound to porphyrin tweezer **2**.

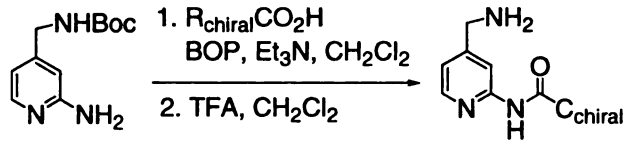

A **8A-15A**

Chiral acids	Predicted ECCD	Δε	A
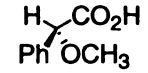 **8** (*S*)	**8A** neg	Not observed	---
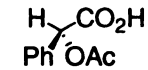 **9** (*S*)	**9A** neg	432 (-35) 424 (+46)	-81
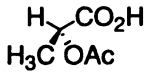 **10** (*S*)	**10A** neg	431 (-28) 423 (+29)	-57
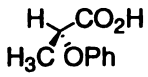 **11** (*S*)	**11A** neg	429 (+70) 421 (-54)	+124
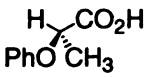 **12** (*R*)	**12A** pos	429 (-58) 420 (+60)	-118
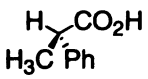 **13** (*R*)	**13A** pos	427 (-15) 417 (+14)	-29
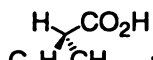 **14** (*S*)	**14A** neg	430 (-33) 422 (+39)	-72
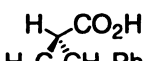 **15** (*R*)	**15A** neg	430 (-6) 422 (+15)	-21

Initially, a simplistic model based on molecular modeling conformational search (Monte Carlo) of the α-chiral carboxylic acid conjugated carrier **A** was used to predict the anticipated sign of the ECCD spectra. Modeling of the carrier **A** derivatized

complexes was initially performed without bound porphyrin. As shown in Figure 3-10, the lowest energy conformations of carrier **A** conjugates predicted a *syn* arrangement of the chiral center's medium group with respect to the amide hydrogen for most of the derivatives (sizes are based on A values).[21] We believe this was predicted in order to facilitate hydrogen bonding between the heteroatom-containing substituent, which is usually the medium group, and the amide proton. Also, this arrangement would lead to staggering of the other two groups at the chiral center (large and small) with respect to the carbonyl.

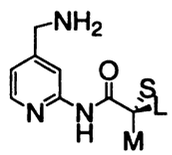

Figure 3-10. Lowest energy conformations of carrier **A** derivatized complexes based on modeling without binding to zinc porphyrin.

Therefore, our expected ECCD signs were dictated by placing the medium group *syn* to the amide hydrogen, which in turn would give rise to a preferred helicity of the bound porphyrin tweezer as a result of avoiding steric interactions with the large group. However, this model did not allow for consistent prediction of ECCD signs. We abandoned this method of analysis since the predictions did not match the observed ECCD spectra, (see Table 3-1, conjugates **8A**, **11A**, **12A**, and **13A**), most probably because we had not incorporated the binding of the zinc porphyrin to the pyridine nitrogen atom into our modeling.

Incorporation of the porphyrin into the modeling of carrier **A** derivatives produced conformers with inconsistent rotation around the C_{aryl}-N_{amide} bond, as shown in Figure 3-11. All of the derivatized carriers produced multiple conformations within 1

kcal/mol that would lead to opposing ECCD spectra. In many cases, the number of conformers expected to show positive ECCD was nearly equal to the number of conformers expected to show negative ECCD (within the lowest 1 kcal/mol).

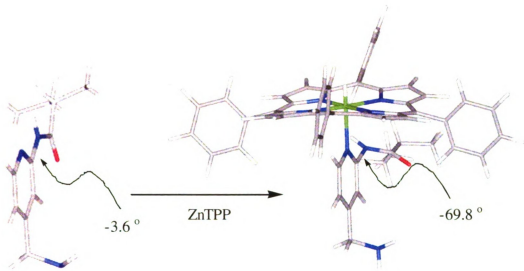

14A **14A** + ZnTPP

Figure 3-11. Based on modeling, binding of the Zn porphyrin to carrier **A** conjugates forces the rotation of the C_{aryl}-N_{amide} bond.

We believe the complication is because upon porphyrin binding with the pyridine nitrogen, unfavorable steric interactions with the amide hydrogen forces the C_{aryl}-N_{amide} bond rotation, as shown in Figure 3-11. The relatively large distance between the site of porphyrin binding and the chiral center might also lead to unpredictable assignments since the rotation of multiple single bonds must be assumed. Therefore, it became apparent that a more rigid carrier should be designed for the stereochemical determination of α-chiral carboxylic acids, which could limit the number of possible conformations upon binding to the zinc porphyrin.

3-2. Stereochemical determination of α-chiral carboxylic acids with carrier B

Carrier **B**, 1,4-diaminobenzene, was proposed as an alternate carrier in order to alleviate the problems associated with carrier **A**. Mono-amidation of 1,4-diaminobenzene (carrier **B**) with α-chiral carboxylic acids provided chiral complexes, which could coordinate with the zinc porphyrin tweezer via the free amino nitrogen and the carbonyl oxygen of the resulting amide group.

It was anticipated that the carrier **B** conjugates would not bind to zinc porphyrin tweezer as strong as carrier **A** derivatives, since the amide carbonyl oxygen in carrier **B** derivatives was not such a good coordination handle to bind to zinc porphyrins as pyridine nitrogen in carrier **A** complexes. However, the disadvantage in binding could be compensated by other factors. Not only binding through the carbonyl oxygen would bring the porphyrin moiety closer to the chiral center, but also the C_{aryl}-N_{amide} bond rotation would be inconsequential in this system. The induced helicity within the porphyrin tweezer would thus be governed only by the rotation of the $C_{carbonyl}$-C_{chiral} bond.

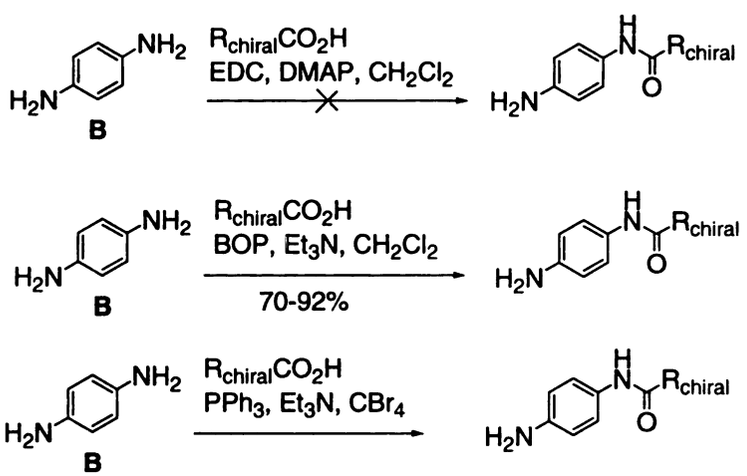

Scheme 3-3. The synthesis of carrier **B** derivatized chiral complexes.

The different methods that were tried for forming the carrier **B** derivatized chiral complexes are summarized in Scheme 3-3. The amidation between the carrier **B** and chiral carboxylic acids was first tried with a standard EDC coupling reaction, however, after the reaction mixture was stirred in the room temperature for 2 days, most of the starting material remains unreacted. Therefore, EDC was not active enough to form amide bond between the carrier **B** and chiral acids. When a more reactive coupling reagent BOP was used instead, this reaction underwent smoothly, and the starting chiral acids were fully consumed. Direct transformation of carboxylic acid and amine to carboxamides could also be achieved by using triphenylphosphine and carbon tetrabromide. This was a quick reaction, and the yield was also quite good. However, to separate the resulting phosphonium salt from the amide product was troublesome.

Therefore, for all the chiral acids, BOP coupling reaction was used to form amides with carrier **B**. In all the coupling reactions, large excess amount of carrier **B**, 1,4-diaminobenzene, was used to improve the conversion of the more expensive chiral acids and to eliminate the generation of diamides. The yield of the coupling reaction varied from 70-92%.

Prior to investigate the complexes generated by coupling carrier **B** to chiral acids by modeling, the binding between the zinc porphyrin tweezer **2** and carrier **B** complexes were investigated by UV-vis, NMR and IR.

The carrier **B** derivatives provide two binding sites to coordinate with zinc porphyrin tweezer **2**, one is the free amino group, without any doubt, and the other one could either be the amide nitrogen or amide oxygen (Figure 3-12). Although it is expected that zinc porphyrins would bind to the amide oxygen[22] because of its higher

electron density, the possibility of binding through amide nitrogen still exists, since nitrogen has high affinity to zinc. The possibility of binding through the amide nitrogen would drastically change the course of our studies, so it was important to fully understand the binding of the carrier **B** derivatives to zinc porphyrins.

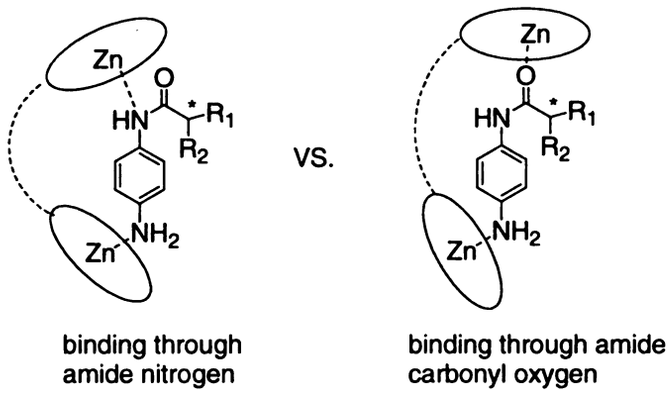

Figure 3-12. The possible binding of carrier **B** derivatives to zinc porphyrin tweezer.

Since we were only concerned about the binding of the amide part of carrier **B** derivatives to zinc porphyrins, zinc tetraphenylporphyrin (ZnTPP) was used in place of zinc porphyrin tweezer in the UV-vis study. Two amides with different bulkiness at the amide nitrogens (*t*-butylformamide and dimethylformamide) were added to zinc tetraphenylporphyrin (ZnTPP). The UV-vis spectra of these two amides binding to ZnTPP are shown in Figure 3-13.

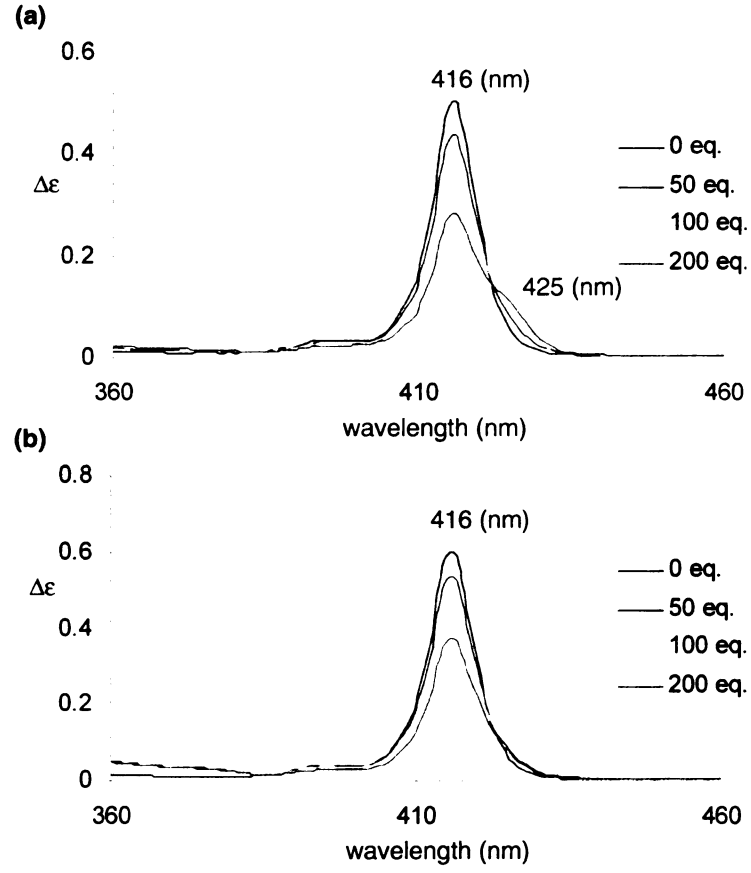

Figure 3-13. UV-vis spectra of adding two amides to ZnTPP. (*a*) titration with *t*-butylformamide; (*b*) titration with dimethylformamide

In spectrum (*a*), with the addition of *t*-butylformamide to ZnTPP, the absorption intensity of the Soret band at 416 nm decreases, and a new peak at 425 nm can be observed. This is confirmed by taking the second derivative of the spectrum (Figure 3-14). The growing shoulder at 425 nm is reasoned to be the bound *t*-butylformamide/ZnTPP complex, which significantly red-shifted the Soret band. On the other hand, as shown in spectrum (*b*), when dimethylformamide is added to the ZnTPP, the Soret band at 416 nm also decreases; however, the new shoulder at 425 nm is nearly negligible.

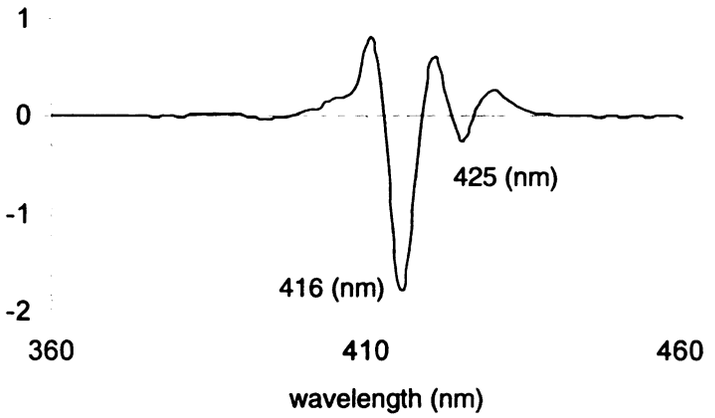

Figure 3-14. The second derivative of the UV-vis spectrum of ZnTPP with *t*-butylformamide (200 eq.).

The much weaker peak at 425 nm in spectrum (*b*) as compared to spectrum (*a*) indicates that the ZnTPP binds to *t*-butylformamide stronger than to dimethylformamide (DMF). The different binding ability of *t*-butylformamide and dimethylformamide to ZnTPP suggests that the amides bind to ZnTPP through amide oxygen instead of nitrogen. If the binding occurred through the nitrogen, DMF should exhibit higher binding affinity, since, in this case, the nitrogen atom is more accessible.

The binding between amides and zinc porphyrin was also studied by NMR. NMR of carrier **B** derivatized (*R*)-phenylpropionic acid **13B** and (*S*)-methylbutyric acid **14B** were taken before and after the addition of zinc porphyrin tweezer **2**, respectively. Since the NMR spectra of both derivatives showed the same trend, the NMR of one compound is shown here. Figure 3-15 depicts the chemical shift of derivative **14B** before and after the binding to zinc porphyrin tweezer **2**. Spectrum (*a*) is the proton NMR of carrier **B** derivatized (*S*)-2-methylbutyric acid **14B** by itself, and spectrum (*b*) is the proton NMR of compound **14B** with 1 equivalent of zinc porphyrin tweezer **2**.

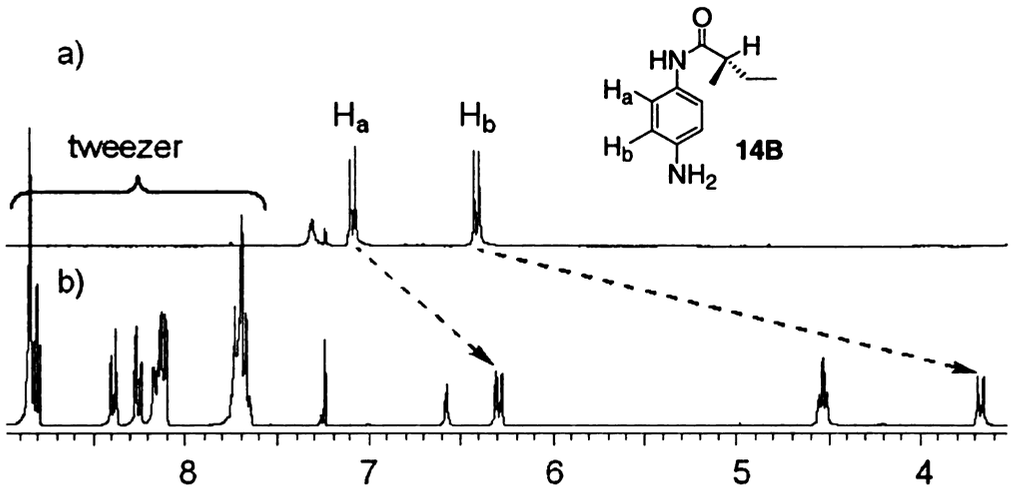

Figure 3-15. The binding study of the chiral conjugates **14B** with zinc porphyrin tweezer **2** by NMR. (*a*) ^{1}H-NMR of carrier **B** derivatized (*S*)-2-methylbutyric acid **14B**; (*b*) ^{1}H-NMR of compound **14B** with zinc porphyrin tweezer (1 equiv) is added.

As expected, the carrier phenyl protons H_a and H_b are upfield shifted after the addition of zinc porphyrin tweezer **2**; this is due to the anisotropic shielding effect of the porphyrin rings when the chiral conjugate binds to the porphyrin tweezer. However, the two sets of carrier phenyl protons shift upfield to a different extent. The aryl protons H_a are upfield shifted by 0.62 ppm while H_b shifts by 2.48 ppm. The different shift indicates that these two sets of protons are at different distance from the porphyrin ring. The larger upfield shift of H_b indicates their closer proximity to the bound porphyrin as compared to H_a. We would have expected a larger upfield shift for H_a if the porphyrin is bound to the amide nitrogen. Therefore, the NMR study of conjugate **14B** indicates that the zinc porphyrin binds to the amide oxygen instead of amide nitrogen.

There could be another explanation for the observation that the two sets of carrier phenyl protons, H_a and H_b, upfield shift to different extent. Considering the possibility

that the zinc porphyrin tweezer binds to the chiral conjugates through the amide nitrogen, because of the steric and electronic difference between the free amino nitrogen and the amide nitrogen, it is anticipated that the two nitrogens will bind the zinc porphyrin with different affinity, and thus the time averaged chemical shift for H_a would experience less of a change as compared to H_b.

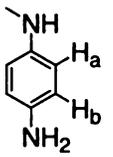

Figure 3-16. The structure of N-methyl-1,4-phenylenediamine.

In order to eliminate this possibility, we have synthesized N-methyl-1,4-phenylenediamine (Figure 3-16), and recorded its proton NMR before and after the addition of zinc porphyrin tweezer **2**. This compound binds zinc porphyrin tweezer through the two amino groups; however, because of the steric difference between the two nitrogens, the primary amino group should bind the zinc porphyrin stronger than the more sterically hindered secondary amino group. If the binding affinity does affect the chemical shift of the protons, then we would expect the two sets of protons to upfield shift to a different extent after the addition of zinc porphyrin tweezer, with H_b upfield shifted more than H_a. Based on NMR analysis, both aryl protons, H_a and H_b, are shifted upfield from 6.6 ppm to 3.5 ppm. Therefore, based on NMR study, we are reasonably confident that the carrier **B** derivatized conjugates bind to the zinc porphyrins through the amide oxygen.

The conclusion, that chiral conjugates bind to zinc porphyrin tweezer by amide oxygen, can be drawn based on both UV-vis and NMR studies, and it was also verified

by IR study of conjugate **14B**. The major change in the IR upon complexation of **14B** with tweezer **2** is a large increase in the intensity of the amide II band. This is also attributed to the binding of the zinc porphyrin to the carbonyl oxygen, which results in a larger C-N amide double bond character and thus an increased intensity in the NH deformation.

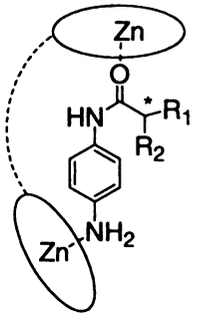

Figure 3-17. The binding of carrier **B** derivatives and zinc porphyrin tweezer based on UV-vis, IR and NMR study.

Based on all the above results, we believe that the carrier **B** derivatized complexes bind to zinc porphyrin tweezer through the free amino nitrogen and the carbonyl nitrogen, as shown in Figure 3-17.

Modeling of the carrier **B** conjugates bound to Zn-TPP (tetraphenylporphyrin), results in a more uniform set of structures as compared to conjugates of carrier **A**. Modeling of the carrier **B** derivatized complexes by itself produces a greater number of consistent conformers. With incorporation of ZnTPP, all conformers of **8B-16B** generated within 1 kcal/mol of the lowest energy conformer lead to predictions of the same ECCD. Modeling of carrier **B** conjugates also generated fewer conformers, indicating a smaller range of viable conformations for these conjugates as compared to the conjugates of carrier **A**.

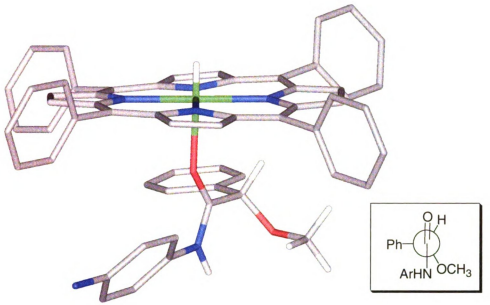

Figure 3-18. Minimized structure of Zn-TPP bound to **9B** (most of the hydrogen atoms deleted for clarity) in which the chiral center has adopted a conformation to minimize steric strain.

As Figure 3-18 illustrates, in all the structures studied, the rotation of the $C_{carbonyl}$-C_{chiral} bond is such that the large group is almost perpendicular to the carbonyl with the small group pointing towards the porphyrin plane and the medium group staggered with respect to the amide proton (insert). We would therefore expect the porphyrin to slide in the direction of the small group. The relative size of the substituents is based on the A values for each.

For those compounds with oxygen containing substituents at the chiral center, the placement of oxygen containing substituents (invariably the medium group in our group of compounds) is more *syn* with respect to the amide hydrogen, which can facilitate hydrogen bonding between the amide hydrogen and the oxygen at the chiral center. This

arrangement leads to the large and small groups bisecting the carbonyl oxygen, and once again dictates the helicity of the bound porphyrin.

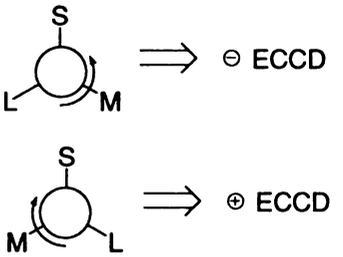

Figure 3-19. Proposed mnemonic for carrier **B** derivatized chiral acids.

A mnemonic has been proposed for carrier **B** derivatized chiral acids based on modeling studies (Figure 3-19). Looking through the $C_{C=O}$-C_{chiral} bond, viewing with the carboxylate in front, clockwise orientation of the large, medium, and small groups based on A values leads to a positive ECCD spectrum with carrier **B** derivatized chiral carboxylic acids, and *vice versa*. The predicted ECCD sign based on the proposed mnemonic for each acid derivative has been compared to the observed sign from CD measurement with zinc porphyrin tweezer **2** in Table 3-2.

The zinc in the zinc porphyrin tweezer **2** could be introduced to the porphyrin tweezer free base by adding zinc salts, such as $Zn(OAc)_2$ or $ZnBr_2$. The zinc porphyrin tweezer synthesized from both zinc salts coordinated with chiral derivatives and exhibited ECCD spectra. The sign of the ECCD spectra were the same for both zinc porphyrin tweezers; however, $Zn(OAc)_2$ porphyrin tweezer showed larger ECCD amplitude upon addition of the chiral substrates as compared to the $ZnBr_2$ derived porphyrin tweezer. To be consistent, all the UV-vis and ECCD studies were carrier out by using $Zn(OAc)_2$ as the porphyrin tweezer zinc source.

Table 3-2. CD predictions and amplitudes of carrier **B** derivatived chiral carboxylic acids bound to porphyrin tweezer **2**.

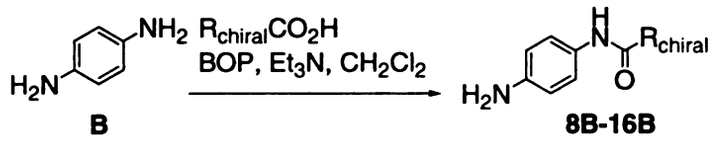

Chiral acids	Predicted ECCD	Mnemonic	Δε	A
8 (*S*)	**8B** neg	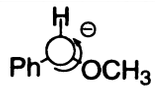	427 (-39) 420 (+43)	-82
9 (*S*)	**9B** neg	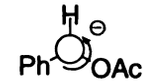	432 (-19) 419 (+22)	-41
10 (*S*)	**10B** neg	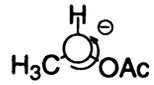	431 (-50) 420 (+38)	-88
11 (*S*)	**11B** neg	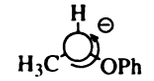	429 (-158) 420 (+116)	-274
12 (*R*)	**12B** pos	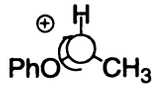	429 (+200) 420 (-83)	+283
13 (*R*)	**13B** pos	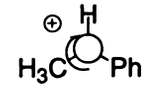	430 (-105) 420 (+85)	-190
14 (*S*)	**14B** neg	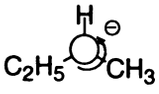	430 (-22) 420 (+26)	-48
16 (*S*)	**16B** neg	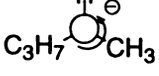	428 (-23) 418 (+27)	-50
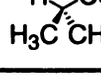 **15** (*R*)	**15B** neg	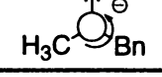	433 (-26) 421 (+28)	-54

Table 3-2 lists the predicted and observed ECCD for compounds **8B-16B**. As mentioned before, the binding of the carrier **B** derivatized conjugates to the zinc porphyrin tweezer is weaker than the binding of carrier **A** derivatized conjugates, so all

the CD measurements for carrier **B** derivatized conjugates were performed at 0 °C, in order to increase the binding of the conjugates with the zinc porphyrin tweezer **2**. Gratifyingly, the sign of the observed ECCD signals matches the predicted values based on the mnemonic presented above (Figure 3-19), except for the compound **13B**, whose explanation will be provided in detail later on. Compounds **11B** and **12B** are a pair of enantiomers, and as expected, they exhibit opposite ECCD spectra.

The ECCD amplitudes of the chiral derivatives at room temperature are much smaller than those at low temperature, but the signs remain the same, except for the (*S*)-2-methylbutyric acid **14B**. It shows small positive ECCD couplet at room temperature, and the sign switches to negative at 0 °C, which matches the predicted sign.

The other acid derivative we need to pay special attention to is the derivative of (*S*)-methoxyphenylacetic acid **8B**. For this derivative, the ECCD sign switched with the addition of great excess of chiral substrate. It showed a positive ECCD sign at room temperature with λ_{ext} 431 nm ($\Delta\varepsilon$ +13) and 424 nm ($\Delta\varepsilon$ -27), A +40, when the chiral substrate was less than 15 equivalents. With increasing amounts of substrate added to the porphyrin tweezer, a new peak growing at 416 nm was observed, and the CD spectrum looked like an overlap of two ECCD couplets with opposite sign. Addition of excess chiral substrate did not completely convert the positive ECCD signal to negative ECCD. When the CD was taken at 0 °C, the same trend was observed (Figure 3-20). When less than 5 equivalents of chiral substrate was added, it also showed a positive ECCD sign with λ_{ext} 431 nm ($\Delta\varepsilon$ +26) and 424 nm ($\Delta\varepsilon$ -40), A +66, and when the chiral substrate was increased to 60 equivalents, the sign of the ECCD switched, exhibiting a negative ECCD couplet with λ_{ext} 427 nm ($\Delta\varepsilon$ -39) and 420 nm ($\Delta\varepsilon$ +43), A –82.

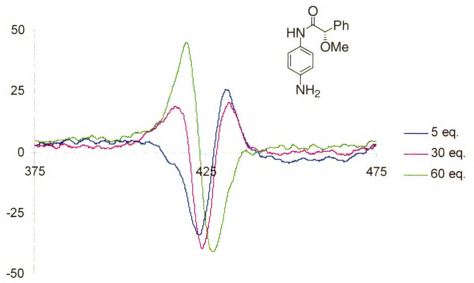

Figure 3-20. The CD spectra of (*S*)-methoxyphenylacetic acid **8B** (different amounts) at 0 °C.

Compound **13B** is a special case in carrier **B** derivatives. If one considers that phenyl is larger than methyl group, then the results obtained for **13B** does not fit the prediction, and in fact a positive ECCD would be expected instead of the negative ECCD spectrum that is observed. However, we believe that possible hydrogen-π interaction between the phenyl and the amide proton, as suggested by others for similar systems,[23-26] effectively places the phenyl group *syn* to the amide hydrogen, thus yielding the observed ECCD. This placement of phenyl group *syn* to the amide hydrogen causes the phenyl group to behave as the medium group when **13B** is bound to tweezer **2**.

The chemical shift of the amide proton for carrier **B** conjugates provides further evidence for the *syn*-like arrangement of the phenyl and the amide hydrogen. The chemical shift of the amide proton for **14B** with ethyl and methyl substituents is at 7.3 ppm and can be considered as the benchmark for the amide proton that does not interact with the groups at the chiral center. The chemical shift for **8B**, **9B**, **10B**, **11B**, and **12B**,

which contain an oxygen substituent ranges from 7.7-8.4 ppm. The downfield shift of these oxygen containing compounds could be indicative of hydrogen bonding between the oxygen and the amide hydrogen. The chemical shift for the amide proton of **13B** however resonates at 6.9 ppm, and the upfield shift arises from the shielding of the amide proton by the phenyl group.

A more direct way to test the existence of hydrogen-π interaction between amide hydrogen and phenyl ring in compound **13B** was to remove the amide hydrogen by replacing it with methyl group. In this way, the removal of the amide hydrogen would eliminate the possible hydrogen-π interaction, and it was expected that this methylated carrier **B** derivative **Me-13B** would show opposite ECCD sign as compared to the original carrier **B** derivative **13B**.

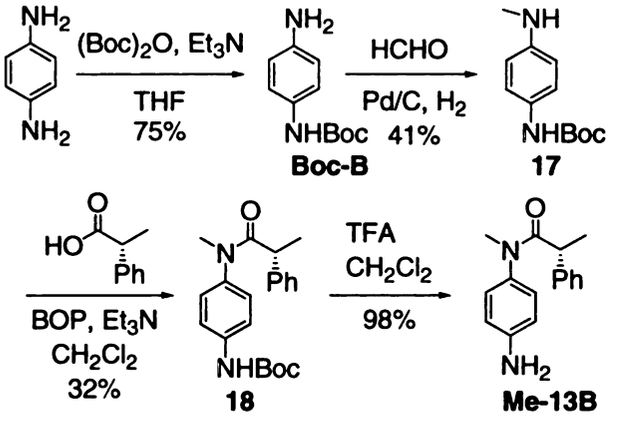

Scheme 3-4. The synthesis of methylated carrier **B** derivative **Me-13B**.

The synthesis of the methylated compound **Me-13B** is summarized in Scheme 3-4. The synthesis of compound **Me-13B** started with carrier **B**, 1,4-phenylenediamine. One of the amino groups was protected by Boc, and the free amino group was mono-methylated to yield compound **17** by reductive amination with formaldehyde, palladium on carbon and hydrogen gas.[27, 28] After the generation of the monomethylated amine **17**,

it was reacted with the chiral (*R*)-2-phenylpropionic acid to form amide **18** under BOP coupling reaction condition. Due to the steric hindrance of the methylated amino group, the reaction did not go to completion even after overnight stirring. The polarities of the resulting amide product **18** and the methylated starting material **17** were similar, and the separation by column chromatography was quite hard, but some of the pure product **18** (32%) was isolated. The Boc protecting group in compound **18** was removed by the standard TFA condition to generate the desired compound **Me-13B**.

The UV-vis and CD spectra were recorded for the complex **Me-13B** by adding it to zinc porphyrin tweezer **2** in methylcyclohexane. The binding between this methylated complex **Me-13B** and zinc porphyrin tweezer **2** was very weak. Upon addition of the chiral complex, the λ_{max} of the Soret band slightly red shifted from 416.0 nm to 416.7 nm, as compared to about 4 nm red shift of the original derivative **13B**. In agreement, the ECCD signal was also very weak, exhibiting a negative ECCD couplet.

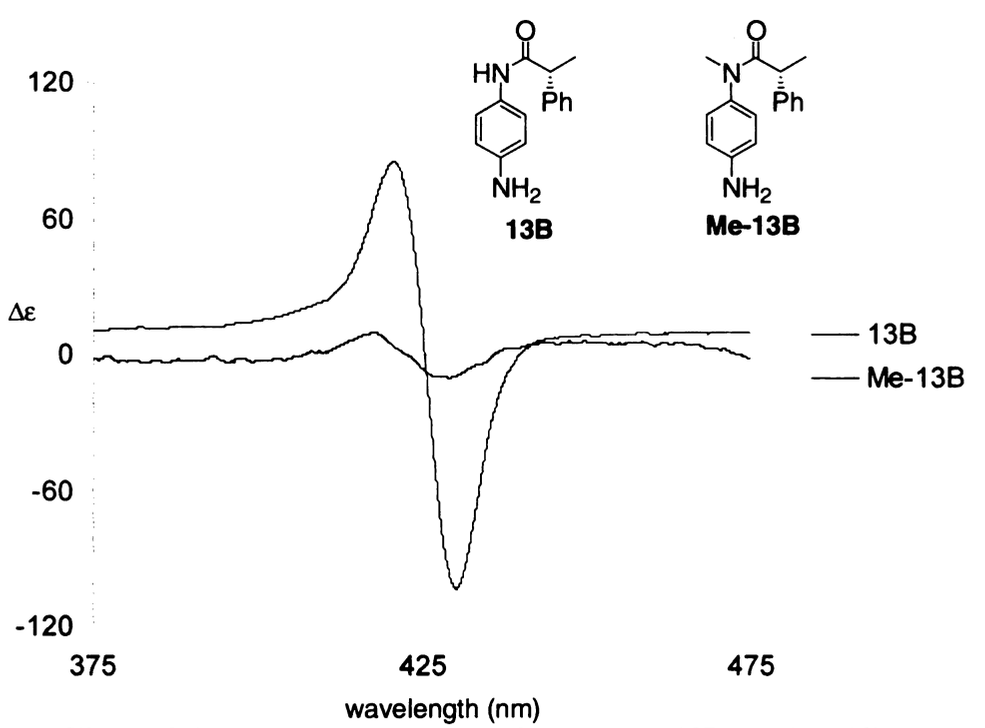

Figure 3-21. The ECCD spectra of compound **13B** and **Me-13B**.

As shown in Figure 3-21, contrary to what we were expecting, the ECCD sign of the methylated conjugate **Me-13B** was the same as that of the original conjugate **13B**, although the amplitude was much smaller, and thus weakening the possibility hydrogen-π interaction postulated between the amide hydrogen and phenyl group. However, we could not draw this conclusion based on the study with compound **Me-13B**, since the ECCD couplet of this compound was so small. This hydrogen-π interaction hypothesis will be discussed in more detail later.

Another possibility for the abnormal behavior of compound **13B** is that the consideration of A values[21] for analysis of **13B** is not valid due to other intramolecular forces, namely stacking interactions. Our modeling of **13B** bound to Zn-TPP suggests that the phenyl group adopts an arrangement parallel to the porphyrin. The probable stacking interaction of the phenyl group could be responsible for the tilting of the porphyrin towards it, thus causing it to behave as a small substituent that results in the observed ECCD.

The coupling between the carrier **B** and the chiral acids could result in both the monoamidation and diamidation products depending on the amount of carrier **B** used in the reaction. The diamidated product could be separated from the monoamidated compound by column chromatography.

Compared to the corresponding monoamides, most of the diamides are less soluble in organic solvents, but at the concentration needed for CD spectroscopy (micromolar), they are sufficiently soluble in methylcyclohexane in order to carry out all the UV-vis and CD studies. The diamides could bind to zinc porphyrin tweezer **2** through the amide oxygens, however, the binding of diamides to the zinc porphyrin

tweezer **2** was not expected to be as strong as the binding of monoamides. From UV-vis, it could be observed that the λ_{max} of the Soret band red shifted with the addition of both monoamides and diamides, however, the wavelength change with the addition of monoamides is a bit larger than that with diamides. The wavelength change for the monoamides binding was usually 4 nm, while it was no more than 2 nm upon the diamides binding.

The chiral diamide of (*S*)-acetoxypropionic acid **10** exhibited the same ECCD sign as the corresponding monoamide when added to the zinc porphyrin tweezer (λ_{ext} 430 nm ($\Delta\varepsilon$ -15) and 419 nm ($\Delta\varepsilon$ +26), A -41), but the amplitude was only half of that of the monoamide. On the other hand, the diamide derivative of (*S*)-methylbutyric acid **14** did not show any ECCD at all. Since taking the ECCD of diamides does not have advantages over monoamides, and because of the poor solubility of the diamides in organic solvents, we have not done an extensive study with these compounds.

3-3. Carrier C for the stereochemical study of chiral carboxylic acids

In the carrier **B** derivatized chiral acids conjugates, the signs of the ECCD spectra are determined by the free rotation around the $C_{C=O}$-C_{chiral} bonds. Based on modeling study (Figure 3-18), the rotation of the $C_{carbonyl}$-C_{chiral} bond was such that the large group was almost perpendicular to the carbonyl with the small group pointed towards the porphyrin plane and the medium group staggered with respect to the amide proton. For those compounds with oxygen containing substituents at the chiral center, the placement of oxygen containing substituents (invariably the medium group in our group of compounds) staggered with respect to the amide hydrogen also facilitated hydrogen bonding between the amide hydrogen and the oxygen at the chiral center.

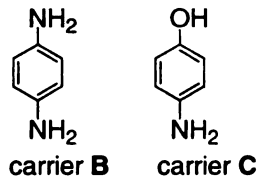

Figure 3-22. The structure of carrier **B** and **C**.

In order to further study the conformation of the $C_{C=O}$-C_{chiral} bond, we chose to use carrier **C**, 4-aminophenol. As shown in Figure 3-22, the only difference between carrier **B** and carrier **C** is that one of the amino functionalities in carrier **B** is replaced by a hydroxyl group in carrier **C**. This hydroxyl group in carrier **C** would be used to derivatize with chiral acids to form an ester linkage. This new carrier **C** was proposed because there is a better understanding of the rotation between carbonyl carbon and the α chiral carbon center in esters than in amides.[29]

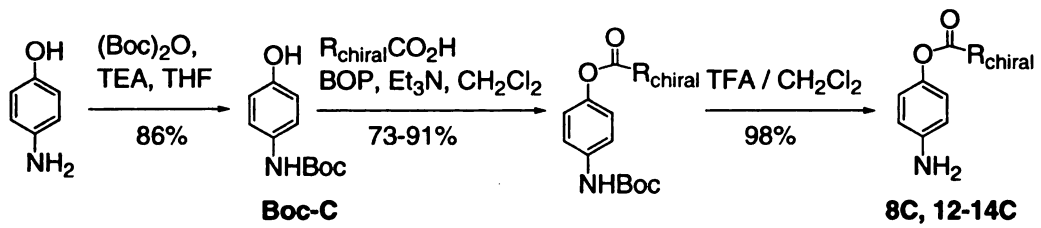

Scheme 3-5. The synthesis of carrier **C** derivatized chiral acids.

The synthesis of carrier **C** derivatized chiral acids is shown in Scheme 3-5. Since in carrier **C**, the amino group was more reactive than the hydroxyl group, it had to be first protected with the Boc protecting group. The free hydroxyl group was esterified with the chiral carboxylic acids activated by BOP, and subsequently the Boc protecting group was removed by treatment with TFA to generate the free amine for CD studies.

Carrier **C** was derivatized with all the chiral carboxylic acids used with the carrier **A** except for **9**, (*S*)-acetylmandelic acid, and **10**, (*S*)-acetoxypropionic acid. These two acids bear an ester functionality that could interfere with the binding between the chiral

conjugates and the zinc porphyrin tweezer, which in turn will complicate the correlation of the stereochemistry of the chiral conjugates to the observed ECCD signs.

Carrier **C** derivatized chiral carboxylic acids bound to zinc porphyrin tweezer through coordination with the nitrogen of the free amino group, and the carbonyl oxygen. However, carrier **C** derivatized conjugates did not bind to zinc porphyrin porphyrin as strong as carrier **B** derivatized conjugates. Although, both carrier **B** and **C** derivatives bind to zinc porphyrins through the carbonyl oxygen, the oxygen in carrier **C** derivatives is less nucleophilic than the oxygen in carrier **B**, since the ester oxygens are less electron donating than the amide nitrogens. Consequently, the binding of the carbonyl oxygen in carrier **C** to zinc porphyrins was weaker. This statement could be supported by UV-vis studies with zinc porphyrin tweezer. The wavelength change of the Soret band upon addition of the carrier **B** derivative was usually 4 nm, while it was less than 2 nm upon the binding to the carrier **C** derivatives.

Table 3-3 lists the observed ECCD for carrier **C** derivatized chiral carboxylic acids. All the measurements were performed at 0 °C in order to increase the binding of the chiral conjugates to the zinc porphyrin tweezer. There was no observable ECCD peak when the measurements were performed at room temperature. All the CD measurements were taken by using methylcyclohexane as the solvent. Other solvents were tested, including benzene, dichloromethane, and acetonitrile, but no ECCD peak was observed when using these solvents. ECCD peaks were observable only in methylcyclohexane and hexane, and since the bisignate ECCD peak was stronger in methylcyclohexane than in hexane, methylcyclohexane was used as the solvent of choice for the ECCD studies.

Table 3-3. CD amplitudes of carrier **C** derivatized chiral carboxylic acids bound to zinc porphyrin tweezer **2**.

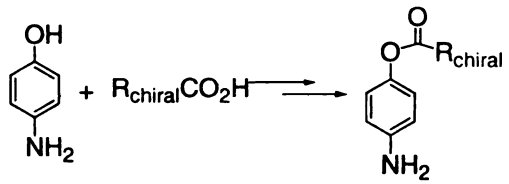

Chiral acid	1st λ(Δε)	2nd λ(Δε)	A (0 °C)
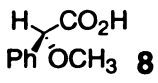 **8** (*S*)	432 (-77)	420 (+55)	-132
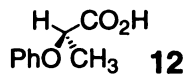 **12** (*R*)	430 (+9)	420 (-4)	+13
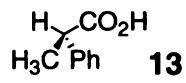 **13** (*R*)	432 (+21)	419 (-14)	+35
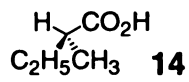 **14** (*S*)	430 (-15)	418 (+7)	-22

The ECCD signs of the carrier **C** derivatized (*R*)-methoxyphenylacetic acid **8C**, (*R*)-phenoxypropionic acid **12C** and (*S*)-methylbutyric acid **14C** were the same with the corresponding carrier **B** derivatives, and it suggested that the rotation around $C_{C=O}$-C_{chiral} bond remained the same for both the carrier **B** and **C** derivatives. However, the ECCD sign of the carrier **C** derivatized (*R*)-2-phenylpropionic acid **13C** was opposite to the ECCD sign of the carrier B derivative **13B**.

In the carrier **B** derivative **13B**, if the phenyl is considered larger than methyl group by A value consideration, then the resultant ECCD sign is opposite to the one proposed by the mnemonic (Section 3-2). This contradiction was explained by the possible hydrogen-π interaction between the amide proton and the phenyl group. This hydrogen-π interaction effectively places the phenyl group *syn* to the amide hydrogen,

instead of perpendicular to the carbonyl as the large group of the other conjugates did, and the sign predicted from this conformation was the same as the observed ECCD sign.

In Section 3-2, the *syn*-like arrangement of the phenyl and the amide hydrogen to facilitate the possible hydrogen-π interaction between the phenyl and the amide proton was partially proved by investigating the chemical shift of the amide proton for carrier **B** conjugates. The chemical shift for the amide proton of **13B** was more upfield shifted when compared to the other conjugates, which could be explained by the shielding of the amide proton by the phenyl group.

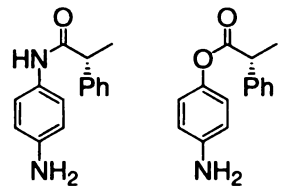

13B **13C**

Figure 3-23. The structure of **13B** and **13C**.

Here, the switching of the sign between the carrier **B** derivatized conjugate **13B** and carrier **C** derivatized compound **13C** gave a more direct evidence of the existence of hydrogen-π interaction between amide hydrogen and phenyl ring. As the structures shown in Figure 3-23, the only difference between these two derivatives was the changing from an amide bond (in compound **13B**) to ester bond (in **13C**). That the elimination of hydrogen-π interaction in compound **13C** resulted in the opposite of ECCD sign further suggested the probable hydrogen-π interaction between amide hydrogen and phenyl ring in carrier **B** derivative.

(*R*)-2-Phenylpropionic acid **13** was also derivatized with carrier **C** by forming an amide bond with the amino group to generate compound **13C'**, structure shown in Figure 3-24. If the ECCD sign of **13C'** was opposite to that of the original compound **13C**, it

would also strengthen the argument for the existence of the hydrogen-π interaction between amide hydrogen and phenyl ring.

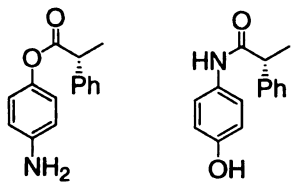

13C **13C'**

Figure 3-24. The structure of **13C** and **13C'**.

A routine BOP coupling of carrier **C**, 4-aminophenol, with (*R*)-2-phenylpropionic acid was not successful, and led to mixtures of ester and amide derivative product. Precedented in the literature, we have found a way to selectively form the amide bond in presence of the hydroxyl functionality (Scheme 3-7).[30] Acyloxytriphenylphosphonium salt **19**, generated *in situ*, is a good acylation reagent, which selectively acylated the amino group of carrier **C**, when the reaction was carried out at low temperature. If the reaction was warmed up to room temperature, the hydroxyl group could also react to form an ester.

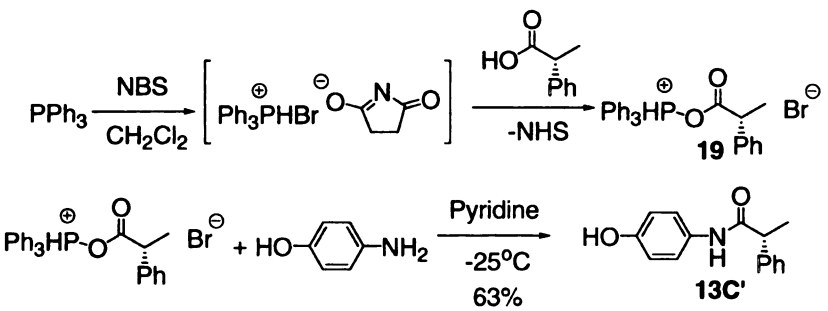

Scheme 3-6. The coupling of carrier **C** with acids to form amide bond.

The coupling of carrier **C** with (*R*)-2-phenylpropionic acid is shown in Scheme 3-6. The acyloxytriphenylphosphonium salt **19** was formed by the treatment of an equimolar mixture of a (*R*)-2-phenylpropionic acid and triphenylphosphine with NBS.

Adding the salt **19** to the carrier **C**, 4-aminophenol, at –25 °C generated the corresponding amides **13C'** in good yield.

No ECCD was observed upon addition of **13C'** to zinc porphyrin tweezer in methylcyclohexane at 0 °C. This might be due to the weak binding between the zinc porphyrin and the phenol. Zinc porphyrins are not known to bind hydroxyl groups well, however, magnesium porphyrins are capable of binding. Similar to metallation of free base porphyrin tweezer with zinc, the corresponding magnesium porphyrin tweezer was synthesized. Addition of **13C'** to magnesium porphyrin tweezer yielded a positive CD couplet, with λ_{ext} 429 nm ($\Delta\varepsilon$ -17) and 420 nm ($\Delta\varepsilon$ +20.8), A -38 at 0 °C. The sign of the ECCD couplet changed from positive in compound **13C** to negative in compound **13C'**.

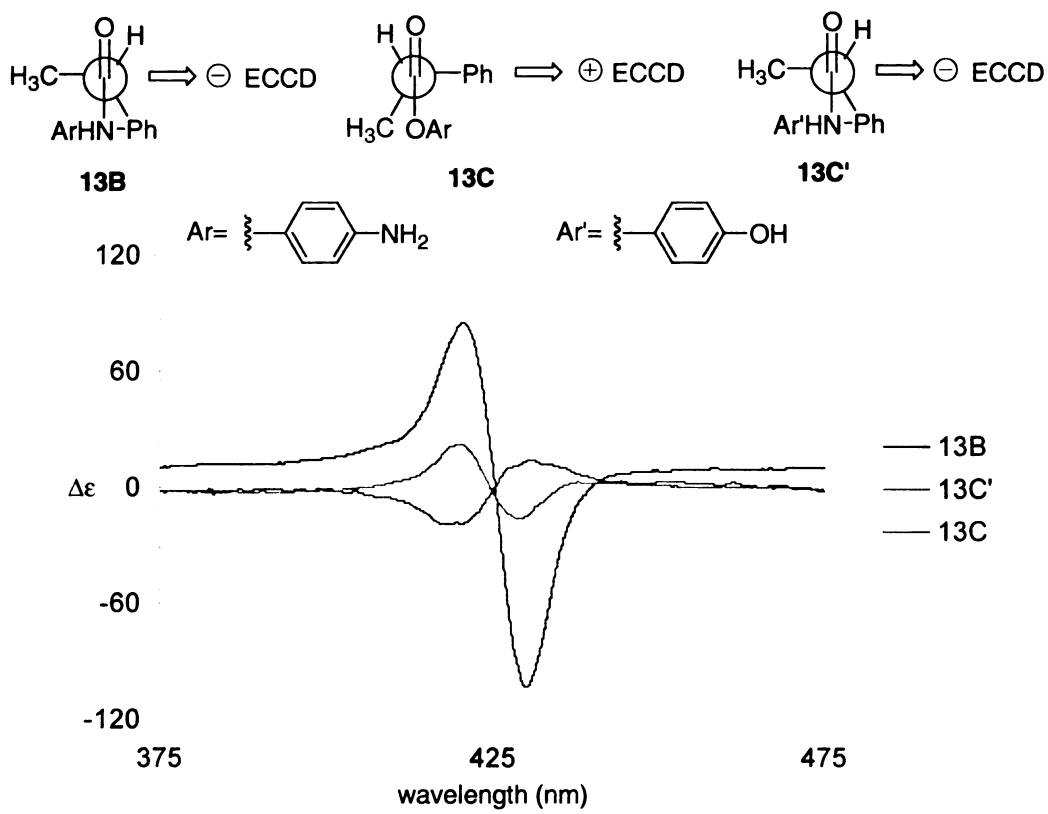

Figure 3-25. The conformations and ECCD of **13B**, **13C** and **13C'**.

From the comparison of ECCD signs of the compound **13B**, **13C** and **13C'** (Figure 3-25), one could deduce that the amide hydrogen does affect the conformation of the compounds, and the hydrogen-π interaction between the amide hydrogen and phenyl group is highly possible.

3-4. Carrier D for the stereochemical study of chiral carboxylic acids

In order to prove that in the comparison of **13C** and **13C'**, the binding between the hydroxyl oxygen to magnesium porphyrin is not the cause of the reversal in the observed ECCD, we chose to utilize carrier **D**, which is 1,4-benzenediol (Figure 3-26).

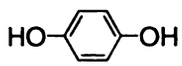

Figure 3-26. Structure of carrier **D**.

One of the hydroxyl groups in carrier **D** would be derivatized with the chiral carboxylic acids to form an ester bond, and the other hydroxyl group together with the resulting ester carbonyl oxygen would serve as the binding sites to porphyrin tweezer. Not surprisingly, no ECCD was observed by addition of carrier **D** derivatized compounds to zinc porphyrin tweezers, since oxygens do not bind to zinc as strongly as nitrogens. In order to improve the binding of the carrier **D** derivatives with the porphyrin tweezer, we decided to use magnesium porphyrin tweezer instead of zinc porphyrin tweezer, because of the high affinity between oxygen and magnesium.

The synthesis of Mg porphryin tweezer was not as easy as the synthesis of Zn porphyrin tweezer **2**. The Zn porphyrin tweezer **2** could be easily synthesized by adding excess amount of $Zn(OAc)_2$ to the porphyrin tweezer free base in CH_2Cl_2 and stirring at room temperature overnight. The zinc porphyrin is very stable and can to be easily purified by column chromatography.

Magnesium porphyrin tweezer was synthesized by adding excess amount of MgI_2 to the porphyrin tweezer free base in CH_2Cl_2 in the presence of bases, such as triethylamine.[31] During the synthesis of magnesium porphyrin tweezer, triethylamine was necessary to keep the reaction mixture basic, because the magnesium ion embedded in porphyrins is very sensitive to acid, and the weak acidic conditions generated in the process of inserting magnesium metal into porphyrins is strong enough to pop the magnesium out. The reaction was completed in 15 minutes and the excess of MgI_2 could be removed by filtration. The removal of the triethylamine from reaction mixture was more of a challenge, since it bound to the porphyrin by coordinating to magnesium. This rendered the magnesium porphyrin tweezer incapable of coordinating to the chiral complexes, and therefore, it was essential to remove all the triethylamine from the Mg porphyrin tweezer system.

Two ways were explored to remove triethylamine from the magnesium porphyrin system. Methanol was added to the triethylamine coordinated magnesium tweezer and the mixture was then extracted by CH_2Cl_2. Methanol was added in the hope that it would replace triethylamine by coordinating to the Mg porphyrin tweezer. However, this method did not work very well. As can be seen from NMR, the replacement was not quantitative. More over, the methanol bound to magnesium porphyrin could not be removed under vacuum, and it would also hinder the coordination of magnesium porphyrins to the chiral complexes.

The other way to remove triethylamine was by washing the triethylamine coordinated tweezer with 5% $NaHCO_3$ aqueous solution and extracting it with CH_2Cl_2.[31] This method worked out very well, and from NMR analysis, it was clear that all the

triethylamine had been removed. A few words have to be said about taking NMRs of magnesium porphyrins. When taking NMR of the magnesium porphyrin tweezer, small amount of deuterated methanol is necessary in order to keep the porphyrins from aggregating.[32] Because of the sensitivity of the magnesium porphyrins to acidic conditions, the magnesium porphyrin tweezer was used without being purified by column chromatography.

Before using the magnesium porphyrin tweezer for CD study, its extinction coefficient (ε) was determined. The absorption of certain concentration of magnesium porphyrin tweezer was measured by UV-vis with spectrophotometric solvents, and the extinction coefficient ε could be calculated based on the Lambert-Beer's Law:[33]

$$A = \varepsilon c l \tag{3-1}$$

where A is the absorbance and it can be read from UV-vis spectrometry, ε is the extinction coefficient, its unit is $M^{-1}cm^{-1}$, c is the concentration of the sample and l is the cell length, which is 1 cm in most cases.

Table 3-4 lists the extinction coefficient ε of Mg porphyrin tweezer in different solvents.

Table 3-4. The extinction coefficient ε of Mg porphyrin tweezer in different solvents.

Solvent	Extinction coefficient (ε)	λ_{max} (nm)
Methylcyclohexane	460,000	420
Dichloromethane	570,000	422
Chloroform	630,000	426
Acetonitrile	580,000	416
Benzene	470,000	426

The esterification between the chiral carboxylic acids and the carrier **D** was easy and straightforward. The conjugates were formed by BOP coupling of the carrier **D** with

chiral carboxylic acids. Again, (*S*)-acetylmandelic acid **9** and (*S*)-acetoxypropionic acid **10** were not used, because these two acids had an ester functionality, which could compete for binding with the magnesium porphyrin tweezer and complicate the observed ECCD spectra.

Table 3-5. The CD data of carrier **D** derivatized chiral acids with magnesium porphyrin tweezer.

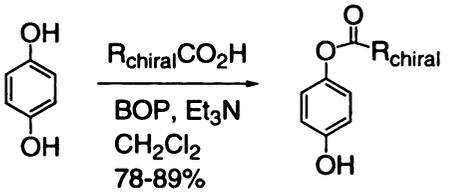

8D, 12D-14D

Chiral acid	1st λ(Δε)	2nd λ(Δε)	A (0 °C)
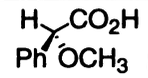 **8** (*S*)	432 (-12)	421 (+27)	-39
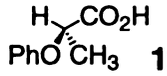 **12** (*R*)	431 (+9)	420 (-11)	+20
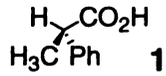 **13** (*R*)	431 (+29)	419 (-14)	+43
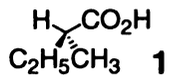 **14** (*S*)	No ECCD peaks		

The ECCD data of the carrier **D** derivatized chiral acids with magnesium porphyrin tweezer are listed in Table 3-5. The measurements were taken in methylcyclohexane at 0 °C. Except for the derivative of (*S*)-methylbutyric acid **14**, which did not show any ECCD peak under these conditions, all the other tested chiral acids derivatives had the same ECCD signs as the corresponding carrier **C** derivatives. The conservation in the sign of ECCD for these two different carrier derivatives indicated that

the binding between hydroxyl oxygen to magnesium porphyrins worked in the same way as amino nitrogen bound to zinc porphyrins.

Although carrier **C** and **D** could both be used to derivatize chiral carboxylic acids and exhibit quite consistent ECCD sign, these two carriers had no remarkable advantage over carrier **B**. Since carrier **B** derivatives have quite strong ECCD signals and zinc porphyrin tweezer is easier to handle than magnesium porphyrin tweezer, carrier **B** is the best carrier candidate for the stereochemical determination of α-chiral carboxylic acids.

3-5. Carrier E and F for the stereochemical study of α-chiral carboxylic acids

As it has been stated above that carrier **B**, 1,4-diaminobenzene, is the best carrier, so far, for the stereochemical determination of α-chiral carboxylic acids. In order to have a better understanding of the interaction of the carrier **B** derivatives with zinc porphyrin tweezer, we proposed a new generation of carriers. Carrier **E**, 4-aminopyridine, is very similar in structure as carrier **B**, structures shown in Figure 3-27.

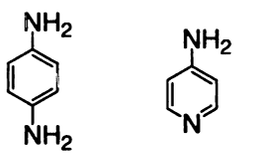

Figure 3-27. Structures of carrier **B** and **E**.

Carrier **E** could be derivatized with chiral carboxylic acids to form an amide bond as carrier **B**. However these two carriers differ from each other with regards to the geometry of binding of the un-derivatized nitrogen through the zinc porphyrin. Carrier **B** derivatives bind to zinc porphyrin tweezer with the free amino nitrogen, while carrier **E** derivatives bind to zinc porphyrin tweezer through the pyridine nitrogen. Since the location of the electron lone pair of the pyridine nitrogen is more defined in comparison

to that of the free amino nitrogen, the location of the zinc porphyrin bound to the pyridine nitrogen of carrier **E** is more predictable compared to that of carrier **B**. The comparison of the two different carrier-derivatized chiral carboxylic acids would enable us to have better understanding of the coordination between the chiral conjugates and zinc porphyrin tweezer.

Carrier **E** was esterified with chiral carboxylic acids by standard BOP reaction conditions without any problem. For preliminary studies, three chiral carboxylic acids were derivatized with the new carrier: (*S*)-2-methoxyphenylacetic acid **8**, (*R*)-phenylpropionic acid **13**, and (*S*)-2-methylbutyric acid **14**.

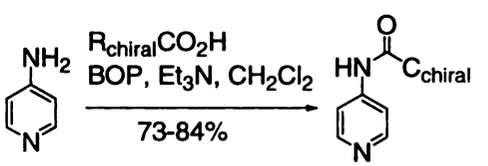

8E, 13E and 14E

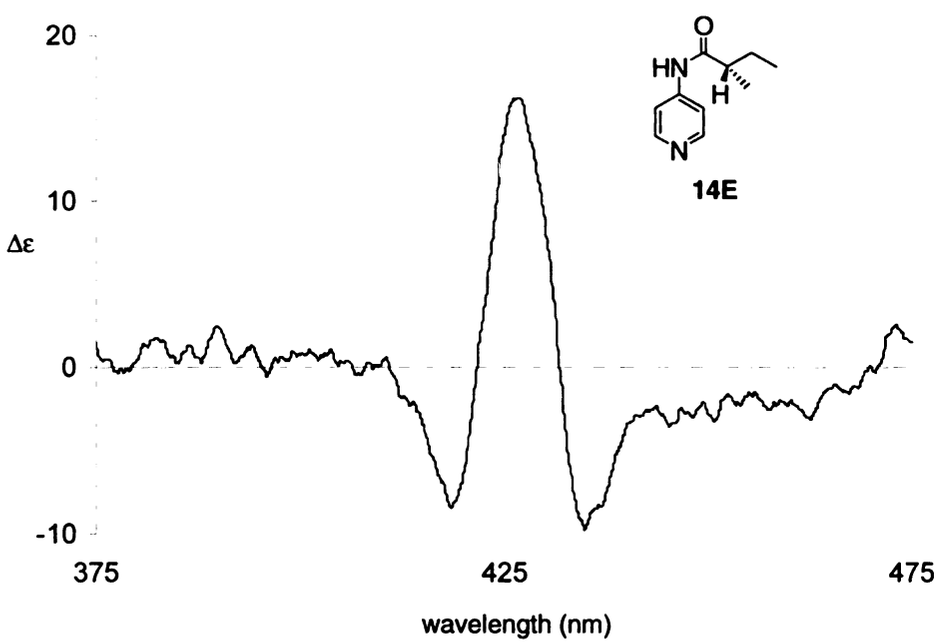

14E

Figure 3-28. The ECCD of carrier **E** derivatized methylbutyric acid **14E**.

However, carrier **E** derivatives did not work as well as expected, according to CD spectra taken by addition of the chiral derivatives to zinc porphyrin tweezer in methylcyclohexane. The (*S*)-2-methoxyphenylacetic acid derivative **8E** showed a positive ECCD couplet, which was opposite to the ECCD observed with carrier **B** conjugate **8B**. On the other hand, the derivatives of (*R*)-phenylpropionic acid **13E** and (*S*)-2-methylbutyric acid **14E** did not exhibit simple ECCD spectra (as shown in Figure 3-28). Both spectra looked like an overlap of two ECCD couplets with opposite signs, and they were not improved when the solution was cooled down to 0 °C.

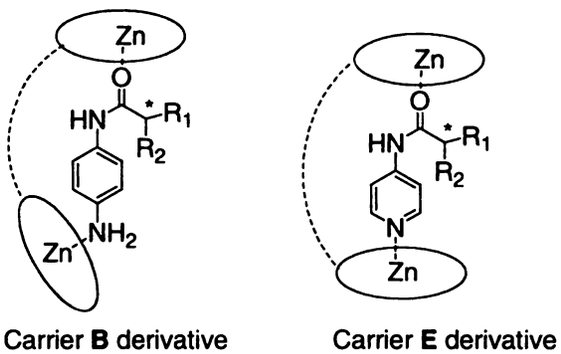

Figure 3-29. Carrier **B** and **E** derivatized amides bind to zinc porphyrin tweezer.

When carrier **B** and carrier **E** derivatives were compared more closely, it was found that actually carrier **E** did not mimic carrier **B** very well in binding to zinc porphyrin tweezer. Zinc porphyrin binds to the nitrogen electron pair, and the location of the electron pair in turn determines the location of the zinc porphyrin. Therefore, as shown in Figure 3-29, when carrier **E** derivatives bound to the zinc porphyrin tweezer, the two zinc porphyrin planes would approach to the amide substrate in a *psuedo-para* fashion, while when it bound to carrier **B** derivatives, the two zinc porphyrin planes would approach the substrate in a *psuedo-meta* fashion.

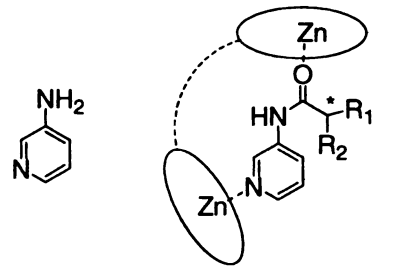

carrier **F** Carrier **F** derivative

Figure 3-30. Structure of carrier **F** and its derivative binds to zinc porphyrin tweezer.

Based on the latter discussion, naturally, 3-aminopyridine was chosen as a new carrier candidate (carrier **F**), since the pyridine nitrogen would be *meta*- to the amide functionality. As shown in Figure 3-30, the carrier **F** derivatives would coordinate with zinc porphyrin tweezer with the resulting amide carbonyl oxygen and pyridine nitrogen. Since the amino group was at *meta* position relative to the pyridine nitrogen, the porphyrin tweezer would approach to the substrate in a *meta* fashion just similar to what was presumed with carrier **B** derivatives.

Carrier **F** was derivatized with chiral carboxylic acids with standard BOP conditions. The chiral derivatives were then added to zinc porphyrin tweezer solution in methylcyclohexane, and CD spectra were measured. The ECCD data for carrier **F** derivatives are shown in Table 3-6, and are compared to those of the carrier **B** derivatives.

Table 3-6. Comparison of the CD data of carrier **B** and **F** derivatives

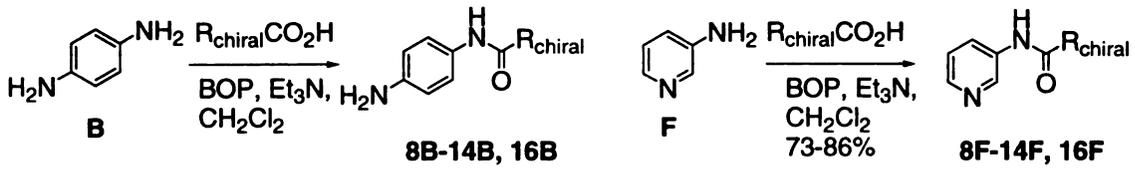

Chiral acids	Carrier **B** derivatives		Carrier **F** derivatives	
	Δε	A	Δε	A
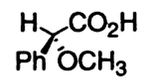 **8** (*S*)	427 (-39) 420 (+43)	-82	430 (-68) 421 (+69)	-137 (r.t)
			426 (+50) 417 (-37)	+87 (0 °C)
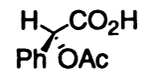 **9** (*S*)	432 (-19) 419 (+22)	-41	429 (+368) 420 (-236)	+604
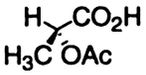 **10** (*S*)	431 (-50) 420 (+38)	-88	430 (+160) 420 (-109)	+269
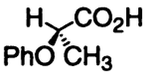 **12** (*R*)	429 (+200) 420 (-83)	+283	426 (-73) 418 (+86)	-159
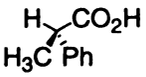 **13** (*R*)	430 (-105) 420 (+85)	-190	429 (-10) 420 (+21)	-31
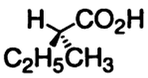 **14** (*S*)	430 (-22) 420 (+26)	-48	428 (+14) 420 (-14)	+28
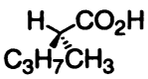 **16** (*S*)	428 (-23) 418 (+27)	-50	429 (+20) 421(-20)	+40

The ECCD amplitudes of the carrier **B** derivatives shown in Table 3-6 were measured at 0 °C, since the amplitudes at room temperature were quite small. As for the carrier **F** derivatives, the amplitudes shown in Table 3-6 were measured at room temperature, except for the derivatives of (*R*)-phenoxypropionic acid **12** and (*S*)-2-methylbutyric acid **14**, which were measured at 0 °C. One thing notable about the carrier **F** derivatives was that the derivatives of the acetyl containing acids, such as **9F** and **10F**,

showed extraordinary large ECCD peaks, especially carboxylic acid **9**, (*S*)-*O*-acetylmandelic acid, which exhibited an amplitude of 604 at room temperature.

The (*S*)-2-methylbutyric acid derivative **14F** showed a small positive ECCD couplet at room temperature, however when it was cooled to 0 °C, the ECCD couplet became much stronger, while the sign remained the same. This observation indicated that the derivative adopted the same conformation at room temperature and at 0 °C, but the population of the CD active conformation increased with the lowering of temperature.

The (*R*)-phenoxypropionic acid derivative **12F** did not show a clear ECCD spectrum at room temperature. It looked like an overlap of two ECCD couplets with opposite signs, which indicated the presence of more than one ECCD active conformation. When the solution was cooled to 0 °C, a strong negative ECCD couplet with λ_{ext} 426 nm ($\Delta\varepsilon$ -73) and 418 nm ($\Delta\varepsilon$ +86), A –159 was observed. The problem of multiple conformations at room temperature was alleviated, and only one of them was dominant at low temperature.

Special attention should be paid to the derivatives of acid **8**, (*R*)-methoxyphenylacetic acid. For its carrier **B** derivative **8B**, as it was mentioned in Section 3-2, the sign of the ECCD couplet changed with the addition of excess chiral substrate. When less than 5 equivalents of chiral substrate was added, it showed a positive ECCD sign and when the chiral substrate increased to 60 equivalents, it showed a negative ECCD couplet. While for its carrier **F** derivative **8F**, the sign of ECCD switched when it was cooled down from room temperature to 0 °C. At room temperature, it showed a negative ECCD sign with λ_{ext} 430 nm ($\Delta\varepsilon$ -77) and 421 nm ($\Delta\varepsilon$ +74), A –151, with a small peak at 414 nm. When the solution was cooled to 0 °C, it switched to a positive

ECCD couplet with λ_{ext} 426 nm ($\Delta\varepsilon$ +42) and 417 nm ($\Delta\varepsilon$ -50), A +92, and this time a small peak could also be observed at 433 nm (Figure 3-31).

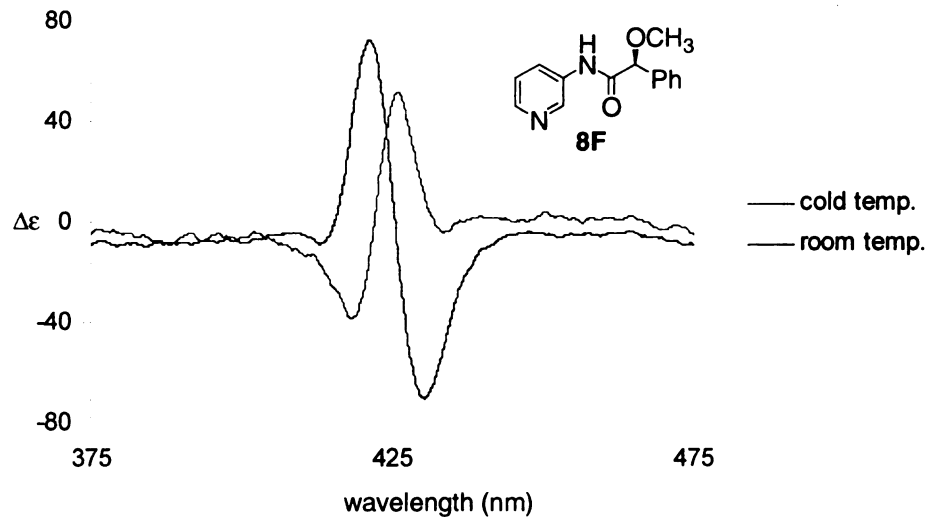

Figure 3-31. The ECCD of compound **8F** at different temperatures.

The switching of the ECCD sign from negative at room temperature to positive at 0 °C indicated that the chiral substrate **8F**, upon binding to the zinc porphyrin tweezer, adopted different conformations at room temperature and at 0 °C. At room temperature, the conformation, which showed positive ECCD signal, was the dominant conformation, and the small peak at 414 nm indicated the existence of small amount of another conformation, which led to a negative ECCD couplet. At 0 °C, the minor conformation at room temperature now became the major one, and the sign of the ECCD spectrum correspondingly switched from negative to positive. The conformation, which used to be the major conformation at room temperature, could only now been observed as a small peak at 433 nm.

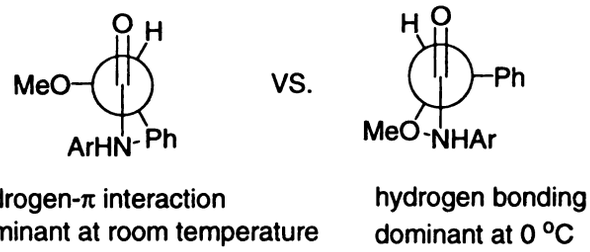

Figure 3-32. Hydrogen bonding vs. hydrogen-π interaction.

The ECCD sign of compound **8F** switched upon the changing of temperature, and this temperature dependence might be explained by the existence of two competing interactions (Figure 3-32), the hydrogen bonding between the amide hydrogen and the methoxy oxygen, and the hydrogen–π interaction between the amide hydrogen and the phenyl group. At room temperature, the hydrogen–π interaction was the major interaction, and it placed the phenyl group gauche to the amide hydrogen, thus leading to the observed negative ECCD spectrum. At 0 °C, the hydrogen bonding between the amide hydrogen and methoxy oxygen dominated, replacing the hydrogen–π interaction to become the major contributor to the conformation. This led to the conformational change that placed the methoxy group gauche to the amide hydrogen, producing a positive ECCD spectrum. However, at this point, we do not have any proof for this hypothesis.

When comparing the CD data of all the carrier **B** and carrier **F** derivatives, what became obvious was that all the carrier **B** derivatives exhibited the opposite ECCD as compared to the carrier **F** derivatives, except for the (*R*)-2-phenylpropionic acid **13**. We do not understand the cause of the sign switching between these two systems, however, it was not likely due to the conformational change around the $C_{C=O}$-C_{chiral} bond, since the amide functionality remained similar for both carrier **B** and carrier **F** derivatives. The different approaches of the zinc porphyrin tweezer adopted upon binding to the substrate

might be one of the possible explanations. As shown in Figure 3-33, the zinc porphyrin tweezer could approach the chiral substrate from opposite side, and this would lead to the observed opposite ECCD sign, even though the conformation around the $C_{C=O}$-C_{chiral} bond remained the same for these two derivatives. So far, due to lack of experimental evidence, this remains a working suggestion.

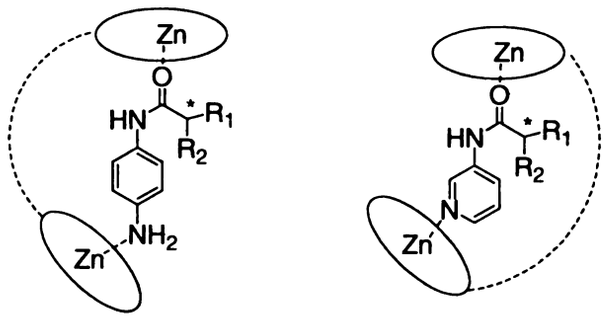

Carrier **B** derivative Carrier **F** derivative

Figure 3-33. The different interactions between the zinc porphyrin tweezer and carrier **B** and carrier **F** derivatives.

3-6. Use of 2-aminopyrazine as the new carrier G

We have also tested the ability of 2-aminopyrazine[34, 35] (carrier **G**) for the stereochemical determination of α-chiral carboxylic acids. 2-Aminopyrazine had an amino group, which could be easily derivatized with chiral carboxylic acids by forming amide bond, while the pyrazine functionality provided two binding sites to coordinate with zinc porphyrin tweezer **2**.

An advantage of this new carrier over all the other carriers tested so far was that the binding position of the zinc porphyrin tweezer relative to the chiral complex could be precisely predicted. Since the direction of the nitrogen lone pairs were fixed, the sign of the ECCD spectrum should only depend on the rotation around the C_{chiral}-$C_{C=O}$ bond (shown in Figure 3-34).

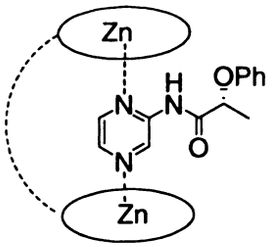

Carrier **G** derivative **12G**

Figure 3-34. The binding of carrier **G** derivatives **12G** to zinc porphyrin tweezer.

The coupling between carrier **G** and (*R*)-phenoxypropionic acid **12** was easily achieved by using BOP as the coupling reagent. However, the resulting chiral conjugate **12G** did not shown any ECCD peaks when added to zinc porphyrin tweezer **2** in methylcyclohexane. The CD was taken both at room temperature and 0 °C.

From the results of the UV-vis experiments, we believe that the chiral complex **12G** did not bind to zinc porphyrin tweezer, since the absorption wavelength λ_{max} of the Soret band did not change upon the addition of the carrier **G** derivative. One possible reason contributing to the lack of binding of the complex **12G** to zinc porphyrin tweezer **2** is that the two nitrogen binding sites in **12G** are very close to each other. In order to improve the binding, we shortened the distance between the two porphyrin planes by synthesizing the zinc porphyrin tweezer **2'** with 1,3-propanediol as the linkage, as shown in Scheme 3-7.

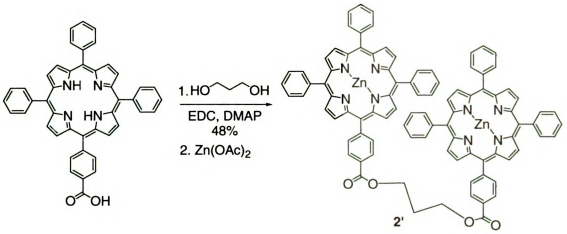

Scheme 3-7. The structure of zinc porphyrin tweezer **2'**, in which 1,3-propanediol serves as the linkage.

The newly synthesized zinc porphyrin tweezer **2'** was tested with carrier **F** derivatized (*S*)-O-acetylmandelic acid **9F**. This complex exhibited a strong positive ECCD spectrum, and the sign of the ECCD spectrum was consistent with previous consideration. However, when the carrier **G** derivative **12G** was added to tweezer **2'**, no ECCD spectrum was observed. UV-vis spectrum also indicated the lack of binding to the porphyrin tweezer. Therefore, 2-aminopyrazine was abandoned due to lack of binding.

3-7. Design of a new carrier H for chiral carboxylic acids

We have also designed a new carrier **H**, *o*-phenylene diamine, for the stereochemical determination of α-chiral carboxylic acids. As it is shown in Scheme 3-8, carrier **H** could form benzimidazoles with chiral carboxylic acid under acidic conditions.[36] The chiral benzimidazole could bind to zinc porphyrin tweezer with the two nitrogen atoms, and the helicity of the zinc porphyrin tweezer would depend on the rotation around the C-C_{chiral} single bond.

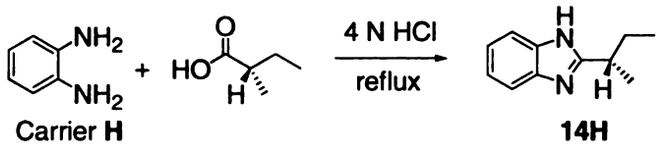

Scheme 3-8. The synthesis of chiral benzimidazole.

(*S*)-2-methylbutyric acid **14** was derivatized with the carrier **H**, to form chiral benzimidazoles **14H** by refluxing in 4 N HCl. The product could be easily precipitated from the reaction mixture by adding ammonium hydroxide. Without further purification, the benzimidazole **14H** was added to the zinc porphyrin tweezer, and UV-vis and CD spectra were obtained. From UV-vis, we observed the red shift of the maximum absorption wavelength, which indicated the binding of the chiral substrate to zinc porphyrin tweezer. CD analysis indicated a small positive ECCD curve at room temperature. Decreasing the temperature did not improve the amplitude of the couplet. The solubility of the chiral benzimidazole **14H** in methylcyclohexane was quite poor, and it began to precipitate out of the solution when up to 1 equivalent of the compound **14H** was added to the zinc porphyrin tweezer.

Although only preliminary studies were performed with the carrier **H**, this method is promising. We plan to optimize the ECCD spectrum by deprotonating the complex to improve the binding of the substrate to zinc porphyrin tweezer, and by varying the solvents for CD measurement.

3-8. Conclusion:

We have utilized a carrier strategy to investigate the chirality of asymmetric carboxylic acids, and for this purpose, we have design carriers **A**-**H** (Figure 3-35).

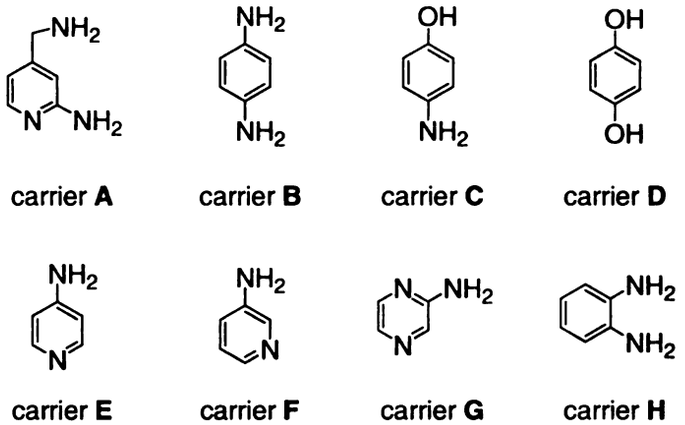

Figure 3-35. Carrier **A**-**H**.

Carrier **A**, which is analogous to the carrier utilized for chiral amines previously studied,[3] does not yield predictable ECCD spectra, most probably due to the unpredictable single bond rotamers between the porphyrin binding site and the chiral center. Carrier **B**, which can generate a more rigid chiral complex, produced consistent ECCD spectra, which can be rationalized and predicted by molecular modeling. Carriers **C** and **D** have similar structures as carrier **B**, and their chiral complexes exhibit consistent ECCD. But their ECCD signals are not as strong as those of carrier **B**; even carrier **D** can only exhibit ECCD with the Mg porphyrin tweezer, which is less stable than the Zn porphyrin tweezer. The derivatives of carrier **F**, 3-aminopyridine, also exhibit consistent ECCD, however, the signs are all opposite to that of the carrier **B** derivatives. So far, we cannot explain the reason for the change in sign. Whether the different approach of the zinc porphyrin tweezer with respect to the chiral substrate could be an explanation is not clear as of yet. As for carriers **E** and **G**, they are not good carriers, since their complexes exhibit complicated ECCD spectra. Finally, the carrier **H**, which is based on a totally different approach, although only briefly studied, provides promising results.

In conclusion, of all the tested carriers, carrier **B**, 1,4-diaminobenzene, is the best for the absolute stereochemical determination of α-chiral carboxylic acids. The use of carrier **B** to determine the stereochemistry of α–chiral carboxylic acids by zinc porphyrin tweezer **2** is displayed in Figure 3-36.

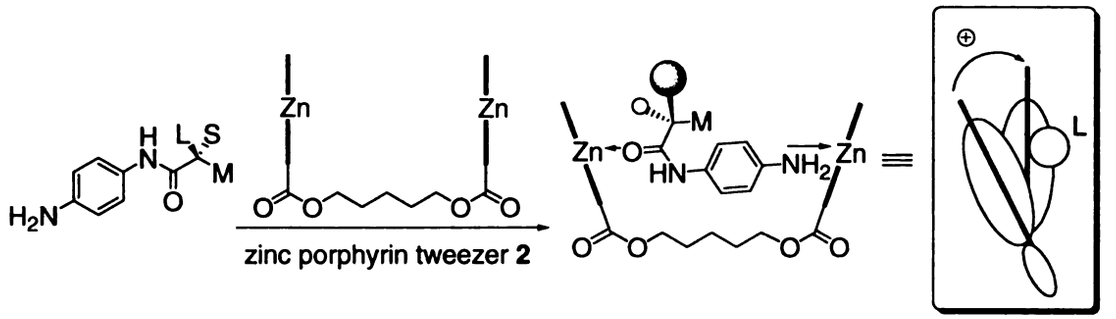

Figure 3-36. The stereochemical study of carrier **B** derivatized α–chiral carboxylic acids with zinc porphyrin tweezer **2**.In summary, the carrier **B** derivatized chiral carboxylic acids bind to zinc porphyrin tweezer **2** with the free amino group and the amide oxygen. When the conjugate binds to porphyrin tweezer, it adopts a conformation to place the medium group gauche to amide hydrogen, and the large and small group (size wise) point towards the porphyrin plane. Accordingly, the zinc porphyrin tweezer adopts the appropriate helicity to minimize the steric interaction with the groups on the chiral center, and the handedness of porphyrin tweezer can be observed by CD measurements. In turn, the absolute stereochemistry of the chiral center can be deduced from the sign of the resulting ECCD spectrum.

3-9. Another approach towards the same goal

As it has been stated at the beginning of this chapter, Nakanishi's lab has developed a very similar idea for absolute stereochemical determination of α-chiral carboxylic acids, by using the Exciton Coupled Circular Dichroic (ECCD) method

together with carrier molecules.[17, 18] The carrier molecule that they used in their studies is 1,3-diaminopropane. The chiral substrate was derivatized with the achiral carrier **X**, to generate a bifunctional amide conjugate that could form a 1:1 host-guest complex with the zinc porphyrin tweezer. The chiral conjugate coordinated to the tweezer host **2** through the free amino nitrogen and the carbonyl oxygen.[37, 38]

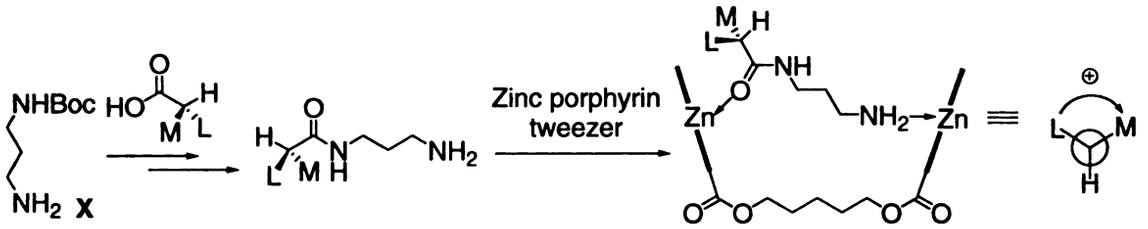

Figure 3-37. The binding of chiral conjugate to zinc porphyrin tweezer.

As depicted in Figure 3-37, in the most favored conformation adopted by the chiral conjugate **X**, the L (large) and M (medium) groups were pointing toward the porphyrin plane. The absolute configuration of the chiral substrate could be correlated to the sign of the ECCD couplet in such manner: viewing with the carboxylic group in the rear, the clockwise orientation of the L, M and H will resulted in a positive ECCD spectrum, and *vice versa*.

The system described above is very similar to the one we developed. Both groups used zinc porphyrin tweezer as the chromophoric host, and the carriers used were diamino compounds, we used 1,4-diaminobenzene while they used 1,3-diaminopropane. Both the carriers' derivatives showed consistent ECCD sign, and mnemonics were proposed to link the observed ECCD spectra to the absolute stereochemical determination of α-chiral carboxylic acids.

However, there was a major difference between these two carrier systems: the mnemonics proposed, which were consistent with the observed ECCD signs, were

opposite to each other. This was due to the different conformations the substrate adopted upon binding to zinc porphyrin tweezer. Figure 3-38 is an example with (*S*)-methylbutyric acid **14**. In our system, the chiral substrate adopted the conformation with the large group (Et) perpendicular to the carbonyl group, while the medium group (Me) was gauche to the amide hydrogen. The porphyrin tweezer differentiated between the large (Et) and small group (H) on the chiral center, which led to a negative ECCD. In their system, the small group (H) was *syn* to the amide hydrogen, and it was the large (Et) and the medium group (Me) that were pointing towards the porphyrin plane, which resulted in a positive ECCD.

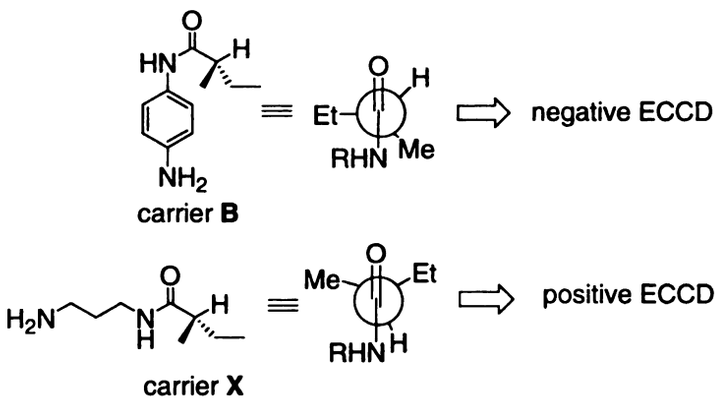

Figure 3-38. Opposite ECCD spectra with the two carriers **B** and **X**.

We do not yet understand what causes the conformational change in these two systems, but they work equally well in determining the absolute stereochemistry of α-chiral carboxylic acids.

Experimental materials and general procedures:

Anhydrous CH_2Cl_2 was dried over CaH_2 and distilled. The solvents used for CD measurements were purchased from Aldrich and were spectra grade. All reactions were performed in dried glassware under nitrogen. Column chromatography was performed using SiliCycle silica gel (230-400 mesh). ^{1}H-NMR spectra were obtained on Varian Inova 300 MHz or 500 MHz instrument and are reported in parts per million (ppm) relative to the solvent resonances (δ), with coupling constants (J) in Hertz (Hz). IR studies were performed on a Galaxy series FTIR 3000 instrument (Matteson). UV-Vis spectra were recorded on a Perkin-Elmer Lambda 40 spectrophotometer, and is reported as λ_{max} [nm]. CD spectra were recorded on a JASCO J-810 spectropolarimeter, equipped with a temperature controller (Neslab 111) for low temperature studies, and is reported as λ [nm] ($\Delta\varepsilon_{max}$ [l mol^{-1} cm^{-1}]). Porphyrin tweezer **2** was synthesized as previously described.[39] α-Chiral carboxylic acids **8**, **9**, **10**, **13**, **14** and **15** were purchased from Aldrich. Compound **11** and **12** was synthesized as previously reported.

General procedure for CD measurement:

All the CD spectra were taken with 1 μM porphyrin tweezer in methylcyclohexane (1 mL) with 40 equiv of the carrier/chiral carboxylic acid conjugate. The CD spectra were measured in millidegrees and normalized into $\Delta\varepsilon/\lambda$ [nm] units. Experiments with carrier **A**, **F** were carried out at room temperature. However, measurements with carrier **B**, **C**, **D** and **H** were performed at 0 °C in order to increase the binding of the carrier with the porphyrin tweezer.

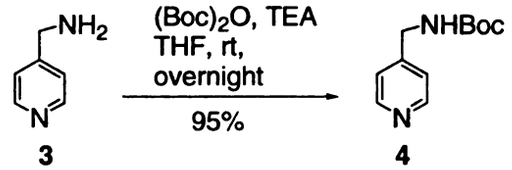

3 4

4-[(*t*-Butoxycarbonyl-amino)methyl] pyridine 4:

To a solution of 4-aminomethylpyridine **3** (0.54 g, 5 mmol) in dry THF (10 mL) was added di-*t*-butyl dicarbonate (1.10 g, 5 mmol) and triethylamine (0.16 mL). A white precipitate was formed and redissolved immediately. The reaction mixture was stirred at room temperature overnight. The solution was filtered and the filtrate was concentrated to yield an oil like liquid. The residue was purified by flash chromatography (9:1 CH_3Cl/MeOH) to yield the title compound **4** (0.9 g, 95%). ^1H NMR (300 MHz, $CDCl_3$) δ 8.54 (d, *J*=5.0 Hz, 2H), 7.20 (d, *J*=5.0 Hz, 2H), 5.10-5.24 (br, 1H), 4.33 (d, *J*=4.7 Hz, 2H), 1.47 (s, 9H).

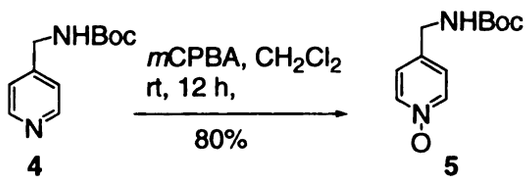

4 5

4-[(*t*-Butoxycarbonyl-amino)methyl] pyridine oxide 5:

To a solution of **4** (0.5 g, 2.4 mmol) in CH_2Cl_2 (10 mL) was added *m*CPBA (1.6 g). The reaction was stirred at room temperature for 18 h and then washed with 0.5 N aqueous NaOH solution (5 mL). The aqueous layer was extracted with CH_2Cl_2 (10 × 10 mL) until no product was left in the aqueous phase. The organic layers were combined and dried by Na_2SO_4. The solvent was removed under reduced pressure, and the residue was purified by column chromatography (9:1 CH_3Cl/MeOH) to yield the pure compound **5** (0.42 g, 80%). ^1H NMR (300 MHz, CD_3OD) δ 8.27 (d, *J*=6.6 Hz, 2H), 7.44 (d, *J*=6.6 Hz, 2H), 4.27 (d, *J*=5.7 Hz, 2H), 1.44 (s, 9H).

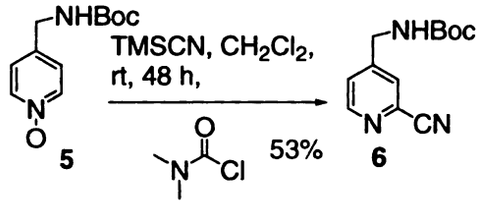

2-Cyano-4-[(*t*-Butoxycarbonyl-amino)methyl] pyridine 6:

To a solution of **5** (0.65 g, 3.15 mmol) in CH_2Cl_2 under N_2 was added TMSCN (0.52 mL, 4.09 mmol). After stirring for 5 minutes, dimethylcarbamyl chloride (0.34 mL, 3.44 mmol) was added. The solution was further stirred at room temperature for 48 h, and then washed with saturated aqueous $NaHCO_3$ solution (5 mL). The aqueous layer was washed with CH_2Cl_2 (3 × 10 mL) and the organic layers were combined and dried over Na_2SO_4. The solvent was removed under reduced pressure, and purified by column chromatography (20:1 CH_2Cl_2/MeOH) to yield the title product **6** (0.42 g, 53%). ^1H NMR (300 MHz, $CDCl_3$) δ 8.64 (d, *J*=5.1 Hz, 2H), 7.63 (d, *J*=6.7 Hz, 1H), 7.44 (d, *J*=5.1 Hz, 2H), 5.32-5.42 (br, 1H), 4.38 (d, *J*=6.2 Hz, 2H), 1.47 (s, 9H).

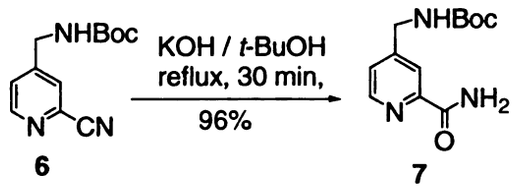

4-[(*t*-Butoxycarbonyl-amino)methyl] pyridine 2-carboxylic acid amide 7:

Finely powdered KOH (50 mg) was added to a solution of 2-cyano-4-[(*tert*-butoxycarbonylamino)methyl] pyridine **6** (50 mg, 0.23 mmole) in *t*-BuOH (2 mL). The reaction mixture was refluxed for 30 min. The mixture was cooled and poured into an aqueous sodium chloride solution (10 mL) followed by extraction with $CHCl_3$ (4 × 20 mL). The organic layers were combined and then dried over anhydrous Na_2SO_4, and the solvent was removed under reduced pressure to afford the amide **7** in 96% yield. ^1H

NMR (300MHz, $CDCl_3$) δ 8.49 (d, *J*=4.9 Hz, 1H), 8.09 (s, 1H), 7.80 (br, 1H), 7.36 (d, *J*=4.9 Hz, 1H), 5.56 (br, 1H), 5.01 (br, 1H), 4.39 (d, *J*=6.6 Hz, 2H), 1.42 (s, 9H). Compound **7** was used in the next reaction without further purification.

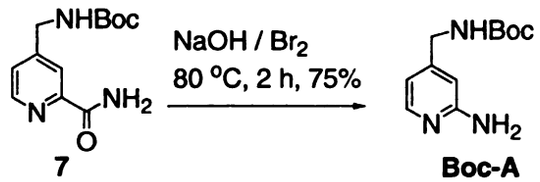

7 **Boc-A**

NHBoc-Carrier A:

A solution of NaOH (60 mg) in water (1 mL) was cooled in an ice-bath, and Br_2 (25 µl) was slowly added to it. The solution was stirred at 0 °C for 15 min, and the amide **4** (100 mg, 0.4 mmole) was added. This mixture was stirred vigorously for 15 min in an ice-bath and subsequently moved into an oil bath, which was maintained at 75 °C with constant stirring for an hour. The solution was saturated with sodium chloride, and extracted with $CHCl_3$ (5 × 25 mL). The combined organic layers were dried over anhydrous Na_2SO_4, and the solvent was removed under reduced pressure. The remaining residue was purified by column chromatography to yield 75% of the pure product. ^1H NMR (300 MHz, $CDCl_3$) δ 7.92 (d, *J*=5.5 Hz, 1H), 6.51 (d, *J*=5.5 Hz, 1H), 6.36 (s, 1H), 5.08 (br, 1H), 4.51 (br, 2H), 4.16 (d, *J*=6.0 Hz, 2H), 1.41 (s, 3H).

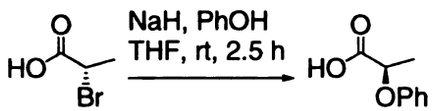

(*R*)-Phenoxypropionic acid and (*S*)-phenoxypropionic acid (11 and 12):

NaH (60% suspension, 20 mg, 0.5 mmole, washed 3 times with hexane) was added to a solution of (*S*)-2-bromopropionic acid (77 mg, 0.5 mmole for synthesis of **5** or (*R*)-2-bromopropionic acid for synthesis of **6**) in THF (5 mL). In a separate vessel NaH (60% suspension, 40 mg, 1 mmole, washed 3 times with hexane) was added to a solution

of phenol (94 mg, 1 mmole) in THF (5 mL). The phenolate solution was cannulated into the 2-bromopropionate solution, and stirred at room temperature for 2.5 h. The reaction was quenched with NaOH solution (10 mL, 2 N NaOH), and kept stirring at room temperature for another hour. The reaction was acidified with HCl (2 N) up to pH=1, and extracted with Et_2O (3 × 25 mL). The Et_2O extract was dried over anhydrous Na_2SO_4 and concentrated. The residue was purified by column chromatography to yield the product. The spectroscopic analysis of the product matched with the reported data. The enantiomeric excess was determined by derivatizing the acids with (*S*)-cyclohexylethylamine, and was determined to be in excess of 90% *ee* for both acids by GC analysis.

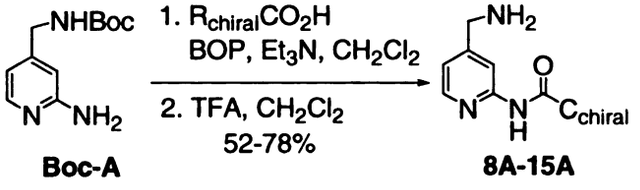

Boc-A **8A-15A**

General procedure for preparation of carrier A/carboxylic acid conjugates (8A-15A):

To a solution of carrier **A** (1 equiv) in CH_2Cl_2 (2 mL), BOP (1.1 equiv), triethylamine (5 equiv), and the chiral carboxylic acid (1 equiv) were added. The solution was stirred at room temperature overnight. After removal of most of the solvent under reduced pressure, the product was purified by silica gel column chromatography to yield the Boc-protected conjugate. The Boc group was removed by stirring overnight in TFA/CH_2Cl_2 (1:4) at room temperature. The solvent was then removed by purging nitrogen. The residue was redissolved in anhydrous CH_2Cl_2, and anhydrous Na_2CO_3 (20 mg) was added. This solution was stirred at room temperature for an hour, and the

Na_2CO_3 was filtered. The solvent was evaporated under reduced pressure to provide analytically pure product.

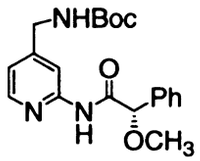

Boc-8A

Boc protected carrier A/carboxylic acid conjugates Boc-8A:

^{1}H NMR (300 MHz, $CDCl_3$) δ 9.17 (br, 1H), 8.24 (d, *J*=4.9 Hz, 1H), 8.14 (s, 1H), 7.45 (m, 5H), 7.00 (d, *J*=4.9 Hz, 1H), 5.03 (br, 1H), 4.73 (s, 1H), 4.30 (d, *J*=6.5 Hz, 2H), 3.43 (s, 3H), 1.46 (s, 9H).

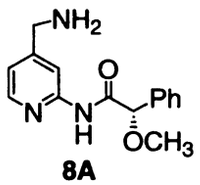

8A

Carrier A/carboxylic acid conjugates 8A:

^{1}H NMR (300 MHz, $CDCl_3$) δ 9.17 (br, 1H), 8.24 (d, *J*=4.9 Hz, 1H), 8.14 (s, 1H), 7.45 (m, 5H), 7.00 (d, *J*=4.9 Hz, 1H), 4.73 (s, 1H), 3.84 (s, 2H), 3.43 (s, 3H), 1.58 (br, 2H).

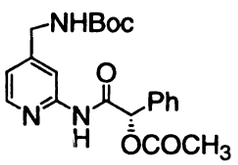

Boc-9A

Boc protected carrier A/carboxylic acid conjugates Boc-9A:

^{1}H NMR (300 MHz, $CDCl_3$) δ 8.75 (br, 1H), 8.23 (d, *J*=4.9 Hz, 1H), 8.14 (s, 1H), 7.50 (m, 2H), 7.41 (m, 3H), 7.03 (d, *J*=4.9 Hz, 1H), 6.21 (s, 1H), 5.02 (br, 1H), 4.33 (d, *J*=6.6, Hz, 2H), 2.27 (s, 3H), 1.47 (s, 9H).

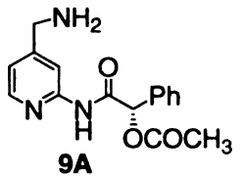

9A

Carrier A/carboxylic acid conjugates 9A:

^{1}H NMR (300 MHz, $CDCl_3$) δ 8.75 (br, 1H), 8.23 (d, *J*=4.9 Hz, 1H), 8.13 (s, 1H), 7.51 (m, 2H), 7.41 (m, 3H), 7.07 (d, *J*=4.9 Hz, 1H), 6.19 (s, 1H), 3.90 (s, 2H), 2.26 (s, 3H).

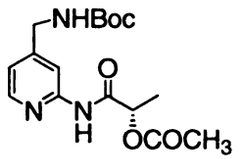

Boc-10A

Boc protected carrier A/carboxylic acid conjugates Boc-10A:

^{1}H NMR (300 MHz, $CDCl_3$) δ 8.66 (br, 1H), 8.23 (d, *J*=4.9 Hz, 1H), 8.14 (s, 1H), 7.03 (d, *J*=4.9 Hz, 1H), 5.35 (q, *J*=6.8 Hz, 1H), 5.02 (br, 1H), 4.33 (d, *J*=6.6 Hz, 2H), 2.22 (s, 3H), 1.56 (d, *J*=6.8 Hz, 3H), 1.48 (s, 9H).

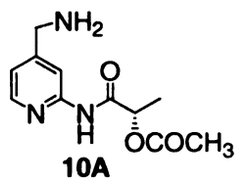

10A

Carrier A/carboxylic acid conjugates 10A:

^{1}H NMR (300 MHz, $CDCl_3$) δ 8.43 (br, 1H), 8.22 (d, *J*=4.9 Hz, 1H), 8.17 (s, 1H), 7.07 (d, *J*=4.9 Hz, 1H), 5.38 (q, *J*=6.6 Hz, 1H), 3.90 (s, 2H), 2.20 (s, 3H), 1.55 (d, *J*=6.6 Hz, 3H).

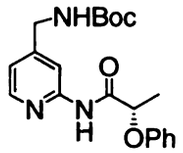

Boc-11A

Boc protected carrier A/carboxylic acid conjugates Boc-11A/12A:

^{1}H NMR (300 MHz, $CDCl_3$) δ 8.66 (br, 1H), 8.16 (m, 2H), 7.24 (m, 3H), 6.99 (m, 3H), 4.95 (br, 1H), 4.79 (q, *J*=6.9 Hz, 1H), 4.33 (d, *J*=6.6 Hz, 2H), 1.61 (d, *J*=6.9 Hz, 3H), 1.45 (s, 9H).

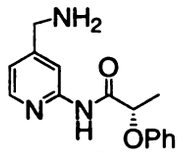

11A

Carrier A/carboxylic acid conjugates 11A/12A:

^{1}H NMR (300 MHz, $CDCl_3$) δ 8.82 (br, 1H), 8.23 (m, 2H), 7.28 (m, 3H), 6.99 (m, 3H), 4.78 (q, *J*=6.9 Hz, 1H), 3.91 (s, 2H), 1.63 (d, *J*=6.9 Hz, 3H).

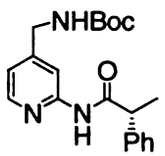

Boc-13A

Boc protected carrier A/carboxylic acid conjugates Boc-13A:

^{1}H NMR (300 MHz, $CDCl_3$) δ 8.54 (br, 1H), 8.14 (d, *J*=5.1 Hz, 1H), 7.96 (s, 1H), 7.38 (m, 5H), 6.93 (d, *J*=5.1 Hz, 1H), 4.93 (br, 1H), 4.30 (d, *J*=6.5 Hz, 2H), 3.72 (q, *J*=7.2 Hz, 1H), 1.57 (d, *J*=7.2 Hz, 3H), 1.44 (s, 9H).

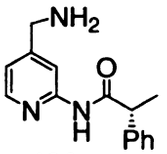

13A

Carrier A/carboxylic acid conjugates 13A:

^{1}H NMR (300 MHz, $CDCl_3$) δ 8.22 (br, 1H), 8.15 (d, *J*=5.1 Hz, 1H), 7.80 (s, 1H), 7.38 (m, 5H), 7.01 (d, *J*=5.1 Hz, 1H), 3.90 (s, 2H), 3.74 (q, *J*=7.2 Hz, 1H), 1.60 (d, *J*=7.2 Hz, 3H).

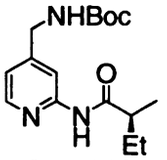

Boc-14A

Boc protected carrier A/carboxylic acid conjugates Boc-14A:

^{1}H NMR (300 MHz, $CDCl_3$) δ 8.21 (m, 2H), 7.99 (br, 1H), 6.95 (d, *J*=4.9 Hz, 1H), 4.95 (br, 1H), 4.36 (d, *J*=6.5 Hz, 2H), 2.27 (m, 1H), 1.78 (m, 1H), 1.51 (m, 1H), 1.43 (s, 9H), 1.22 (d, *J*=6.9 Hz, 1H), 0.94 (t, *J*=6.9 Hz, 3H).

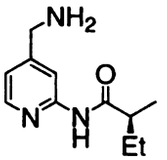

14A

Carrier A/carboxylic acid conjugates 14A:

^{1}H NMR (300 MHz, $CDCl_3$) δ 8.24 (m, 2H), 7.95 (br, 1H), 7.01 (d, *J*=4.9 Hz, 1H), 3.88 (s, 2H), 2.27 (m, 1H), 1.72 (m, 1H), 1.52 (m, 1H), 1.22 (d, *J*=6.9 Hz, 1H), 0.94 (t, *J*=6.9 Hz, 3H).

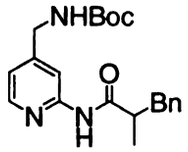

Boc-15A

Boc protected carrier A/carboxylic acid conjugates Boc-15A:

^{1}H NMR (300 MHz, $CDCl_3$) δ 8.12 (d, *J*=5.1 Hz, 1H), 7.81 (s, 1H), 7.25 (m, 6H), 6.92 (d, *J*=5.1 Hz, 1H), 5.03 (br, 1H), 4.30 (d, *J*=6.5 Hz, 2H), 3.08 (m, 1H), 2.66 (m, 2H), 1.60 (d, *J*=7.2 Hz, 3H), 1.46 (s, 9H).

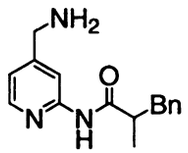

15A

Carrier A/carboxylic acid conjugates 15A:

^{1}H NMR (300 MHz, $CDCl_3$) δ 8.12 (d, *J*=5.1 Hz, 1H), 7.70 (s, 1H), 7.25 (m, 5H), 6.92 (d, *J*=5.1 Hz, 1H), 3.87 (s, 2H), 3.08 (m, 1H), 2.66 (m, 2H), 1.60 (d, *J*=7.2 Hz, 3H).

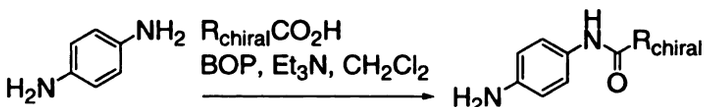

B **8B-16B**

General procedure for preparation of carrier B/carboxylic acid conjugates:

To a solution of carrier **B** (5 equiv) in CH_2Cl_2 (4 mL), BOP (1.1 equiv), triethylamine (5 equiv), and the chiral carboxylic acid (1 equiv) were added. The solution was stirred at room temperature overnight. After removal of most of the solvent under reduced pressure, the product was purified by silica gel flash column chromatography to yield the carrier **B**/acid conjugate ready for use for CD analysis.

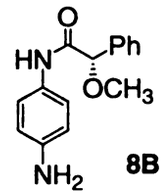

8B

Carrier B/carboxylic acid conjugates 8B:

^{1}H NMR (300 MHz, $CDCl_3$) δ 8.34 (br, 1H), 7.39 (m, 7H), 6.62 (d, *J*=8.8 Hz, 2H), 4.68 (s, 1H), 3.41 (s, 3H), 2.61 (br, 2H).

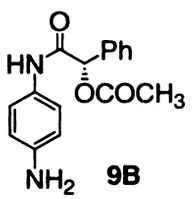

9B

Carrier B/carboxylic acid conjugates 9B:

^{1}H NMR (300 MHz, $CDCl_3$) δ 7.78 (br, 1H), 7.51 (m, 2H), 7.40 (m, 3H), 7.28 (d, *J*=8.2 Hz, 2H), 6.63 (d, *J*=8.2 Hz, 2H), 6.18 (s, 1H), 3.31 (br, 2H), 2.23 (s, 3H).

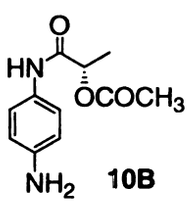

10B

Carrier B/carboxylic acid conjugates 10B:

^{1}H NMR (300 MHz, $CDCl_3$) δ 7.68 (br, 1H), 7.28 (d, *J*=8.8 Hz, 2H), 6.63 (d, *J*=8.8 Hz, 2H), 5.30 (q, *J*=7.14 Hz, 1H), 3.63 (br, 2H), 2.15 (s, 3H), 1.51 (d, *J*=7.14 Hz, 3H).

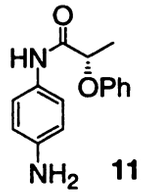

11B/12B

Carrier B/carboxylic acid conjugates 11B/12B:

^{1}H NMR (300 MHz, $CDCl_3$) δ 8.06 (br, 1H), 7.33 (m, 4H), 7.02 (m, 3H), 6.65 (d, *J*=8.8 Hz, 2H), 4.77 (q, *J*=6.6 Hz, 1H), 3.63 (br, 2H), 1.66 (d, *J*=6.6 Hz, 3H).

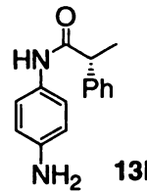

13B

Carrier B/carboxylic acid conjugates 13B:

^{1}H NMR (300 MHz, $CDCl_3$) δ 7.34 (m, 5H), 7.14 (d, *J*=8.8 Hz, 2H), 6.81 (br, 1H), 6.58 (d, *J*=8.8 Hz, 2H), 3.66 (q, *J*=7.1 Hz, 1H), 3.55 (br, 2H), 1.57 (d, *J*=7.1 Hz, 3H).

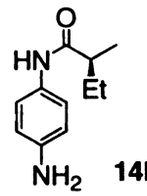

14B

Carrier B/carboxylic acid conjugates 14B:

^{1}H NMR (300 MHz, $CDCl_3$) δ 7.31 (br, 1H), 7.09 (d, *J*=8.8 Hz, 2H), 6.41 (d, *J*=8.8 Hz, 2H), 3.39 (br, 2H), 2.03 (m, 1H), 1.51 (m, 1H), 1.26 (m, 1H), 0.99 (d, *J*=6.6 Hz, 1H), 0.73 (t, *J*=6.6 Hz, 3H).

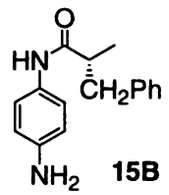

15B

Carrier B/carboxylic acid conjugates 15B:

^{1}H NMR (300 MHz, $CDCl_3$) δ 7.22 (m, 5H), 7.07 (d, *J*=8.8 Hz, 2H), 6.69 (br, 1H), 6.57 (d, *J*=8.8 Hz, 2H), 2.99 (m, 1H), 2.71 (m, 1H), 2.04 (m, 1H), 1.23 (d, *J*=6.6 Hz, 1H).

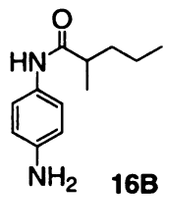

16B

Carrier B/carboxylic acid conjugates 16B:

^{1}H NMR ($CDCl_3$, 300 MHz) δ 7.30 (d, *J*=8.8 Hz, 2H), 7.12 (br, 1H), 6.67 (d, *J*=8.8Hz, 2H), 3.50 (br, 2H), 2.31 (m, 1H), 1.73 (m, 1H), 1.35 (m, 2H), 1.22 (d, *J*=6.6 Hz, 3H), 0.94 (d, *J*=7.7 Hz, 3H).

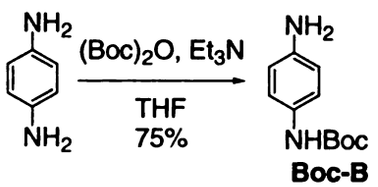

Boc-B

Boc-protected carrier B:

To a solution of carrier **B**, 1,4-diaminobenzene, (0.54 g, 5 mmol) in dry THF (10 mL) was added di-*t*-butyl dicarbonate (1.10 g, 5 mmol) and triethylamine (0.16 mL). A white precipitate was formed and redissolved immediately. This reaction mixture was stirred at room temperature overnight. The reaction was concentrated under reduced pressure, and the residue was purified by flash chromatography (75% yield). ^{1}H NMR

($CDCl_3$, 300 MHz) δ 6.98 (d, *J*=7.7 Hz, 2H), 6.50 (d, *J*=8.2 Hz, 2H), 3.35 (br, 2H), 1.34 (s, 9H).

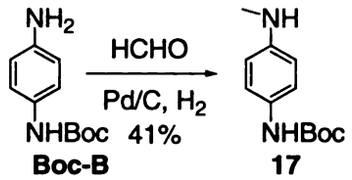

Methylated Boc-protected carrier B 17:

The protected carrier **Boc-B** (41.6 mg, 0.2 mmol) was dissolved in EtOAc (1 mL). Formaldehyde (0.25 mmol) and Pd/C (10 mg) were added. This solution was then hydrogenated with atmospheric pressure H_2 for 20 h. The black powder was filtered, and the filtrate was concentrated under reduced pressure, and purified by column chromatography to yield the title product **17** (41%). ^1H NMR ($CDCl_3$, 300 MHz) δ 7.14 (d, *J*=7.7 Hz, 2H), 6.51 (d, *J*=8.8 Hz, 2H), 3.51 (br, 1H), 2.74 (s, 3H), 1.48 (s, 9H).

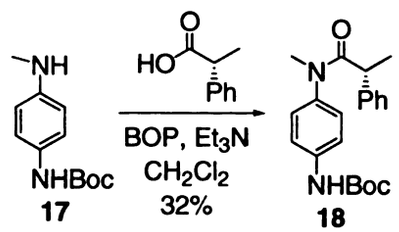

Methylated Boc-B/carboxylic acid conjugate 18:

To a solution of Boc protected carrier compound **17** (111 mg, 0.5 mmol) in CH_2Cl_2 (6 mL), BOP (250 mg, 0.55 mmol), triethylamine (1 mL), and the chiral acid (75 mg, 0.5 mmol) were added. The solution was stirred at room temperature overnight. After removal of most of the solvent under reduced pressure, the product was purified by silica gel flash chromatography (32% yield). ^1H NMR ($CDCl_3$, 300 MHz) δ 7.28 (d, *J*=8.8 Hz, 2H), 7.04 (d, *J*=7.7 Hz, 2H), 6.94 (d, *J*=8.2 Hz, 2H), 6.75 (m, 2H), 6.85 (d, *J*=8.2 Hz, 2H), 4.56 (q, *J*=6.6 Hz, 1H), 3.07 (s, 3H), 1.36 (s, 9H), 1.28 (d, *J*=6.0 Hz, 3H).

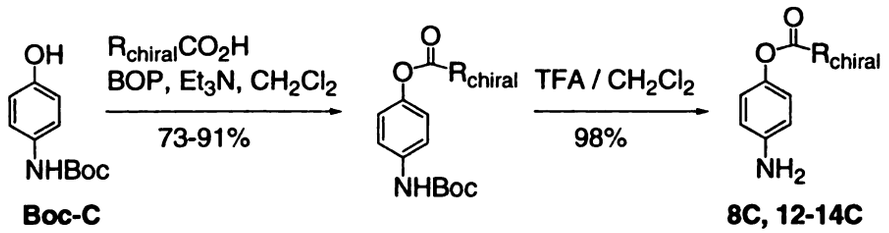

Boc-C **8C, 12-14C**

General procedure for preparation of carrier C/carboxylic acid conjugates:

To a solution of carrier **Boc-C** (5 equiv) in CH_2Cl_2 (4 mL), BOP (1.1 equiv), triethylamine (5 equiv), and the chiral carboxylic acid (1 equiv) were added. The solution was stirred at room temperature overnight. After removal of most of the solvent under reduced pressure, the product was purified by silica gel column chromatography to yield the Boc-protected acid conjugate. The Boc group was removed by stirring overnight in TFA/CH_2Cl_2 (1:4) at room temperature. The solvent was then removed by purging nitrogen. The residue was redissolved in anhydrous CH_2Cl_2, and anhydrous Na_2CO_3 (20 mg) was added. This solution was stirred at room temperature for an hour, and the Na_2CO_3 was filtered. The solvent was evaporated under reduced pressure to provide analytically pure product.

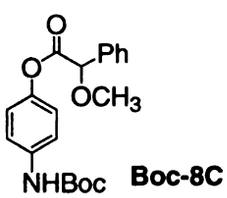

Boc-8C

Boc protected carrier C/carboxylic acid conjugates Boc-8C:

^{1}H NMR ($CDCl_3$, 300 MHz) δ 7.56 (m, 2H), 7.40 (m, 3H), 7.32 (d, *J*=8.8 Hz, 2H), 6.92 (d, *J*=8.8 Hz, 2H), 6.62 (br, 1H), 5.00 (s, 1H), 3.51 (s, 3H), 1.49 (s, 9H).

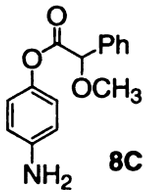

8C

Carrier C/carboxylic acid conjugates 8C:

^{1}H NMR ($CDCl_3$, 300 MHz) δ 7.56 (m, 2H), 7.40 (m, 3H), 6.78 (d, *J*=8.8 Hz, 2H), 6.61 (d, *J*=8.8 Hz, 2H), 4.99 (s, 1H), 3.52 (s, 3H).

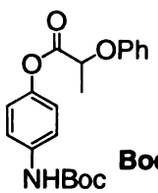

Boc-12C

Boc protected carrier C/carboxylic acid conjugates Boc-12C:

^{1}H NMR ($CDCl_3$, 300 MHz) δ 7.35 (m, 4H), 6.96 (m, 5H), 6.54 (br, 1H), 4.98 (d, *J*=7.1 Hz, 1H), 1.78 (q, *J*=7.1 Hz, 3H), 1.50 (s, 9H).

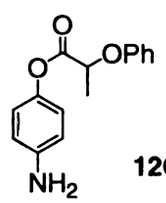

12C

Carrier C/carboxylic acid conjugates 12C:

^{1}H NMR ($CDCl_3$, 300 MHz) δ 7.33 (m, 2H), 6.98 (m, 3H), 6.82 (m, 4H), 5.76 (br, 1H), 4.95 (q, *J*=7.1 Hz, 1H), 1.78 (d, *J*=7.1 Hz, 3H).

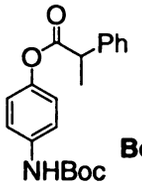

Boc-13C

Boc protected carrier C/carboxylic acid conjugates Boc-13C:

^{1}H NMR ($CDCl_3$, 300 MHz) δ 7.40-7.31 (m, 7H), 6.94 (d, *J*=8.8 Hz, 2H), 6.58 (br, 1H), 3.98 (q, *J*=7.1 Hz, 1H), 1.64 (d, *J*=7.1 Hz, 3H), 1.49 (s, 9H).

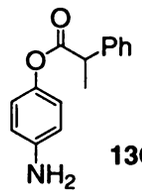

13C

Carrier C/carboxylic acid conjugates 13C:

^{1}H NMR ($CDCl_3$, 300 MHz) δ 7.36 (m, 5H), 6.79 (d, *J*=8.8 Hz, 2H), 6.64 (d, *J*=8.8 Hz, 2H), 3.92 (q, *J*=7.1 Hz, 3H), 3.32 (br, 2H), 1.62 (t, *J*=7.1 Hz, 3H).

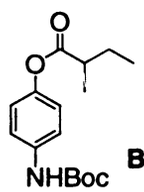

Boc-14C

Boc protected carrier C/carboxylic acid conjugates Boc-14C:

^{1}H NMR ($CDCl_3$, 300 MHz) δ 7.36 (d, *J*=8.8 Hz, 2H), 6.98 (d, *J*=8.8 Hz, 2H), 6.64 (br, 1H), 2.61 (m, 1H), 1.83 (m, 1H), 1.63 (m, 1H), 1.50 (s, 9H), 1.27 (q, *J*=7.1 Hz, 3H), 1.02 (t, *J*=7.1 Hz, 3H).

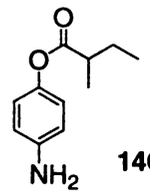

14C

Carrier C/carboxylic acid conjugates 14C:

^{1}H NMR ($CDCl_3$, 300 MHz) δ 6.88 (d, *J*=8.8 Hz, 2H), 6.69 (d, *J*=8.8 Hz, 2H), 3.39 (br, 2H), 2.60 (m, 1H), 1.81 (m, 1H), 1.64 (m, 1H), 1.26 (q, *J*=7.1 Hz, 3H), 1.02 (t, *J*=7.1 Hz, 3H).

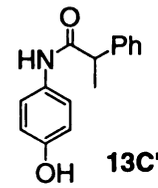

13C'

The synthesis of compound 13C':

To a stirred solution of PPh_3 (26.8 mg, 0.10 mmol), (*R*)-phenylpropionic acid (10 mg, 0.1 mmol) in anhydrous CH_2Cl_2 (0.5 mL) at 0 °C was added NBS (20 mg, 1.12 mmol) in one portion. The mixture was set aside at room temperature, while making the other solution. 4-Aminophenol (10.9 mg, 0.10 mmol) and pyridine (10.1 mg, 1.28 mmol) was dissolved in THF (0.5 mL), and the mixture was cooled to –25 °C. Then the first solution was added dropwise. The cooling bath was removed after 15 min and warm to room temperature. The solvent was removed under reduced pressure, and the residue was separated by column chromatography to yield the title compound (63%). ^{1}H NMR ($CDCl_3$, 300 MHz) δ 7.39 (m, 5H), 7.22 (d, *J*=8.8 Hz, 2H), 5.97 (br, 2H), 6.75 (d, *J*=8.8 Hz, 2H), 5.76 (br, 2H), 3.72 (q, *J*=7.1 Hz, 3H), 1.57 (t, *J*=7.1 Hz, 3H).

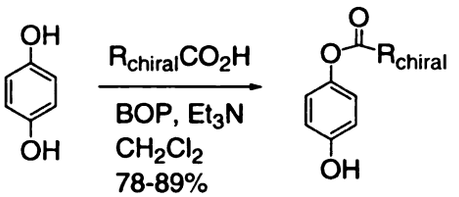

8D, 12D-14D

General procedure for preparation of carrier D/carboxylic acid conjugates:

To a solution of carrier **D** (5 equiv) in CH_2Cl_2 (4 mL), BOP (1.1 equiv), triethylamine (5 equiv), and the chiral acid (1 equiv) were added. The solution was stirred at room temperature overnight. After removal of most of the solvent under reduced pressure, the product was purified by silica gel column chromatography.

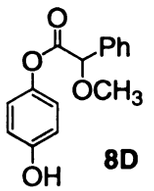

8D

Carrier D/carboxylic acid conjugates 8D:

^{1}H NMR ($CDCl_3$, 300 MHz) δ 7.56 (m, 2H), 7.42 (m, 3H), 6.84 (d, *J*=8.8 Hz, 2H), 6.75 (d, *J*=8.8 Hz, 2H), 5.73 (br, 2H), 4.99 (s, 1H), 3.50 (s, 3H).

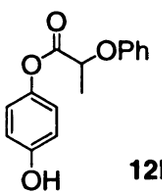

12D

Carrier D/carboxylic acid conjugates 12D:

^{1}H NMR ($CDCl_3$, 300 MHz) δ 7.32 (m, 3H), 7.02 (m, 2H), 6.87 (d, *J*=8.8 Hz, 2H), 6.79 (d, *J*=8.8 Hz, 2H), 4.98 (q, *J*=7.1 Hz, 1H), 1.78 (d, *J*=7.1 Hz, 3H).

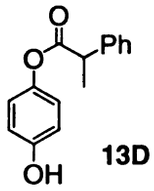

13D

Carrier D/carboxylic acid conjugates 13D:

^{1}H NMR ($CDCl_3$, 300 MHz) δ 7.36 (m, 5H), 6.82 (d, *J*=8.8 Hz, 2H), 6.76 (d, *J*=8.8 Hz, 2H), 5.23 (br, 2H), 3.96 (q, *J*=7.1 Hz, 3H), 1.62 (t, *J*=7.1 Hz, 3H).

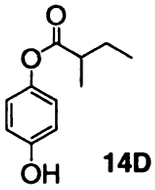

14D

Carrier D/carboxylic acid conjugates 14D:

^{1}H NMR ($CDCl_3$, 300 MHz) δ 6.90 (d, *J*=8.8 Hz, 2H), 6.77 (d, *J*=8.8 Hz, 2H), 6.38 (br, 2H), 2.62 (m, 1H), 1.83 (m, 1H), 1.67 (m, 1H), 1.28 (q, *J*=7.1 Hz, 3H), 0.99 (t, *J*=7.1 Hz, 3H).

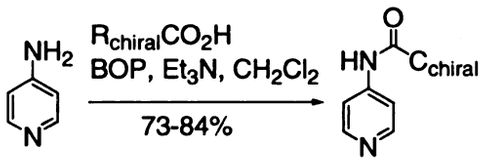

8E, 13E and 14E

General procedure for preparation of carrier E/carboxylic acid conjugates:

To a solution of carrier **E** (5 equiv) in CH_2Cl_2 (4 mL), BOP (1.1 equiv), triethylamine (5 equiv), and the chiral carboxylic acid (1 equiv) were added. The solution was stirred at room temperature overnight. After removal of most of the solvent under reduced pressure, the product was purified by silica gel column chromatography.

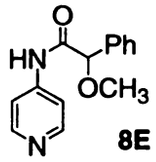

8E

Carrier E/carboxylic acid conjugates 8E:

^{1}H NMR ($CDCl_3$, 300 MHz) δ 8.79 (br, 1H), 8.45 (d, *J*=5.5 Hz, 2H), 7.56 (d, *J*=5.5 Hz, 2H), 7.37 (m, 5H), 4.74 (s, 1H), 3.41 (s, 1H).

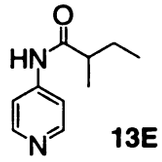

13E

Carrier E/carboxylic acid conjugates 13E:

^{1}H NMR ($CDCl_3$, 300 MHz) δ 8.45 (d, *J*=5.5 Hz, 2H), 7.64 (br, 1H), 7.58 (d, *J*=5.5 Hz, 2H), 2.39 (m, 1H), 1.79 (m, 1H), 1.57 (m, 1H), 1.24 (d, *J*=6.6 Hz, 3H), 0.99 (d, *J*=7.7 Hz, 3H).

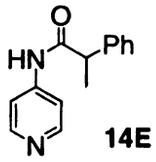

14E

Carrier E/carboxylic acid conjugates 14E:

^{1}H NMR ($CDCl_3$, 300 MHz) δ 8.30 (d, *J*=5.5 Hz, 2H), 7.44 (br, 1H), 7.57 (d, *J*=5.5 Hz, 2H), 7.27 (m, 5H), 3.77 (q, *J*=6.6 Hz, 1H), 1.62 (d, *J*=6.0 Hz, 3H).

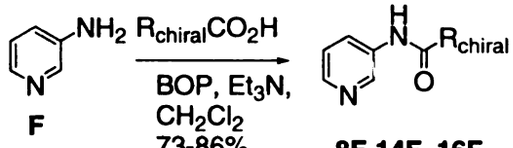

F **8F-14F, 16F**

General procedure for preparation of carrier F/carboxylic acid conjugates:

To a solution of carrier **F** (5 equiv) in CH_2Cl_2 (4 mL), BOP (1.1 equiv), triethylamine (5 equiv), and the chiral carboxylic acid (1 equiv) were added. The

solution was stirred at room temperature overnight. After removal of most of the solvent under reduced pressure, the product was purified by silica gel column chromatography.

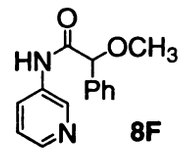

8F

Carrier F/carboxylic acid conjugates 8F:

^{1}H NMR ($CDCl_3$, 300 MHz) δ 8.64 (m, 2H), 8.39 (d, *J*=4.9 Hz, 1H), 8.13 (d, *J*=9.4 Hz, 1H), 7.58 (m, 5H), 7.23 (m, 1H), 4.80 (s, 1H), 3.45 (s, 3H).

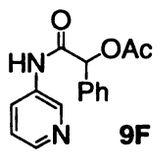

9F

Carrier F/carboxylic acid conjugates 9F:

^{1}H NMR ($CDCl_3$, 300 MHz) δ 8.57 (m, 2H), 8.34 (d, *J*=4.9 Hz, 1H), 8.18 (d, *J*=9.4 Hz, 1H), 7.51 (m, 2H), 7.40 (m, 3H), 7.23 (m, 1H), 6.19 (s, 1H), 2.27 (s, 3H).

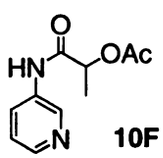

10F

Carrier F/carboxylic acid conjugates 10F:

^{1}H NMR ($CDCl_3$, 300 MHz) δ 8.61 (s, 1H), 8.39 (d, *J*=4.9 Hz, 1H), 8.22 (d, *J*=8.2 Hz, 1H), 8.10 (br, 1H), 7.30 (m, 1H), 5.37 (q, *J*=7.1 Hz, 1H), 2.12 (s, 1H), 1.58 (d, *J*=7.1 Hz, 3H).

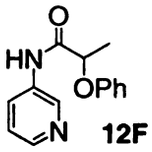

12F

Carrier F/carboxylic acid conjugates 12F:

^{1}H NMR ($CDCl_3$, 300 MHz) δ 8.62 (s, 1H), 8.37 (m, 2H), 8.20 (d, *J*=9.4 Hz, 1H), 7.40 (m, 3H), 7.23 (m, 3H), 4.85 (q, *J*=7.1 Hz, 1H), 1.69 (d, *J*=6.6 Hz, 3H).

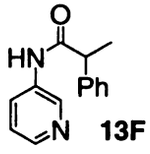

13F

Carrier F/carboxylic acid conjugates 13F:

^{1}H NMR ($CDCl_3$, 300 MHz) δ 8.45 (s, 1H), 8.32 (d, *J*=4.4 Hz, 1H), 8.20 (d, *J*=8.2 Hz, 1H), 7.48 (m, 6H), 3.78 (q, *J*=7.1 Hz, 1H), 1.63 (d, *J*=7.1 Hz, 3H).

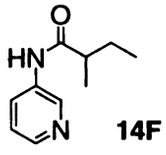

14F

Carrier F/carboxylic acid conjugates 14F:

^{1}H NMR ($CDCl_3$, 300 MHz) 8.61 (s, 1H), 8.37-8.22 (m, 2H), 7.43 (br, 1H), 7.33 (m, 1H), 2.37 (m, 1H), 1.79 (m, 1H), 1.57 (m, 1H), 1.22 (d, *J*=6.6 Hz, 3H), 1.01 (d, *J*=7.2 Hz, 3H).

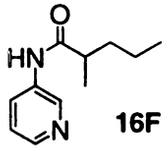

16F

Carrier F/carboxylic acid conjugates 16F:

^{1}H NMR ($CDCl_3$, 300 MHz) δ 8.53 (s, 1H), 8.37 (d, *J*=4.4 Hz, 1H), 8.19 (d, *J*=7.7 Hz, 1H), 7.37 (br, 1H), 7.26 (m, 1H), 2.36 (m, 1H), 1.70 (m, 1H), 1.42 (m, 2H), 1.22 (d, *J*=7.1 Hz, 3H), 0.89 (d, *J*=7.1 Hz, 3H).

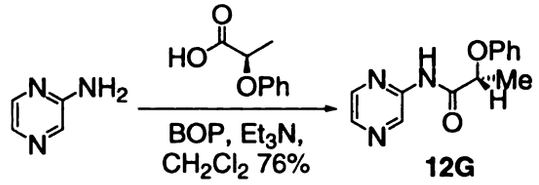

Carrier G derivative 12G:

To a solution of carrier **G** (5 equiv) in CH_2Cl_2 (4 mL), BOP (1.1 equiv), triethylamine (5 equiv), and the chiral acid (1 equiv) were added. The solution was stirred at room temperature overnight. After removal of most of the solvent under reduced pressure, the product was purified by silica gel flash chromatography. ^{1}H NMR ($CDCl_3$, 300 MHz) δ 9.71 (s, 1H), 8.78 (br, 1H), 8.37 (d, *J*=2.2 Hz, 1H), 8.21 (d, *J*=2.2 Hz, 1H), 7.28 (m, 2H), 6.98 (m, 3H), 4.82 (q, *J*=7.1 Hz, 1H), 1.64 (d, *J*=6.6 Hz, 3H).

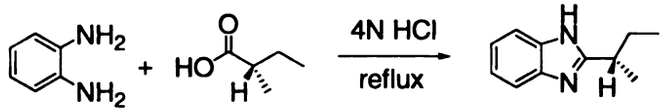

Carrier **H** **14H**

Carrier H derivative 14H:

o-Phenyldiamine (54 mg, 0.5 mmole) and (*S*)-2-methylbutyric acid (51 mg, 0.5 mmol) were dissolved in 4 N HCl (2 mL), and the solution was refluxed for 8 h, until it turned to dark red. It was then cooled to room temperature, and enough ammonium hydroxide was added in order to get precipitate. The precipitate was filtered and washed with water. It was then dried with a vacuum, however, the yield of this reaction was not determined because of the very small amount of the product. ^{1}H NMR ($CDCl_3$, 300 MHz) δ 7.60 (br, 1H), 7.26 (m, 4H), 3.04 (q, *J*=6.9 Hz, 1H), 1.86 (m, 2H), 1.46 (d, *J*=6.9 Hz, 3H), 0.96 (t, *J*=7.2 Hz, 3H).

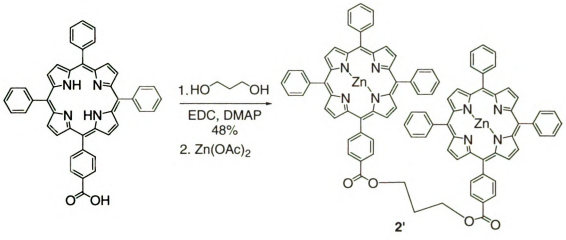

Porphyrin tweezer 2':

To a solution of porphyrin acid (90 mg, 0.14 mmol) and 1,3-propanediol (5 mg, 0.05 mmol) in anhydrous CH_2Cl_2 (4 mL) was added EDC (27 mg, 0.14 mmol) and DMAP (18 mg, 0.14 mmol). The reaction mixture was stirred at room temperature overnight and $Zn(OAc)_2$ (50 mg) was added. The reaction was stirred for another 2 h, and it was then applied directly to silica gel column and purified (CH_2Cl_2) to afford the title compound **2'** (48%). ^{1}H NMR ($CDCl_3$, 300 MHz) δ 8.94-9.04 (m, 16H), 8.48 (d, *J*=8.0 Hz, 4H), 8.17-8.23 (m, 16H), 7.46-7.54 (m, 18H), 4.71 (t, *J*=6.6 Hz, 4H), 2.43 (t, *J*=6.6 Hz, 2H).

Reference:

1. Harada, N.; Nakanishi, K. *Circular Dichroic Spectroscopy: Exciton Coupling in Orgainc Stereochemistry*, ed.; University Science Books: Mill Valley, **1983**.

2. Huang, X. F.; Rickman, B. H.; Borhan, B.; Berova, N.; Nakanishi, K. *J. Am. Chem. Soc.* **1998**, *120*, 6185.

3. Huang, X.; Borhan, B.; Rickman, B. H.; Nakanishi, K.; Berova, N. *Chem. Eur. J.* **2000**, *6*, 216.

4. Tyrrell, E.; Tsang, M. W. H.; Skinner, G. A.; Fawcett, J. *Tetrahedron* **1996**, *52*, 9841.

5. Nagai, Y.; Kusumi, K. *Tetrahedron Lett.* **1995**, *36*, 1853.

6. Kusumi, K.; Yabuuchi, T.; Ooi, T. *Chirality* **1997**, *9*, 550.

7. Mizutani, J.; Tahara, S. *Tetrahedron Lett.* **1996**, *37*, 4737.

8. Ferreiro, M. J.; Latypov, S. K.; Quinoa, E.; Riguera, R. *J. Org. Chem.* **2000**, *65*, 2658.

9. Barker, R. *Organic Chemistry of Biological Compounds*; Prentice-Hall: New Jersey, **1971**.

10. Seco, J. M.; Quinoa, E.; Riguera, R. *Tetrahedron: Asymmetry* **2001**, *12*, 2915.

11. Berova, N.; Nakanishi, K. *Circular Dichroism, Principles and Applications*, 2nd ed.; Wiley-VCH: New York, **2000**.

12. Rickman, B. H.; Matile, S.; Nakanishi, K.; Berova, N. *Tetrahedron* **1998**, *54*, 5041.

13. Hor, K.; Gimple, O.; Schreier, P.; Humpf, H. -U. *J. Org. Chem.* **1998**, *63*, 322.

14. Nakaya, T.; Tomomoto, T.; Imoto, M. *Bull. Chem. Soc. Jpn.* **1967**, *40*, 691.

15. Andersson, L.; Kenne, L. *Carbohydr. Res.* **2003**, *338*, 85.

16. Barth, G.; Voelter, W.; Mosher, H. S.; Bunnenberg, E.; Djerassi, C. *J. Am. Chem. Soc.* **1970**, *92*, 875.

17. Proni, G.; Pescitelli, G.; Huang, X.; Quraishi, N. Q.; Nakanishi, K.; Berova, N. *Chem. Commun.* **2002**, 1590.

18. Proni, G.; Pescitelli, G.; Huang, X.; Nakanishi, K.; Berova, N. *J. Am. Chem. Soc.* **2003**, *125*, 12914.

19. Hall, J. H.; Gisler, M. *J. Am. Chem. Soc.* **1976**, *41*, 3769.

20. Fehrentz, J. A.; Castro, B. *Synthesis* **1983**, 676.

21. Eliel, E. L.; Wilen, S. H. *Stereochemistry of Organic Compounds*; John Wiley & Sons, Inc.: New York, **1994**.

22. Sigel, H.; Martin, R. B. *Chem. Rev.* **1982**, *82*, 385.

23. Kurtan, T.; Nesnas, N.; Li, Y. Q.; Huang, X. F.; Nakanishi, K.; Berova, N. *J. Am. Chem. Soc.* **2001**, *123*, 5962.

24. Jimenez, A. I.; Cativiela, C.; Gomez-Catalan, J.; Perez, J. J.; Aubry, A.; Paris, M.; Marraud, M. *J. Am. Chem. Soc.* **2000**, *122*, 5811.

25. Adams, H.; Harris, K. D. M.; Hembury, G. A.; Hunter, C. A.; Livingstone, D.; McCabe, J. F. *Chem. Commun.* **1996**, 2531.

26. Crisma, M.; Formaggio, F.; Valle, G.; Toniolo, C.; Saviano, M.; Iacovino, R.; Zaccaro, L.; Benedetti, E. *Biopolymers* **1997**, *42*, 1.

27. Klotz, P.; Chatrenet, B.; Coppo, M.; Rousseau, B.; Goeldner, M.; Hirth, C. *J. Labeled Compd. Radiopharm.* **1991**, *XXIX*, 149.

28. Kessler, P.; Chatrenet, B.; Goeldner, M.; Hirth, C. *Synthesis* **1990**, 1065.

29. Latypov, S. K.; Galiullina, N. F.; Aganov, A. V.; Kataev, V. E.; Riguera, R. *Tetrahedron* **2001**, *57*, 2231.

30. Froyen, P. *Tetrahedron Lett.* **1997**, *38*, 5359.

31. Lindsey, J. S.; Woodford, J. N. *Inorg. Chem.* **1995**, *34*, 1063.

32. O'Shea, D. F.; Miller, M. A.; Matsueda, H.; Lindsey, J. S. *Inorg. Chem.* **1996**, *35*, 7325.

33. Pecsok, R. L.; Shields, L. D.; Cairns, T.; Mcwilliam, I. B. *Modern Methods of Chemical Analysis*, 2nd. ed.; John Wiley & Sons, Inc.: New York, **1976**.

34. Hara, H.; van der Plas, H. C. *J. Heterocyclic Chem.* **1982**, *19*, 1285.

35. van der Haak, H. J. W.; van der Plas, H. C.; van Veldhuizen, B. *J. Org. Chem.* **1981**, *46*, 2134.

36.

37.

38.

39.

36. Wang, H.; Partch, R.; Li, Y. *J. Org. Chem.* **1997**, *62*, 5222.

37. Weiss, J. *J. Inclusion Phenom. Macrocyclic Chem.* **2001**, *40*, 1.

38. Mizutani, J.; Kurahasci, T.; Murakami, T.; Matsumi, N.; Ogoshi, H. *J. Am. Chem. Soc.* **1997**, *119*, 8991.

39. Huang, X.; Rickman, B.; Borhan, B.; Berova, N.; Nakanishi, K. *J. Am. Chem. Soc.* **1998**, *120*, 6185.

Chapter 4

The stereochemical determination of α-chiral halocarboxylic acids

In chapter 3, we have shown in detail the absolute stereochemical determination of α-chiral carboxylic acids by using different carriers in conjunction with porphyrin tweezer. The extension of this methodology was applied to the stereochemical determination of α-chiral halocarboxylic acids. α-Chiral halocarboxylic acids were first derivatized with carrier **A** and carrier **B**. The syntheses of (*R*)-2-bromopropionic acid derivatives, **A-1-Br** and **B-1-Br**, are shown in Scheme 4-1.

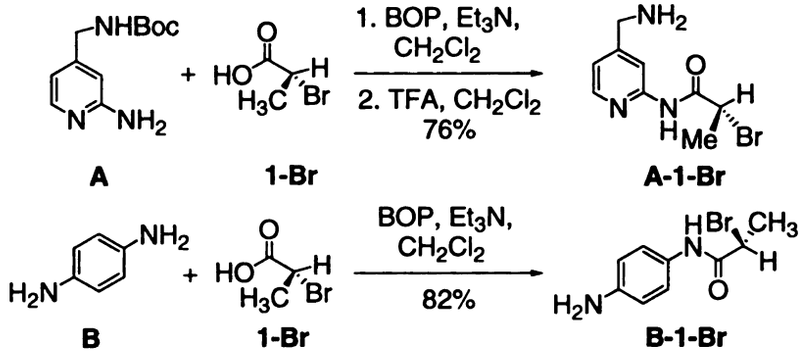

Scheme 4-1. The derivitization of (*R*)-2-bromopropionic acid **1-Br** to carrier **A** and **B**.

The carrier **A** derivative **A-1-Br** showed a small positive ECCD sign with λ_{ext} 427 nm (Δε +9) and 420 nm (Δε -13), A +21 at room temperature. But since carrier **A** derivatives were found unreliable for stereochemical assignment in our previous studies, further use of this carrier was abandoned.

The carrier **B** derivative **B-1-Br** exhibited a very strong negative ECCD sign with λ_{ext} 430 nm (Δε -236) and 421 nm (Δε +136), A -372 at room temperature, and the signal became even stronger (A = –643) when it was cooled to 0 °C. However, this sign was opposite to the predicted sign from the proposed mnemonic in Section 3-2, shown in

Figure 4-1. According to A values,[1] bromo was considered as the medium group, and methyl group as large, thus a positive ECCD was predicted.

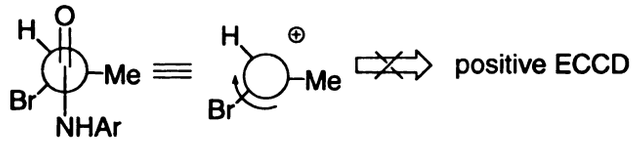

Figure 4-1. The contradiction of the observed ECCD sign vs. the predicted sign based on the mnemonic.

4-1. Synthesis of α-chiral halocarboxylic acids and the ECCD data of carrier B derivatives.

The deviation observed with (*R*)-2-bromopropionic acid derivative **B-1-Br** was investigated with a series of α-chiral halocarboxylic acids. In order to study the behaviors of the α-chiral halocarboxylic acids derivatives in more detail, a series of α-chiral halocarboxylic acids were synthesized from chiral amino acids and derivatized with carrier **B**. The general procedures for the synthesis of α-chiral halocarboxylic acids from amino acids are shown in Scheme 4-2.

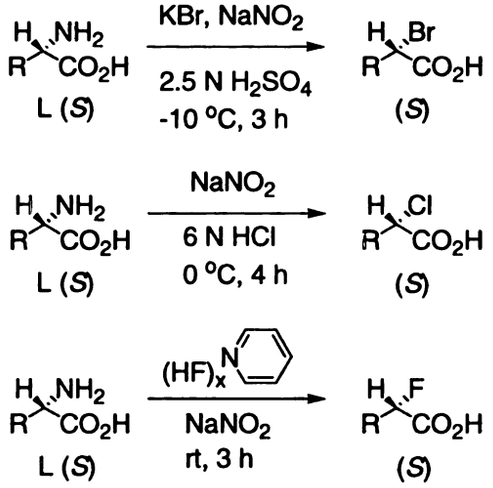

Scheme 4-2. The synthesis of α-chiral halocarboxylic acids.

The α-chiral halocarboxylic acids could be easily synthesized from optically pure amino acids.[2] Bromination of the L-(*S*)-amino acids with potassium bromide and sodium nitrite in 2.5 N sulfuric acid afforded α-chiral bromocarboxylic acids. The chiral α-chlorocarboxylic acids and α-fluorocarboxylic acids could also be synthesized in a similar manner. α-Chloro chiral carboxylic acids were produced by adding sodium nitrite to a vigorously stirred solution of L-(*S*)-amino acids in 2.5 N HCl, and α-fluoro chiral carboxylic acids were synthesized by treating L-(*S*)-amino acids with sodium nitrite and hydrogen fluoride-pyridine as the reaction solvent. These reactions proceeded with retention of stereochemistry,[2] and it was the result of double inversion at the chiral center, as shown in Scheme 4-3.

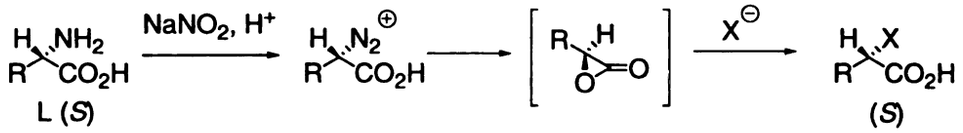

Scheme 4-3. The mechanism of the α-chiral halocarboxylic acids synthesis.

Under the acidic reaction conditions, sodium nitrite reacted with the amino group to generate a diazo intermediate. The diazo moiety was a good leaving group, which was subsequently replaced by the free carboxylic acid functionality to form a very unstable lactone intermediate, which upon nucleophilic attack of the halide formed the chiral halocarboxylic acids.

The reactions were completed in four hours, and the products were easily separated from the reaction mixture by extraction with dichloromethane. The crude yield of these chiral carboxylic acids varied from 42% to 67%. Without further purification, these chiral acids were coupled with carrier **B**, 1,4-diaminobenzene. The amino acids

utilized for our studies were L-alanine, L-valine, L-leucine, L-isoleucine and L-phenylalanine.

The enantiomeric ratio for each of the α-chiral halocarboxylic acids was determined by derivatizing the chiral acids with chiral (*S*)-methylbenzylamine by BOP coupling reaction. The reaction was stirred at room temperature overnight, and was analyzed by GC-MS to determine the retention time of the two diastereomers. The diastereomeric ratio was then determined by calculating GC peak areas. The enantiomeric ratio of the α-chiral halocarboxylic acids is listed in table 4-1.

Table 4-1. The enantiomeric ratio for chiral α-halogen carboxylic acids.

Chiral acids	X = Br	X = Cl	X = F
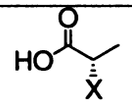 **1**	99%	99%	50%
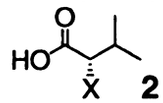 **2**	90%	90%	64%
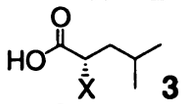 **3**	90%	90%	>80%
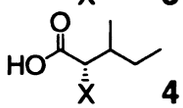 **4**	80%	80%	80%
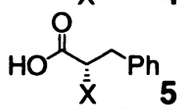 **5**	90%	75%	56%

The synthesized α-chiral halocarboxylic acids were coupled to carrier **B** with standard BOP coupling reaction, and all the reactions underwent smoothly. The carrier **B** derivatized complexes were then added to zinc porphyrin tweezer for spectroscopic evaluation.

Table 4-2. The CD data of carrier **B** derivatives of α-chiral halocarboxylic acids.

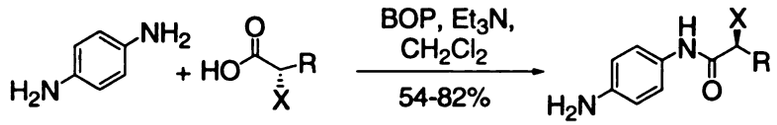

Chiral acids derivatives	X = Br		X = Cl		X = F	
	Δε	A	Δε	A	Δε	A
HO, X, O **1**	(*R*) 430 (-236) 421 (+136)	-372	(*S*) 429 (+25) 421 (-38)	+63	(*S*) 428 (+34) 419 (-31)	+65
HO, X, O **2(*S*)**	429 (+103) 421 (-91)	+194	429 (+132) 421 (-82)	+214	428 (+114) 420 (-93)	+207
HO, X, O **3(*S*)**	429 (+107) 421 (-75)	+182	429 (+24) 421 (-30)	+54	429 (+31) 420 (-30)	+61
HO, X, O **4(*S*)**	429 (+94) 421 (-81)	+175	429 (+108) 421 (-124)	+232	429 (+96) 420 (-66)	+162
HO, X, Ph, O **5(*S*)**	429 (+47) 421 (-43)	+90	429 (+22) 421 (-19)	+41	428 (+18) 419 (-22)	+40

The CD data for all the chiral α-halogen carboxylic acids derivatized with carrier **B**, 1,4-diaminobenzene, are summarized in Table 4-2. The CDs were taken by adding the chiral conjugates to zinc porphyrin tweezer in methylcyclohexane at room temperature. All the derivatives exhibited ECCD spectra that were consistent for all α-chiral halocarboxylic acids, i.e., ECCD for (*R*)-acids were negative and ECCD for (*S*)-acids were positive.

A chiral iodocarboxylic acid was also synthesized to see that if the ECCD sign for the chiral iodo compounds would be consistent with the other halogen containing carboxylic acids derivatives. The α-chiral bromo-, chloro-, and fluoro- carboxylic acids were synthesized from natural amino acids in a single step,[2] in which the free amino group was transformed to diazo intermediate, and then replaced by halogens. However,

since the iodo functionality was too reactive, the chiral α-iodocarboxylic acid could not be synthesized by this simple method.

Alternatively, the chiral iodocarboxylic acids could be synthesized by the Finkelstein[3] reaction starting with the corresponding chiral bromo carboxylic acids. As shown in Scheme 4-4, the (*S*)-2-iodopropionic acid **1-I** was synthesized by refluxing (*R*)-2-bromopropionic acid **1-Br** in acetonitrile overnight with excess amount of potassium iodide. In this process, the stereochemistry at the chiral center was inverted.

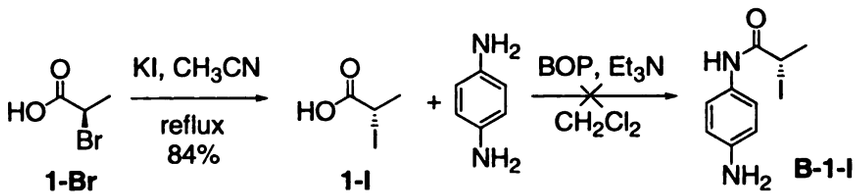

Scheme 4-4. The attempted synthesis of carrier **B** derivatized iodocarboxylic acid **B-1-I**.

Without any further purification, the (*S*)-2-iodopropionic acid **1-I** was coupled with carrier **B**, 1,4-diaminobenzene, by a standard BOP coupling. However, this routine amidation reaction did not yield the desired product and led to many unidentified compounds. The problem could be that the iodide was too reactive, and might be displaced by nucleophilic attack with another molecule of 1,4-diaminobenzene.

In order to synthesize the carrier **B** derivatized chiral iodocarboxylic acid **B-1-I**, the order of the reactions was changed. As illustrated in Scheme 4-5, the free amino group in the carrier **B** was first protected with Boc, and then esterified under BOP coupling condition with (*R*)-bromopropionic acid to form **BocB-1-Br**. The synthesis of desired compound **B-1-I** was finished by replacing the bromo with iodo group by the Finkelstein reaction,[3] and followed by deprotection.

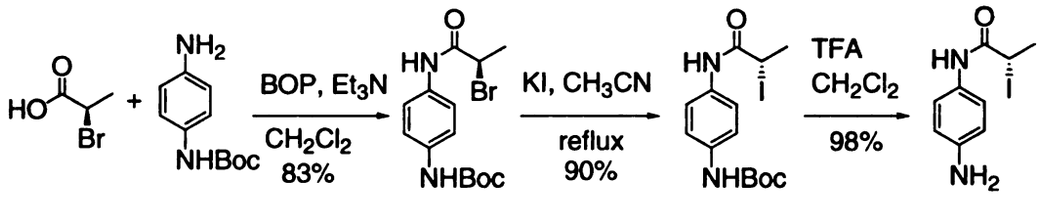

1-Br **BocB-1-Br** **B-1-I**

Scheme 4-5. The synthesis of carrier **B** derivatized (*S*)-2-iodopropionic acid **B-1-I**.

The complex **B-1-I** was added to zinc porphyrin tweezer in methylcyclohexane and led to a positive ECCD sign at 0 °C (λ_{ext} 431 nm ($\Delta\varepsilon$ +21) and 417 nm ($\Delta\varepsilon$ -28), A +48), which is consistent with all the other carrier **B** derivatized α-chiral halocarboxylic acids. However, the iodo complex **B-1-I** was unstable and reproducible ECCD could not be obtained if the iodo compound was stored for days.

As described above, carrier **B** derivatives of chiral α-halogen carboxylic acids exhibit consistent ECCD spectra for all types of halogens tested thus far, with negative ECCD for (*R*) and positive ECCD for (*S*) chirality. However, the observed ECCD of carrier **B** derivatives of chiral α-halocarboxylic acids are opposite to the sign predicted based on the mnemonic proposed for carrier **B** (see Section 3-2).

Figure 4-2 illustrated the observed and predicted ECCD of carrier **B** derivatized (*S*)-2-bromo-3-methylbutyric acid **B-2-Br**. According to the proposed mnemonic for carrier **B**, the large *i*-Pr group was perpendicular to the carbonyl group, and the medium bromo group was gauche to amide hydrogen. The counterclockwise orientation from large to medium to small group would result in a negative ECCD couplet. However, the chiral complex exhibited a strong positive ECCD couplet, with λ_{ext} 429 nm ($\Delta\varepsilon$ +103) and 421 nm ($\Delta\varepsilon$ -91), A +194.

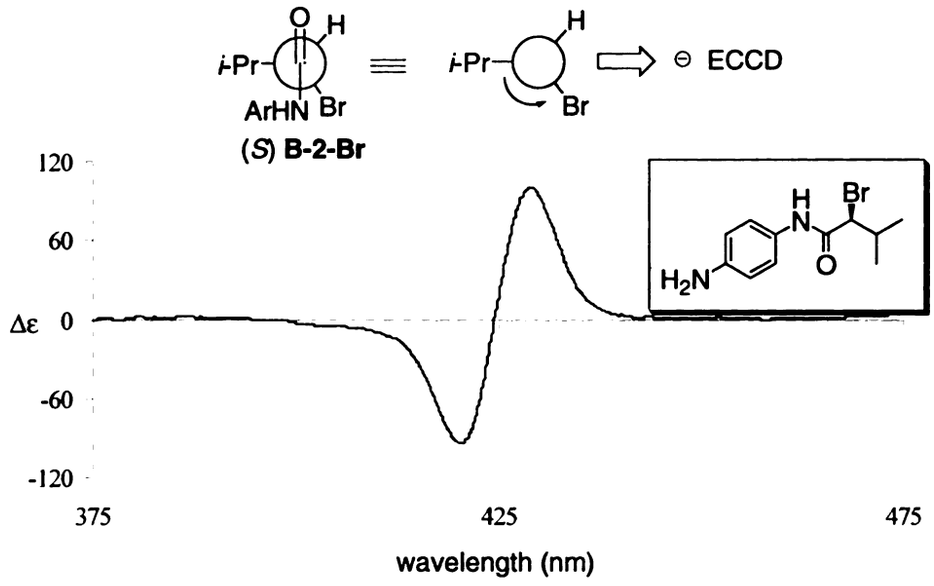

Figure 4-2. The observed and predicted ECCD of **B-2-Br**.

4-2. Explanations for the unexpected ECCD of carrier B derivatized α-chiral halocarboxylic acids

In order to explain the inconsistency between the observed ECCD of the carrier **B** derivitized chiral α-halocarboxylic acids and the predicted signs based on the proposed mnemonic (see Section 3-2), three hypotheses were proposed (Figure 4-3).

(*a*) Electronic factors overcome the steric control of the substituents in determining the sign of the ECCD couplet, by causing the halogens to behave as the large group and positioning themselves perpendicular to carbonyl;

(*b*) The halogen on the chiral center and not the carbonyl oxygen coordinates with the zinc porphyrin tweezer, resulting in a new orientation between the two interacting porphyrins;

(*c*) The carbonyl oxygen and the halogen on the chiral center cooperatively bind to the zinc porphyrin tweezer in a bi-dentate fashion leading to a new paradigm for binding porphyrins.

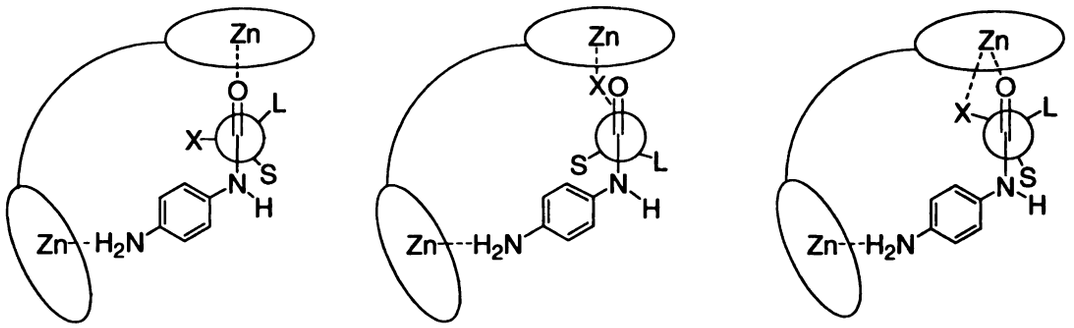

Figure 4-3. Possible conformations leading to the observed ECCD sign: (***a***) halogen behaves as the large group and is perpendicular to carbonyl; (***b***) the halogen binds to zinc porphyrin tweezer; (***c***) cooperative binding of halogen and the carbonyl oxygen to zinc porphyrin tweezer.

4-2.1. Determining the rotation of C_{α}-$C_{c=o}$ bond by NMR study

From the latter discussion, it was clear that the configuration of the C_{chiral}-$C_{C=O}$ bond could adopt various rotomers. The rotation around the C_{chiral}-$C_{C=O}$ bond directly dictated the observed ECCD sign, so it was critical to understand the rotation around the C_{chiral}-$C_{C=O}$ bond. We relied on NMR of carrier **B** derivatives and other amides to investigate the single bond conformation.

The (*R*)-2-bromopropionic acid **1-Br** was derivatized with (*R*) and (*S*)-2-phenylmethylamine **6**. The preferred conformation of the amide bond has been extensively studied and understood, placing the hydrogen on the chiral amine center *syn* to the carbonyl oxygen due to $A_{1,3}$ strain (Figure 4-4).[4-7] With the amide conformation locked, we were interested in determining the preferred conformation around the C_{chiral}-$C_{C=O}$ bond using NMR. Depending on the favored conformation of the C_{chiral}-$C_{C=O}$ bond, the substituents on the chiral center would be placed either inside or outside the

anisotropic cone of the neighboring phenyl group, experiencing different shielding effects.

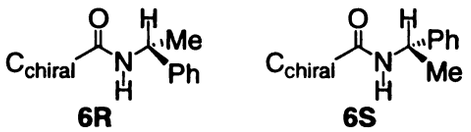

Figure 4-4. The conformation of the amide part in the derivatives.

Standard BOP coupling between the (*R*)-2-bromopropionic acid **1-Br** and chiral amines (*R*) and (*S*)-2-phenylmethylamine **6** provided diastereomers **6R** and **6S**, the NMR spectra of which (in $CDCl_3$) are shown in Figure 4-5.

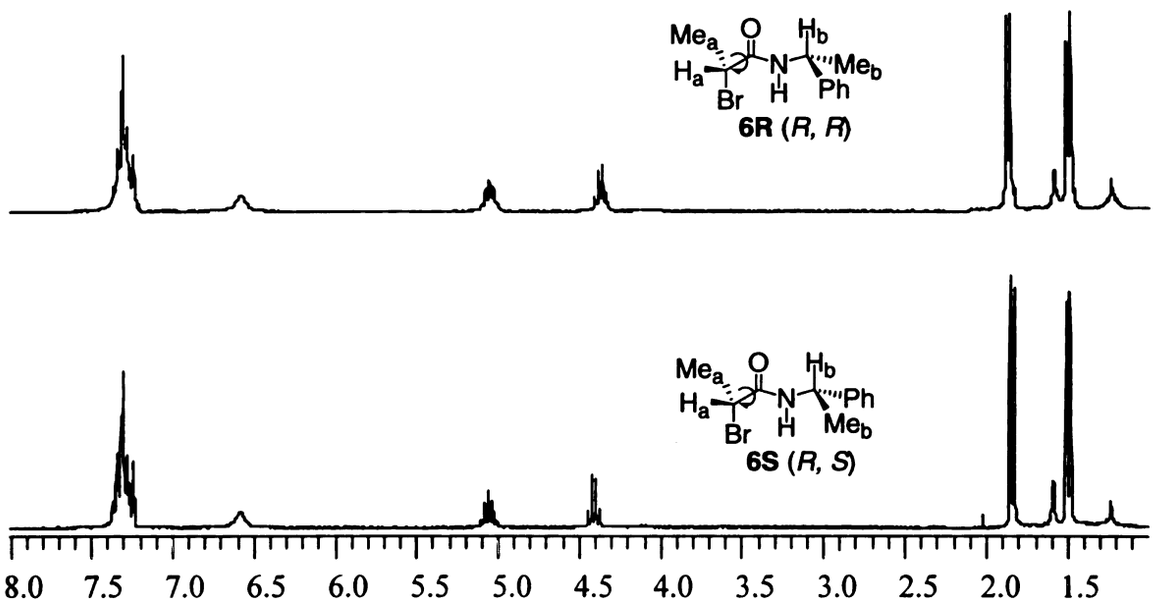

Figure 4-5. NMR of compounds **6R** and **6S**.

In the spectra shown in Figure 4-5, H_a appears at ~4.4 ppm, and the methyl group (Me_a) resonated at ~1.8 ppm. H_a shifts downfield in the **6S** (*R*, *S*) diastereomer, while Me_a has slightly upfield shifted. Same results were obtained both at room temperature and 0 °C. These results suggested that, as shown in Figure 4-5, in the **6R** (*R*, *R*) diastereomer case, the methyl group on the carboxylic acid chiral center (Me_a) is on the

same side of the phenyl group, while the corresponding hydrogen (H_a) is on the same side as the methyl group of the amide chiral center (Me_b).

Although the above study provided important indication for the preferred conformation of the free **6R** and **6S** in solution, we were reluctant in using these results to extrapolate conformational information for the complexed porphyrin tweezer system. Upon binding to the zinc porphyrin tweezer, the C_{chiral}-$C_{C=O}$ bond conformation could change, making the above analysis ambiguous. Therefore, these results were not conclusive to be of help for the actual system.

4-2.2. The study with carrier B derivative of 2-trifluoromethylpropionic acid

As discussed before, we were interested in determining the cause of the unique behavior of α-chiral halocarboxylic acids as compared to the other α-chiral carboxylic acids we had already studied (see Section 3-2). One of the suggestions was that the strong electronegativity of the halogens overcame the steric factor by forcing the halogen substituents to behave as the large group.[8, 9]

In order to address this issue, we were interested in synthesizing α-trifluoromethyl containing chiral acids, and derivatize them with carrier **B**. These carboxylic acids have a strong electron withdrawing group, $-CF_3$, and their complexation with porphyrin tweezers were expected to give us some insight into our hypotheses for the α-chiral halocarboxylic acids derivatives. In particular, if the ECCD signs of the carrier **B** derivatized α-trifluoromethyl chiral carboxylic acids were consistent with those of chiral halocarboxylic acid derivatives, the electronegativity argument expressed before could be valid. If not, we need to address this issue otherwise.

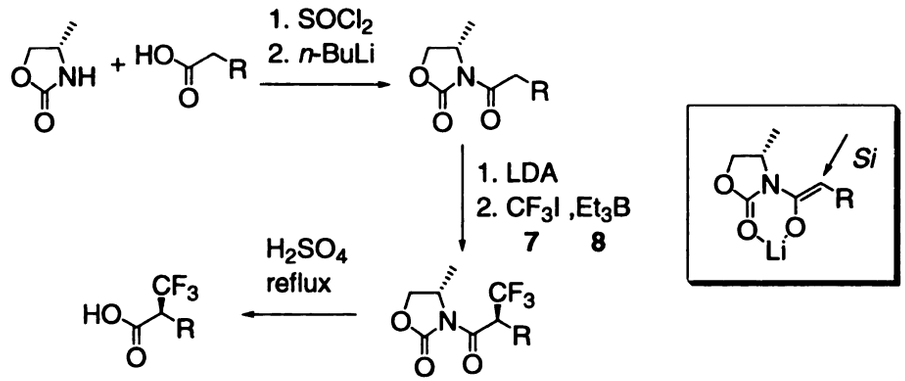

Scheme 4-6. The proposed synthesis of chiral 2-trifluoromethyl carboxylic acids.

The plan for synthesizing the trifluoromethyl containing chiral acids is shown in Scheme 4-6. In order to introduce the trifluoromethyl group at the α position in a stereoselective manner, a chiral auxiliary is necessary. After the carboxylic acid was coupled with the Evans' chiral auxiliary, a chiral imide enolate could be generated by treatment with LDA. Trifluoromethylation was then accomplished by addition of excess amount of iodotrifluoromethane **7** in the presence of triethylborane **8**, which was to accelerate this reaction.[10] The trifluoromethyl radical thus adds with a C(α)-*si*-face preference to the Li-chelated transition state. At the final step, the chiral auxiliary could be removed by hydrolysis to provide the desired chiral 2-trifluoromethyl carboxylic acids.[4] Although the aforementioned synthetic scheme looks promising, several problems were encountered when the chemistry was actually applied.

Both of the reagents used in the above scheme, trifluoromethyl iodide **7** and triethylborane **8**, are commercially available. However, due to their high expense, we decided to synthesize them. The syntheses of those two compounds have been previously reported and are not complicated.[11, 12, 13]

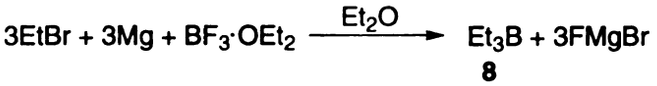

Scheme 4-7. The synthesis of triethylborane **8**.

As shown in Scheme 4-7, triethylborane **8** could be easily synthesized by reacting trifluoroborane etherate with ethyl magnesium bromide, generated *in situ*.[11, 12] The challenge lies in the separation and purification of the product from the reaction mixture, mostly because triethylborane is pyrophoric. Upon exposure to air, even during transferring between flasks, triethylborane caught fire, which made its purification by distillation impossible. So finally, triethylborane was purchased in order to move on with the rest of the synthesis.

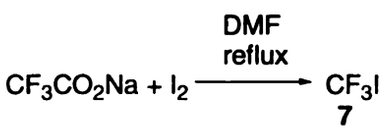

Scheme 4-8. The synthesis of trifluoromethyl iodide **7**.

At the same time, trifluoromethyl iodide **7** could be synthesized by refluxing iodine with sodium salt of trifluoroacetic acid in dry dimethylformamide, as illustrated in Scheme 4-8.[13] Since the boiling point of the resulting trifluoromethyl iodide is about –40 °C, it could be distilled from the reaction mixture and collected by cooling the collecting flask at –78 °C. Although the synthesis of the trifluoromethyl iodide **7** proceeded smoothly, its storing and handling for further use was problematic. The rubber septum used to cover the trifluoromethyl idodide container became very brittle and stiff when the flask was kept in the –80 °C freezer. Moreover, since the trifluoromethyl iodide was a gas at room temperature, it was very hard to determine the extract amount used in the trifluoromethylation reaction.

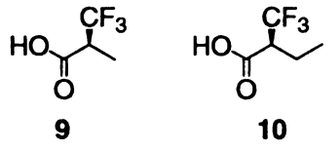

Figure 4-6. The structures of 2-trifluoromethylpropionic acid **9** and 2-trifluoromethylbutyric acid **10**.

With the reagents **7** and **8** in hand, we were ready to synthesize 2-trifluoromethyl chiral carboxylic acids. The first two targets were 2-trifluoromethylpropionic acid **9**, and 2-trifluoromethylbutyric acid **10**, the structures of which are shown in Figure 4-6.

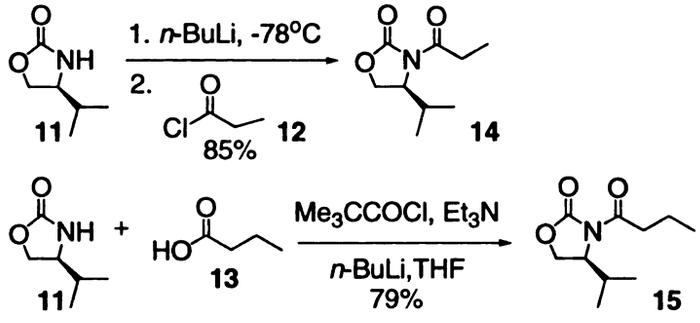

Scheme 4-9. The amidation with Evans' chiral auxiliary.

The first step for the synthesis of trifluoromethyl containing chiral acids involved the coupling of the acids or acid derivatives, with the Evans' chiral auxiliary (*S*)-4-isopropyl-2-oxazolidinone **11**. In our case propionyl chloride **12** and butyric acid **13** were used, as shown in Scheme 4-9, in order to form the chiral amides with oxazolidinone **11**. Propionyl chloride **12** could directly react with the Evans' chiral auxiliary **11** under strong basic conditions to generate the chiral amide **14** at low temperature.[4] On the other hand, butyric acid **13** had to be activated with pivaloyl chloride to form a more reactive mixed anhydride first, which was then coupled with the deprotonated chiral auxiliary **11** to form the chiral amide **15**.[14]

Although both of the reactions worked, column chromatography purification was needed to acquire pure products **14** and **15**. However, the identification of the product eluted was problematic, since all the starting materials and products of the above reactions were neither UV active or showed strong color in the presence of different dyes. Therefore, GC-MS was used to determine the component in each of the fractions of the column, instead of normal TLC analysis, making the process very tedious. Ultimately, pure products were separated from the reaction mixture at decent yields (Scheme 4-9).

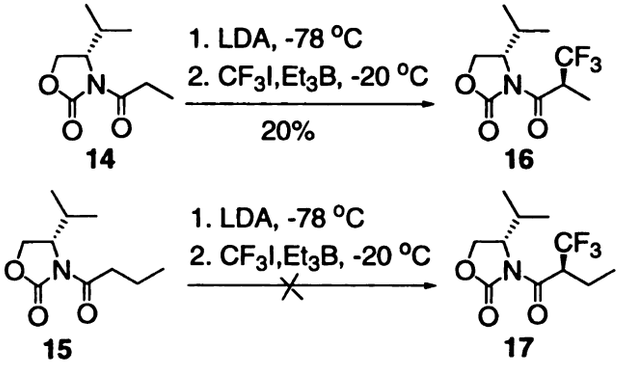

Scheme 4-10. The introduction of trifluoromethyl group to the α position.

The critical step for the synthesis of chiral trifluoromethyl carboxylic acids was the introduction of the trifluoromethyl group to the α position of the amides **14** and **15** in a chiral fashion, as shown in Scheme 4-10. The enolate formed by LDA, which was generated *in situ* by treating diisopropylamine with *n*-BuLi at –78 °C, reacted with trifluoromethyl iodide **7** and triethylborane **8** at –20 °C. As it had been mentioned before, trifluoromethyl iodide **7** is a gas at room temperature, and it could not be added to the reaction vessel by syringes, so the cold trifluoromethyl iodide **7** was poured into the reaction mixture, which inevitably led to a brief contact with air. Since these reactions were carried out at very small scales (1 mmol), they were extremely sensitive to moisture.

When two reactions in Scheme 4-10 were set up side by side, compound **16** was obtained at roughly 20% yield, but only traces of amide **17** could be identified.

The separation and purification of compound **16** proved to be troublesome, due to the very similar polarities of the starting amide **14** and the product **16**. In addition, none of the two compounds were neither UV active or show visible spot with any dyes. Once again, GC-MS was used for the determination of the components of each of the column fractions. Unfortunately, after several attempts the product, amide **16**, could not be separated from the starting amide **14** by column chromatography, since each of the fractions was a combination of the two at similar ratios. Although pure product **16** could not be isolated at this point, it was decided to proceed to the next step using the amide mixture. The logic behind it was that after coupling with carrier **B**, 1,4-diaminobenzene, the isolation of the desired product would be easier, since now it is UV active.

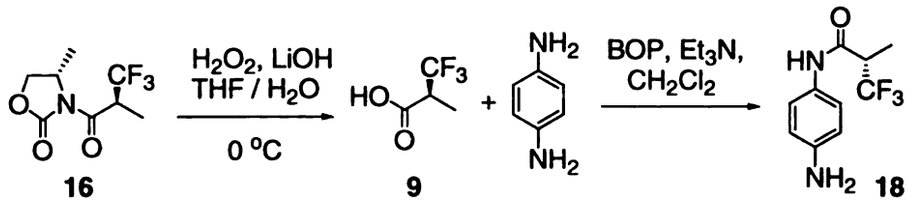

Scheme 4-11. The synthesis of carrier **B** derivatized 2-trifluoromethylpropionic acid **18**.

The coupling of carrier **B** with 2-trifluoromethylpropionic acid **9** is shown in Scheme 4-11. The removal of the chiral auxiliary was achieved by hydrolyzing the mixed amides **14** and **16** with lithium hydroxide and hydrogen peroxide at 0 °C, which provided a mixture of the desired chiral carboxylic acid **18** and propionic acid.[4] Finally the mixed carboxylic acids were coupled with carrier **B** under standard BOP coupling condition. The reaction provided a rather complicated mixture of UV active compounds, which underwent separation by column chromatography to yield the pure conjugate **18**,

as identified by MS. Since the starting materials of the above reactions were mixtures, the yields of these reactions were not determined.

With the pure compound **18** in hand, we were ready to evaluate its binding to zinc porphyrin tweezer under standard condition, methylcyclohexane at 0 °C, and compared the result with those obtained from α-chiral carboxylic acid derivatives. The ECCD spectrum of **18** binding to the tweezer revealed a weak negative couplet with λ_{ext} 423 nm ($\Delta\varepsilon$ -13.3) and 414 nm ($\Delta\varepsilon$ +10), A –23.3.

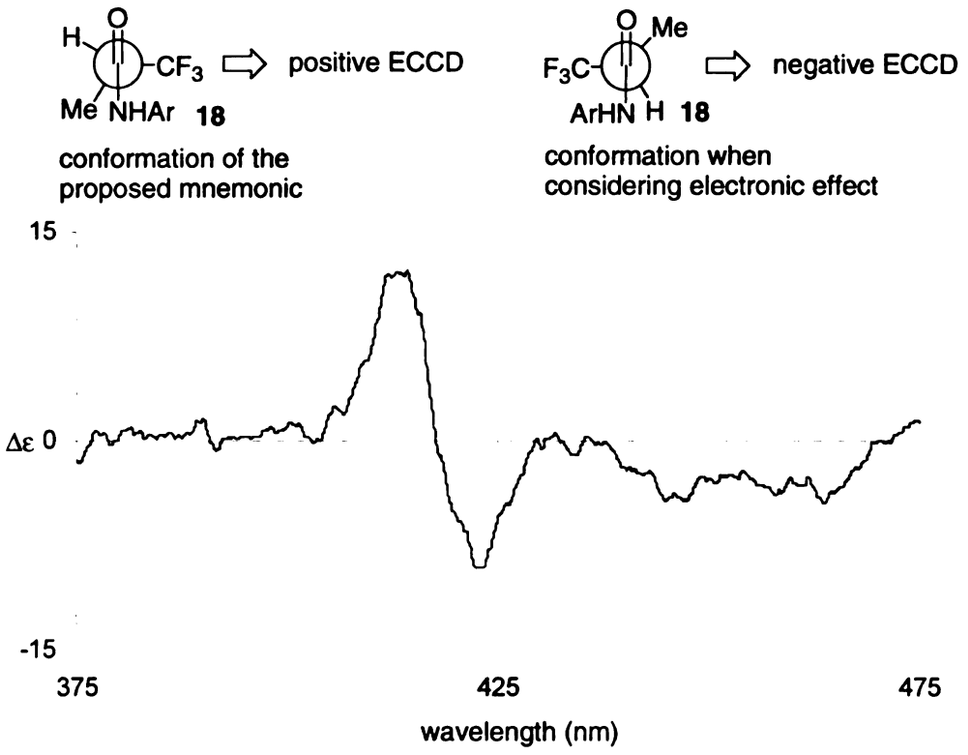

Figure 4-7. The two possible conformations for compound **18** and its ECCD spectrum.

As shown in Figure 4-7, according to A values,[1] trifluoromethyl group (CF_3) is larger than methyl group (CH_3) in size, and thus the observed ECCD of this complex is opposite to the predicted sign based on the proposed mnemonic for carrier **B** derivatives. If the electronic effect of the trifluoromethyl group is considered, the conformation of the $C_{C=O}$-C_{chiral} bond changes. Although CF_3 is still the large group and perpendicular to the

amide carbonyl, the small group (H) is now staggered with respect to the amide proton, and the medium group (CH_3) points to the porphyrin plane. This new conformation would lead to the observed negative ECCD spectrum. This experiment might suggest that the electronic effect of the strong electron withdrawing group at the chiral center play a role in the stereochemical determination of α-chiral halocarboxylic acid.

However, the ECCD of carrier **B** derivatized 2-trifluoromethylpropionic acid **18** was not reproducible after the compound was stored on sodium carbonate (to keep the amino from being protonated) for a day. This might be due to the rapid epimerization at the chiral center, since the α hydrogen, which is also adjacent to the strong electron withdrawing trifluoromethyl group, is very acidic and could epimerize in either acidic or basic condition.

4-2.3. The possibility of σ*–π interaction

As mentioned before, the strong electron withdrawing effect of halogen atoms could also affect the ECCD signs of carrier **B** derivatized chiral halocarboxylic acids by σ*–π interaction,[15] which would cause the halogens to behave as the large group instead of medium group by electronic effects.

When Heathcock and coworkers studied the addition of nucleophiles to chiral aldehydes according to Felkin-Ahn model,[16] they observed that "the simple steric effects are at least as important as σ*–orbital energies in determining which was the 'large' group for the purpose of applying the Felkin model." Since carbon-heteroatom bonds have significant lower σ*–orbital energies than carbon-carbon bond, the major conformer should have the heteroatom perpendicular to the carbonyl, acting as the large group.

According to their results, they determined the order of ligand preferences for the perpendicular position: MeO> t-Bu> Ph> *i*-Pr> Et> Me> H.

When we first predicted the ECCD signs of carrier **B** derivatized α-halocarboxylic acids based on the proposed mnemonic for carrier **B** derivatives, the large, medium and small group on the chiral center were defined based on their A values.[1] Halogens are smaller than alkyl groups but larger than hydrogen, so they are considered as the medium group. But when the σ*–π interactions are considered, the halogens could behave as the large group by electronic effect and could be perpendicular to the carbonyl group. If this approach is valid, our previously proposed mnemonic could also be successfully applied to the α-chiral halocarboxylic acid derivatives.

Although this σ*–π interaction theory could give an explanation for our results of the α-chiral halocarboxylic acid derivatives, it could at the same time complicate some of the previously discussed cases where heteroatoms, besides halogens, were involved. For example, as discussed in the previous chapter, the derivatives of oxygen containing acids, such as (*S*)-acetylmandelic acid derivative **9B** and (*S*)-acetoxypropionic acid derivative **10B**, did not place the heteroatom, oxygen, perpendicular to the carbonyl group.

A possible explanation for this different behavior could be the hydrogen bonding between the amide hydrogen and the heteroatom oxygen in preference to the possible σ*–π interaction. Because of the hydrogen bonding, the oxygen containing substituent is locked in the gauche position relative to the $C_{C=O}$-C_{C-N} bond, instead of being perpendicular to carbonyl group, as the σ*–π interaction would predict (Figure 4-8).

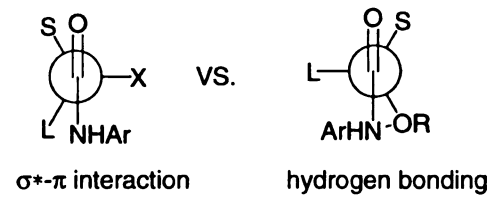

Figure 4-8. The conformations dictated by σ*–π interaction and hydrogen bonding.

If the above hypothesis is true, when the specified hydrogen bonding is eliminated from the system, the complex should adopt a conformation in order to put the oxygen perpendicular to the carbonyl group in favor of the σ*–π interaction. In order to test this statement, we decided to methylate the amide nitrogen and therefore remove the hydrogen available for hydrogen bonding. (*S*)-2-phenoxypropionic acid was the substrate of choice, since its carrier **B** derivative **11B** exhibited the strongest ECCD observed (see Section 3-2).

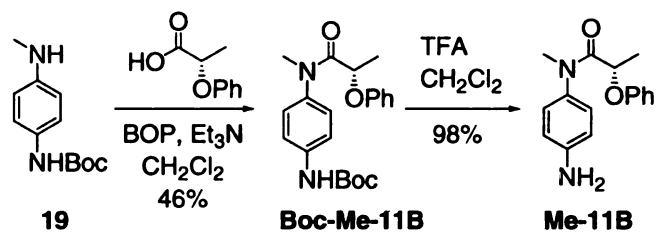

Scheme 4-12. The synthesis of methylated carrier **B** derivative **Me-11B**.

The synthesis of the monomethylated carrier **B** derivatized (*S*)-2-phenoxypropionic acid **Me-11B** is shown in Scheme 4-12. The N-methylated carrier **19** was coupled with the (*S*)-2-phenoxypropionic acid **11** under standard BOP coupling condition, and subsequently Boc deprotection with trifluoroacetic acid yielded the N-methylated compound **Me-11B**. The chiral complex **Me-11B** was then added to zinc porphyrin tweezer in methylcyclohexane to measure its ECCD. To our satisfaction, the

methylated carrier **B** derivative **Me-11B** showed a positive ECCD spectrum, opposite to that of the original carrier **B** derivative **11B** (Figure 4-9).

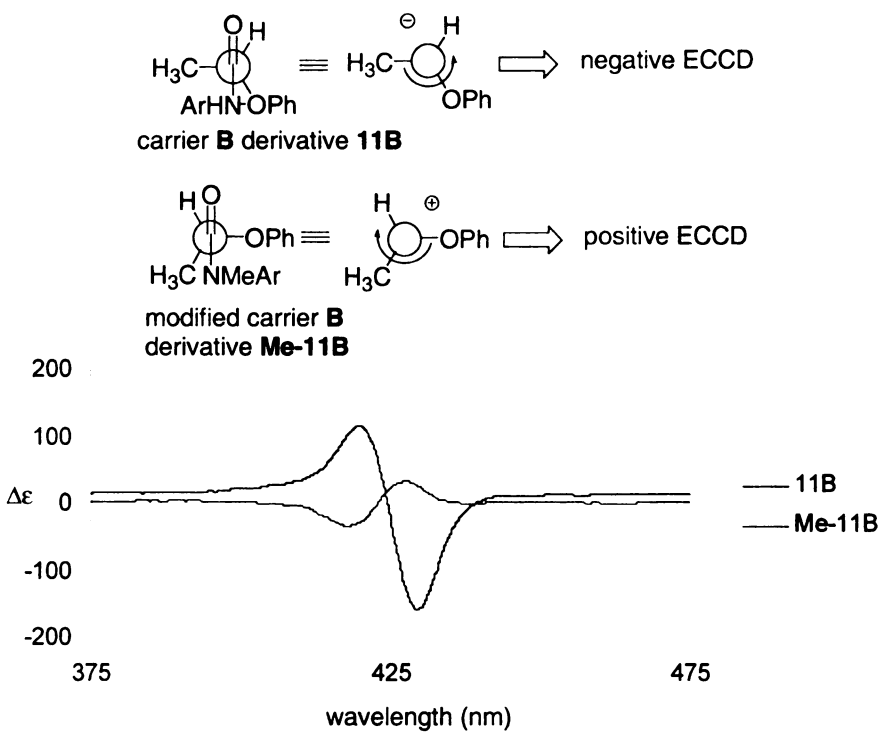

Figure 4-9. The conformations and ECCD of **11B** and **Me-11B**.

According to the above observations, a conformational change of the chiral complexes is implied (Figure 4-9). In particular, for the original carrier **B** derivative **11B**, which contains an amide hydrogen, the oxygen on the chiral center is gauche to the $C_{C=O}$-C_{C-N} bond to form a hydrogen bond. This conformation predicts a negative ECCD spectrum, which is consistent with the observation. In the case of the modified derivative **Me-11B**, however, the amide hydrogen is eliminated, and according to $\sigma^*-\pi$ interaction, the oxygen now becomes the large group because of the electronic effects. This new conformation dictates a positive ECCD spectrum, which is also consistent with the observed ECCD sign.

In order to obtain additional evidence for the validity of the above theory, the carrier **B** derivatized (*R*)-2-bromopropionic acid **1Br** was chosen to undergo methylation. In this case, since there was no chance for hydrogen bonding in either the original derivative **B-1-Br** or the methylated derivative **MeB-1-Br**, we did not expect to see an ECCD sign switch.

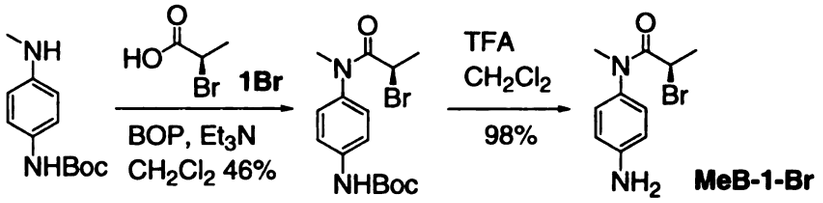

Scheme 4-13. The synthesis of modified carrier **B** derivative **MeB-1-Br**.

(*R*)-2-bromopropionic acid **1Br** was coupled with the methylated carrier **B** as shown in Scheme 4-13. However, the chiral complex **MeB-1-Br** did not show any ECCD spectrum when it was added to zinc porphyrin tweezer in methylcyclohexane, either at room temperature or at 0 °C.

According to the experiments performed so far, the σ^*–π interaction could be a possible explanation for the behavior of the carrier **B** derivatized α-chiral halocarboxylic acids. However, although we had some evidence, we were still not able to provide a strong proof for this theory.

4-2.4. The NMR study to determine the interaction between zinc porphyrin tweezer and carrier B derivatized α-chiral halocarboxylic acids

During all the previous studies, we were trying to consider the electronic effect of the halogens in the carrier **B** derivatized chiral halocarboxylic acid cases. As mentioned before, the halogens could behave as the large group due to their strong electronegativity or due to σ^*–π interactions as shown in Figure 4-3*a*.

Besides the electron effect of the halogens, there are two other possible explanations for the observed ECCD of the carrier **B** derivatized α-chiral halocarboxylic acids. Both cases involved binding between the chiral complex and the zinc porphyrin tweezer. When the carrier **B** derivatized α-chiral halocarboxylic acids bind to zinc porphyrin tweezer, it is certain that the free amino group of the conjugate would bind to one of the zinc porphyrins of the tweezer. What we were not so sure about is, which atom of the chiral complex would preferentially bind to the other porphyrin of the tweezer. As mentioned before, it is possible that the halogen atom binds to the zinc porphyrin, instead of the carbonyl oxygen (Figure 4-3*b*), or that there is a cooperative binding of both halogen atom and carbonyl oxygen to zinc porphyrin (Figure 4-3*c*). In order to investigate these two hypotheses (Figure 4-3*b* and *c*), we undertook a NMR study of a series of different amides binding to zinc tetraphenylporphyrin (ZnTPP).

When a substrate binds to ZnTPP, because of the strong diamagnetic anisotropy of the porphyrin ring, the protons on the substrate will shift upfield. The tighter the substrate binds to ZnTPP, the closer it is to the porphyrin plane, and the larger upfield shifts the protons will "sense". Therefore, by comparing the change of the proton chemical shift of various substrates, we could estimate how well they bind to ZnTPP.

Table 4-3. Change in proton chemical shift upon addition to ZnTPP.

	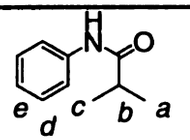 **20**	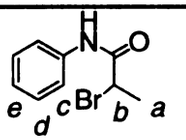 **21**	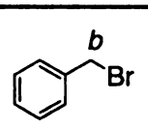 **22**	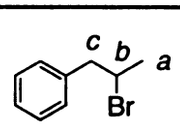 **23**	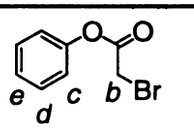 **24**	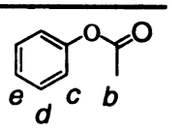 **25**
a	0.019	0.093		0		
b	0.084	0.177	0.023	0.004	0.014	0.029
c	0.068	0.104		0.008	0.017	0.028
d	0	0.036			0.013	0.015
e	0	0.024			0.010	0.013

The changes in proton chemical shift of these substrates upon binding to ZnTPP are shown in Table 4-3. All the NMR studies were performed in $CDCl_3$ at room temperature, and the ratio between the substrates and ZnTPP was roughly 1:1.

All the substrates underwent an upfield shift upon addition to ZnTPP, which indicated that all the substrates bound to ZnTPP to some extent. Among them, substrate **21**, the α-bromo amide, showed the most significant upfield shift, which suggested the tightest binding. Substrate **20**, which lacked the α-bromo moiety, also showed binding to ZnTPP, but not as strong as its α-bromo analogue, which suggests that the halogen atom participates in the binding. On the other hand, when substrates **22** and **23**, which bore a bromine atom but lacked a carbonyl group were tested, they experienced very small shift upon introduction to ZnTPP. This indicated that the bromine by itself did not bind to ZnTPP. The next substrates tried were esters **24** and **25**, one with a α-bromo and the other without. Based on the small change of the chemical shift of these two substrates, we could conclude that they both did not bind to ZnTPP strongly, and the bromine atom does not seem to participate in the binding of esters to ZnTPP.

Overall, the results presented in Table 4-3 suggested the cooperative binding of the α-bromo and the carbonyl oxygen of amides to ZnTPP. Interestingly, the above statement was not true in the case of esters.

In order to investigate whether the same cooperative binding occurs for all the α-halo amides and that it is not specific for α-bromo amide, the α-chloro and α-fluoro amides were also tested. Just as the α-bromo case, the NMRs were taken in $CDCl_3$ at room temperature, with the ratio between the amide substrates and the ZnTPP being

about 1:1. The binding results, expressed as the change of the haloamides chemical shifts upon addition to ZnTPP, are shown in Table 4-4.

Table 4-4. The change in chemical shifts of haloamides upon addition of ZnTPP.

	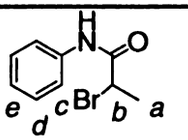	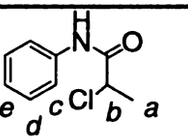	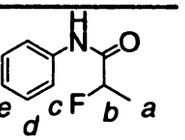
	21	**26**	**27**
a	0.093	0.080	0.092
b	0.177	0.162	0.156
c	0.104	0.095	0.104
d	0.036	0.022	0.021
e	0.024	0.017	0.016

According to the numbers obtained in Table 4-4, all the haloamides bound to ZnTPP with the same relative affinity. The proposed cooperative binding in α-bromoamides seems to exist for both α-fluoroamides and α-chloroamides.

The NMR studies listed in Table 4-3 and 4-4 suggests that the carrier **B** derivatized α-chiral halocarboxylic acids bind to zinc porphyrin tweezer with both the carbonyl oxygen and the halogen atom at the chiral center. In order to have a better understanding of the rotation around the $C_{C=O}$-C_{chiral} bond, a tertiary α-bromoamide **28** was synthesized, and the change of its chemical shift upon addition to ZnTPP was followed by NMR (Figure 4-10).

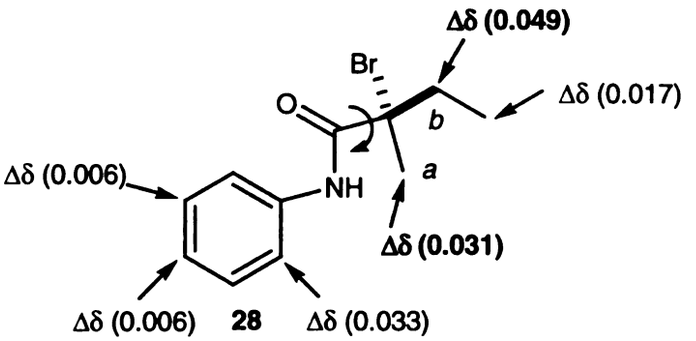

Figure 4-10. The change of chemical shift of bromoamide **28** upon addition of ZnTPP.

Once more, NMR experiments were carried out in $CDCl_3$ at room temperature, with the ratio between the amide substrate and ZnTPP being nearly 1:1. The fact that all the protons of amide **28** shifted upfield suggested that the amide substrate bound to ZnTPP. In order to understand the rotation around the $C_{C=O}$-C_{chiral} bond, we needed to determine the positions of the methyl group (S) and the ethyl group (L) relative to the porphyrin plane. Therefore, we were interested in protons *a*, the protons of the methyl group, and protons *b*, the protons on the methylene of the ethyl group. A comparison of the change of the chemical shift between these two protons was a direct measurement of the proximity of these two sets of protons to the porphyrin ring. The larger the change of the chemical shift, the closer the protons were to the porphyrin plane. As shown in Figure 4-10, protons *b* experienced a larger change of chemical shift as compared to protons *a*, which suggested that the ethyl group was in closer proximity to the porphyrin ring as compared to the methyl group.

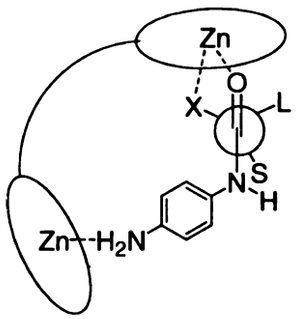

Figure 4-11. The interaction of carrier **B** derivatized α-chiral halocarboxylic acids with zinc porphyrin tweezer.

According to the above experiments, the suggested conformation of the carrier **B** derivatized α-chiral halocarboxylic acids upon binding to zinc porphyrin tweezer is shown in Figure 4-11: (1) There is a cooperative binding of the α-halogens and carbonyl

oxygen to zinc porphyrin; (2) The $C_{C=O}$-C_{chiral} bond adopts such a conformation that the large group is gauche to the carbonyl and the small group is *syn* to $C_{C=O}$-C_{C-N} bond.

4-3. The study of the interaction between the zinc porphyrin tweezer and carrier B derivatized α-chiral halocarboxylic acids by forming five-membered α-halolactams

Although, according to the results presented above we have acquired some NMR evidence to show the interactions between the zinc porphyrin tweezer and carrier **B** derivatized α-chiral halocarboxylic acids, we thought we should support our suggestion of the novel cooperative binding through another approach. In particular, we were interested in constraining the free rotation around the $C_{C=O}$-C_{chiral} bond, so that, by removing this variable, the experimental results would reflect directly the nature of the cooperative binding.

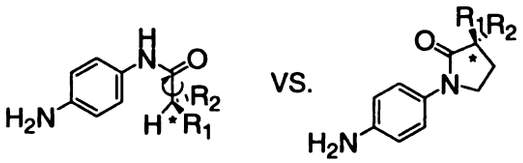

Figure 4-12. The carrier **B** derivatives versus the five-membered chiral α-lactams.

In order to achieve that, we decided to utilize five-membered chiral α-lactams (Figure 4-12). For these systems, there is no rotation around the $C_{C=O}$-C_{chiral} bond, since that bond is now frozen in a five-membered ring. Therefore, the ECCD sign will be dictated only by the interaction of the chiral center with the zinc porphyrins.

As shown in Figure 4-13, for most chiral five-membered lactams, when they bind to zinc porphyrin tweezer, the porphyrin plane should "slide away" from the large group on the chiral center and cover the small group to minimize the steric interaction between the chiral substituent and the porphyrin plane. However, when one of the substituents on

the chiral center is a halogen and the other one is a hydrogen, and if the stated cooperative binding of the halogen and carbonyl oxygen to zinc porphyrin really exists, the porphyrin should slide toward the halogen, even though it is the large group. Therefore, if cooperative halogen binding exists, this specific α-halolactam and all the other five-membered α-chiral lactams should induce the opposite chirality upon binding to zinc porphyrin tweezer, which will be exhibited as opposite ECCD sign

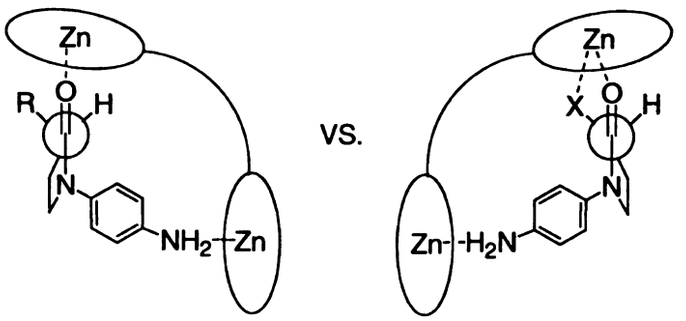

Figure 4-13. The comparison of interaction of a five-memered lactam and the α-halolactam with zinc porphyrin tweezer.

4-3.1. The synthesis of chiral α-substituted-γ-butyrolactams

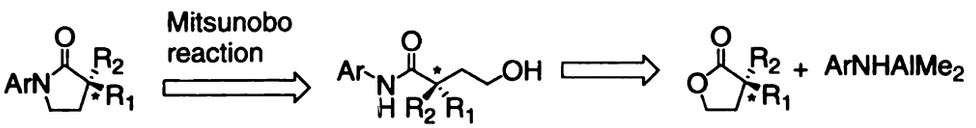

29 **30** **31**

Figure 4-14. The synthesis of five-membered α-chiral lactams from α–chiral–γ–butyrolactones.

The synthesis of five-membered α-chiral lactams **29** has been previously reported,[17] starting with α–chiral–γ–butyrolactones **31** (Figure 4-14). The five-membered α-chiral lactams **29** could be synthesized by Mitsunobo reaction[18] from 4-hydroxy-butyramide **30**, which was synthesized by opening an α–chiral–γ–butyrolactone **31** with aromatic amine and trimethylaluminum.[19] During this process, the

stereochemistry of the chiral center is retained. Since we need to synthesize a library of five-membered α-chiral lactams, the real task lies in the synthesis of different α–chiral–γ–butyrolactones.

Our first synthetic target was chiral α–chloro–γ–butyrolactone **32**, which would eventually afford the corresponding lactam. As shown in Scheme 4-14, the proposed synthesis of **32** started with the reaction of chiral homoserine **33** with sodium nitrite, in aqueous hydrochloric acid solution, which was a general method for converting amino groups to halogens,[2] with overall retention of stereochemistry. Treatment of the chiral alcohol **34** with acid would then lead to the formation of lactone **32**.

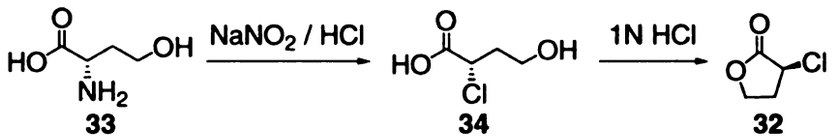

33 **34** **32**

Scheme 4-14. The synthesis of chiral α–chloro–γ–butyrolactone **32**.

However, the aforementioned synthesis did not proceed as expected. When L-homoserine **33** was treated with sodium nitrite in the presence of hydrochloric acid, besides the anticipated conversion of the amino group to chloro, the condition was acidic enough for the ring closure to occur. This reaction could cause a serious problem, since, although we obtained the desired butyrolactone **32**, we could not be certain of whether or not the stereochemistry of the chiral center was retained.

As stated before (see Section 4-1), in the process of converting amino groups to halogens, the stereochemistry of the chiral center is retained because of the participation of the adjacent carboxylic acid. However, in the above reaction, when direct conversion of the homoserine **33** to butyrolactone **32** occurred, the acid functionality also reacted with the free hydroxyl group to form the five-membered lactone ring, and this

complicated the stereochemical determination of the chiral center. If the lactone formation was faster than the substitution reaction, the stereochemistry at the chiral center would be reversed, while if the replacement of the diazo group by acid was faster than the lactone formation, then the stereochemistry should be retained.

In order to avoid this problem, another approach was adopted, which involved the closing of the five-membered lactone ring before converting the amino groups to halogens under the standard sodium nitrite method. In this way, the stereochemistry of the chiral center should be reversed. The commercially available (*S*)-homoserine lactone hydrochloride **35** was used as the starting material. As shown in Scheme 4-15, the (*S*)-homoserine lactone **35** was converted to α-chloro-γ-butyrolactone **32** by treatment with potassium nitrite and aqueous hydrochloric acid, and the stereochemistry of the chiral center switched from (*S*) to (*R*).

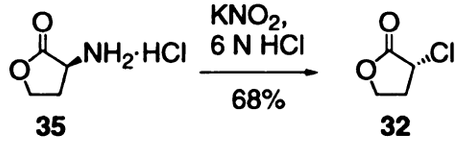

35 **32**

Scheme 4-15. The synthesis of α-chloro-γ-butyrolactone **32**.

The next target was chiral α-phenoxy-γ-butyrolactone **36**, which could be synthesized from α-chloro-γ-butyrolactone **32** by replacing the chloro group with a phenoxy group (Scheme 4-16). In order to eliminate the possible racemization at the chiral center under strong basic condition, excess amount of phenol was pretreated with sodium hydride, and then the α-chloro-γ-butyrolactone **32** was added into the reaction.

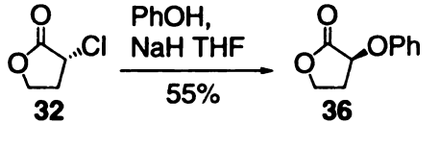

32 **36**

Scheme 4-16. The synthesis of α-phenoxy-γ-butyrolactone **36**.

With the two of chiral butyrolactones **32** and **36** in hand, we were ready to convert them to the corresponding chiral lactams **37** and **38**. Scheme 4-17 presents the conversion of (*R*)-α-phenoxy-γ-butyrolactone **36** to its corresponding lactam **38**.

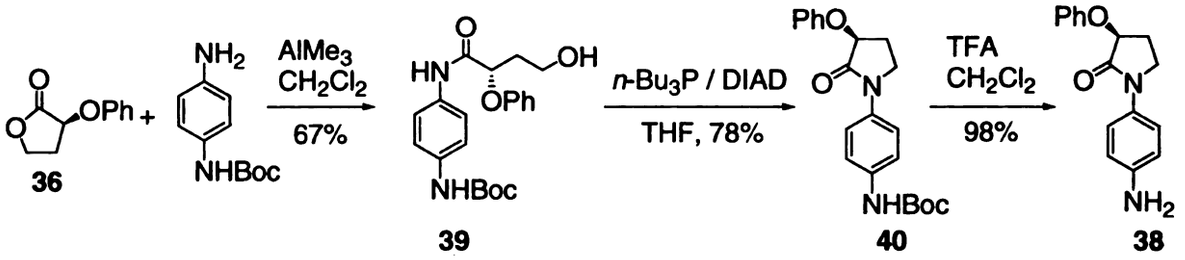

Scheme 4-17. Converting butyrolactone to butyrolactam.

The Boc-protected carrier **B** was first reacted with trimethylaluminum in order to obtain the corresponding dimethylaluminum amide, which was then treated with (*R*)-α-phenoxy-γ-butyrolactone **36** to form the amide **39**. Cyclodehydration of amide **39** was achieved by Mitsunobu reaction to yield the Boc-protected lactam **40**. The Boc protecting group on lactam **40** was then removed by stirring in TFA and CH_2Cl_2 to yield the desired chiral butyrolactam **38**. The chiral α-chloro-γ-butyrolactone **32** could be converted to its corresponding lactam **37** in the same manner.

The pure butyrolactams **37** and **38** were then added to zinc porphyrin tweezer in methylcyclohexane, and their ECCD were measured. The (*R*)-α-chloro-γ-butyrolactam **37** exhibited a positive ECCD curve at both room temperature and 0 °C, upon addition to zinc porphyrin tweezer. Although the ECCD amplitude at 0 °C was larger than that at room temperature, the shape of the peak was not as symmetric. On the other hand, the (*S*)-α-phenoxy-γ-butyrolactam **38** showed a negative ECCD spectrum at room temperature, which disappeared when cooled to 0 °C. The enantiomeric ratios for these

two compounds before Boc deprotection were determined by chiral HPLC, to be ~80% for (*R*)-α-chloro-γ-butyrolactam **37**, but only 33% for (*S*)-α-phenoxy-γ-butyrolactam **38**.

Although 80% is an acceptable value, 33% *ee* for compound **38** is not. Since it was derived from (*R*)-α-chloro-γ-butyrolactone **32** by replacing the chloro group with phenoxy, racemization must have taken place during that process. The possibility of racemization in the substitution step was foreseen, and in order to minimize it, less than one equivalent of sodium phenoxide was used. However, the precaution was obviously not enough. In order to improve the enantioselectivity of the substitution reaction, the chiral α-bromo-γ-butyrolactone **39** was synthesized. Since bromide is a better leaving group than chloride, the substitution reaction described above should work better. The synthesis of (*S*)-α-phenoxy-γ-butyrolactam **38** through the α-bromo-γ-butyrolactone **41** is shown in Scheme 4-18.

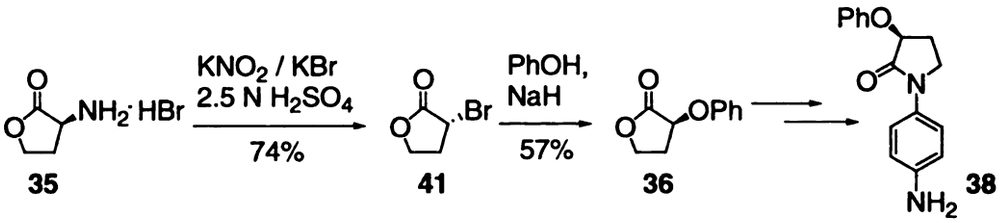

Scheme 4-18. Second route for the synthesis of (*S*)-α-phenoxy-γ-butyrolactam **38**.

The (*S*)-α-bromo-γ-butyrolactone **41** was synthesized in the standard way by stirring chiral homoserine lactone hydrobromide **35** with sodium nitrite and potassium bromide in diluted sulfuric acid solution. The product was extracted and used without further purification. The bromide compound **41** was then combined with 1 eq. of sodium phenoxide to generate (*S*)-α-pheonxy-γ-butyrolactone **36**, which was subsequently converted to the (*S*)-α-phenoxy-γ-butyrolactam **38** as described before. To our surprise,

the enantiomeric excess determined by chiral HPLC was only 7%, even worse than what was previously obtained.

So far, the attempts to synthesize chiral α-phenoxy-γ-butyrolactone **36** by replacing halogens with sodium phenoxide to secure high enantiomeric ratio had failed. Another approach could be the use of Mitsunobu reaction, which could then lead to an enantiomerically pure lactam **38** (Scheme 4-19).

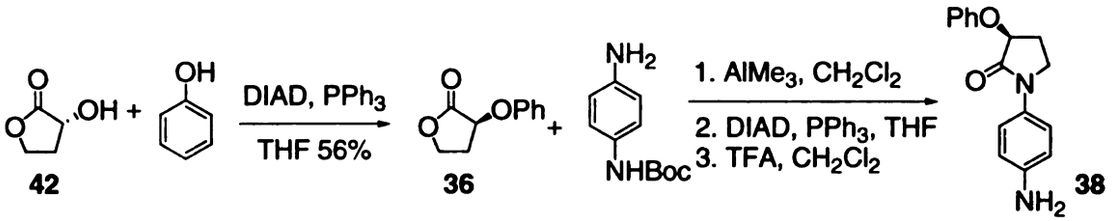

Scheme 4-19. Third route for the synthesis of (*S*)-α-phenoxy-γ-butyrolactam **38**.

The synthesis of chiral α-phenoxy-γ-butyrolactone **36** by Mitsunobu reaction[18] started with (*R*)-α-hydroxy-γ-butyrolactone **42** reacting with phenol in the presence of DIAD and PPh_3. The desired chiral (*S*)-α-phenoxy-γ-butyrolactone **36** was separated (56% yield).[20] The (*S*)-α-phenoxy-γ-butyrolactone **36** was then reacted with the Boc protected carrier **B** in the presence of trimethylaluminum, followed by an another Mitsunobu reaction to close the lactam ring, and deprotection with TFA and CH_2Cl_2 afforded the final (*S*)-α-phenoxy-γ-butyrolactam **38**.[17] This time, a greater than 99% *ee* was determined for lactam **38**, before Boc deprotection. When lactam **38** was added to the zinc porphyrin tweezer in methylcyclohexane at room temperature, a negative ECCD spectrum was obtained.

By using α-hydroxy-γ-butyrolactone **42** as the starting material, more oxygen containing chiral butyrolactones could be synthesized, since the hydroxyl group could be easily converted to other functionalities.

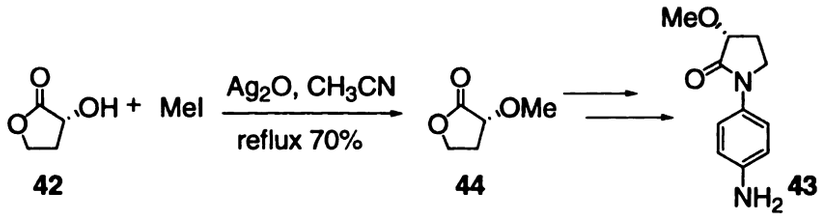

Scheme 4-20. The synthesis (*R*)-α-methoxy-γ-butyrolactam **43**.

In particular, the next target was α-methoxy-γ-butyrolactam **43**, and its synthesitic plan is depicted in Scheme 4-20.[21] The corresponding (*R*)-α-methoxy-γ-butyrolactone **44** could be easily synthesized from (*R*)-α-hydroxy-γ-butyrolactone **42** by reacting with methyl iodide under refluxing condition in the presence of silver oxide. In this process, the stereochemistry of the chiral center should be retained.[21] The (*R*)-methoxybutyrolactone **44** was then converted to its corresponding (*R*)-α-methoxy-γ-butyrolactam **43** according to the protocol previously describe by using $AlMe_3$ and then Mitsunobu reaction conditions.[17]

Since the chiral α-methoxy-γ-butyrolactone **44** was easily synthesized from the chiral α-hydroxy-γ-butyrolactone **42** by using methyl iodide and silver oxide,[21] it was expected that more alkoxybutyrolactones could be synthesized in the same manner, and the attempted syntheses are shown in Scheme 4-21.

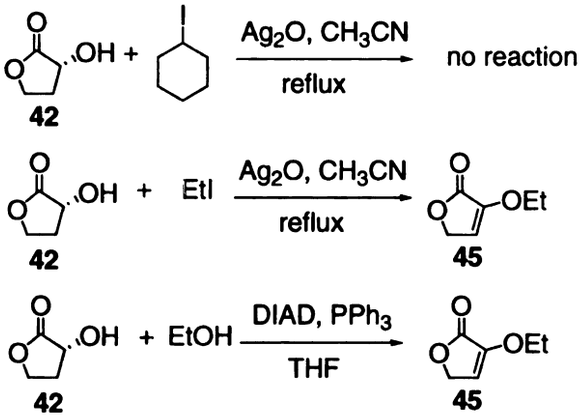

Scheme 4-21. The attempted synthesis of α-alkoxy-γ-butyrolactones.

Cyclohexyl iodide reacted with α-hydroxy-γ-butyrolactane **42** in the presence of silver oxide. The reaction mixture was refluxed in acetonitrile for over 2 days; however, there was no conversion to the desired product. This might be due to the fact that the secondary iodide was too sterically hindered, and therefore a less sterically hindered primary iodide, ethyl iodide, was tested.

The reaction condition with ethyl iodide was similar to that of methyl iodide, however, the product separated from the reaction mixture was not the desired alkylated lactone, but the α,β–unsaturated lactone **45** with the hydroxyl group being converted to ethyl ether. The mechanism leading to this unexpected product is still unclear, however, it is obvious that even ethyl iodide was not active enough to convert the α-hydroxy-γ-butyrolactone **42** to the corresponding ethoxy lactone by using the silver oxide method. We also tried to synthesize the ethoxy lactone by Mitsunobu reaction of ethanol and α-hydroxy-γ-butyrolactone **42**. Once more, the only product obtained was the same α,β–unsaturated lactone **45**. Mitsunobu reaction works well when an alcohol reacts with a carboxylic acid, but not when two alcohols react with each other.[22] In the reaction with phenol (Scheme 4-19), since phenol is quite acidic, the reaction provided the desired phenoxy lactone **36**. However, since ethanol is not as acidic, the reaction failed to provide the desired Mitsunobu product.

Up to this point, all attempts to obtain chiral α-ethoxy-γ-butyrolactone had failed. Since even ethyl iodide was not active enough to convert the α-hydroxy-γ-butyrolactone **42** to ethoxy lactone by using silver oxide reaction conditions, more reactive iodides such as allylbromide and benzylbromide were tried (Scheme 4-22).

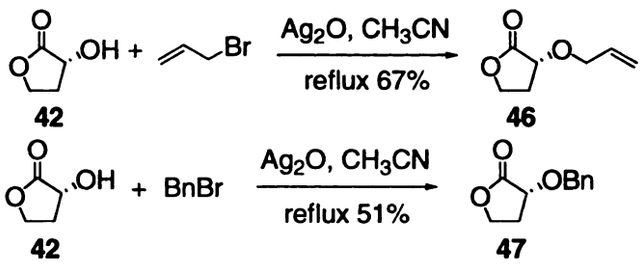

Scheme 4-22. The synthesis of chiral benzoxy and allyoxy lactones.

When allylbromide or benzylbromide reacted with (*R*)-α-hydroxy-γ-butyrolactone **42** under silver oxide conditions, both reactions yielded a mixture of products with the desired alkoxy compound **46** and **47** being the major product with satisfactory yield. However, for both these reactions, the α,β–unsaturated lactones were generated also.

In addition, two more chiral alkoxy, (*S*)-α-naphthyloxy-γ-butyrolactone **48** and (*S*)-α-*p*-*tert*-butylphenoxy-γ-butyrolactone **49** were synthesized by using Mitsunobu reaction, as shown in Scheme 4-23. One thing to be noticed with these Mitsunobu reactions is that the reaction did not work when *n*-Bu_3P was used instead of PPh_3.

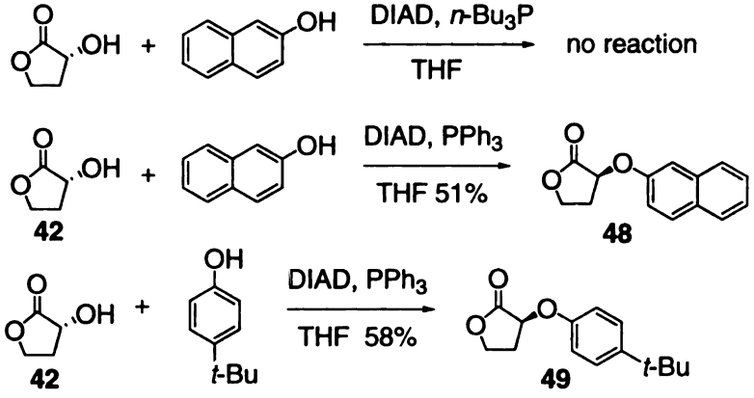

Scheme 4-23. The synthesis of (*S*)-α-naphthyloxy-γ-butyrolactone **48** and (*S*)-α-*p*-*tert*-butylphenoxy-γ-butyrolactone **49**.

With these new chiral lactones in hand, we moved on to the syntheses of the corresponding carrier **B** derivatized chiral butyrolactams, with the protocols described

before. The conversions were uneventful, and hydrogenation of (*R*)-α-allyloxy-γ-butyrolactam **50** with Pd/C yielded (*R*)-α-propoxy-γ-butyrolactam **51** (Scheme 4-24). Upon addition of these derivatized chiral lactams to zinc porphyrin tweezer in methylcyclohexane at room temperature, the ECCD data were obtained and are shown in Table 4-5.

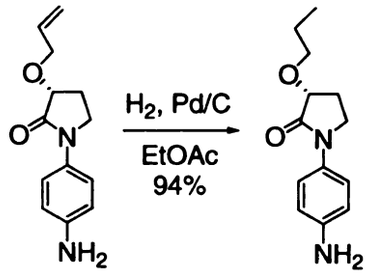

50 **51**

Scheme 4-24. The hydrogenation of lactam **50** to **51**.

Table 4-5. The CD data of chiral butyrolactams.

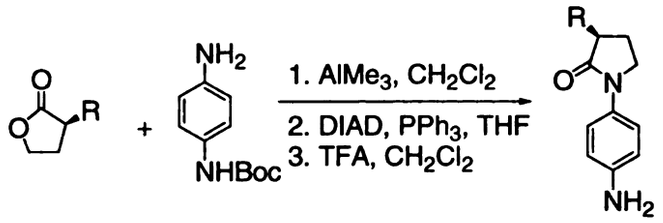

	Expected sign	1st λ(Δε)	2nd λ(Δε)	Amplitude
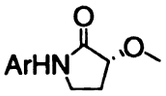 **52**(*R*)	negative	429 (-32)	417 (+30)	-62
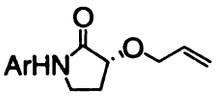 **50**(*R*)	negative	429 (-34)	417 (+19)	-53
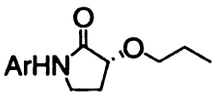 **51**(*R*)	negative	429 (-23)	417 (+27)	-50
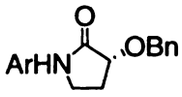 **53**(*R*)	negative	431 (-12)	416 (+12)	-24
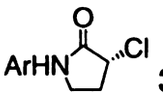 **37**(*R*)	positive	426 (+34)	418 (-23)	+57
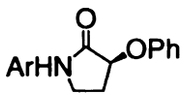 **38**(*S*)	positive	427 (-17)	418 (+25)	-42
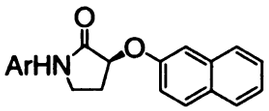 **54**(*S*)	positive	427 (-17)	418 (+34)	-51
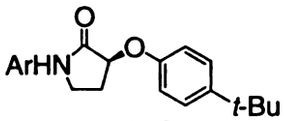 **55**(*S*)	positive	427 (-14)	417 (+14)	-28

As it is shown in Figure 4-15, when the four chiral (*R*)-α-alkoxy-γ-butyrolactams **50-53** bind to zinc porphyrin tweezer, the two substitutions, the alkoxy group and hydrogen, on the chiral center are pointing toward the porphyrin plane. Since the alkoxy groups are larger in size than hydrogen, the porphyrin slides away from the alkoxy group

and covers the small hydrogen group. The counterclockwise orientation of the two porphyrin rings leads to a negative ECCD sign for all four of them.

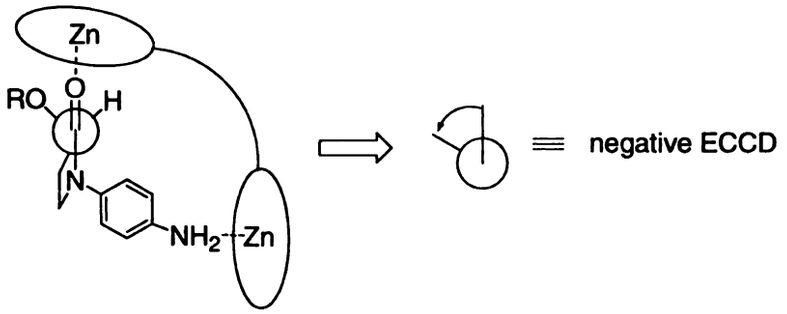

Figure 4-15. The conformation of (*R*)-α-alkoxy-γ-butyrolactams **50-53** binding to zinc porphyrin tweezer.

As for the (*R*)-α-chloro-γ-butyrolactam **37**, although its stereochemistry is the same as the four chiral alkoxybutyrolactams **50-53**, the sign of its ECCD spectrum is opposite to those of the chiral alkoxybutyrolactams, and this is due to the cooperative binding of the chlorine and the carbonyl oxygen with the zinc porphyrin tweezer. As shown in Figure 4-16, although chlorine is larger than hydrogen in size, because of the cooperative binding, the bound porphyrin slides away from the small hydrogen to cover the large chlorine. The clockwise-orientated porphyrin tweezer results in a positive ECCD sign.

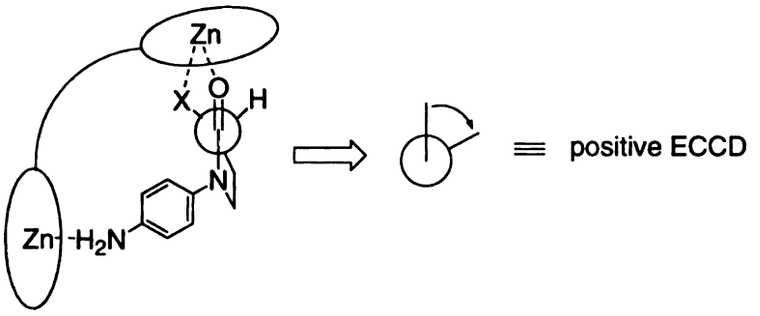

Figure 4-16. The conformation of (*R*)-α-chloro-γ-butyrolactam **37** binding to zinc porphyrin tweezer.

For the last three chiral butyrolactams **38**, **54** and **55**, since there is no halogen present in the molecules, there should be no cooperative binding and thus it should follow the same trend as butyrolactam **50-53** by adopting the same conformation as shown in Figure 4-15. However, they exhibited opposite ECCD sign as we expected. In order to explain this contradiction, we turn to the possible π–stacking interaction between the aromatic group on the chiral center and the porphyrin ring. As shown in Figure 4-17, this π–stacking interaction brings the porphyrin plane close to the aromatic substitution at the chiral center, in spite of the fact that it is larger than hydrogen. The aryl ring in essence creates a modified bi-dentate mode of binding, leading to a counterclockwise orientation of the porphyrin tweezer that results in a negative ECCD spectrum.

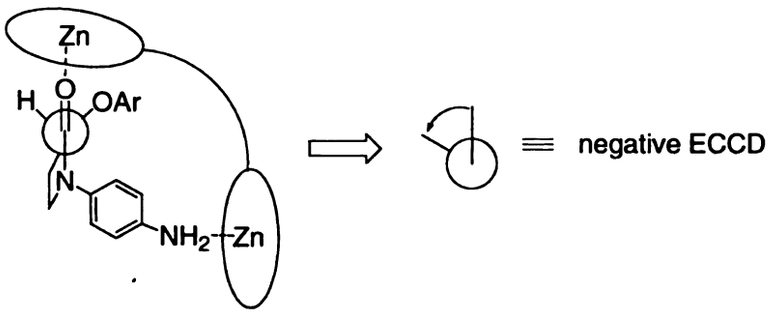

Figure 4-17. The conformation of chiral α-alkoxy-γ-butyrolactams **38**, **54** and **55** binding to zinc porphyrin tweezer.

4-3.2. The synthesis of chiral α-alkyl-γ-butyrolactams

The chiral butyrolactams synthesized contain either halogen, or alkoxy groups at the chiral center. However, in order to complete our library, we needed to obtain a few chiral α-alkyl-γ-butyrolactams. For the synthesis of the chiral α-alkyl-γ-butyrolactams, a similar scheme as before was followed, by starting with chiral α-alkyl-γ-butyrolactones.

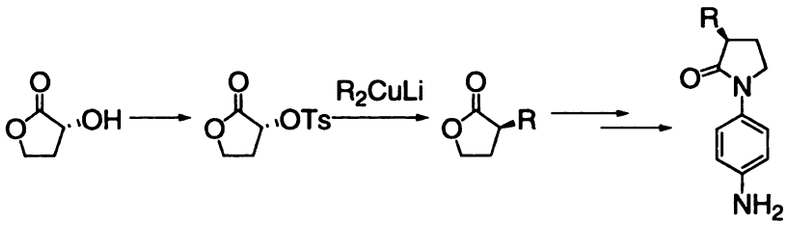

Scheme 4-25. The synthesis of chiral α-alkyl-γ-butyrolactams using cuprates.

The first attempt to synthesize the chiral α-alkyl-γ-butyrolactones, shown in Scheme 4-25, was by placing a good leaving group, such as a tosylate or triflate, at the chiral center, which was then replaced by a cuprate. Since, replacement of an α-tosylate with different kinds of cuprates was reported,[23] we decided to follow that protocol and make chiral α-tosyl-γ-butyrolactone **54** from chiral α-hydroxy-γ-butyrolactone **42**.

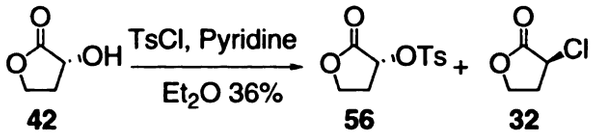

Scheme 4-26. The synthesis of (*R*)-α-tosyl-γ-butyrolactone **56**.

As shown in Scheme 4-26, the first conditions tried in order to synthesize (*R*)-α-tosyl-γ-butyrolactone **56** was to react (*R*)-α-hydroxy-γ-butyrolactone **42** with TsCl, using pyridine as the base in ether. The reaction was completed overnight, followed by diluted HCl solution to remove the pyridine. However, after column chromatography, two products were separated with close polarity and close yield (nearly 1:1 ratio). One of the compounds was the desired tosylate **56**, while the other one was the unexpected chlorobutyrolactone **32**. The generation of the unexpected chlorobutyrolactone **32** was rationalized by the addition of diluted HCl in the quenching step. The hydrochloric acid could replace the tosylate group in product **56** and resulted in the formation of the chloro

byproduct **32**. Also, the chloride generated during the reaction of the alcohol with tosyl chloride could have resulted in the formation of **32**.

In an attempt to investigate if HCl was indeed the source of Cl, the same reaction was repeated, using diluted H_2SO_4 instead of HCl to neutralize the excess amount of pyridine. However, as before, the same byproduct, chlorobutyrolactone **32**, was formed in the reaction with similar yields. Therefore, we knew that the neutralization step did not lead to the formation of the chloro byproduct **32**. Since HCl was not the source of Cl, the only other explanation could be that the chlorine came from the starting material TsCl. Since TsCl was used in the reaction as the source of the tosylate group, the generation of the chloro byproduct **32** was inevitable under this reaction condition.

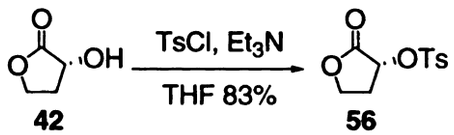

42 **56**

Scheme 4-27. Second route for the synthesis of (*R*)-α-tosyl-γ-butyrolactone **56**.

Another reaction condition was tried to eliminate the generation of the unwanted chlorobutyrolactone byproduct (Scheme 4-27). The new reaction utilized THF as the solvent, and triethylamine as the base instead of pyridine. Under this new reaction condition the only product generated was the desired tosylate lactone **56**, without any formation of the chloro byproduct **32**.

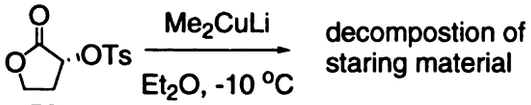

56

Scheme 4-28. The first reaction of (*R*)-α-tosyl-γ-butyrolactone **56** with dimethylcuprate.

The (*R*)-α-tosyl-γ-butyrolactone **56** was ready to be converted to the chiral alkylbutyrolactones by reacting with organocuprates. As shown in Scheme 4-28, the first

organocuprate used was lithium dimethylcuprate. Generally, the reactions with organocuprates are kept at –78 °C to keep the organocuprates from decomposing. However, the lithium dimethylcuprate is quite stable, and the reaction could be carried out at relatively high temperature (-10 °C) to facilitate the replacement of the leaving group.[23] The lithium dimethylcuprate was made by adding methyllithium into cuprous iodide at 0 °C in ether. The reaction initially showed a bright yellow color, and with the addition of methyllithium, the yellow color gradually disappeared. After the generation of lithium dimethylcuprate, the (*R*)-α-tosyl-γ-butyrolactone **56** was dissolved in ether and added to the cuprate solution at –20 °C in salt-ice bath. Unfortunately, the (*R*)-α-tosyl-γ-butyrolactone **56** does not dissolve in ether well, and when it was added into dimethylcuprate, it became very sticky and precipitated out of the reaction mixture. The reaction was kept at –10 °C, and at this temperature, the starting material (*R*)-α-tosyl-γ-butyrolactone **56** decomposed.

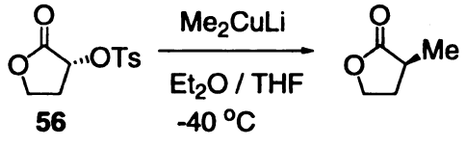

56

Scheme 4-29. The second reaction of compound **56** with dimethylcuprate.

The reaction was repeated, only this time, as shown in Scheme 4-29, the reaction was kept at lower temperature to prevent the decomposition of **56**. The solvent mixture of Et_2O and THF (1:1 ratio) was used to increase the solubility of the starting material. All the starting tosylate **56** disappeared in 4 hours, and from GC-MS, we could observe four major peaks, with one of them being possibly the desired α-methyl-γ-butyrolactone. However, the isolation of the desired product from the reaction mixture by column chromatography was not successful. After the reaction mixture was loaded to silica

column, it could not be recovered in any of the fraction. This might due to the low boiling point of the product, which could result in the vaporization of the compound in the process of removing solvents under reduced pressure.

In order to increase the boiling point of the product, we decided to use lithium dibutylcuprate instead to react with the (*R*)-α-tosyl-γ-butyrolactone **56**. The procedure for this reaction is the same as dimethylcuprate, with the *in situ* generation of lithium dibutylcuprate first, and then react it with (*R*)-α-tosyl-γ-butyrolactone. Since the dibutylcuprate is not as stable as dimethylcuprate, the reaction temperature was kept at – 78 °C. Since, as mentioned before, the (*R*)-α-tosyl-γ-butyrolactone **56** was not very soluble in ether, the reaction took place in a solvent mixture of ether and THF (Scheme 4-30). The reaction mixture was kept for 4 h, and only starting material **56** was recovered.

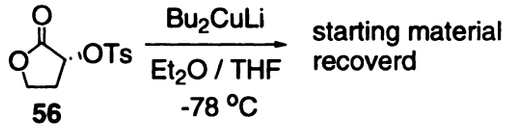

56

Scheme 4-30. The reaction of (*R*)-α-tosyl-γ-butyrolactone **56** with dibutylcuprate.

Attempts to synthesize chiral α-alkyl-γ-butyrolactones by reacting organocuprate with tosylate **56** had failed. An alternative route for the synthesis of these compounds could be the Reformatsky reaction. The general Reformatsky reaction calls for α-bromo compounds reacting with aldehydes in the presence of activated zinc. However, there have been no examples of using alkyl halides instead of aldehydes in the Reformatsky reaction. From literature search, a palladium catalyzed coupling reaction of a Reformatsky reagent with allylic acetates to add the allylic group to the α–position of the Reformatsky reagent was found,[24] as shown in Scheme 4-31.

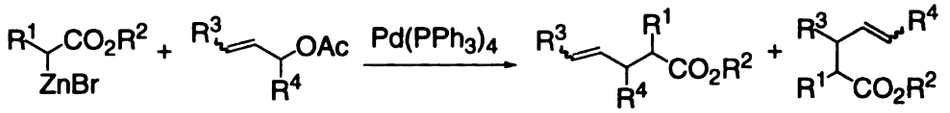

Scheme 4-31. A palladium catalyzed coupling reaction of Reformatsky reagent with allylic acetates.

The same palladium catalyzed coupling reaction could be used to in our synthesis to generate the chiral α-allyl-γ-butyrolactones by reacting the chiral α-bromo-γ-butyrolactone **39** with allyl acetate, as shown in Scheme 4-32.

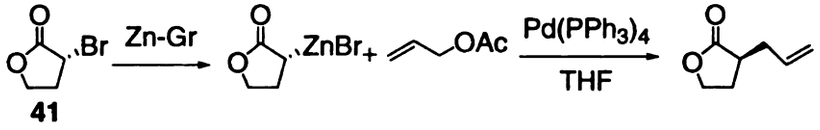

Scheme 4-32. The proposed synthesis of chiral α-allyl-γ-butyrolactones by palladium catalyzed Reformatsky reagent utilizing zinc on graphite.

One critical factor for the Reformatsky reaction is the preparation of highly reactive zinc. There are several ways to activate zinc metal. One way is by the potassium-graphite (C_8K) reduction of the corresponding zinc halide ($ZnCl_2$)[25] in ethereal solvents according to equation 3-1.[26, 27]

$$2C_8K + ZnCl_2 \rightarrow C_{16}Zn + 2KCl \qquad (3\text{-}1)$$

Potassium-graphite (C_8K) was prepared by heating graphite powder under argon to about 150 °C, and adding freshly cleaned potassium in pieces. The heating did not stop until the potassium melts, which generated the pyrophoric potassium-graphite. It was then covered with THF, and solid anhydrous $ZnCl_2$ was added. The reaction was stirred at 70 °C for half an hour, at which time the zinc-graphite was made. This was a dangerous reaction to perform, since potassium is pyrophoric especially at high temperatures. After the zinc-graphite was made, it was cooled to 0 °C, and the chiral α-

bromo-γ-butyrolactone **41** was added dropwise to generate the Reformatsky reagent. The solution was then warmed up to room temperature, and the palladium catalyst and allyl acetate were added. The mixture was stirred for an hour before it was quenched by aqueous acid. However, this reaction failed, and the starting α-bromo-γ-butyrolactone **41** was recovered. One of the possible reasons for the failure could be the unsuccessful activation of zinc by potassium-graphite.

In the mean time, a much milder way to prepare highly reactive zinc was found, formed by the reduction of anhydrous zinc chloride with 2.1 equivalent of lithium and a small amount of naphthalene in freshly distilled glyme under an argon atmosphere.[28] In this activation, lithium serves as the reducing agent,[29] and naphthalene acts as an electron carrier. The best solvent for the reduction is glyme, since the use of THF leads to a zinc powder of much reduced reactivity while reduction does not proceed at all in ether. After the mixture was stirred overnight, very fine black particles could be observed at the bottom of the reaction flask, which indicated the generation of activated zinc powder. The glyme was then removed by syringe, and THF was injected into the flask serving as the solvent for the following palladium catalyzed coupling reaction.

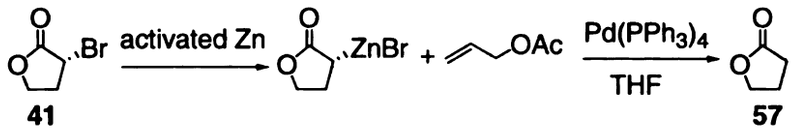

41 **57**

Scheme 4-33. Palladium coupling reaction of Reformatsky reagent with allyl acetate.

The coupling reaction was carried out in the same way as described above (Scheme 4-33), but this time, the separated compound from the reaction mixture was the plain butyrolactone **57**. The generation of butyrolactone **57** indicated the successful

formation of the Reformatsky reagent, however, the palladium coupling reaction provided the reduced product instead of the coupling product.

Since the synthesis of chiral α-alkyl-γ-butyrolactones with palladium catalyzed reaction failed, an alternative way was proposed, which involved the use of chiral auxiliaries. The proposed synthesis is shown in Scheme 4-34.

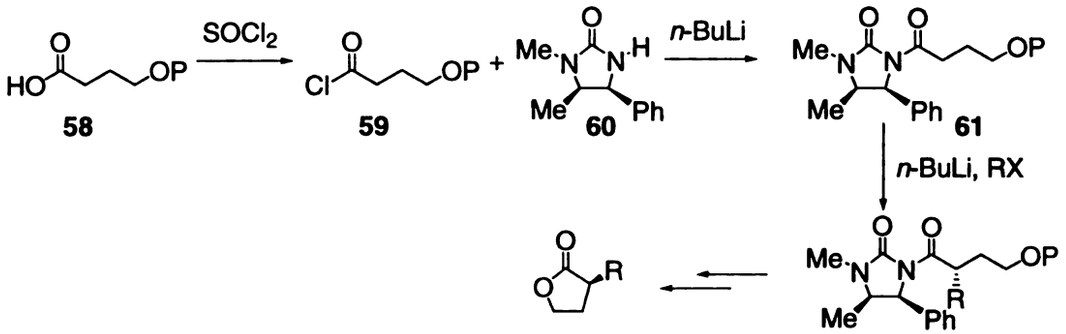

Scheme 4-34. The proposed synthesis of chiral α-alkyl-γ-butyrolactones with chiral auxiliary.

According to the proposed scheme, the protected γ-hydroxy-carboxylic acid **58** was converted to the more reactive acyl chloride **59**, which then reacted with chiral auxiliary **60**[30] in the presence of *n*-BuLi. The R group (R=Me, allyl, and benzyl) could be introduced in a chiral fashion to the α position by *n*-BuLi treatment and addition of the corresponding alkyl halide. The standard deprotection of the hydroxyl group, and the removal of the chiral auxiliary would result in the formation of the desired chiral α-alkyl-γ-butyrolactones.

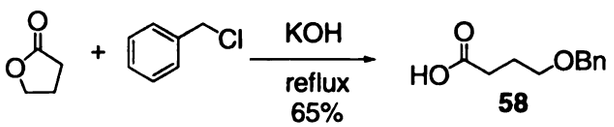

Scheme 4-35. The synthesis of benzyl protected γ-hydroxy-carboxylic acid **58**.

The benzyl protected γ-hydroxy-carboxylic acid **58** was synthesized following published procedures,[31] as shown in Scheme 4-35. Butyrolactone was refluxed in toluene in the presence of benzyl chloride and potassium hydroxide, and in this way, the hydroxyl group could be selectively protected in the presence of the carboxylic functionality.

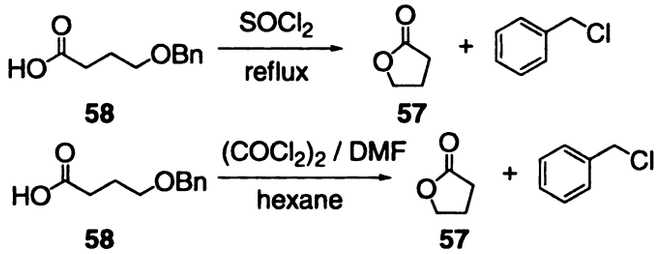

Scheme 4-36. The attempted conversion of the acid **58** to acyl chloride.

As shown in Scheme 4-36, the benzyl protected γ-hydroxy-carboxylic acid **58** could then be converted to the corresponding acyl chloride **59** by refluxing in $SOCl_2$. However, the starting material **58** decomposed under the reaction condition, and benzyl chloride and butyrolactone **57** were isolated from the reaction instead. Another way to convert carboxylic acid **58** to the acyl chloride **59** was by using oxalyl chloride and catalytic amount of DMF in hexane.[32] This reaction was carried out at both room temperature and refluxing condition. However, in both cases, only benzyl chloride and butyrolactone **57** were generated, instead of the desired acid chloride **59**.

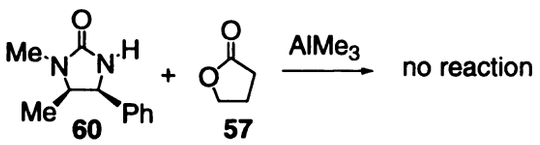

Scheme 4-37. The attempted reaction between chiral auxiliary **60** and butyrolactone **57**.

Since the conversion of benzyl protected γ-hydroxybutyic acid **58** to acyl chloride **59** failed, we thought we might be able to couple it to the chiral auxiliary **60** directly. Since butyrolactones can be opened with amines in the presence of $AlMe_3$ (Scheme 4-

16),[19] we tried to react the chiral auxiliary **60** and butyrolactone directly, as shown in Scheme 4-37. However, this reaction did not work, which might be due to the fact that the anion generated on the chiral auxiliary **60** was too stable to react with the butyrolactone.

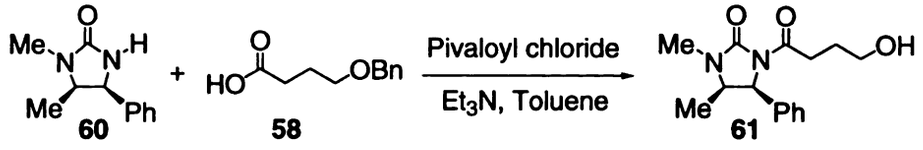

Scheme 4-38. The coupling of chiral auxiliary **60** with acid **58** by generating mixed anhydride.

As shown in Scheme 4-38, another way to couple the chiral auxiliary **60** with the benzyl protected γ-hydroxybutyic acid **58** was by converting the carboxylic acid to a more reactive mixed anhydride by treating it with pivaloyl chloride.[33] This reaction was refluxed in toluene, and the desired conjugate **61** was formed along with some byproducts. This reaction, although promising, had to be optimized, and at the same time, we came across a published procedure on the synthesis of chiral α-alkyl-γ-butyrolactones, which we decided to follow.

After many unsuccessful attempts, the chiral α-alkyl-γ-butyrolactones were finally synthesized by following A. I. Meyers' method, which utilizes chiral 2-methyloxazoline as the chiral auxiliary.[34] The chiral 2-methyloxazoline **62** is commercially available, and could be used to prepare either enantiomer of the α-alkyl-γ-butyrolactones as shown in Scheme 4-39. For our purpose, we follow the procedures to synthesize chiral lactones with (*S*) configuration.

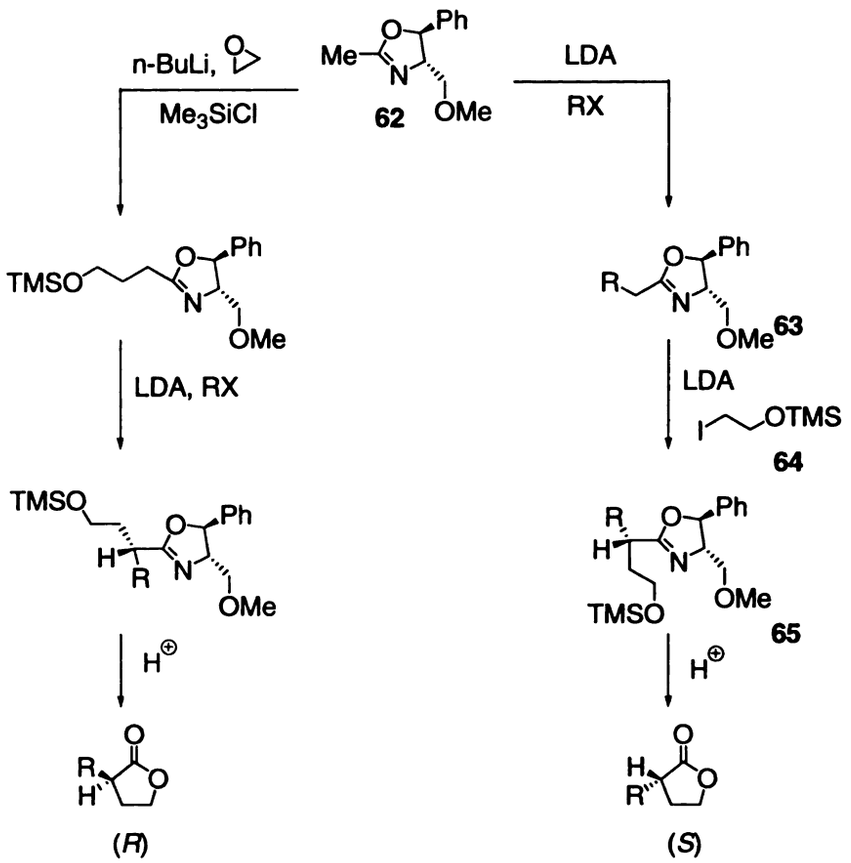

Scheme 4-39. The synthesis of chiral butyrolactones with chiral 2-methyloxazoline **62**.

According to the published scheme,[34] alkylation of chiral 2-methyloxazoline **62** forms the 2-alkyloxazoline **63**. Ethylene oxide could not be introduced to 2-alkyloxazoline **63** after LDA deprotonation due to its poor reactivity at –78 °C to –98 °C, and therefore, a synthetic equivalent, 2-(trimethylsilyloxy)ethyl iodide **64** was used instead, affording compound **65**. The subsequent acidic hydrolysis produces the (*S*) lactones.

Scheme 4-40 rationalizes the absolute configuration of chiral butyrolactones.[34] The deprotonation of the 2-alkyloxazoline **63** with LDA results in the generation of two enolates with a ratio of 95:5, favoring the Z enolate. These two enolates do not equilibrate under the reaction condition, and are subjected to bottom-side alkylation

leading to compound **65** as the major product. Upon acidic hydrolysis, the chiral lactones with (*S*) configuration are produced. However, a small amount of chiral lactones with the opposite configuration could be generated in the same process. Bottom-side alkylation of the minor enolate and some (~10%) top-side alkylation of the major enolate provide 15-20% of the opposite enantiomer.

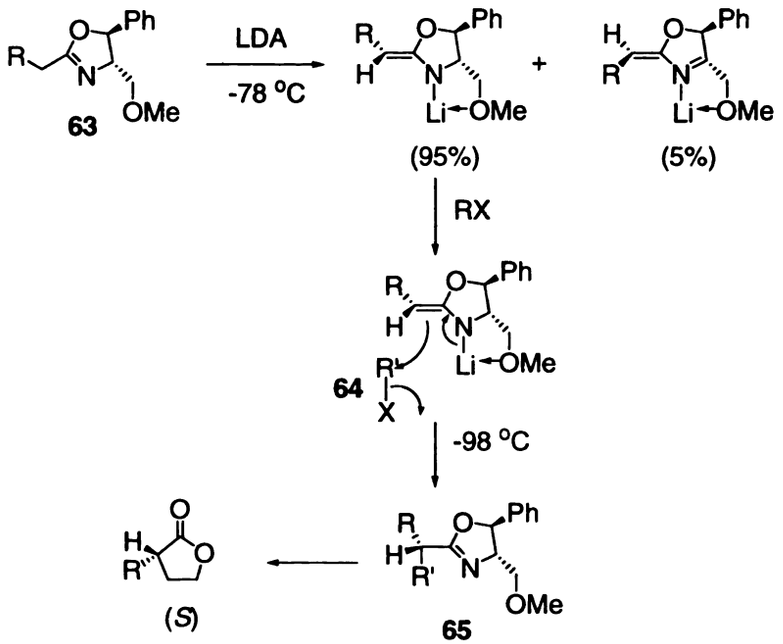

Scheme 4-40. Rationale for the absolute configuration of chiral butyrolactones.

The syntheses of (*S*)-2-methyl-γ-butyrolactone **66** and (*S*)-allyl-γ-butyrolactone **67** were achieved following the published procedure, with one modification. In stead of using 2-(trimethylsilyloxy)ethyl iodide **63** as the alkylation reagent, 2-(OTBS)ethyl iodide **68** was used, because of the unsuccessful synthesis of 2-(trimethylsilyloxy)ethyl iodide **64**.

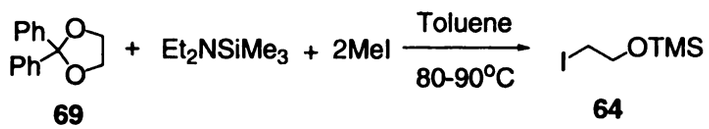

Scheme 4-41. The published synthesis of 2-(trimethylsilyloxy)ethyl iodide **64**.

We have tried to synthesize 2-(trimethylsilyloxy)ethyl iodide **64** according to the published synthesis shown in Scheme 4-41.[35, 36] The 1:2 mixture of Et_2NSiMe_3 and MeI could act as synthetic equivalent of Me_3SiI,[37] and they could be handled without special care. According to the reference, the reaction of benzophenone ethylene acetal **69** with 1 equivalent of Et_2NSiMe_3 and 2 eq. of MeI could afford the desired 2-(trimethylsilyloxy)ethyl iodide **64** as the major product.

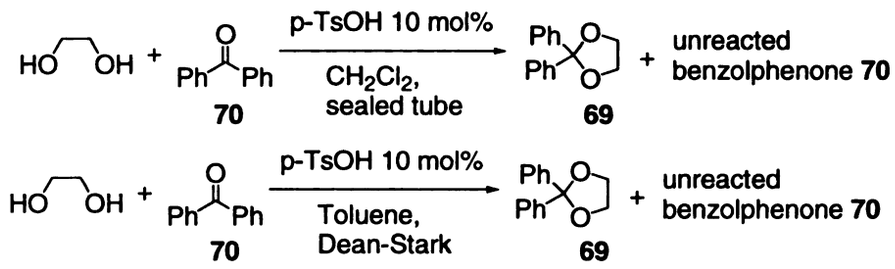

Scheme 4-42. The reactions for the synthesis of benzophenone ethylene acetal **69**.

The benzophenone ethylene acetal **69** could be synthesized by reacting benzophenone **70** with ethylene glycol. However, since the benzophenone **70** is sterically crowded, the synthesis of benzophenone ethylene acetal **69** was not very efficient. Benzophenone was condensed with ethylene glycol, using TsOH as the catalyst. Two different reaction conditions were tried (Scheme 4-42), either using CH_2Cl_2 as the solvent and heating in a sealed tube, or using Dean-Starks trap with benzene as the solvent. Both the reactions worked, however, did not go to completion, and the starting material **70** could not be separated from the product **69**.

Since the benzophenone ethylene acetal **69** could not be synthesized efficiently, and 2-(trimethylsilyloxy)ethyl iodide **64** is too reactive to survive the column if we synthesize it from ethylene glycol by iodonation followed by silylation, we turned to a

more stable synthetic equivalent, the 2-(OTBS)ethyl iodide **68**. The conventional synthesis of the 2-(OTBS)ethyl iodide **68** from ethylene glycol is shown in Scheme 4-43.

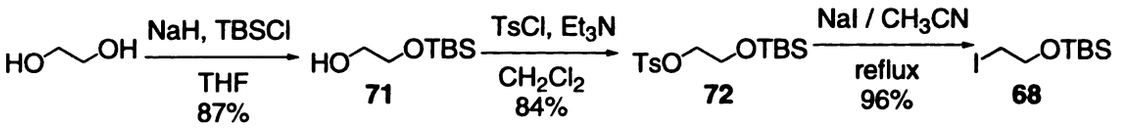

Scheme 4-43. The synthesis of 2-(OTBS)ethyl iodide **68**.

The synthesis of 2-(OTBS)ethyl iodide **68** started with ethylene glycol. Monosilylation of the ethylene glycol to compound **71** could be achieved by addition of NaH and TBSCl in THF. The free hydroxyl group was then converted to tosylate **72**, which was a good leaving group, and was replaced by iodide, according to the Finkelstein reaction,[3] to yield the desired 2-(OTBS)ethyl iodide **68**.

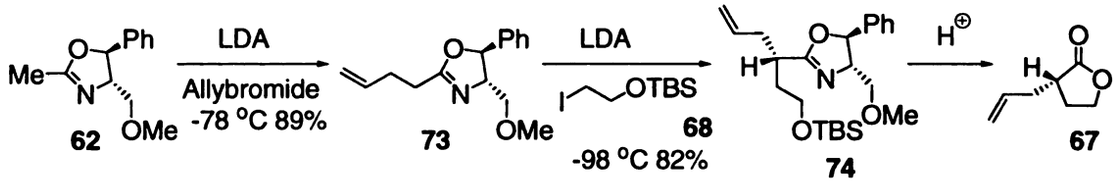

Scheme 4-44. The synthesis of (*S*)-2-allyl-γ-butyrolactone **67**.

With the 2-(OTBS)ethyl iodide **68** in hand, (*S*)-2-methyl-γ-butyrolactone **66** and (*S*)-allyl-γ-butyrolactone **67** were synthesized in the same manner; the synthesis of (*S*)-2-allyl-γ-butyrolactone **67** is shown in Scheme 4-44. The alkylation of 2-alkyloxazoline **62** with allylbromide provided compound **73** with 89% yield. The following alkylation of compound **73** with 2-(OTBS)ethyl iodide **68** was the critical step. It is important to keep the alkylation below –98 °C, since when the reaction was tried at –78 °C, product **74** was not generated but instead starting material **73** was recovered. This could be due to E_2 elimination of iodide **68** at warmer temperature. The alkylation reaction between compound **73** and **68** finished in 2 h at –98 °C. This was a clean reaction, and the pure

alkylation product **74** could be easily separated by column chromatography. The alkylation product **74** was then hydrolyzed under acidic conditions to form the (*S*)-2-allyl-γ-butyrolactone **67**. The hydrolysis was carried out at refluxing 4.5 N HCl for only 15 minutes to avoid possible racemization.

However, the synthesized (*S*)-2-allyl-γ-butyrolactone **67** was not very pure by NMR. This was unexpected, since the starting material **74** was very clean, and the hydrolysis should not provide any other product than the desired butyrolactone **67**. However, despite the fact that the (*S*)-2-allyl-γ-butyrolactone **67** was not very pure, it was still used as starting material for the synthesis of (*S*)-2-allyl-γ-butyrolactam **75**. It was thought that perhaps the impurity would be easier to remove in a later step.

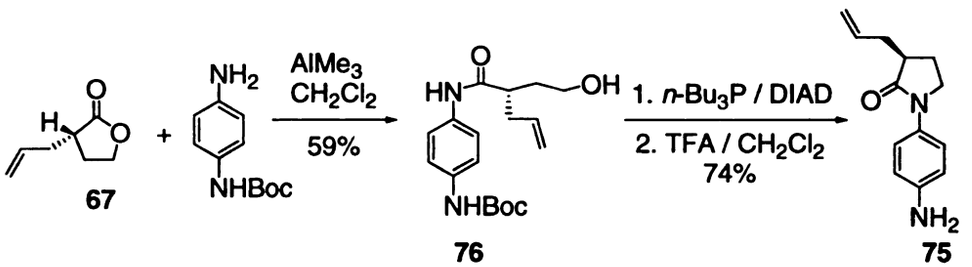

Scheme 4-45. The synthesis of (*S*)-2-allyl-γ-butyrolactam **75**.

Scheme 4-45 shows the synthesis of (S)-2-allyl-γ-butyrolactam **75** from the chiral lactone **67**. The (*S*)-2-allyl-γ-butyrolactone **67** reacted with Boc-protected carrier **B** in the presence of trimethylaluminum, and the cyclodehydration of the resulting amide **76** by Mitsunobu reaction formed the chiral lactam **75**. Although the desired lactam **75** was the major product, the pure compound could not be separated from the reaction mixture. There were several other compounds with very close polarity as the desired lactam, and the desired product **75** could not be separated from the byproducts by column

chromatography. Although it was not surprising that other products were present, since the starting material was not pure, we did not anticipate the separation problem.

In order to synthesize (*S*)-2-allyl-γ-butyrolactone **67**, we closely followed the published procedure, however, with one small difference. In the published protocol, the alkylation product **74** of 2-(OTBS)ethyl iodide **68** reacting with 2-allyl-oxazoline **73** was hydrolyzed without any purification, while in our synthesis, it was purified by column chromatography before undergoing acidic hydrolysis. Perhaps, the alkylation product decomposed easily after subjecting the silicon column, which could yield all the byproducts we could not separate.

The reactions for the synthesis of (*S*)-2-allyl-γ-butyrolactone **67** were repeated as shown in Scheme 4-44. This time, the alkylation product **74** was hydrolyzed under acidic condition as soon as it was extracted from the reaction mixture without any further purification. After the hydrolysis reaction, the desired chiral butyrolactone **67** could be easily purified by column chromatography. After the pure (*S*)-2-allyl-γ-butyrolactone **67** was secured, it was subsequently converted into the corresponding (*S*)-2-allyl-γ-butyrolactam **75** as shown in Scheme 4-45.

The absolute stereochemistry of the (*S*)-2-allyl-γ-butyrolactone **67** was proved by taking the optical rotation in ethanol.[38] Since the conversion of the chiral lactone to chiral lactam did not affect the stereochemistry of the chiral center,[17] the final 2-allyl-γ-butyrolactam **75** should also have the (*S*) configuration.

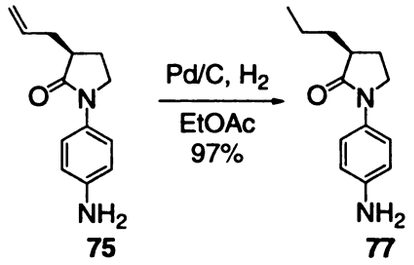

Scheme 4-46. The synthesis of (*S*)-2-propyl-γ-butyrolactam **77**.

The (*S*)-2-allyl-γ-butyrolactam **75** could be easily transformed to (*S*)-2-propyl-γ-butyrolactam **77** by hydrogenation with Pd/C and hydrogen gas. This reaction finished overnight, yielding compound **77** as the sole product, not requiring further purification. Another chiral 2-alkyllactam, (*S*)-2-methyl-γ-butyrolactam **78**, was also synthesized in the same manner, through (*S*)-2-methyl-γ-butyrolactone **65**, by using MeI as the alkylation reagent, instead of allylbromide. These chiral 2-alkyllactams were added to zinc porphyrin tweezer solution at room temperature, and the ECCD data were recorded and shown in Table 4-6.

Table 4-6. The ECCD data of (*S*)-2-alkyl-γ-butyrolactams

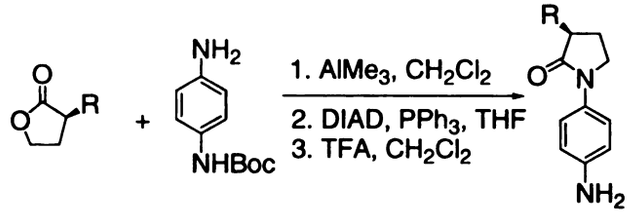

	1st λ(Δε)	2nd λ(Δε)	Amplitude
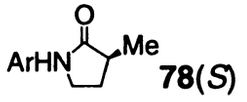 **78**(*S*)	428 (-47)	419 (+36)	-83
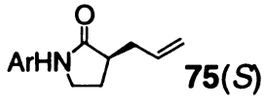 **75**(*S*)	427 (-41)	418 (+38)	-79
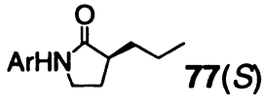 **77**(*S*)	428 (-24)	420 (+37)	-61

As listed in Table 4-6, the ECCD signs for the chiral 2-alkyl-γ-butyrolactams **75**, **77** and **78** were very consistent, with (*S*) configuration showing negative ECCD. However, this sign was opposite to what we expect for the chiral butyrolactams, as shown in Figure 4-18. At this point, we cannot explain this contradiction. We believe that the assigned stereochemistry of the synthesized compounds is correct, since their synthesis was based on well established protocols. However, in an attempt to eliminate the possibility that the above result is due to the wrong stereochemistry assignment, we are currently involved in trying to verify the absolute stereochemistry of the chiral center by synthesizing these chiral substrates following an independent synthetic route. If the results of the second independently synthesized compounds agree with what previously observed, we will have to consider other possibilities for the unexpected observations.

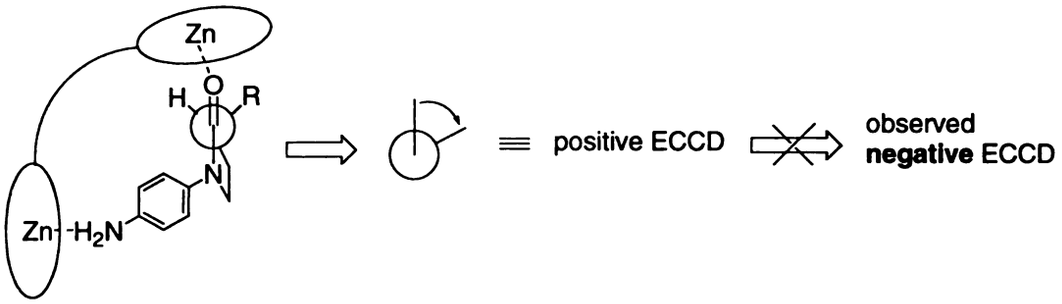

Figure 4-18. The observed ECCD sign is opposite to the predicted sign based on model.

Conclusion:

The absolute stereochemistry of α-chiral halocarboxylic acids can be determined by derivatizing them with carrier **B**, 1,4-diaminobenzene. Upon addition to porphyrin tweezer, (*R*) configuration acids show negative ECCD and (*S*) configuration exhibits positive ECCD. The observed ECCD is opposite to the predicted sign based on the proposed mnemonic in Section 3-2, which we propose is due to the cooperative binding

of the halogen and carbonyl oxygen to zinc porphyrin. This statement has been supported by UV-vis, NMR and IR studies.

We have also tried to prove the above novel binding by synthesizing α-chiral butyrolactams, which can be easily obtained from α-chiral butyrolactones. We compared the sign of the α-chloro butyrolactam with that of the other lactams, and the results match our hypothesis. However, when the substituent on the chiral center is an alkyl group, the observed ECCD sign is opposite to our expectation. We cannot find a plausible explanation for this observation.

Experimental materials and general procedures:

Anhydrous CH_2Cl_2 was dried over CaH_2 and distilled. The solvents used for CD measurements were purchased from Aldrich and were spectra grade. All reactions were performed in dried glassware under nitrogen. Column chromatography was performed using SiliCycle silica gel (230-400 mesh). ^{1}H-NMR spectra were obtained on Varian Inova 300 MHz or 500 MHz instrument and are reported in parts per million (ppm) relative to the solvent resonances (δ), with coupling constants (J) in Hertz (Hz). IR studies were performed on a Galaxy series FTIR 3000 instrument (Matteson). UV/Vis spectra were recorded on a Perkin-Elmer Lambda 40 spectrophotometer, and is reported as λ_{max} [nm]. CD spectra were recorded on a JASCO J-810 spectropolarimeter, equipped with a temperature controller (Neslab 111) for low temperature studies, and is reported as λ [nm] ($\Delta\varepsilon_{max}$ [l mol^{-1} cm^{-1}]). Porphyrin tweezer **2** was synthesized as previously described.[39]

General procedure for CD measurement:

All the CD spectra were taken with 1 μM porphyrin tweezer in methylcyclohexane (1 mL) with 40 equiv of the carrier/chiral acid conjugate. The CD spectra were measured in millidegrees and normalized to $\Delta\varepsilon/\lambda$ [nm] units.

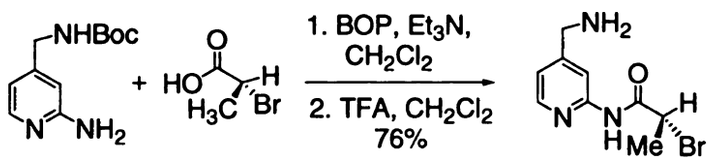

A **1-Br** **A-1-Br**

Carrier A conjugated acid A-1-Br:

To a solution of carrier **A** (1 equiv) in CH_2Cl_2 (2 mL), BOP (1.1 equiv), triethylamine (5 equiv), and the chiral acid (1 equiv) were added. The solution was

stirred at room temperature overnight. After removal of most of the solvent under reduced pressure, the product was purified by silica gel flash chromatography to yield the Boc-protected conjugate. The Boc group was removed by stirring overnight in TFA/CH_2Cl_2 (1:4) at room temperature. The solvent was then removed by purging nitrogen. The residue was redissolved in anhydrous CH_2Cl_2, and anhydrous Na_2CO_3 (20 mg) was added. This solution was stirred at room temperature for an hour, and the Na_2CO_3 was filtered. The solvent was evaporated under reduced pressure to provide analytically pure product.

Boc-A-1-Br:

^{1}H NMR (300 MHz, $CDCl_3$): δ 8.66 (br, 1H), 8.16 (m, 2H), 7.24 (m, 3H), 6.99 (m, 3H), 4.95 (br, 1H), 4.79 (q, *J*=6.9 Hz, 1H), 4.49 (d, *J*=6.6 Hz, 2H), 1.88 (d, *J*=6.9 Hz, 3H), 1.45 (s, 9H).

A-1-Br:

^{1}H NMR (300 MHz, $CDCl_3$): δ 8. 82 (br, 1H), 8.2 (m, 2H), 7.28 (m, 3H), 6.99 (m, 3H), 4.68 (q, *J*=6.9 Hz, 1H), 3.91 (s, 2H), 1.92 (d, *J*=6.9 Hz, 3H).

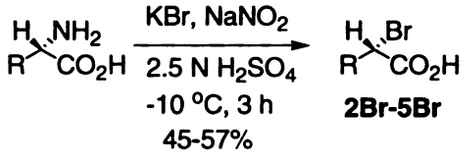

The general procedure to synthesize chiral α-bromocarboxylic acids:

Sodium nitrite (0.22 g, 3.24 mmol) was added to a solution of amino acid (1 mmol) and potassium bromide (0.78 g, 6.56 mmol) in 2.5 N sulfuric acid (9 mL) at –10 °C, and the reaction mixture was stirred for 3 h, and then extracted with CH_2Cl_2 (3 × 25 mL). The combined organic layers were dried over sodium sulfate and evaporated. The crude acid (45-57%) was ready to couple with the carrier **B** without further purification.

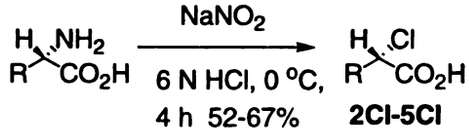

The general procedure to synthesize chiral α-chlorocarboxylic acids:

To a vigorously stirred solution of amino acid (1 mmol) in 6 N HCl (3 mL) at 0 °C was added freshly pulverized sodium nitrite in small portions. This mixture was stirred for 4 h at 0 °C and then extracted with CH_2Cl_2 (3 × 25 mL). The combined extracts were dried over sodium sulfate and solvent was removed under reduced pressure. The crude acid (52%-67%) was coupled with carrier **B** without further purification.

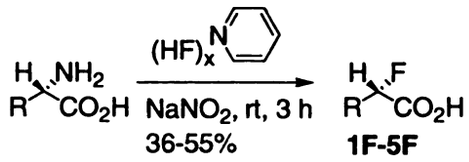

The general procedure to synthesize chiral α-fluorocarboxylic acids:

Sodium nitrite (0.26 g, 3.77 mmol) was added to a solution of amino acid (1.1 mmol) in hydrogen fluoride-pyridine (2 mL) at –10°C, and the reaction mixture was stirred for 3 h at room temperature, at which time the reaction was quenched with water (10 mL). The resulting solution was adjusted to pH 4.0 with solid sodium bicarbonate. The mixture was extracted with CH_2Cl_2 (3 × 25 mL). The combined organic layers were dried over sodium sulfate and solvent was removed under reduced pressure. The crude acid was ready to couple with the carrier **B** without further purification.

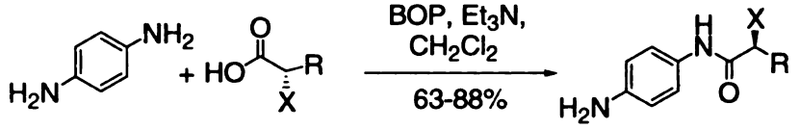

General procedure for preparation of carrier B/halocarboxylic acid conjugates:

To a solution of carrier **B** (5 equiv) in CH_2Cl_2 (4 mL), BOP (1.1 equiv), triethylamine (5 equiv), and the chiral acid (1 equiv) were added. The solution was stirred at room temperature overnight. After removal of most of the solvent under reduced pressure, the product was purified by silica gel flash chromatography to yield the carrier **B** / acid conjugate ready for use for CD analysis.

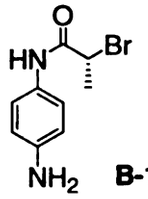

B-1-Br

Carrier B/bromocarboxylic acid conjugates B-1-Br:

^{1}H NMR ($CDCl_3$, 300 MHz) δ 7.91 (br, 1H), 7.30 (d, *J*=8.8 Hz, 2H), 6.67 (d, *J*=8.8 Hz, 2H), 4.56 (q, *J*=7.1 Hz, 1H), 3.63 (br, 2H), 1.98 (d, *J*=7.1 Hz, 3H).

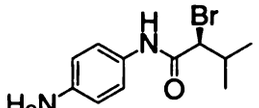

B-2-Br

Carrier B/bromocarboxylic acid conjugates B-2-Br:

^{1}H NMR (300Hz, $CDCl_3$) δ 8.12 (br, 1H), 7.30 (d, *J*=8.8 Hz, 2H), 6.68 (d, *J*=8.8 Hz, 2H), 4.43 (d, *J*=4.4 Hz, 1H), 2.48 (m, 1H), 1.12 (d, *J*=6.6 Hz, 3H), 1.05 (d, *J*=6.6 Hz, 3H).

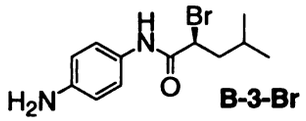

B-3-Br

Carrier B/bromocarboxylic acid conjugates B-3-Br:

^{1}H NMR (300Hz, $CDCl_3$) δ 8.02 (br, 1H), 7.30 (d, *J*=8.8 Hz, 2H), 6.68 (d, *J*=8.8 Hz, 2H), 4.44 (m, 1H), 1.98 (m, 3H), 1.00 (d, *J*=6.6 Hz, 3H), 0.95 (d, *J*=6.6 Hz, 3H).

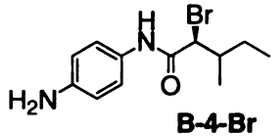

B-4-Br

Carrier B/bromocarboxylic acid conjugates B-4-Br:

^{1}H NMR (300Hz, $CDCl_3$) δ 8.04 (br, 1H), 7.30 (d, *J*=8.8 Hz, 2H), 6.60 (d, *J*=8.8 Hz, 2H), 4.43 (d, *J*=4.9 Hz, 1H), 2.25 (m, 1H), 1.61 (m, 1H), 1.35 (m, 1H), 1.09 (d, *J*=6.6 Hz, 3H), 0.95 (y, *J*=7.5 Hz, 3H).

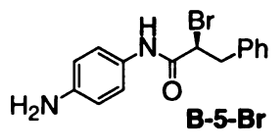

B-5-Br

Carrier B/bromocarboxylic acid conjugates B-5-Br:

^{1}H NMR (300Hz, $CDCl_3$) δ 7.76 (br, 1H), 7.30 (m, 5H), 7.21 (d, *J*=8.8 Hz, 2H), 6.65 (d, *J*=8.8 Hz, 2H), 4.60 (m, 1H), 3.62 (m, 1H), 3.35 (m, 1H).

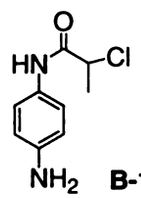

B-1-Cl

Carrier B/bromocarboxylic acid conjugates B-1-Cl:

^{1}H NMR ($CDCl_3$, 300 MHz) δ 7.89 (br, 1H), 7.31 (d, *J*=8.8 Hz, 2H), 6.67 (d, *J*=8.8 Hz, 2H), 4.60 (q, *J*=7.1 Hz, 1H), 3.64 (br, 2H), 1.95 (d, *J*=7.1 Hz, 3H).

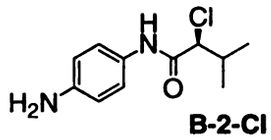

B-2-Cl

Carrier B/chlorocarboxylic acid conjugates B-2-Cl:

^{1}H NMR (300Hz, $CDCl_3$) δ 8.20 (br, 1H), 7.31 (d, *J*=8.8 Hz, 2H), 6.67 (d, *J*=8.8 Hz, 2H), 4.42 (d, *J*=3.3 Hz, 1H), 2.66 (m, 1H), 1.12 (d, *J*=6.6 Hz, 3H), 1.01 (d, *J*=6.6 Hz, 3H).

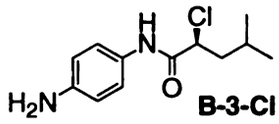

B-3-Cl

Carrier B/chlorocarboxylic acid conjugates B-3-Cl:

^{1}H NMR (300Hz, $CDCl_3$) δ 8.12 (br, 1H), 7.32 (d, *J*=8.8 Hz, 2H), 6.68 (d, *J*=8.8 Hz, 2H), 4.46 (m, 1H), 1.98 (m, 3H), 1.00 (m, 6H).

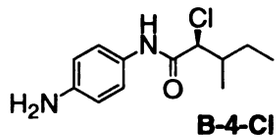

B-4-Cl

Carrier B / chlorocarboxylic acid conjugates B-4-Cl:

^{1}H NMR (300Hz, $CDCl_3$) δ 8.20 (br, 1H), 7.30 (d, *J*=8.8 Hz, 2H), 6.68 (d, *J*=8.8 Hz, 2H), 4.45 (d, *J*=3.7 Hz, 1H), 2.39 (m, 1H), 1.53 (m, 1H), 1.35 (m, 1H), 1.11 (d, *J*=7.1 Hz, 3H), 0.95 (t, *J*=6.7 Hz, 3H).

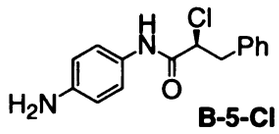

B-5-Cl

Carrier B/chlorocarboxylic acid conjugates B-5-Cl:

^{1}H NMR (300Hz, $CDCl_3$) δ 7.98 (br, 1H), 7.32 (m, 5H), 7.23 (d, *J*=8.8 Hz, 2H), 6.67 (d, *J*=8.8 Hz, 2H), 4.68 (m, 1H), 3.54 (m, 1H), 3.31 (m, 1H).

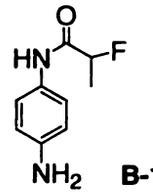

B-1-F

Carrier B/fluorocarboxylic acid conjugates B-1-F:

^{1}H NMR ($CDCl_3$, 300 MHz) δ 7.84 (br, 1H), 7.34 (d, *J*=8.8 Hz, 2H), 6.69 (d, *J*=8.8 Hz, 2H), 5.19-5.03 (dd, 1H), 3.66 (br, 2H), 1.71 (m, 3H).

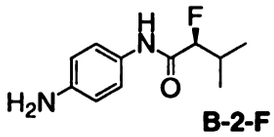

B-2-F

Carrier B/fluorocarboxylic acid conjugates B-2-F:

^{1}H NMR (300Hz, $CDCl_3$) δ 7.81 (br, 1H), 7.35 (d, *J*=8.8 Hz, 2H), 6.69 (d, *J*=8.8 Hz, 2H), 4.86 (dd, 1H), 2.41 (m, 1H), 1.15 (d, *J*=7.1 Hz, 3H), 1.01 (d, *J*=7.1 Hz, 3H).

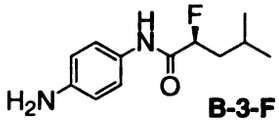

B-3-F

Carrier B/fluorocarboxylic acid conjugates B-3-F:

^{1}H NMR (300Hz, $CDCl_3$) δ 7.85 (br, 1H), 7.35 (d, *J*=8.8 Hz, 2H), 6.68 (d, *J*=8.8 Hz, 2H), 5.04 (m, 1H), 1.98 (m, 3H), 1.02 (m, 6H).

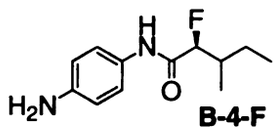

B-4-F

Carrier B/fluorocarboxylic acid conjugates B-4-F:

^{1}H NMR (300Hz, $CDCl_3$) δ 7.83 (br, 1H), 7.35 (d, *J*=8.8 Hz, 2H), 6.69 (d, *J*=8.8 Hz, 2H), 4.89 (m, 1H), 2.16 (m, 1H), 1.57 (m, 1H), 1.30 (m, 1H), 1.11 (d, *J*=7.1 Hz, 3H), 0.95 (t, *J*=7.1 Hz, 3H).

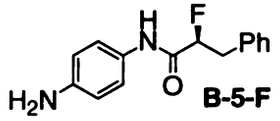

B-5-F

Carrier B/fluorocarboxylic acid conjugates B-5-F:

^{1}H NMR (300Hz, $CDCl_3$) δ 7.62 (br, 1H), 7.32 (m, 5H), 7.23 (d, *J*=8.8 Hz, 2H), 6.63 (d, *J*=8.8 Hz, 2H), 5.22-5.16 (dd, 1H), 3.44-3.21 (m, 2H).

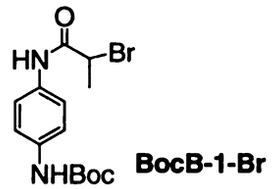

BocB-1-Br

Carrier B/bromocarboxylic acid conjugates BocB-1-Br:

^{1}H NMR ($CDCl_3$, 300 MHz) δ 7.99 (br, 1H), 7.44 (d, *J*=8.8 Hz, 2H), 7.38 (d, *J*=7.7 Hz, 2H), 6.44 (br, 1H), 4.50 (q, *J*=7.1 Hz, 1H), 1.98 (q, *J*=7.1 Hz, 1H), 1.48 (s, 9H).

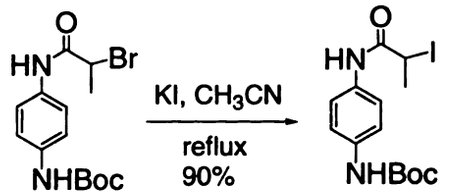

BocB-1-Br **BocB-1-I**

Carrier B/bromocarboxylic acid conjugates BocB-1-I:

The bromo compound **BocB-1-Br** (34 mg, 0.1 mmol) and KI (83 mg, 0.5 mmol) was dissolve in acetonitrile. The mixture was refluxed overnight, and the precipitate was filtered away, and the filtrate was concentrated under reduced pressure. The residue was purified by column chromatography to provide the title compound (90%). ^{1}H NMR ($CDCl_3$, 300 MHz) δ 7.79 (br, 1H), 7.24 (d, *J*=8.8 Hz, 2H), 7.15 (d, *J*=7.7 Hz, 2H), 6.30 (br, 1H), 4.41 (q, *J*=7.1 Hz, 1H), 1.90 (q, *J*=7.1 Hz, 1H), 1.41 (s, 9H).

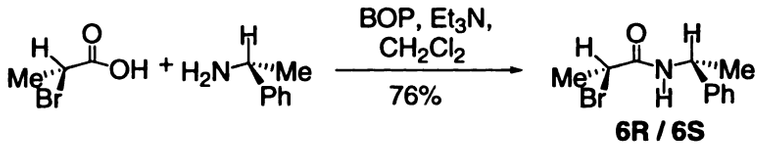

Coupling of (*R*)-2-bromopropionic acid with (*R*)/(*S*)-methylbenzylamine 6R/6S:

(*R*)-2-bromopropionic acid (15.3 mg, 0.1 mmol) and (*R*)-methylbenzylamine (12.1 mg, 0.1 mmol) were dissolved in anhydrous dichloromethane (2 mL). To this solution was added EDC (20 mg, 0.11mmol) and DMAP (15 mg, 0.12 mmol). This mixture was stirred at room temperature overnight. The solvent was removed, and the product was purified by column chromatography (76%). ^{1}H NMR (300Hz, $CDCl_3$) δ 7.31 (m, 5H), 6.58 (br, 1H), 5.15 (m, 1H), 4.37 (q, *J*=6.8 Hz, 1H), 1.87 (d, *J*=7.8 Hz, 3H), 1.50 (d, *J*=6.8 Hz, 3H).

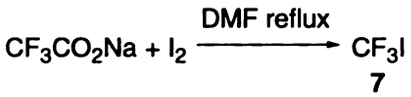

Synthesis of trifluoromethyl iodide 7:

A mixture of iodine (0.15 mol) and dry sodium salt of trifluoroacetic acid (0.1 mol) was mixed in of dry dimthylformamide (40 mL) in a round-bottomed flask and heated to reflux under a condenser cooled with water maintained above the boiling point of the fluoroalkyl iodide product. A syringe was inserted to top of the condenser, and the other end was in a small round-bottom flask, which was cooled with dry ice-acetone bath. The gaseous product was collected over an hour period. The product was kept at –78 °C freezer, and used without further purification.

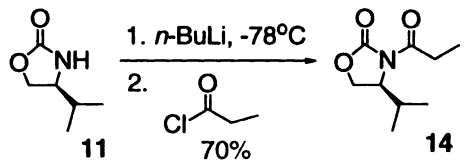

Synthesis of chiral amide 14:

To (*S*)-4-isopropyl-2-oxazolidinone (260 mg, 2 mmol) dissolved in dry THF (4 mL), was added *n*-BuLi (2.5 N in hexane, 1 mL) at –78 °C. After it was stirred for half an hour, propionyl chloride (200 mg, 2.1 mmol) was added into the solution. The reaction was stirred at –78 °C for 2 h. The reaction was quenched with 1 mL of saturated aqueous sodium bisulfate, and then extracted with ether (3 × 10 mL). The ether layer was dried with Na_2SO_4, and concentrated. The residue was purified by column chromatography, to yield the compound (70% yield). ^{1}H NMR (300Hz, $CDCl_3$) δ 4.44-4.06 (m, 3H), 2.91 (q, *J*=6.6 Hz, 2H), 2.38 (m, 1H), 1.18 (t, *J*=6.6 Hz, 3H).

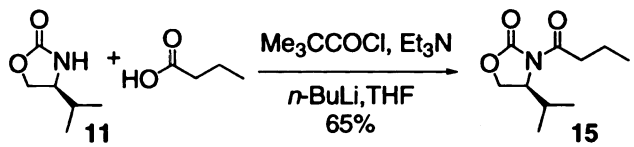

Synthesis of chiral amide 15:

To a stirred solution of butyric acid (176 mg, 2 mmol) in THF (1 mL) at –20 °C was added Me_3CCOCl (0.24 mL, 2.2 mmol) dropwise over 2 min. After 10 min, Et_3N (0.33 mL, 2.4 mmol) was added and the resulting mixture was allowed to warm to –10 °C for an hour. In a separate flask, commercially available (*S*)-4-isopropyl-2-oxazolidinone **11** (260 mg, 2 mmol) was dissolved in dry THF (4 mL), the resulting solution was cooled to –78 °C, and to this solution was added *n*-BuLi in hexane (2.5 N solution, 1 mL). This cold gel-like solution was poured into the mixed anhydride prepared above. After this mixture was stirred at –78 °C for 30 min, it was quenched with aqueous sodium bisulfate

(1 N, 2 mL). THF was removed under reduced pressure, and the residue was extracted with ethyl acetate (3 × 10mL). The organic layer was dried over Na_2SO_4, and concentrated. The residue was purified by column, and afforded **15** in 65% yield. ^1H NMR (300Hz, $CDCl_3$) δ 4.44-4.06 (m, 3H), 2.93 (m, 1H), 2.38 (m, 1H), 1.79 (m, 1H), 1.57 (m, 1H), 1.24 (d, *J*=6.59 Hz, 3H), 0.99 (d, *J*=7.69 Hz, 3H).

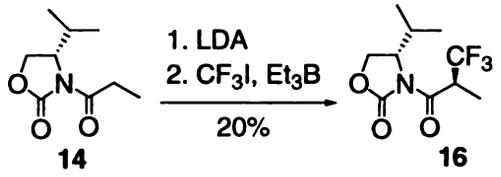

Synthesis of trifluoromethyl amide 16:

Diisopropylamine (0.2 mL, 1.4 mmol) was dissolved in THF (4 mL), and cooled it to –78 °C. *n*-BuLi in hexane (2.5 N solution, 0.5 mL) was added into the solution. The solution was briefly warmed to 0 °C, and then cooled back to –78 °C. Amide **14** (185 mg, 1 mmol) dissolved in 1 mL of THF was added to this solution via cannula, and the solution was then stirred at –78 °C for an hour. CF_3I was added into the solution with triethylborane, and was stirred at –78 °C for another 10 minutes, before it was warmed to –20 °C for 2 hours. The reaction was quenched with saturated aqueous sodium bisulfate (2 mL). THF was removed under reduced pressure, and the residue was extracted with ethyl acetate (3 × 10mL). The organic layer was dried over Na_2SO_4, and concentrated. The residue was purified by column, but still was a mixture of starting amide **14** and the desired product **16**.

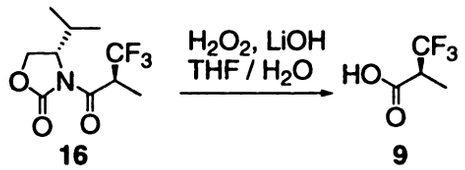

16 9

Synthesis of (*R*)-trifluoromethylpropionic acid 9:

To the mixture of amide **16** and **14**, was added THF and water (4 mL, 3:1), and then H_2O_2 (0.3 mL) and aqueous LiOH (1 mmol, in 1mL of water) were successively added into the reaction mixture. The reaction was stirred at 0 °C for an hour, and then it was quenched with sodium sulfate solution (1 mL). THF was removed under reduced pressure, and the residue was extracted with ethyl acetate (3 × 10mL). The organic layer was dried over Na_2SO_4, and concentrated to afford the mixed carboxylic acids.

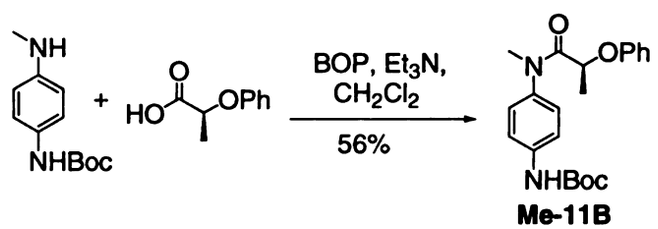

Me-11B

Methylated Boc-B/carboxylic acid conjugate 11 Me-11B:

To a solution of Boc protected carrier **B** (111 mg, 0.5 mmol) in CH_2Cl_2 (6 mL), BOP (250 mg, 0.55 mmol), triethylamine (1 mL), and the chiral carboxylic acid (83 mg, 0.5 mmol) were added. The solution was stirred at room temperature overnight. After removal of most of the solvent under reduced pressure, the product was purified by silica gel flash chromatography (56% yield). ^{1}H NMR ($CDCl_3$, 300 MHz) δ 7.28 (d, *J*=8.8 Hz, 2H), 7.04 (d, *J*=7.7 Hz, 2H), 6.94 (d, *J*=8.2 Hz, 2H), 6.75 (m, 2H), 6.85 (d, *J*=8.2 Hz, 2H), 4.56 (q, *J*=6.6 Hz, 1H), 3.07 (s, 3H), 1.36 (s, 9H), 1.28 (d, *J*=6.0 Hz, 3H).

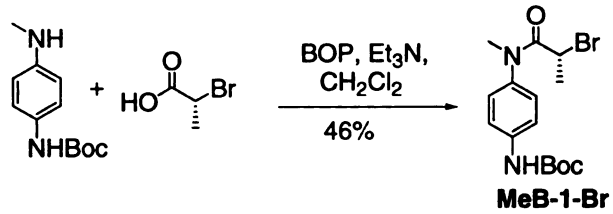

MeB-1-Br

Methylated Boc-B/carboxylic acid conjugate MeB-1-Br:

To a solution of Boc protected carrier **B** (111 mg, 0.5 mmol) in CH_2Cl_2 (6 mL), BOP (250 mg, 0.55 mmol), triethylamine (1 mL), and the chiral carboxylic acid (76 mg, 0.5 mmol) were added. The solution was stirred at room temperature overnight. After removal of most of the solvent under reduced pressure, the product was purified by silica gel flash chromatography (46% yield). ^{1}H NMR ($CDCl_3$, 300 MHz) δ 7.38 (d, *J*=8.8 Hz, 2H), 7.18 (d, *J*=7.7 Hz, 2H), 6.60 (br, 1H), 4.56 (q, *J*=6.6 Hz, 1H), 3.12 (s, 3H), 1.68 (d, *J*=6.0 Hz, 3H),1.48 (s, 9H).

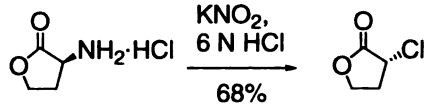

35 **32**

The synthesis of α-chloro-γ-butyrolactone 32:

Sodium nitrite (0.22 g, 3.24 mmol) was added to a solution of homoserine **35** (137 mg, 1 mmol) and potassium bromide (0.78 g, 6.56 mmol) in 2.5 N sulfuric acid (9 mL) at −10 °C, and the reaction mixture was stirred for 3 h, and then extracted with CH_2Cl_2 (3 × 25 mL). The combined organic layers were dried over sodium sulfate and evaporated. The residue was purified by column chromatography and provided the pure title compound (68% yield). ^{1}H NMR ($CDCl_3$, 300 MHz) δ 4.51 (m, 1H), 4.38 (m, 2H), 2.75 (m, 1H), 2.46 (m, 1H).

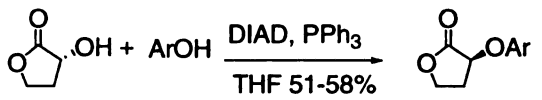

42 **36, 48 and 49**

General procedure for the synthesis of (*S*)-α-aryloxy-γ-butyrolactones:

Aromatic alcohol (0.5 mmol), (*R*)-α-hydroxy-γ-butyrolactone **42** (51 mg, 0.5 mmol) and PPh_3 (131 mg, 0.5 mmol) were dissolved in THF (3 mL) and cooled to 0 °C. DIAD (106 mg, 0.5 mmol) were added to the reaction mixture dropwise. The reaction was slowly warmed up to room temperature, and stirred overnight. The reaction was quenched with saturated $NaHCO_3$ (5 mL) and extract with CH_2Cl_2 (3 × 10 mL). The organic layers were combined and dried over Na_2SO_4. The solvent was removed under reduced pressure, and the residue was purified by column chromatography to provide the desired compound.

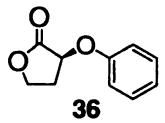

36

(*S*)-α-phenoxy-γ-butyrolactone 36:

^1H NMR ($CDCl_3$, 300 MHz) δ 7.29 (m, 2H), 7.03 (m, 3H), 4.93 (t, *J*=7.7 Hz, 1H), 4.46 (m, 1H), 4.30 (m, 1H), 2.68 (m, 1H), 2.42 (m, 1H), 1.28 (s, 9H); ^{13}C NMR ($CDCl_3$, 300 MHz) δ 173.3, 157.1, 129.3, 122.0, 115.9, 72.3, 65.2, 29.9.

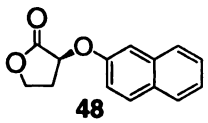

48

(*S*)-α-naphthyloxy-γ-butyrolactone 48:

^1H NMR ($CDCl_3$, 300 MHz) δ 7.75 (m, 3H), 7.44-7.18 (m, 4H), 5.05 (t, *J*=7.7 Hz, 1H), 4.46 (m, 1H), 4.33 (m, 1H), 2.74 (m, 1H), 2.42 (m, 1H); ^{13}C NMR ($CDCl_3$, 300 MHz) δ

173.1, 154.8, 134.1, 129.5, 129.4, 127.4, 126.7, 126.3, 124.0, 118.5, 108.7, 72.0, 65.2, 29.4.

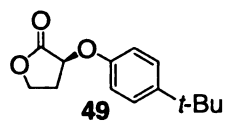

49

(*S*)-α-*p*-*tert*-butylphenoxy-γ-butyrolactone 49:

^{1}H NMR ($CDCl_3$, 300 MHz) δ 7.30 (d, *J*=8.8 Hz, 2H), 6.93 (d, *J*=8.8 Hz, 2H), 4.90 (t, *J*=8.2 Hz, 1H), 4.47 (m, 1H), 4.33 (m, 1H), 2.65 (m, 1H), 2.40 (m, 1H), 1.28 (s, 9H); ^{13}C NMR ($CDCl_3$, 300 MHz) δ 173.3, 154.5, 145.1, 126.1, 114.6, 72.2, 64.4, 33.9, 31.0, 29.3.

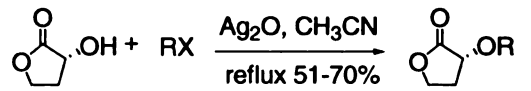

42 **44, 46 and 47**

General procedure for the synthesis of (*R*)-α-alkoxy-γ-butyrolactones 44, 46 and 47:

(*R*)-α-hydroxy-γ-butyrolactone **42** (51 mg, 0.5 mmol), alkyl halides (2 mmol) and silver oxide (2 mmol) was refluxed in acetonitrile (5 mL) overnight. The precipitate was filtered away, and the filtrate was concentrated under reduced pressure. The residue was purified by column chromatography to yield the pure title product.

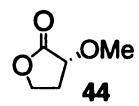

44

(*R*)-α-methoxy-γ-butyrolactone 44:

^{1}H NMR ($CDCl_3$, 300 MHz) δ 4.39 (m, 1H), 4.28 (m, 1H), 4.07 (m, 1H), 3.58 (s, 3H), 2.49 (m, 1H), 2.11 (m, 1H).

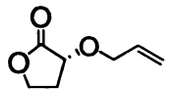

46

(*R*)-α-allyloxy-γ-butyrolactone 46:

^{1}H NMR ($CDCl_3$, 300 MHz) δ 5.79 (m, 1H), 5.15 (m, 2H), 4.38-4.06 (m, 5H), 2.39 (m, 1H), 2.12 (m, 1H); ^{13}C NMR ($CDCl_3$, 300 MHz) δ 174.7, 133.3, 117.7, 72.3, 70.8, 65.0, 29.3.

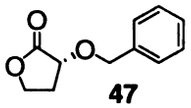

47

(*R*)-α-benzoxy-γ-butyrolactone 47:

^{1}H NMR ($CDCl_3$, 300 MHz) δ 7.34 (m, 5H), 4.90 (d, *J*=11.5 Hz, 1H) 4.70 (d, *J*=11.5 Hz, 1H), 4.36 (m, 1H), 4.16 (m, 2H), 2.41 (m, 1H), 2.23 (m, 1H); ^{13}C NMR ($CDCl_3$, 300 MHz) δ 174.7, 133.6, 128.2, 127.7, 72.7, 71.8, 65.1, 29.5.

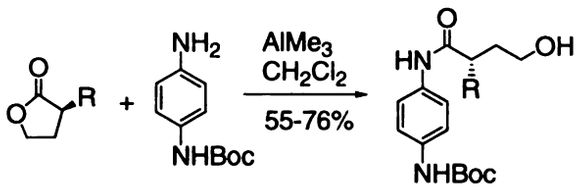

General procedure for the synthesis of amides:

To a solution of **Boc-B** (1.5 eq.) in anhydrous CH_2Cl_2 (5 mL) at room temperature was added trimethylaluminum (2.0 N in hexane, 1.6 eq.) dropwise, under nitrogen. The resulting mixture was stirred for 15 min, then the α-chiral butyrolactone (1eq.) in CH_2Cl_2 (2 mL) was added slowly and stirring was continued at room temperature overnight. The reaction was quenched with aqueous citric acid (2 N, 2 mL), glycerin (5 drops) and saturated aqueous potassium sodium tartrate (10 mL), and kept stirring for another 6 h. The reaction mixture was extracted with CH_2Cl_2 (3 × 10 mL). The combined organic

extract were dried over Na_2SO_4, and concentrated. The residue was purified by column chromatography to yield the pure amides.

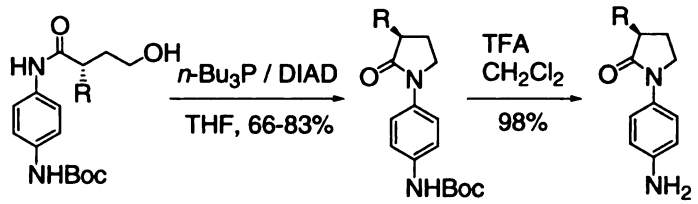

General procedure for the synthesis of chiral butyrolactams:

Tri-n-butylphosphine (1.1 eq.) was added to a solution of DIAD (1.1 eq.) in dry THF (2 mL) at room temperature. The resulting mixture was stirred for 5 min, then added dropwise to a solution of chiral amide (1 eq.) in THF (1 mL) at 0 °C under nitrogen. The reaction mixture was allowed to warm slowly to room temperature and stirred overnight. The reaction was quenched with saturated $NaHCO_3$ (5 mL) and extracted with CH_2Cl_2 (2 × 10 mL). The combined organic extract were dried over Na_2SO_4, and concentrated. The residue was purified by column chromatography to yield the Boc protected lactam as a white solid. Some times, the lactam could not be separated from the byproduct from DIAD. The Boc group was removed by stirring overnight in TFA/CH_2Cl_2 (1:4) at room temperature. The solvent was then removed by purging nitrogen. The residue was redissolved in anhydrous CH_2Cl_2, and anhydrous Na_2CO_3 (20 mg) was added. This solution was stirred at room temperature for an hour, and the Na_2CO_3 was filtered. The solvent was evaporated under reduced pressure to provide analytically pure product.

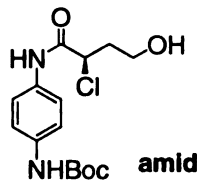

amide 37

Amide 37:

^{1}H NMR ($CDCl_3$, 300 MHz) δ 9.04 (br, 1H), 7.31 (d, *J*=8.8 Hz, 2H), 7.22 (br, 1H), 7.16 (d, *J*=8.8 Hz, 2H), 4.48 (m, 1H), 3.62 (m, 2H), 2.13 (m, 1H), 1.97 (m, 1H), 1.36 (s, 9H); ^{13}C NMR ($CDCl_3$, 300 MHz) δ 167.5, 153.0, 135.2, 132.0, 120.8, 118.9, 57.9, 56.7, 48.6, 37.4, 28.0.

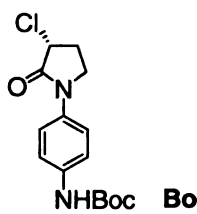

Boc-37

Boc-protected lactam Boc-37:

^{1}H NMR ($CDCl_3$, 300 MHz) δ 7.54 (d, *J*=8.8 Hz, 2H), 7.38 (d, *J*=8.8 Hz, 2H), 6.57 (br, 1H), 4.51 (m, 1H), 3.98 (m, 1H), 3.79 (m, 1H), 2.67 (m, 1H), 2.35 (m, 1H), 1.49 (s, 9H); ^{13}C NMR ($CDCl_3$, 300 MHz) δ 168.6, 152.5, 135.5, 133.6, 120.6, 118.6, 80.4, 55.8, 46.0, 29.3, 28.1.

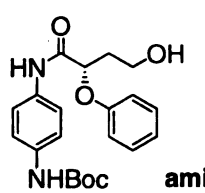

amide 39

Amide 39:

^{1}H NMR ($CDCl_3$, 300 MHz) δ 8.17 (br, 1H), 7.41 (d, *J*=8.8 Hz, 2H), 7.30 (m, 3H), 7.03-6.95 (m, 4H), 6.47 (br, 1H), 4.85 (t, *J*=6.6 Hz, 1H), 3.87 (m, 2H), 2.32 (br, 1H), 2.24 (m, 2H), 1.49 (s, 9H).

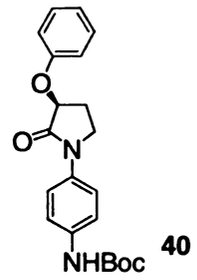

40

Boc-protected lactam 40:

^{1}H NMR ($CDCl_3$, 300 MHz) δ 7.43 (d, *J*=9.3 Hz, 2H), 7.22 (d, *J*=8.8 Hz, 2H), 7.18 (m, 2H), 6.95-6.80 (m, 3H), 6.49 (br, 1H), 4.83 (t, *J*=7.6 Hz, 1H), 3.82 (m, 2H), 2.64 (m, 1H), 2.33 (m, 1H), 1.48 (s, 9H).

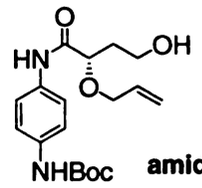

amide 50

Amide 50:

^{1}H NMR ($CDCl_3$, 300 MHz) δ 8.43 (br, 1H), 7.40 (d, *J*=8.8 Hz, 2H), 7.27 (d, *J*=8.8 Hz, 2H), 6.99 (br, 1H), 5.89 (m, 1H), 5.25 (m, 2H), 4.06 (m, 3H), 3.71 (m, 2H), 3.19 (br, 1H), 1.99 (m, 2H), 1.49 (s, 9H); ^{13}C NMR ($CDCl_3$, 300 MHz) δ 170.7, 152.6, 134.9, 133.1, 131.8, 120.4, 118.9, 118.2, 80.0, 77.8, 71.6, 58.7, 35.2, 28.0.

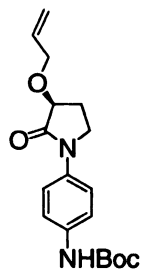

Boc-50

Boc protected lactam Boc-50:

^{1}H NMR ($CDCl_3$, 300 MHz) δ 7.59 (d, *J*=8.8 Hz, 2H), 7.35 (d, *J*=8.8 Hz, 2H), 6.57 (br, 1H), 5.97 (m, 1H), 5.26 (m, 2H), 4.43 (m, 1H), 4.25-4.17 (m, 2H), 3.87-3.60 (m, 2H), 2.42 (m, 1H), 2.06 (m, 1H), 1.48 (m, 9H).

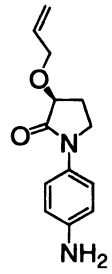

50

Lactam 50:

^{1}H NMR ($CDCl_3$, 300 MHz) δ 7.35 (d, *J*=8.8 Hz, 2H), 6.66 (d, *J*=8.8 Hz, 2H), 5.96 (m, 1H), 5.26 (m, 2H), 4.43 (m, 1H), 4.20 (m, 2H), 3.87-3.60 (m, 2H), 2.44 (m, 1H), 2.06 (m, 1H).

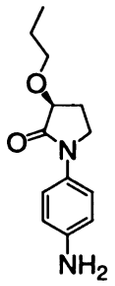

51

Lactam 51:

^{1}H NMR ($CDCl_3$, 300 MHz) δ 7.37 (d, *J*=8.8 Hz, 2H), 6.65 (d, *J*=8.8 Hz, 2H), 4.11 (m, 1H), 3.87 (m, 1H), 3.74 (m, 1H), 3.65 (m, 1H), 3.53 (m, 1H), 2.41 (m, 1H), 2.06 (m, 1H), 1.60 (m, 2H), 0.92 (t, *J*=7.1 Hz, 3H).

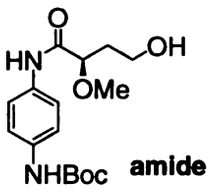

amide 52

Amide 52:

^{1}H NMR ($CDCl_3$, 300 MHz) δ 8.33 (br, 1H), 7.46 (d, *J*=8.2 Hz, 2H), 7.31 (d, *J*=8.2 Hz, 2H), 6.62 (br, 1H), 3.88 (d, *J*=6.6 Hz, 1H), 3.77 (d, *J*=6.0 Hz, 2H), 3.48 (s, 3H), 2.04 (m, 2H), 1.49 (s, 9H).

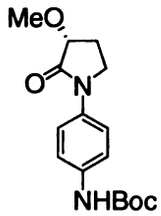

Boc-52

Boc protected lactam Boc-52:

^{1}H NMR ($CDCl_3$, 300 MHz) δ 7.52 (d, *J*=8.8 Hz, 2H), 7.33 (d, *J*=8.8 Hz, 2H), 6.57 (br, 1H), 4.05 (t, *J*=7.7 Hz, 1H), 3.71 (m, 2H), 3.57 (s, 3H), 2.45 (m, 1H), 2.04 (m, 1H), 1.49 (s, 9H).

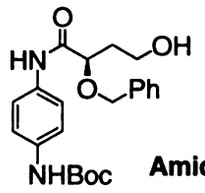

Amide 53

Amide 53:

^{1}H NMR ($CDCl_3$, 300 MHz) δ 8.37 (br, 1H), 7.34 (m, 9H), 6.62 (br, 1H), 4.62 (s, 2H), 4.13 (t, *J*=6.0 Hz, 1H), 3.76 (m, 2H), 2.62 (br, 1H), 2.05 (m, 2H), 1.49 (s, 9H), ^{13}C NMR ($CDCl_3$, 300 MHz) δ 170.5, 152.5, 136.1, 134.7, 131.9, 128.5, 128.2, 127.8, 120.4, 118.7, 80.3, 78.5, 73.1, 59.1, 35.3, 28.0.

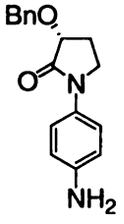

53

Lactam 53:

^{1}H NMR ($CDCl_3$, 300 MHz) δ 7.36 (m, 7H), 6.65 (d, *J*=8.8 Hz, 2H), 4.99 (d, *J*=12.1 Hz, 1H), 4.79 (d, *J*=12.1 Hz, 1H), 4.20 (t, *J*=7.7 Hz, 1H), 3.87-3.62 (m, 2H), 2.35 (m, 1H), 2.12 (m, 1H).

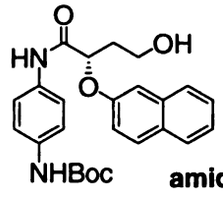

amide 54

Amide 54:

^{1}H NMR ($CDCl_3$, 300 MHz) δ 8.27 (br, 1H), 7.79-7.63 (m, 3H), 7.43 (m, 4H), 7.22 (m, 4H), 6.60 (br, 1H), 4.50 (t, *J*=6.0 Hz, 1H), 3.87 (m, 2H), 2.72 (br, 1H), 2.28 (m, 2H), 1.49 (s, 9H); ^{13}C NMR ($CDCl_3$, 300 MHz) δ 169.4, 154.3, 152.6, 135.1, 133.8, 131.5, 129.8, 129.4, 127.3, 126.8, 126.4, 124.2, 120.7, 118.7, 118.0, 108.9, 80.2, 60.2, 58.3, 35.1, 28.1.

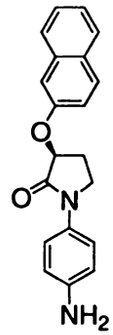

54

Lactam 54:

^{1}H NMR ($CDCl_3$, 300 MHz) δ 7.73 (m, 3H), 7.41-7.20 (m, 6H), 6.73 (d, *J*=8.8 Hz, 2H), 5.15 (t, *J*=6.0 Hz, 1H), 3.85 (m, 1H), 2.77 (br, 1H), 2.23 (m, 1H), 1.49 (s, 3H).

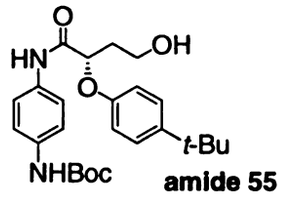

amide 55

Amide 55:

^{1}H NMR ($CDCl_3$, 300 MHz) δ 8.28 (br, 1H), 7.40 (d, *J*=8.8 Hz, 2H), 7.28 (m, 4H), 6.89 (d, *J*=8.8 Hz, 2H), 6.72 (br, 1H), 4.80 (t, *J*=6.0 Hz, 1H), 3.83 (m, 2H), 2.86 (br, 1H), 2.21 (m, 2H), 1.49 (s, 9H), 1.25 (s, 9H); ^{13}C NMR ($CDCl_3$, 300 MHz) δ 169.9, 154.5, 152.3, 144.8, 135.1, 131.6, 126.3, 120.9, 118.7, 114.3, 101.2, 80.2, 58.5.

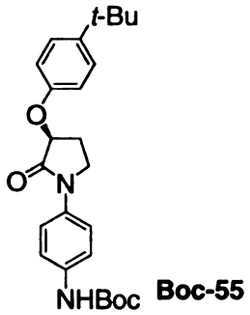

Boc-55

Boc protected lactam Boc-55:

^{1}H NMR ($CDCl_3$, 300 MHz) δ 7.66 (d, *J*=9.09 Hz, 2H), 7.42 (d, *J*=8.79 Hz, 2H), 7.35 (d, *J*=9.09 Hz, 2H),7.05 (d, *J*=8.79 Hz, 2H), 6.51 (br, 1H), 5.03 (t, *J*=7.62 Hz, 1H), 3.89 (m, 2H), 2.70 (m, 1H), 2.33 (m, 1H), 1.55 (s, 9H), 1.34 (s, 9H).

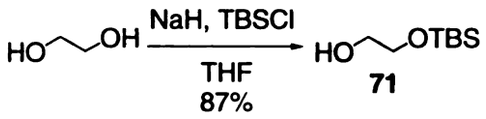

71

Monosilylated ethylene glycol 71:

NaH (60% suspension, 80 mg, 2 mmole, washed 3 times with hexane) was added to a solution of ethylene glycol (124 mg, 2 mmole) in THF (5 mL) at 0 °C. After this mixture was stirred at room temperature for an hour, TBSCl (300 mg, 2 mmol) was added into the solution, and the reaction was stirred at room temperature overnight. The reaction was quenched with brine, and extracted with CH_2Cl_2 (3 × 20 mL). The organic layer was combined and dried over Na_2SO_4. The residue was purified by column chromatography to yield the title compound (87%). ^{1}H NMR ($CDCl_3$, 300 MHz) δ 3.69 (m, 2H), 3.60 (m, 2H), 0.81 (s, 9H), 0 (s, 6H).

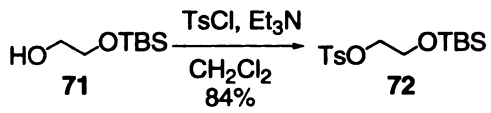

Tosylate 72:

Monosilylated ethylene glycol **71** (176 mg, 0.1 mmol), and Et_3N (1 mL) were dissolved in CH_2Cl_2 (10 mL). TsCl (380 mg, 0.2 mmol) was slowly added in small portion at 0 °C. The reaction was allowed to warm to room temperature, and stirred overnight. The solvent was removed under reduced pressure, and the residue was purified by column chromatography to yield the title compound (84%). ^1H NMR ($CDCl_3$, 300 MHz) δ 7.79 (d, *J*=8.2 Hz, 2H), 7.32 (d, *J*=8.2 Hz, 2H), 3.81 (t, *J*=6.6 Hz, 2H), 3.81 (t, *J*=6.6 Hz, 2H), 2.43 (s, 3H), 0.81 (s, 9H), 0 (s, 6H).

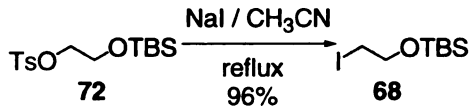

TBS-protected iodoethanol 68:

Tosylate **72** (165 mg, 0.5 mmol) was dissolved in CH_3CN (10 mL) together with NaI (10 mg, 1 mmol). This mixture was refluxed overnight, and the precipitate was filtered away, and the filtrate was concentrated under reduced pressure. The residue was purified by column chromatography to yield the title compound (96%). ^1H NMR ($CDCl_3$, 300 MHz) δ 3.81 (t, *J*=6.59 Hz, 2H), 3.18 (t, *J*=6.59 Hz, 2H), 0.89 (s, 9H), 0 (s, 6H).

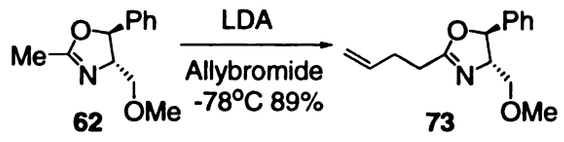

The alkylated product 73:

To a solution of lithium diisopropylamide (LDA) (1.55 mmol) in THF was added a solution of chiral auxiliary (318 mg, 1.55 mmol) **62** in THF (2 mL) dropwise at –78 °C. The mixture was stirred for 45 min at –78 °C, and a solution of allylbromide (0.48 g, 4 mmol) in THF was added slowly. After complete addition, the mixture was stirred an additional 4 h, allowed to slowly warm to –50 °C, and quenched by pouring into ice-water. The aqueous mixture was extracted (3 × 30 mL) with ether, and the combined ether layers were dried with Na_2SO_4, and concentrated. Following column chromatography affords the title compound as clear oil (89% yield). ^{1}H NMR ($CDCl_3$, 300 MHz) δ 7.32 (m, 5H), 5.83 (m, 1H), 5.23 (d, *J*=6.6 Hz, 2H), 5.03 (m, 2H), 4.09 (m, 1H), 3.58 (m, 1H), 3.48 (m, 1H), 3.38 (s, 3H), 2.50-2.40 (m, 4H).

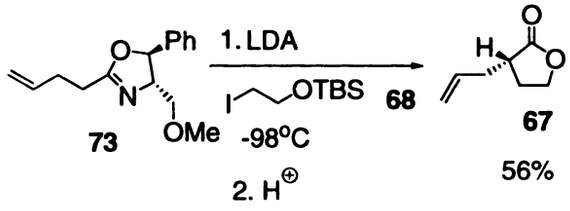

(*S*)-2-Allyl-γ-butyrolactone 67:

To a solution of LDA (1.1 eq.) was added the compound **73** (246 mg, 1 mmol) in THF dropwise at –78 °C, and the mixture was stirred at –78 °C for 45 min. The reaction was then cooled to –98 °C, and **68** (1.03 g, 4 mmol) was slowly added. The reaction was kept at –98 °C for 2 h, and then at –78 °C for 4 h. After being warmed slowly to 0 °C, the solution was quenched with ammonium chloride solution, and extracted with ether (4 × 20 mL). The ether extract was dried over Na_2SO_4, and concentrated. The crude alkylated

product was hydrolyzed immediately in 20 mL of refluxing 4.5 N HCl for 15 min. The solution was cooled down to room temperature, and extracted with ether (4 × 20 mL). The ether extract was dried over Na_2SO_4, and concentrated. Column chromatography provided the pure title product in 56% yield. ^1H NMR ($CDCl_3$, 300 MHz) δ 5.77 (m, 1H), 5.11 (m, 2H), 4.34-4.16 (m, 2H), 2.63 (m, 2H), 2.42 (m, 2H), 1.99 (m, 1H); ^{13}C NMR ($CDCl_3$, 300 MHz) δ 182.6, 134.1, 117.4, 66.2, 38.5, 34.0, 27.5.

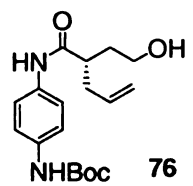

76

Allyl amide 76:

^1H NMR ($CDCl_3$, 300 MHz) δ 7.67 (br, 1H), 7.37 (d, *J*=8.8 Hz, 2H), 7.26 (d, *J*=8.8 Hz, 2H), 6.50 (br, 1H), 5.78 (m, 1H), 5.09 (m, 2H), 3.70 (m, 2H), 2.50 (m, 2H), 2.24 (m, 1H), 1.95 (br, 1H), 1.81 (m, 2H), 1.49 (s, 9H); ^{13}C NMR ($CDCl_3$, 300 MHz) δ 168.1, 153.2, 135.2, 134.3, 132.7, 120.5, 128.9, 117.0, 80.2, 60.0, 44.2, 36.5, 34.4, 28.0.

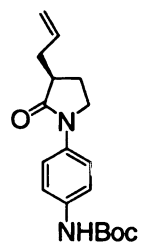

Boc-75

Boc protected lactam Boc-75:

^1H NMR ($CDCl_3$, 300 MHz) δ 7.52 (d, *J*=8.8 Hz, 2H), 7.34 (d, *J*=8.8 Hz, 2H), 6.49 (br, 1H), 5.78 (m, 1H), 5.07 (m, 2H), 3.71 (m, 2H), 2.65 (m, 2H), 2.25 (m, 2H), 1.79 (m, 1H), 1.48 (s, 9H); ^{13}C NMR ($CDCl_3$, 300 MHz) δ 174.7, 152.5, 135.1, 134.3, 120.1, 118.5, 116.7, 80.1, 46.6, 42.5, 35.1, 28.0, 23.6, 21.6.

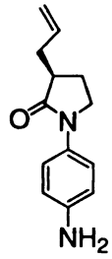

75

Allyl lactam 75:

^{1}H NMR ($CDCl_3$, 300 MHz) δ 7.42 (d, *J*=8.8 Hz, 2H), 6.70 (d, *J*=8.8 Hz, 2H), 5.83 (m, 1H), 5.17 (m, 2H), 3.75 (m, 2H), 2.70 (m, 2H), 2.31 (m, 2H), 1.82 (m, 1H).

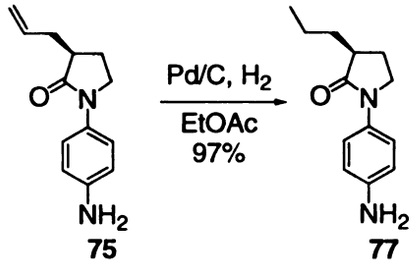

75 **77**

Propyl lactam 77:

To the allyllactam **75** (21.6 mg, 0.1 mmol) in EtOAc (5 mL) was added Pd/C (5 mg). This reaction was then hydrogenated at atmospheric pressure for 20 h. The black powder was filtered, and the filtrate was concentrated under reduced pressure to yield the pure product (97%). ^{1}H NMR ($CDCl_3$, 300 MHz) δ 7.51 (d, *J*=8.8 Hz, 2H), 7.32 (d, *J*=8.8 Hz, 2H), 6.57 (br, 1H), 3.72 (m, 2H), 2.55 (m, 1H), 2.27 (m, 1H), 1.77 (m, 1H), 1.48 (s, 9H), 1.22 (d, *J*=7.14 Hz, 3H), 0.99 (m, 4H); ^{13}C NMR ($CDCl_3$, 300 MHz) δ 175.2, 152.3, 134.1, 120.1, 118.6, 80.1, 46.6, 42.8, 33.0, 28.0, 24.4, 21.6, 13.7.

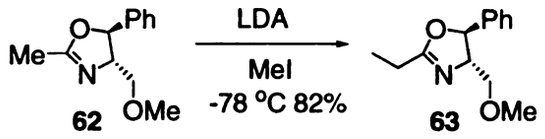

The alkylated product 63:

To a solution of lithium diisopropylamide (LDA) (1.55 mmol) in THF was added a solution of chiral auxiliary (318 mg, 1.55 mmol) **62** in THF (2 mL) dropwise at –78 °C. The mixture was stirred for 45 min at –78 °C, and a solution of methyl iodide (0.64 g, 4 mmol) in THF was added slowly. After complete addition, the mixture was stirred an additional 4 h, allowed to slowly warm to –50 °C, and quenched by pouring into ice-water. The aqueous mixture was extracted (3 × 30 mL) with ether, and the combined ether layers were dried with Na_2SO_4, and concentrated. Column chromatography affords the title compound as clear oil (82% yield). ^{1}H NMR ($CDCl_3$, 300 MHz) δ 7.30 (m, 5H), 5.24 (d, *J*=6.6 Hz, 2H), 4.07 (m, 1H), 3.58 (m, 1H), 3.48 (m, 1H), 3.38 (s, 3H), 2.38 (t, *J*=7.7 Hz, 2H), 1.21 (t, *J*=7.7 Hz, 3H).

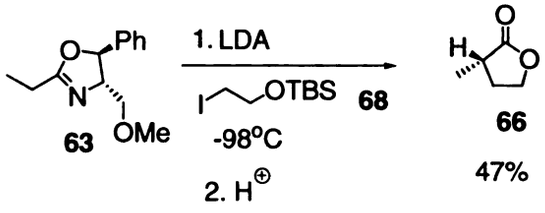

(*S*)-2-Methyl-γ-butyrolactone 66:

To a solution of LDA (1.1 eq.) was added the compound **63** (220 mg, 1 mmol) in THF dropwise at –78 °C, and the mixture was stirred at –78 °C for 45 min. The reaction was then cooled to –98 °C, and **68** (1.03 g, 4 mmol) was slowly added. The reaction was kept at –98 °C for 2 h, and then at –78 °C for 4 h. After being warmed slowly to 0 °C, the solution was quenched with ammonium chloride solution, and extracted with ether (4 × 20 mL). The ether extract was dried over Na_2SO_4, and concentrated. The crude alkylated

product was hydrolyzed immediately in 20 mL of refluxing 4.5 N HCl for 15 min. The solution was cooled down to room temperature, and extracted with ether (4 × 20 mL). The ether extract was dried over Na_2SO_4, and concentrated. Column chromatography provided the pure title product in 47% yield. ^{1}H NMR ($CDCl_3$, 300 MHz) δ 4.40-4.22 (m, 2H), 2.62-2.53 (m, 2H), 1.96 (m, 1H), 1.32 (d, *J*=7.1 Hz, 3H).

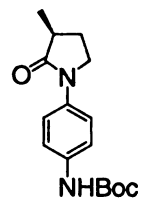

Boc-78

Boc protected lactam Boc-78:

^{1}H NMR ($CDCl_3$, 300 MHz) δ 7.53 (d, *J*=8.8 Hz, 2H), 7.34 (d, *J*=8.8 Hz, 2H), 6.46 (br, 1H), 3.74 (m, 2H), 2.63 (m, 1H), 2.34 (m, 1H), 1.73 (m, 1H), 1.48 (s, 9H), 1.27 (d, *J*=7.1 Hz, 3H); ^{13}C NMR ($CDCl_3$, 300 MHz) δ 174.7, 158.8, 134.2, 133.0.1, 119.0.4, 75.3, 60.0, 38.4, 36.2, 28.0, 17.4.

Reference:

1. Eliel, E. L.; Wilen, S. H. *Stereochemistry of Organic Compounds*; John Wiley & Sons, Inc.: New York, **1994**.

2. Iida, K.; Kajiwara, M., *J. Labeled Compd. Radiopharm.* **1991**, *XXIX*, 201.

3. Matins, M. A. P.; Sinhorin, A. P.; Zimmermann, N. E. K.; Znatta, N.; Bonacorso, H. G.; Bastos, G. P. *Synthesis* **2001**, *13*, 1959.

4. Tyrrell, E.; Tsang, M. W. H.; Skinner, G. A.; Fawcett, J. *Tetrahedron* **1996**, *52*, 9841.

5. Nagai, Y.; Kusumi, K. *Tetrahedron Lett.* **1995**, *36*, 1853.

6. Kusumi, K.; Yabuuchi, T.; Ooi, T. *Chirality* **1997**, *9*, 550.

7. Mizutani, J.; Tahara, S. *Tetrahedron Lett.* **1996**, *37*, 4737.

8. Proni, G.; Pescitelli, G.; Huang, X.; Quraishi, N. Q.; Nakanishi, K.; Berova, N. *Chem. Commun.* **2002**, 1590.

9. Proni, G.; Pescitelli, G.; Huang, X.; Nakanishi, K.; Berova, N. *J. Am. Chem. Soc.* **2003**, *125*, 12914.

10. Iseki, K.; Nagai, T.; Kobayashi, Y. *Tetrahedron Lett.* **1993**, *34*, 2169.

11. Liou, K.; Yang, P.; Lin, Y. *J. Organomet. Chem.* **1985**, *294*, 145.

12. Jadhav, P. K.; Bhat, K. S.; Perumal, P. T.; Brown, H. C. *J. Am. Chem. Soc.* **1992**, *114*, 385.

13. Paskovich, R.; Gaspar, P.; Hammond, G. S. *J. Org. Chem.* **1967**, *32*, 833.

14. Ghosh, A. K.; Hussain, K. A.; Fidanze, S. *J. Org. Chem.* **1997**, *62*, 6080.

15. Anh, N. T.; Eisenstein, O. *Nouv. J. Chem.* **1977**, *1*, 61.

16. Lodge, E. P.; Heathcock, C. H. *J. Am. Chem. Soc.* **1987**, *109*, 3353.

17. Bell, I. M.; Beshore, D. C.; Gallicchio, S. N.; Williams, T. M. *Tetrahedron Lett.* **2000**, *41*, 1141.

18. Mitsunobu, O. *Synthesis* **1981**, 1.

19. Basha, A.; Lipton, M.; Weinreb, S. M. *Tetrahedron Lett.* **1977**, *18*, 4171.

20. Mitsunobu, O.; Eguchi, M. *Bull. Chem. Soc. Jpn.* **1971**, *44*, 3427.

21. Finch, N.; Fitt, J. J.; Hsu, I. H. S. *J. Org. Chem.* **1975**, *40*, 206.

22. Mitsunobu, O.; Yamada, M. *Bull. Chem. Soc. Jpn.* **1967**, *40*, 935.

23. Johnson, C. R.; Dutra, G. A. *J. Am. Chem. Soc.* **1973**, *95*, 7777.

24. Boldrini, G. P.; Mengoli, M.; Tagliavini, E.; Trombini, C.; Umani-ronchi, A. *Tetrahedron Lett.* **1986**, *27*, 4223.

25. Boldrini, G. P.; Savoia, D.; Tagliavini, E.; Trombini, C.; Umani-ronchi, A. *J. Org. Chem.* **1983**, *48*, 4108.

26. Braga, D.; Ripamonti, A.; Savoia, D.; Trombini, C.; Umani-ronchi, A. *J. Chem. Soc., Chem. Commun.* **1978**, 927.

27. Savoia, D.; Tagliavini, E.; Trombini, C.; Umani-ronchi, A. *J. Org. Chem.* **1981**, *46*, 5340.

28. Rieke, R. D.; Li, P. T.; Burns, T. P.; Uhm, S. T. *J. Org. Chem.* **1981**, *46*, 4323.

29. Rieke, R. D.; Kavaliunas, A. V.; Rhyne, L. D.; Fraser, D. J. *J. Am. Chem. Soc.* **1979**, *101*, 246.

30. Cardillo, G.; D'Amico, A.; Orena, M.; Sandri, S. *J. Org. Chem.* **1988**, *53*, 2354.

31. Lermer, L.; Neeland, E. G.; Ounsworth, J. P.; Sims, R. J.; Tischler, S. A.; Weiler, L. *Can. J. Chem.* **1992**, *70*, 1427.

32. Eberlein, T. H. *J. Org. Chem.* **1992**, *57*, 3479.

33. Prashad, M.; Kim, H.; Har, D.; Repic, O.; Blacklock, T. J. *Tetrahedron Lett.* **1998**, *39*, 9369.

34. Meyers, A. I.; Yamamoto, Y.; Mihelich, E. D.; Bell, R. A. *J. Org. Chem.* **1980**, *45*, 2792.

35. Iwata, A.; Tang, H.; Kunai, A. *J. Org. Chem.* **2002**, *67*, 5170.

36. Detty, M. R.; Seidler, M. D. *J. Org. Chem.* **1981**, *46*, 1283.

37. Ohshita, J.; Iwata, A.; Kanetani, F.; Kunai, A.; Yamamoto, Y.; Matui, C. *J. Org. Chem.* **1999**, *64*, 8024.

38. Sato, T.; Hanayama, K.; Tujisawa, T. *Tetrahedron Lett.* **1988**, *29*, 2197.

39. Huang, X.; Rickman, B.; Borhan, B.; Berova, N.; Nakanishi, K. *J. Am. Chem. Soc.* **1998**, *120*, 6185.

Chapter 5

The chiral aggregation of porphyrin acids

It is well-known that porphyrins tend to self-align into one-dimensional aggregate under appropriate conditions, creating novel supramolecular architectures.[1-3] Three types of interactions have been proposed for porphyrin aggregation:[4, 5] (1) free-base porphyrins aggregate via a weak π-π stacking and/or van der Waals interaction;[6] (2) some metalloporphyrins exhibit a strong metal-π interactions that can be abolished by ligand binding to the metal and a strong metal-side chain binding; (3) the aggregation of porphyrins can also be reinforced by hydrogen-bond interactions between the substituents on the porphyrin periphery.[7-9]

Upon self-assembly, the porphyrins can form two different kinds of aggregates: the "face-to-face" *H*-type and the "edge-to-edge" *J*-type[10] (Figure 5-1). It is known that the Soret bands of *H*-type and *J*-type aggregates appear at shorter and longer wavelength, respectively, compared to the Soret bands of the corresponding porphyrin monomers.[11, 12] This could be interpreted on the basis of the exciton coupling mechanism.[13, 14]

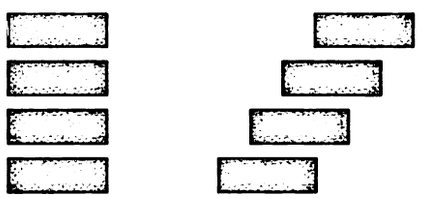

H-aggregation *J*-aggregation

Figure 5-1. The self-assembly of porphyrins.

Some porphyrin aggregates have attracted a lot of attention for mimicking the self-assembly of bacteriochlorophyll *c*,[15, 16] the main pigment of chlorosomes (green sacs), the light-harvesting organelles of green photosynthetic bacteria. The study of porphyrin aggregates could potentially give access to artificial and robust devices for

photochemical energy conversion.[17, 18] Porphyrin aggregates[19] have also been studied for serving as a new generation of optoelectronic devices for telecommunications, optical switching and information storage.[20-22]

Since porphyrins can easily aggregate, we were interested in investigating if the porphyrins could aggregate in a chiral fashion upon addition of chiral substances. If so, we would like to investigate the possibility of determining the stereochemistry of chiral compounds by studying the helicity induced within porphyrin aggregates, analyzed by ECCD.

In order to investigate the above hypothesis, zinc porphyrin acid was synthesized. Porphyrin acids should readily aggregate in non-polar solvents, such as hexane, and methylcyclohexane, while the acid functionality should align the porphyrin planes through hydrogen bonds and polar interactions. In addition, as we saw before for the zinc porphyrin tweezer case, the zinc atom can serve as a binding site to coordinate with chiral substrates.

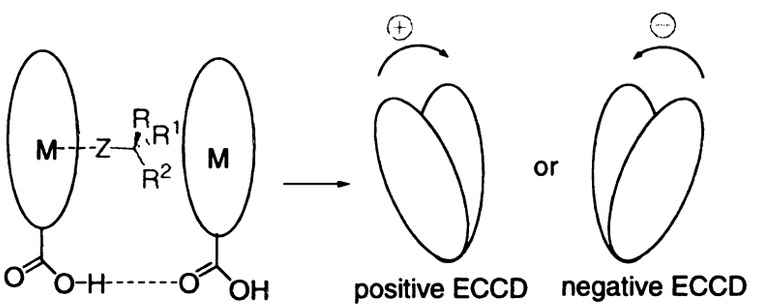

Figure 5-2. Porphyrin acid aggregate as a chromophoric host to determine the stereochemistry of chiral substrates.

A schematic representation of the postulated aggregation idea is shown in Figure 5-2. Upon binding of the chiral substrate, the porphyrin aggregate will adopt the chirality of the substrate, resulting in a preferred helicity, which can be observed as an ECCD

spectrum. The sign of the observed ECCD spectrum, in turn, reflects the absolute stereochemistry of the chiral substrate.

5-1. Determination of extinction coefficient (ε) of zinc porphyrin acid

In order to determine the exact concentration of the zinc porphyrin acid aggregate, it is important to know the extinction coefficient (ε) of the zinc porphyrin acid. We have found two published extinction coefficients (ε) for zinc porphyrin acid. ε=353,000 $M^{-1}cm^{-1}$ in methanol,[23] and ε=602,559 $M^{-1}cm^{-1}$ in CH_3Cl.[24] Although the extinction coefficient of the same compound varies when measured in different solvents, it should not be so different as what we found in these two reports. In fact, when these numbers were compared with our experimental results, with the same amount of porphyrin being added to different solvents (MeOH and $CHCl_3$), and the UV-vis was recorded, we did not observed the degree of difference as reported. Since the published numbers contradicted each other, we decided to determine the ε for the porphyrin carboxylic acid ourselves. The process, which was more troublesome than anticipated, is described in the next part.

5-1.1. Determination of extinction coefficient (ε) by Lambert-Beer's Law

The first way to determine an extinction coefficient was by using Lambert-Beer's law (6-1):

$$A = \varepsilon c l \qquad (6\text{-}1)$$

where A is the absorption observed by UV-vis, ε is the extinction coefficient, c is the concentration of the compound, and l is the length of the UV cell, which is 1 cm.

According to this equation, the extinction coefficient (ε) of a compound could be easily determined if the concentration of the solution is known: $\varepsilon = \frac{A}{cl}$.

Zinc porphyrin acid can be prepared by addition of zinc acetate to porphyrin acid free-base in dichloromethane. Since the zinc porphyrin acid decomposes very easily, it was purified by column chromatography before use. The dried zinc porphyrin acid was then carefully weighted, and known volume of freshly distilled dichloromethane was added to make a porphyrin acid stock solution of known concentration. A known amount of that was then diluted with methylcyclohexane and the spectrum was recorded. Since the concentration of the zinc porphyrin acid was known, the ε of zinc porphyrin acid in methylcyclohexane could be calculated according to the above equation.

The measurement was repeated twice and the extinction coefficient (ε) was calculated. However, the results of those two measurements were not in good agreement. In one case, a ε of 150,000 $M^{-1}cm^{-1}$ was calculated, while in the other case, the number dropped to only 83,000 $M^{-1}cm^{-1}$. Compared to the reported extinction coefficient (ε) of zinc porphyrin methyl ester (ε=550,000 $M^{-1}cm^{-1}$ in CH_2Cl_2),[25] our measured ε were considered inaccurate. The inconsistency of the two measurements urged us to try to rationalize it, and we believe that it is due to the aggregation of zinc porphyrin acid in methylcyclohexane. The self-aggregation of zinc porphyrin acid in solution would result in the deviation from the Lambert-Beer's law, and consequently, the extinction coefficient of porphyrin acid cannot be determined this way.

5-1.2. Determination of extinction coefficient (ε) of zinc porphyrin acid based on that of zinc porphyrin methyl ester

Since the determination of extinction coefficient (ε) of zinc porphyrin acid by Lambert-Beer's law failed because of the inevitable self-aggregation of porphyrin acid in methylcyclohexane, we had to find another way to determine it.

Zinc porphyrin acid could be easily converted to zinc porphyrin methyl ester by addition of a methylation reagent, such as, $TMSCHN_2$. Since the extinction coefficient (ε) of zinc porphyrin methyl ester is known, we could calculate its exact concentration in the solution and therefore, upon conversion to the methyl ester, we could determine the extinction coefficient of zinc porphyrin acid.

$$acid + TMSCHN_2 \rightarrow methylester \qquad (6\text{-}2)$$

For a diluted zinc porphyrin acid, its absorption A_{acid} could be determined by UV-vis. By addition of $TMSCHN_2$, it was converted to the corresponding methyl ester, while the excess of $TMSCHN_2$ could be easily removed by purging the cell with nitrogen gas. When the residue was dissolved in fresh solvent, the only thing left was the zinc porphyrin methyl ester, whose absorption A_{ester} could also be recorded by UV-vis. During this conversion, the concentration of the starting acid should be equal to that of the product methyl ester, and based on the Lambert-Beer's equation: $A = \varepsilon cl$, we could deduce this equation (6-3):

$$\varepsilon_{acid} = \frac{A_{acid}}{A_{ester}} \times \varepsilon_{ester} \qquad (6\text{-}3)$$

A_{acid} and A_{ester} are the absorption of the porphyrin acid and methyl ester, respectively, which can be obtained from the UV-vis spectra, and ε_{acid} and ε_{ester} are the extinction coefficient of porphyrin acid and methyl ester, with ε_{ester}=550,000 $M^{-1}cm^{-1}$ in CH_2Cl_2.[25]

Based on this method, the extinction coefficient of zinc porphyrin acid in CH_2Cl_2 was found to be 580,000 $M^{-1}cm^{-1}$. Since it is quite close to the published figure ε=602,559 M^{-1} cm^{-1} in CH_3Cl, we are quite satisfied with it. Since the zinc porphyrin

acid aggregates in methylcyclohexane, there is no need to deduce its extinction coefficient.

5-2. The zinc porphyrin acid aggregate with carrier F derivatized (*S*)-*O*-acetylmandelic acid 9F

The idea of using zinc porphyrin aggregate as chromophoric host was tested briefly, but we have observed some interesting phenomena. The first chiral complex tested for the zinc porphyrin acid aggregate system was the carrier **F** derivatized (*S*)-*O*-acetylmandelic acid **9F**, since this substrate exhibited the largest ECCD amplitude when added to the zinc porphyrin tweezer in methycyclohexane, (A = +604). The structures of carrier **F** derivatized (*S*)-*O*-acetylmandelic acid **9F** and zinc porphyrin acid are illustrated in Figure 5-3.

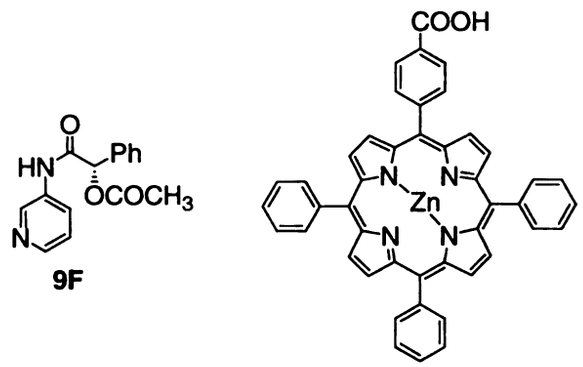

Figure 5-3. The structures of the carrier **F** derivatized (*S*)-*O*-acetylmandelic acid **9F** and zinc porphyrin acid.

When the carrier **F** derivatized (*S*)-*O*-acetylmandelic acid **9** was added to the freshly made zinc porphyrin acid in methylcyclohexane at 0 °C, a positive ECCD spectrum was obtained (Figure 5-4).

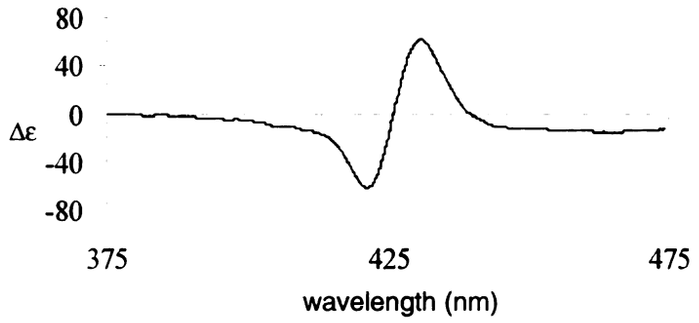

Figure 5-4. The addition of chiral substrate **9F** to zinc porphyrin acid in methylcyclohexane leads to a positive ECCD.

However, this porphyrin acid aggregate was not as stable as the zinc porphyrin tweezer system. As shown in Figure 5-5, the amplitudes of the ECCD spectra decreased significantly with time. After an hour, the amplitude dropped to nearly one third of the original.

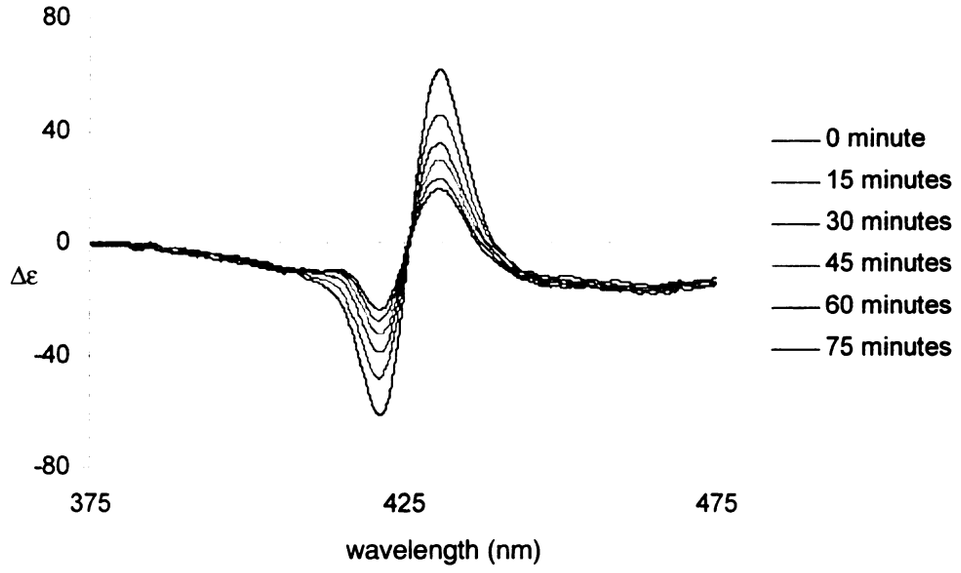

Figure 5-5. The time study of zinc porphyrin acid aggregate with **9F**.

We had not observed the decrease in amplitude when zinc porphyrin tweezer was used as the chromophoric host. The decreasing of the ECCD amplitude of zinc porphyrin

acid aggregate might suggest the instability of the zinc porphyrin acid aggregate. However, the change in the amplitude could also be caused by photo bleaching: the degradation of the zinc porphyrin acid under the prolonged light radiation. In order to test this possibility, we added the chiral substrate **9F** to zinc porphyrin acid, and divided this solution into two. One portion was kept in the CD machine, under the radiation of light all the time, while the other one was shielded away from light. After an hour, CD spectra were measured for both solutions, and the amplitudes for both solutions were much smaller than that taken an hour ago (Figure 5-6). This experiment excluded the possibility of photo bleaching.

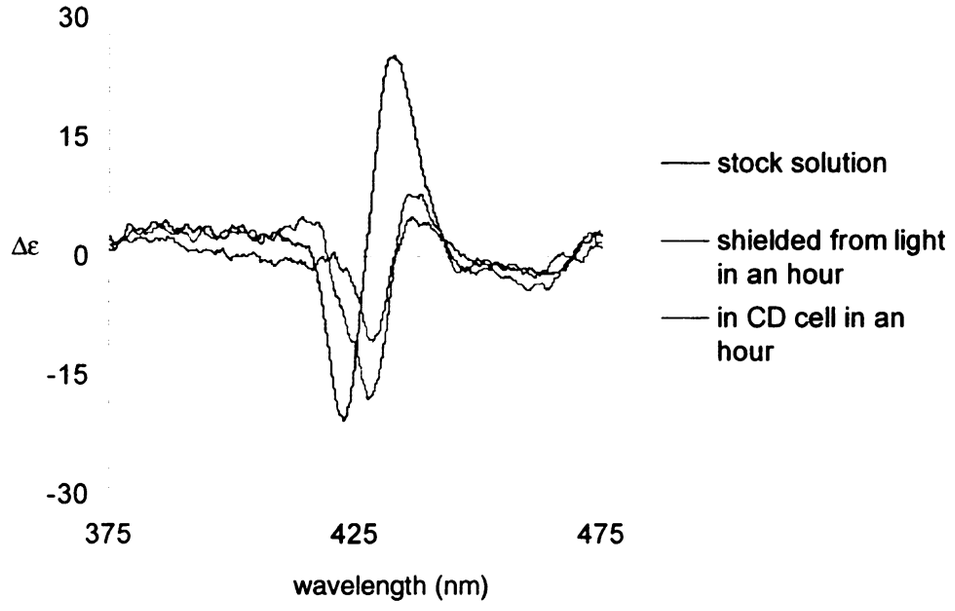

Figure 5-6. The photo bleaching study.

Some preliminary studies were also performed for the binding between zinc porphyrin acid and the carrier **F** derivatized (*S*)-*O*-acetylmandelic acid. As shown in Figure 5-7, the addition of the carrier **F** derivatized (*S*)-*O*-acetylmandelic acid **9F** to zinc porphyrin acid exhibited positive ECCD spectra at 0 °C, while the amplitudes of ECCD

spectra varied with the amount of chiral complex present. The maximum amplitude was reached with the addition of 1 equivalent of chiral complex. From the ECCD spectra, it was clear that the ECCD signals were sensitive to the amount of chiral complex in the system, since there was nearly no ECCD signal upon addition of more than 10 equivalents of chiral complex. On the other hand, for the system with zinc porphyrin tweezer as the chromophoric host, more than 100 equivalent of chiral complex has to be added before the disappearance of ECCD peaks.[26]

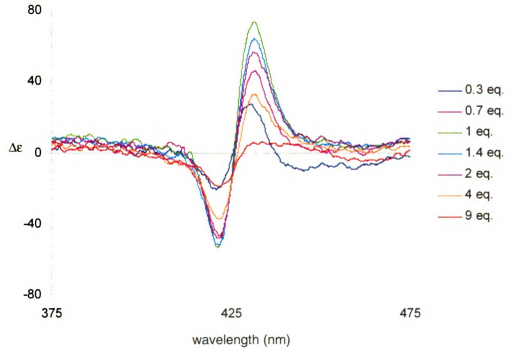

Figure 5-7. The titration of zinc porphyrin acid with **9F**.

When zinc porphyrin acid aggregates coordinate with the chiral substrate, it is the zinc atom, which serves as the binding site. This can be proved by adding the chiral substrate to free-base porphyrin acid, in which no CD was observed. From UV-vis, it could be seen that there was no binding between the substrate and porphyrin acid free base, since the absorption wavelength λ_{max} of the porphyrin acid Soret band remained the

same before and after the addition of the chiral substrate. However, when the substrate was added into zinc porphyrin acid, a new peak was observed at 427 nm in the UV-vis spectrum.

The above experiment eliminates the possibility of the carboxylic acid functionality on the porphyrin periphery binding to the chiral substrate. Instead, the carboxylic acid functionality on the porphyrin plays an important role in the porphyrin aggregation. When the acid functionality was esterified as a methyl ester, as shown in Figure 5-8, the amplitude of the ECCD spectrum decreased significantly upon addition of **9F**, even though the sign stayed the same.

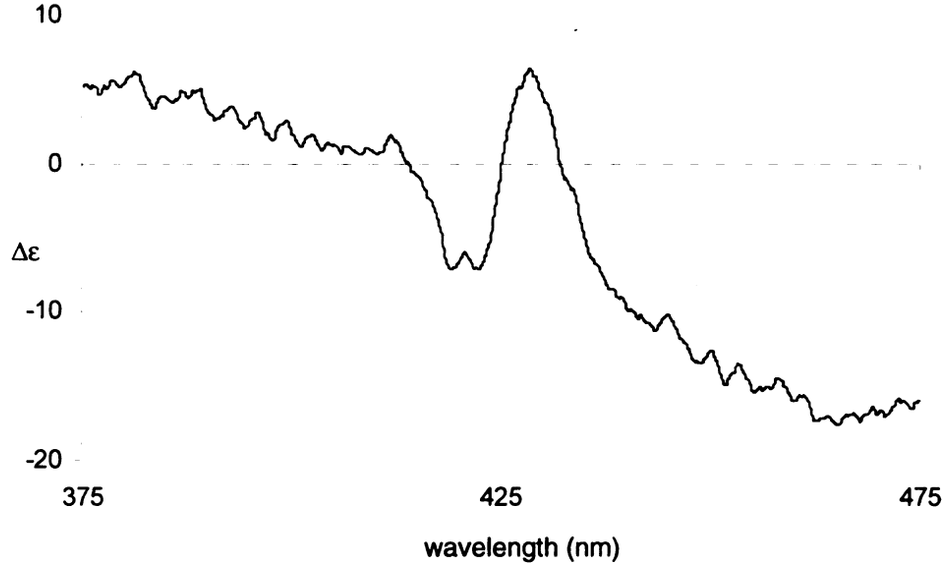

Figure 5-8. The ECCD of **9F** in zinc porphyrin methyl ester.

The above studies indicated that the carboxylic acid functionality could help the aggregation and alignment of the zinc porphyrin aggregates by hydrogen bonding. The importance of hydrogen bonding could also be seen by addition of base, which resulted in reducing the hydrogen bonds and increase of charge repulsion between aggregating carboxylates. When an inorganic base, such as sodium carbonate, was added into the

mixture of zinc porphyrin acid and chiral substrate **9F**, the amplitude of the ECCD spectrum decreased (Figure 5-9). However, the addition of sodium carbonate was not as effective as expected in disrupting the hydrogen-bonding network. This might be due to the limited solubility of the base and also the porphyrin carboxylate in methylcyclohexane. On the other hand, as shown in Figure 5-10, no ECCD was observed, when the zinc porphyrin tweezer was pre-treated with sodium carbonate before the addition of the chiral substrate **9F**.

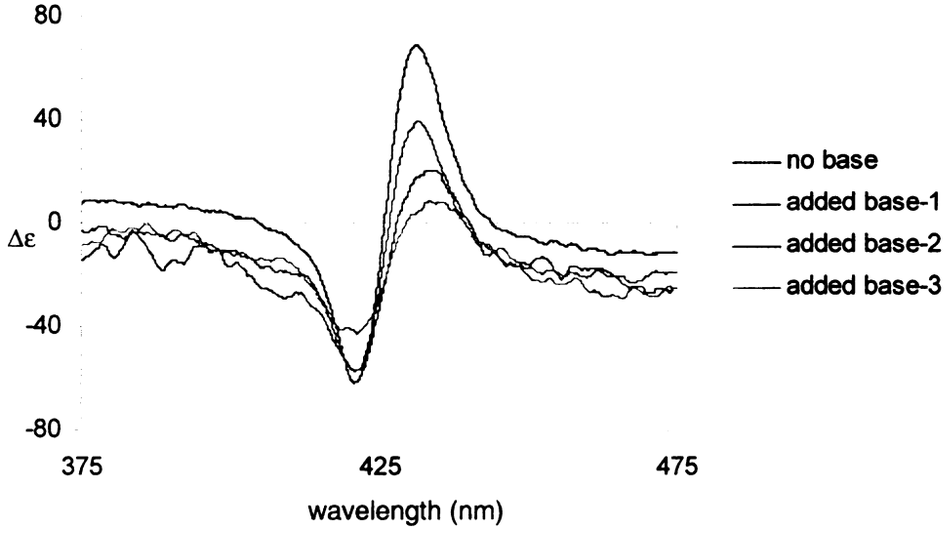

Figure 5-9. The addition of sodium carbonate to zinc porphyrin tweezer.

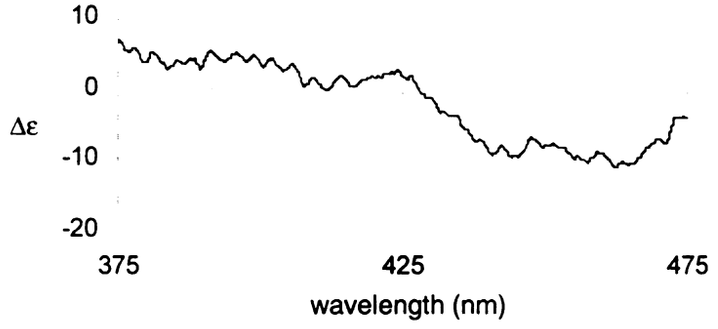

Figure 5-10. The CD spectrum of **9F** adds to pre-treated zinc porphyrin acid.

Furthermore, when an organic base such as diisopropylmethylamine was added to the zinc porphyrin acid solution with the chiral substrate present, the ECCD peak decreased very quickly, and finally disappeared. This could be due to two separate reasons: (a) diisopropylmethylamine deprotonates the carboxylic acid, disrupting the hydrogen bond network, which we believe is responsible for the alignment of the porphyrin aggregates, and therefore is lost; (b) diisopropylmethylamine displaces the chiral conjugate and bind to zinc, which again leads to the loss of ECCD. Therefore, more time needs to be spent on this subject to verify the nature of the chiral species formed.

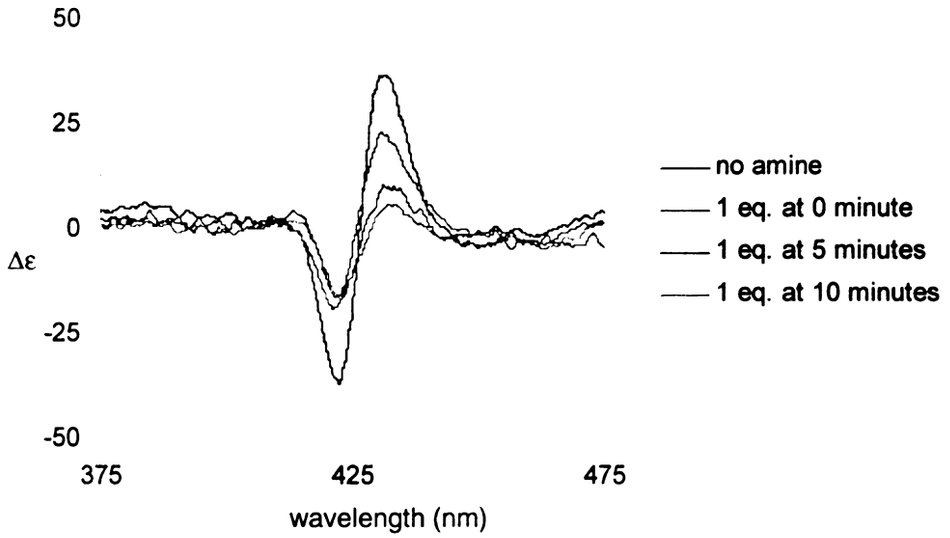

Figure 5-11. Adding diisopropylmethylamine (1eq.) to zinc porphyrin acid with **9F**.

5-3. Other chiral substrates for the zinc porphyrin acid aggregates

The zinc porphyrin acid system exhibited ECCD upon addition of carrier **F** derivatized (*S*)-*O*-acetylmandelic acid **9F**, and all the other carrier **F** derivatized chiral acids (see Section 3-5) were also tested, however, none of them exhibited a distinctively clear ECCD signal, except for the (*S*)-methoxyphenylpropionic acid's derivative **8F**. A

positive ECCD was observed, however, not as strong as that of the substrate **9F**. At the same time, chiral monoamines and diamines were also tested, and only L-lysine methyl ester showed a small positive ECCD spectrum with the addition of zinc porphyrin acid. The structures of **8F** and L-lysine methyl ester are shown in Figure 5-12.

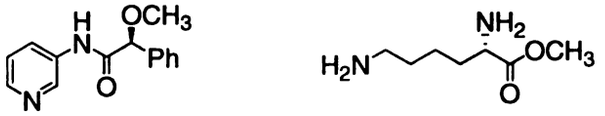

8F L-lysine methyl ester

Figure 5-12. Structures of (*S*)-methoxyphenylpropionic acid derivative **8F** and L-lysine methyl ester.

5-4. Porphyrin aggregates with other porphyrin compounds

As mentioned before, the zinc porphyrin acid can aggregate in methylcyclohexane, and upon the binding of a chiral complex, the aggregate can adopt a preferred helicity, which can be observed as ECCD spectrum. In the process, zinc serves as the binding site to coordinate with the chiral substrate, and the carboxylic functionality helps the alignment of the porphyrin aggregates by forming hydrogen bonds. It is natural to wonder if porphyrin compounds with other functionalities, such as alcohols, can also exhibit the same behavior. In order to test this, we have synthesized two porphyrin mono-alcohols by derivatizing porphyrin acid with diols.

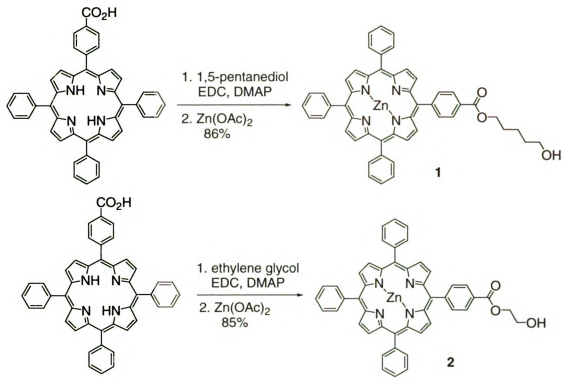

Scheme 5-1. The synthesis of porphyrin mono-alcohols **1** and **2**.

As shown in Scheme 5-1, the porphyrin acid was derivatized with 1,5-pentanediol and ethylene glycol, to generate two porphyrin mono-alcohols **1** and **2**, respectively. Zinc was inserted into these two porphyrin alcohols by addition of zinc acetate to the porphyrin solution. The carrier **F** derivatized (*S*)-*O*-phenylmandelic acid **9F** was then added to the resulting zinc porphyrin mono-alcohols and CD spectra were recorded. When the chiral complex was added to porphyrin mono-alcohol **1**, an asymmetric positive ECCD peak was observed λ_{ext} 430 nm ($\Delta\varepsilon$ +11) and 422 nm ($\Delta\varepsilon$ -17), A +28, while when it was added to the mono-alcohol **2**, the ECCD signals became stronger. As shown in Figure 5-13, although the ECCD peak for the zinc porphyrin mono-alcohol **2** was not as strong as that of the zinc porphyrin acid, the system was more stable as the ECCD signal did not decrease with time.

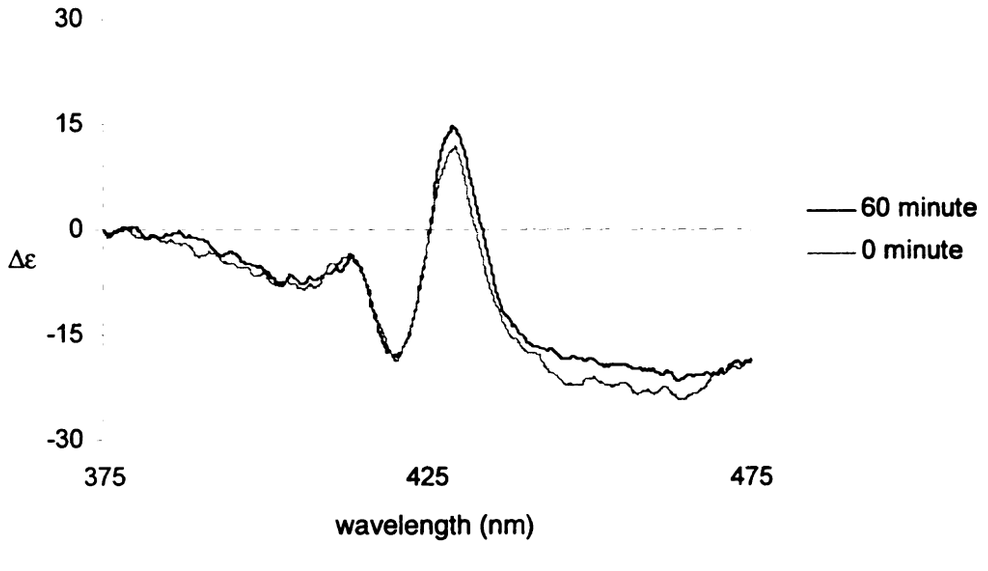

Figure 5-13. The time study of zinc porphyrin mono-alcohol **2** with carrier **F** derivatized (S)-*O*-phenylmandelic acid **9F**.

Conclusion:

Although we have only carried out preliminary studies on the porphyrin aggregates, the obtained results are very encouraging. It appears that it is possible to transfer the chirality of a small molecule to a zinc-porphyrin aggregate, which can be observed by ECCD. As a proof of concept, upon addition of derivatized carboxylic acids **8F** and **9F** as well as L-Lysine methyl ester to a zinc porphyrin carboxylic acid solution, an ECCD spectrum was observed. However, the system is very dynamic, changing significantly with time, while it fails to produce positive results with other chiral compounds. At the same time, it was observed that the acid functionality on the porphyrin periphery is very critical for the success of the system, since if replaced by the corresponding methyl ester the ECCD is reduced. We believe that the hydrogen bonding between the carboxylic acid groups dictates directionality to the aggregate, essentially for the formation of an ECCD active complex. In an attempt to explore the above

hypothesis, alcohols were used to direct the aggregate formation and the preliminary results were very promising (currently further studies were carried out in the lab (Marina Tanasova) by using polyols as the aggregate directing group).

The porphyrin aggregate system, although promising, has to be further optimized and proven valid for a wide range of substrates. If consistent results are obtained it could be potentially used as an alternative to the porphyrin tweezer system having the advantage of requiring less steps for its synthesis.

Experimental materials and general procedures:

Anhydrous CH_2Cl_2 was dried over CaH_2 and distilled. The solvents used for CD measurements were purchased from Aldrich and were spectra grade. All reactions were performed in dried glassware under nitrogen. Column chromatography was performed using SiliCycle silica gel (230-400 mesh). ^{1}H-NMR spectra were obtained on Varian Inova 300 MHz or 500 MHz instrument and are reported in parts per million (ppm) relative to the solvent resonances (δ), with coupling constants (J) in Hertz (Hz). UV-Vis spectra were recorded on a Perkin-Elmer Lambda 40 spectrophotometer, and is reported as λ_{max} [nm]. CD spectra were recorded on a JASCO J-810 spectropolarimeter, equipped with a temperature controller (Neslab 111) for low temperature studies, and is reported as λ [nm] ($\Delta\varepsilon_{max}$ [l mol^{-1} cm^{-1}]). Porphyrin acid was synthesized as described in Chapter 2, and all the other starting materials were purchased from Aldrich.

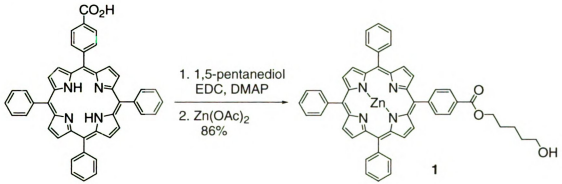

1

Porphyrin alcohol 1:

To a solution of porphyrin acid (90 mg, 0.14 mmol) and 1,5-pentanediol (50 mg, 0.5 mmol) in anhydrous CH_2Cl_2 (4 mL) was added EDC (27 mg, 0.14 mmol) and DMAP (18 mg, 0.14 mmol). The reaction mixture was stirred at room temperature overnight and $Zn(OAc)_2$ (50 mg) was added. The reaction was stirred for another 1 h, and it was applied directly to silica gel column and purified (CH_2Cl_2) to afford the title compound **1**

(86%). ^{1}H NMR ($CDCl_3$, 300 MHz) δ 8.76-8.85 (m, 8H), 8.42 (d, *J*=8.3 Hz, 2H), 8.29 (d, *J*=8.3 Hz, 2H), 8.19-8.21 (m, 6H), 7.71-7.79 (m, 9H), 4.71 (d, *J*=6.0 Hz, 2H), 3.82 (d, *J*=6.0 Hz, 2H), 2.13 (m, 4H), 1.91 (m, 2H).

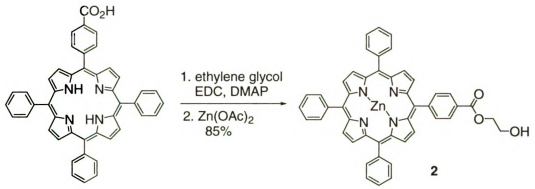

2

Porphyrin alcohol 2:

To a solution of porphyrin acid (90 mg, 0.14 mmol) and ethylene glycol (62 mg, 1 mmol) in anhydrous CH_2Cl_2 (4 mL) was added EDC (27 mg, 0.14 mmol) and DMAP (18 mg, 0.14 mmol). The reaction mixture was stirred at room temperature overnight and $Zn(OAc)_2$ (50 mg) was added. The reaction was stirred for another 1 h, and it was applied directly to silica gel column and purified (CH_2Cl_2) to afford the title compound **2** (86%). ^{1}H NMR ($CDCl_3$, 300 MHz) δ 8.76-8.85 (m, 8H), 8.42 (d, *J*=8.3 Hz, 2H), 8.29 (d, *J*=8.3 Hz, 2H), 8.19-8.21 (m, 6H), 7.71-7.79 (m, 9H), 4.54 (d, *J*=6.0 Hz, 2H), 4.41 (d, *J*=6.0 Hz, 2H).

Reference:

1. Engelkamp, H.; Middelbeek, S.; Nolte, R. J. M. *Science* **1999**, *284*, 785.

2. van Nostrum, C. F.; Picken, S. J.; Schouten, A. -J.; Nolte, R. J. M. *J. Am. Chem. Soc.* **1995**, *117*, 9957.

3. Drager, S. A.; Zangmeister, R. A. P.; Armstrong, N. R.; O'Brien, D. F. *J. Am. Chem. Soc.* **2001**, *123*, 3595.

4. Abraham, R. J.; Eivazi, F.; Pearson, H.; Smith, K. M. *J. Chem. Soc., Chem. Commun.* **1976**, 698.

5. Abraham, R. J.; Fell, S. C.; Pearson, H.; Smith, K. M. *Tetrahedron* **1979**, *35*, 1759.

6. Tamaru, S.; Uchino, S.; Takeuchi, M.; Ikeda, M.; Hatano, T.; Shinka, S. *Tetrahedron Lett.* **2002**, *43*, 3751.

7. Luboradzki, R.; Gronwald, O.; Ikeda, M.; Shinka, S.; Reinhoudt, D. N. *Tetrahedron* **2000**, *56*, 9595.

8. Melendez, R. E.; Carr, A. J.; Linton, B. R.; Hamilton, A. D. *Struct. Bond.* **2000**, *96*, 31.

9. Seto, C. T.; Whitesides, G. M. *J. Am. Chem. Soc.* **1993**, *115*, 905.

10. Leighton, P.; Cowan, J. A.; Abraham, R. J.; Sanders, J. K. M. *J. Org. Chem* **1988**, *53*, 733.

11. Akins, D. L.; Zhu, H. R.; Guo, C. *J. Phys. Chem.* **1996**, *100*, 5420.

12. Maiti, N. C.; Ravikanth, M.; Mazumdar, S.; Perisasmy, N. *J. Phys. Chem.* **1995**, *99*, 17192.

13. Kasha, M. *Physical Processes in Radiation Biology*; Academic Press: New York, **1964**.

14. Davydov, A. S. *Theory of Molecular Excitions*; Plenum Press: New York, **1971**.

15. Balaban, T. S.; Eichhofer, A.; Lehn, J. -M. *Eur. J. Org. Chem.* **2000**, *6*, 4047.

16. Balaban, T. S.; Leitich, J.; Holzwarth, A. R.; Schaffner, K. *J. Phys. Chem. B* **2000**, *104*, 1362.

17. Gratzel, M. *Nature* **2001**, *414*, 338.

18. Brabec, C. J.; Shaheen, S. E.; Fromherz, T.; Padinger, F.; Hummelen, J. C.; Dhanabalan, A.; Hanssen, R. A. J.; Sariciftci, N. S. *Synth. Met.* **2001**, 121, 1517.

19. Plater, M. J.; Aiken, S.; Bourhill, G. *Tetrahedron* **2002**, *58*, 2405.

20. Chemla, D. S.; Zyss, J. *Nonlinear Optical Properties of Organic Molecules and Crystals*; Academic: Orlando, FL, **1987**.

21. Prasad, P. N.; Williams, D. J. *Introduction to Nonlinear Optical Effects in Molecules and Polymers*; Wiley: New York, **1991**.

22. Burland, D. M.; Miller, R. D.; Walsh, C. A. *Chem. Rev.* **1994**, *94*, 31.

23. Matile, S.; Berova, N.; Nakanish, K. *J. Am. Chem. Soc.* **1995**, *117*, 7021.

24. Faustino, M. A.; Neves, M. G. P. M. S.; Vicente, M. G. H.; Cavaleiro, J. A. S.; Neumann, M.; Brauer, H. -D.; Jori, G. *Photochem. Photobiol.* **1997**, *66*, 405.

25. Berova, N.; Nakanish, K.; Woody, R. W. *Cicular Dichroism: Principles and Applications*, 2nd ed.; John Wiley & Sons, Inc. Publication: New York, **2000**;

26. Huang, X. F.; Rickman, B. H.; Borhan, B.; Berova, N.; Nakanishi, K. *J. Am. Chem. Soc.* **1998**, *120*, 6185.

Chapter 6

The attempted synthesis of boronic porphyrin tweezer

Since it has been very well known that boronic acids can form stable complexes with sugars and diols even in aqueous solution,[1-3] numerous arylboronic acids have been prepared and studied as sugar receptors.[4, 5] However, the simple arylboronic acids form stable complexes with a variety of sugars and thus they are not useful as specific receptors or sensors for a specific sugar.

A specific carbohydrate can be recognized by appropriate manipulation of two boronic acids in the same molecule, with the precise placement of the recognition element in the proper position and orientation for optimal complementarity to the guest. Figure 6-1 is an example of a computer-based designed receptor, specifically for glucopyranose.[3] Its high affinity to glucose has been evaluated by fluorescence experiments, exhibiting a 400-folder greater affinity for glucose than any of the other sugars.

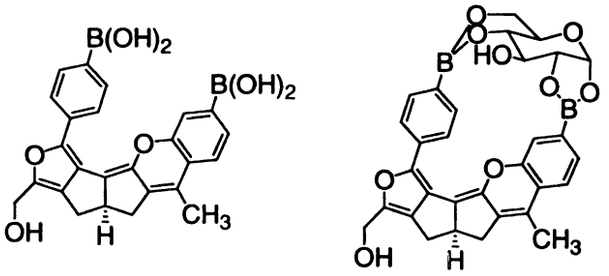

Figure 6-1. A receptor for glucopyranose and its glucose complex.

It has been demonstrated that porphyrins, bearing boronic acid functionalities, can bind to carbohydrates and the binding could be observed by ECCD spectra (Figure 6-2).[6, 7] However, they have high affinities for all the carbohydrates, and are not specific receptors for a single sugar.

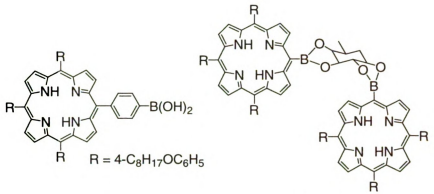

Figure 6-2. The boronic porphyrin and its binding to sugars.

We are interested in designing artificial carbohydrate receptors, which show selectivity for a specific carbohydrate. Of particular interest are glucose sensors for potential application in the maintenance of blood glucose levels in patients with diabetes.[8, 9] In order to achieve this goal, we wanted to design boronic acid based porphyrin receptors, which upon binding to specific substrates will exhibit ECCD spectra. In the previous chapters, we have demonstrated the ability of zinc porphyrin tweezer for the stereochemical determination of chiral substrates. An extension of these is boronic porphyrin tweezers **1** and **2** designed specifically as receptor molecules for carbohydrates.

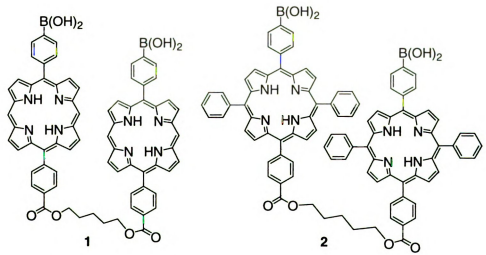

Figure 6-3. The structure of boronic porphyrin tweezer **1** and **2**.

The boronic porphyrin tweezers **1** and **2** can bind to carbohydrates by forming covalent bonds between the boron on the porphyrin periphery and the oxygen of the sugars. Since the sugars are all chiral, the binding to the boronic porphyrin tweezer **1** or **2** will induce helicity of the porphyrin host, which can provide fingerprint spectra for the carbohydrates. The boronic porphyrin tweezers can be synthesized from the *para*-substituted porphyrin carboxylic acids by a standard EDC coupling with a diol. The challenge lies in the synthesis of the *para*-substituted porphyrin carboxylic acid **3** and **4**, which are proposed to be synthesized by MacDonald "2+2" cyclization method.[10]

The synthesis of porphyrin acid **3** relies on introducing the 10-, 20- *meso* carbon of the porphyrin as formyl group at the 1-, and 9- position of one dipyrromethane **5**, and then condensing it with another dipyrromethane **5**, which has no substitution at 1-, and 9-position, under acidic condition (Scheme 6-1).[11]

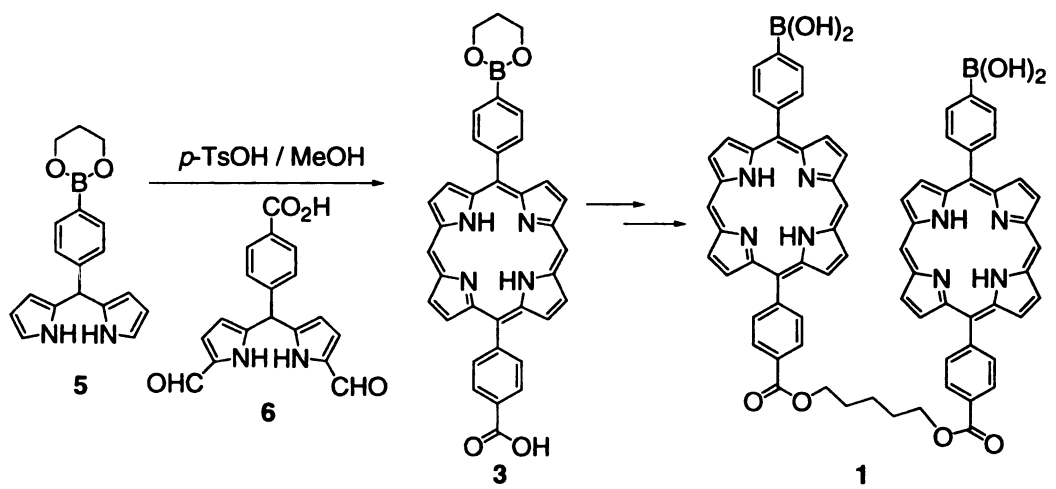

Scheme 6-1. Proposed synthesis of porphyrin tweezer **1** by MacDonald "2+2" cyclization.

As for tweezer **2**, since there are two extra phenyl groups at 5- and 15- position, its "2+2" cyclization synthesis requires the condensation of dipyrromethane-dicarbinol **7**,

instead of dipyrromethane-dialdehyde **6**, with dipyrromethane **5**. Its proposed synthesis is illustrated in Scheme 6-2.[10]

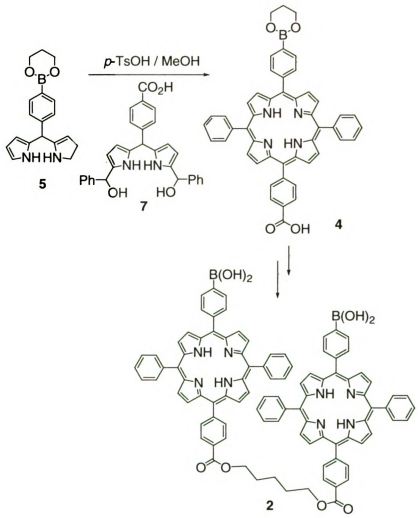

Scheme 6-2. Proposed synthesis of porphyrin tweezer **2** by MacDonald "2+2" cyclization.

6-1. Synthesis of porphyrin tweezer 1

For the synthesis of porphyrin tweezer **1**, dipyrromethane **5** could be easily synthesized by reacting protected 4-boronic benzaldehyde with pyrrole under acidic condition, as shown in Scheme 6-3. The boronic acid functionality of the 4-boronic benzaldehyde was protected with 1,3-propanediol[12] before it was condensed with excess

amount of distilled pyrrole to form the 5-phenyldipyrromethane **5**, by using TFA as the acidic catalyst. Excess pyrrole is required to maximize formation of dipyrromethane, and lowering the pyrrole/benzaldehyde ratio favors formation of higher oligomer and polymer.

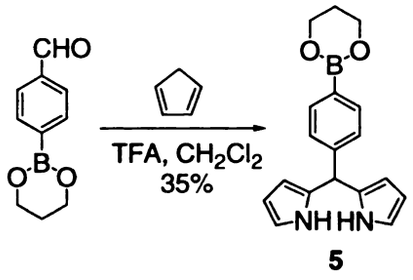

5

Scheme 6-3. Synthesis of dipyrromethane **5**.

Scheme 6-4 shows the proposed synthesis of dipyrromethane-dialdehyde **6** from 2-pyrrole-carboxylic acid **8**. The synthesis of dipyrromethane-dialdehyde **6** started by using 2-pyrrole-carboxylic acid **8** as the starting material. After it was condensed with 4-carboxymethylbenzaldehyde **9** to form the dipyrromethane **10**, the methyl ester could be converted to carboxylic acid functionality by hydrolysis, and consequently, the carboxylate functionality in compound **11** would be reduced to aldehyde to finish the synthesis of dipyrromethane-dialdehyde **6**.[13]

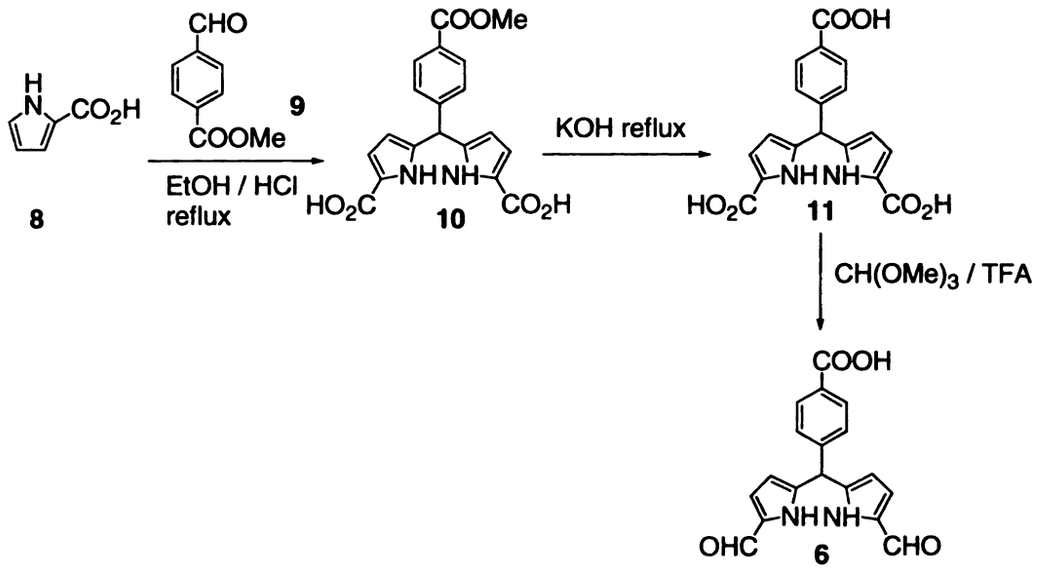

Scheme 6-4. The proposed synthesis of dipyrromethane-dialdehyde **6** from 2-pyrrole-carboxylic acid **8**.

As shown in Scheme 6-4, the 2-pyrrole-carboxylic acid **8** was condensed with 4-carboxymethylbenzaldehyde **9** in refluxing HCl and ethanol to form dipyrromethane **10**.[14] However, under this harsh condition, only black polymeric like material was generated instead of the desired dipyrromethane product **10**. Thus the carboxylic acid functionality in acid **8** had to be protected by forming esters to survive the strong acidic condition for the synthesis of dipyrromethane **10**.

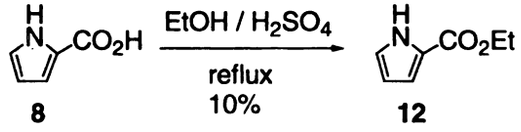

Scheme 6-5. The esterification of 2-pyrrole-carboxylic acid **8**.

The conversion of carboxylic acid **8** to ethyl ester **12** was carried out according to published procedures by refluxing in an acidic solution of ethanol (Scheme 6-5).[15] However, only very small amount of desired product **12** (the yield was about 10%) was

generated, with the majority of the isolated product being some black powder, which probably was a polymer since it did not dissolve in any solvent.

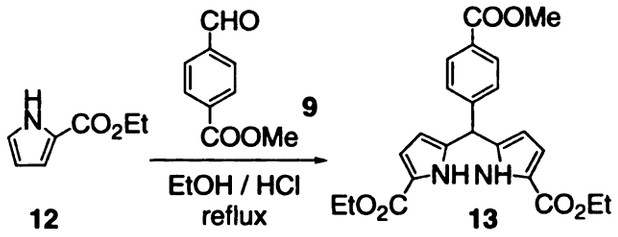

Scheme 6-6. The condensation of ethyl ester **12** with aldehyde **9**.

The ethyl ester **12** and 4-carboxymethylbenzaldehyde **9** were then condensed to generate dipyrromethane **13**, by refluxing in an acidic solution of ethanol for 4 hours (Scheme 6-6). The desired product **13** was afforded as a precipitate.[14] However, the synthesis of dipyrromethane-dialdehyde **6** as outlined in Scheme 6-4 was not pursued because of perceived problems. First of all, since compound **11** with three carboxylic acid functionalities, was going to be synthesized by hydrolysis of compound **13**, it would be very hard to extract it from the water. Secondly, to convert compound **11** to dipyrromethane-dialdehyde **6**, the reduction of the carboxylic acid functionality on the pyrrole ring could also compromise the carboxylic acid functionality on the phenyl ring. Since the dipyrromethane-dialdehyde **6** might also be synthesized by using pyrrole as starting material, we focused on this strategy.

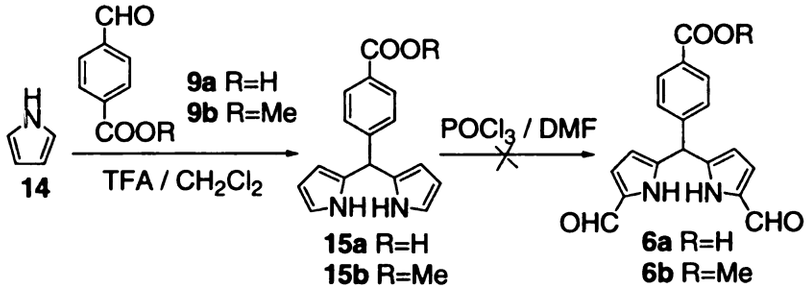

Scheme 6-7. Unsuccessful synthesis of dipyrromethane-dialdehydes **6a and 6b** from pyrrole.

As depicted in Scheme 6-7, pyrrole **14** was condensed with 4-carboxybenzaldehyde **9a** and 4-methoxycarbonylbenzaldehyde **9b** by using TFA as acidic catalyst to furnish the dipyrromethane **15a** and **15b**.[16] Compared to the harsh condition of refluxing in EtOH and HCl, the TFA condition is a much milder way to generate dipyrromethane and provides higher yields. Unfortunately, this reaction did not work on 2-substituted pyrrole, such as the 2-pyrrolcarboxylic acid **8** or its corresponding ethyl ester **12**. The Vilsmeier reaction to install formyl groups onto the dipyrromethane **15a** and **15b**,[17, 18] failed to provide the desired product **6a** or **6b**.

The two different schemes (Scheme 6-4 and 6-7) to synthesize dipyrromethane-dialdehyde **6** had failed, and therefore, at this point, we directed our attention toward the synthesis of boronic porphyrin tweezer **2**.

6-2. Synthesis of boronic porphyrin tweezer 2

6-2.1. Synthesis of boronic porphyrin tweezer 2 by MacDonald "2+2" cyclization

The synthesis of porphyrin tweezer **2** by MacDonald "2+2" cyclization method requires the condensation of dipyrromethane **5** and dipyrromethane-dicarbinol **7**. The synthesis of dipyrromethane **5** is demonstrated in Scheme 6-3, and the challenge here was to synthesize the dipyrromethane-dicarbinol **7**. The synthesis of boronic porphyrin acid **4** through the condensation of dipyrromethane **5** and dipyrromethane-dicarbinol **7** is shown in Scheme 6-8.

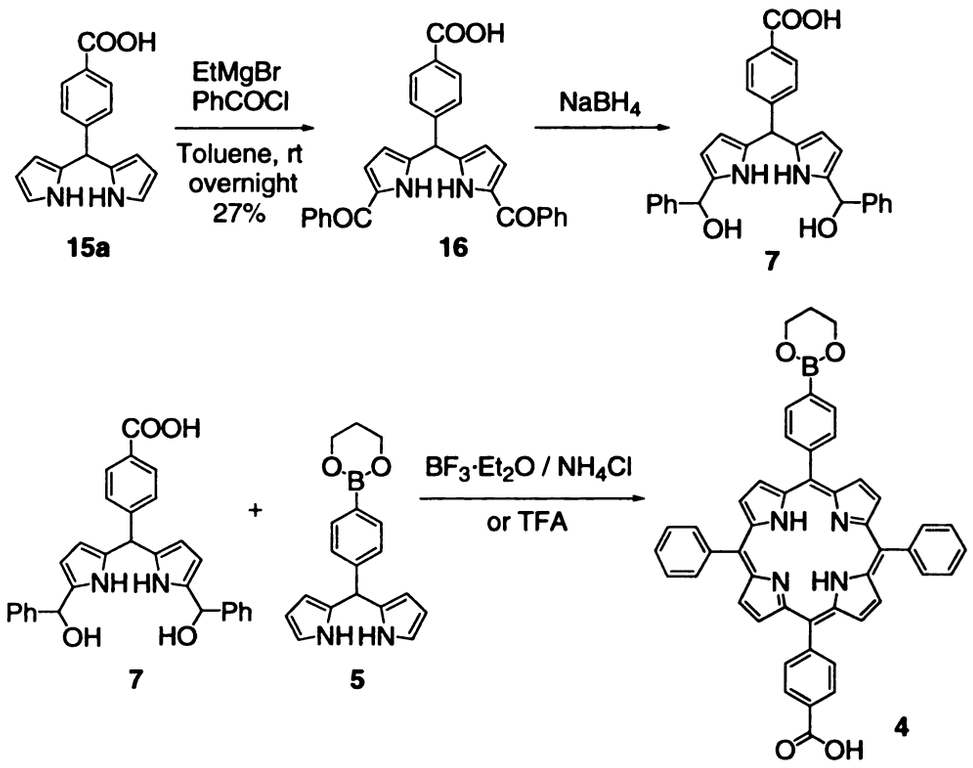

Scheme 6-8. Proposed synthesis of boronic porphyrin acid **4**.

Scheme 6-8 depicts the proposed synthetic pathway to secure the protected boronic acid **4**. The treatment of dipyrromethane **15a** with excess amount of EtMgBr and benzoyl chloride successfully introduced benzoyl groups to the 1- and 9- position of compound **15a**. This process generated both the mono-acylated and di-acylated dipyrromethane, which were easily separated by column chromatography.[16] According to literature precedent,[16] the ratio between the mono- and di-acylated products should be 1:5. It was found that prolonging the reaction time increased the yield of the di-acylated product; even so a low yield of **16** was isolated. The reduction of diacyl dipyrromethane **16** to dicarbinol **7** was achieved with excess $NaBH_4$ in THF/methanol.[19] This reduction reaction proceeded well, however, we were unable to extract product **7** from the reaction mixture, due to its high polarity.

Since the carboxylic acid **7** was too polar, we planned to decrease its polarity by synthesizing the corresponding methyl ester **17** instead. As shown in Scheme 6-9, the dipyrromethane methyl ester **15b** was used as the starting material. When dipyrromethane **15b** was treated, under the Friedel-Craft reaction condition, with benzoyl chloride in the presence of $AlCl_3$,[19, 20] it yielded both mono- and di-acylated products, which were easily separated by column chromatography. Unfortunately, the diacylated product that was isolated from reaction mixture was not the desired compound **17**, but byproduct **18**, with one substituent at the α-position and the other at β-position.

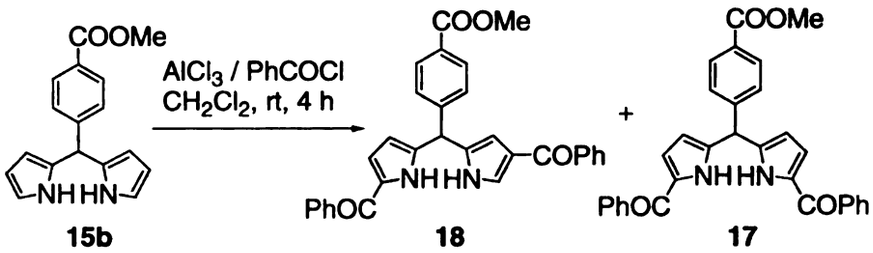

Scheme 6-9. Synthesis of dipyrromethane-dicarbinol **17**.

The reaction to synthesize symmetrically substituted compound **17** by Friedel-Crafts condition was repeated several times. In one of the reactions, it was noticed that on TLC, there was a spot just right above the mono-acylated product. It did not seem to be the desired di-acylated product, since it lacked the characteristic bright color most the dipyrromethane compounds exhibit in bromine vapor, and also because according to the literature,[19] generally di-acylated products moved slower than mono-acylated products. However, this spot was isolated, and it was identified by NMR to be the desired symmetric compound **17**.

The yield of the **17** varied with reaction time and the amount of Lewis acid and benzoyl chloride used in the reaction. It seems like, the longer the reaction time; the lower the yield of the desired symmetrically substituted product **17**, while the yield of the

asymmetrically substituted byproduct **18** was increasing. The yield of compound **17** ranged from 15% to 40%. We had also tried to introduce the two benzoyl groups of **17** in a step-wise fashion, however, the reaction stopped at the mono-acylated product stage. We tried different conditions, but we could not add the second benzoyl group to the mono-acylated compound, and at the end of the reactions, the mono-acylated starting material was recovered.

After the symmetrically diacylated dipyrromethane **17** was made, it was ready to condense with dipyrromethane **5** to synthesize the *para*-substituted porphyrin **4**. Since the final target of our synthesis was the porphyrin tweezer **2**, there were two pathways to synthesize it by using the diacylated dipyrromethane **17** as the starting material (Scheme 6-10): pathway **I** was to synthesize a porphyrin carboxylic acid **4** first, and then form the linkage between the two porphyrins by simple esterification; pathway **II** would introduce the linkage between two of the dipyrromethane **17** first, and then build two porphyrins on the dipyrromethane dimer **19** in a single step.

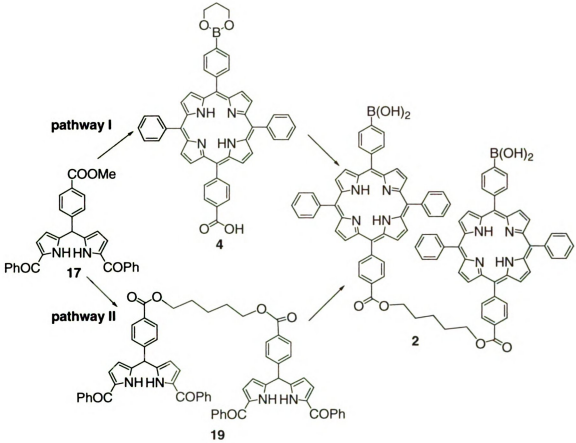

Scheme 6-10. Two pathways for the synthesis of porphyrin tweezer **2**.

To synthesize porphyrin tweezer **2**, pathway **II** was attempted first, which required the synthesis of the dipyrromethane dimer **19**. With dipyrromethane carboxylic acid **16** in hand, esterification with 1,5-pentanediol utilizing EDC as the coupling reagent should afford the dipyrromethane dimer **19**. However, the standard esterification reaction failed, there was no formation of either the diester **19**, or the monoester (Scheme 6-11). This might be due to the impurities in the carboxylic acid **16**, since the purification of the acid **16** by column chromatography was not very effective, and it had to be precipitated out of the column fractions to get purer product.

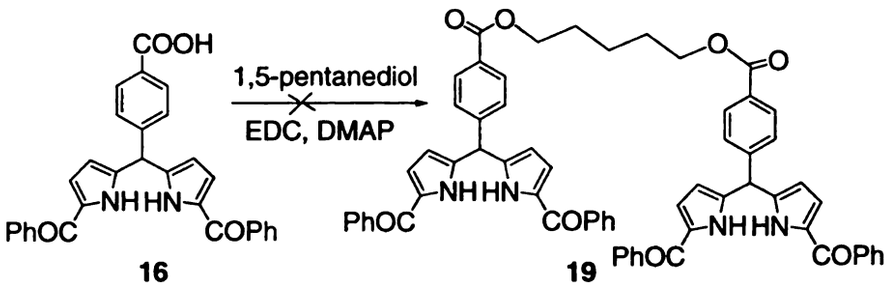

Scheme 6-11. The unsuccessful EDC coupling of compound **16** and 1,5-pentanediol.

In order to obtain pure carboxylic acid **16**, its corresponding methyl ester **17** was hydrolyzed under basic condition, as shown in Scheme 6-12. The routine hydrolysis, by refluxing the dipyrromethane methyl ester **17** in a mixture of THF and aqueous sodium hydroxide solution overnight, provided a very polar compound as the only product. This product was so polar that it did not move on the TLC plate by even using 10% MeOH in CH_2Cl_2 as the developing solvent. However, it was demonstrated not to be the desired carboxylic acid **16** by NMR. This hydrolysis reaction was repeated several times, and each time same product was observed.

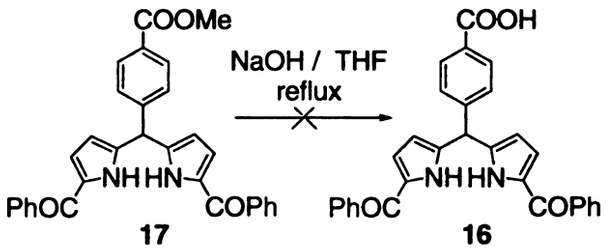

Scheme 6-12. The unsuccessful hydrolysis of methyl ester **17** to acid **16**.

Since the attempt of securing dipyrromethane carboxylic acid **16** failed, we turned to an alternate way to synthesize the dipyrromethane dimer **19**. As shown in Scheme 6-13, a simpler dipyrromethane dimer **20** was synthesized first, and then the benzoyl groups would be introduced in the α-position of pyrroles of compound **20** by Friedel-Crafts reaction. However, this was a risky plan, since installing four benzoyl groups in one

single reaction could result in many byproducts and the yield of the desired product **19** was sure to be low. Having that in mind, this method was still worth trying because the starting material **15a** was very easy to synthesize.

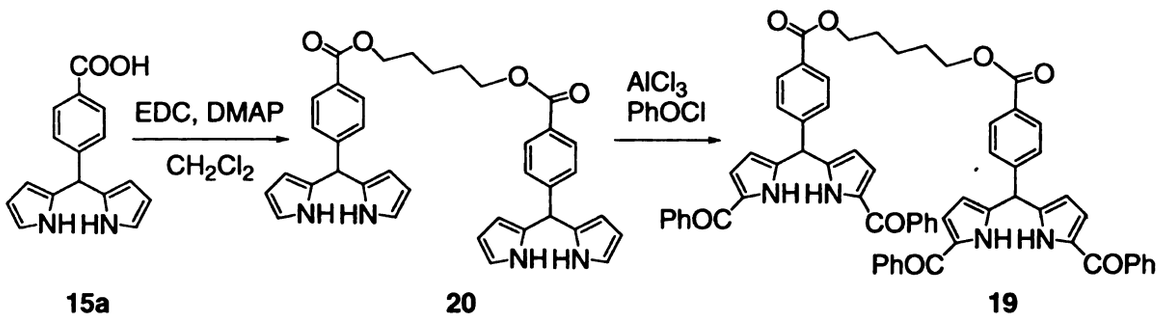

Scheme 6-13. Alternate way to synthesize dimer **19**.

As shown in Scheme 6-14, the dipyrromethane dimer **20** was easily synthesized from the dipyrromethane carboxylic acid **15a** by esterifying with 1,5-pentanediol under standard EDC reaction condition. Synthesizing dimer **20** stepwise from carboxylic acid **15a** could improve the yield of the dimer **20**.

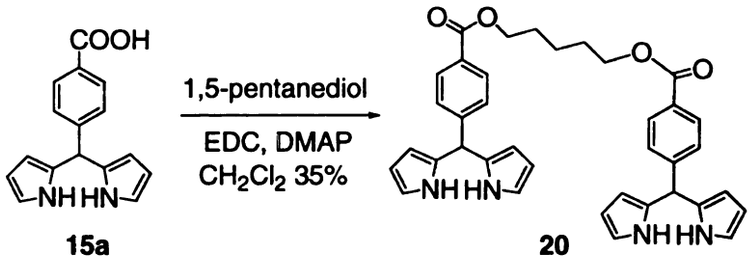

Scheme 6-14. The synthesis of dimer **20**.

As shown in Scheme 6-15, the isolated dimer **20** was then treated under Friedel-Crafts reaction condition to install the benzoyl groups. Although the Friedel-Crafts reaction was successfully applied to introduce benzoyl groups with the dipyrromethane methyl ester **15b**, it did not work for the dimer **20**. This reaction was repeated a couple of times, and in all the reactions starting material **20** was recovered.

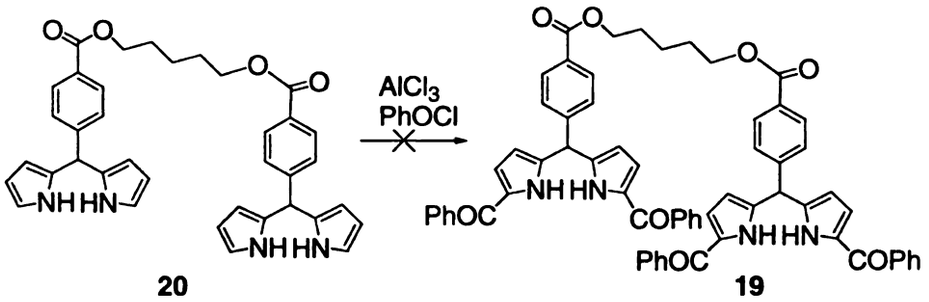

Scheme 6-15. The unsuccessful Friedel-Crafts reaction to synthesize dimer **19**.

Since we were unable to introduce four benzoyl groups with dimer **20**, we turned back to the original idea of installing benzoyl groups first, and then forming dimer **19**. As is illustrated in Scheme 6-11, the EDC coupling reaction of carboxylic acid **16** with 1,5-pentanediol failed to provide compound **19**, and methyl ester **17** could not be hydrolyzed to provide the carboxylic acid **16** (Scheme 6-12), an alternate method was needed to form the dimer **19** directly from the methyl ester **17**, without forming the carboxylic acid **16** first.

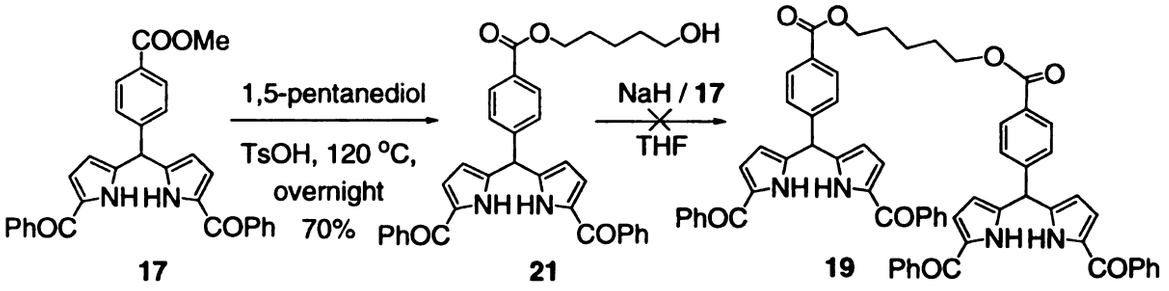

Scheme 6-16. The first attempt to synthesize compound **19** from methyl ester **17**.

As shown in Scheme 6-16, we planned to synthesize the monoester **21** from the methyl ester **17** by transesterificating with 1,5-pentanediol first, and then transform the monoester **21** to the diester **19** by reacting with equal amount of methyl ester **17** in presence of a base, such as sodium hydride. The monoester **21** was easily synthesized from methyl ester **17** via transesterification, by heating in 1,5-pentanediol in the presence of TsOH as the acidic catalyst. But once again, the attempt to synthesize the diester **19**

from the monoester **21** was unsuccessful. Even after stirring at room temperature overnight, the reaction did proceed, and heating it to reflux resulted in the decomposition of starting material **21**.

According to the literature, methyl esters can be directly transformed to diesters using sodium metal, as shown in Scheme 6-17.[21] Although the stoichiometry of the reaction calls for half equivalent of the diol, since the reaction was performed in a large scale, the diol was used as a solvent. In our case, the working scale did not allow for the use of 1,5-pentanediol as a solvent. Therefore, THF was chosen to serve as the solvent. Treatment of methyl ester **17** with sodium metal and half equivalent of 1,5-pentanediol in THF generated the desired diester **19** in 30% yield. The addition of THF drastically decreased the reaction rate and the yield of the desired product **19** was much worse than the reported.

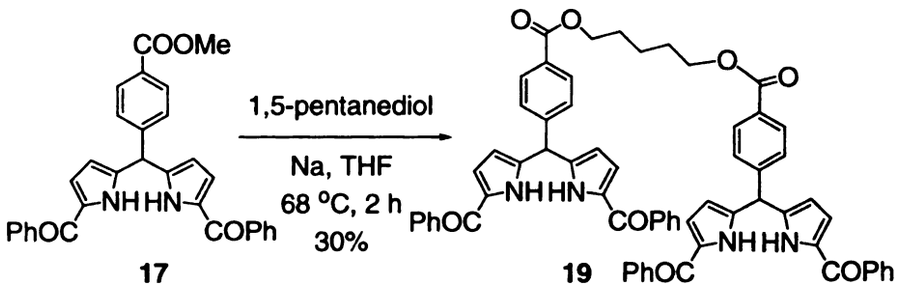

Scheme 6-17. Directly synthesis of diester **19** from methyl ester **17**.

With compound **19** in hand, it seemed we were not far away from securing the final porphyrin tweezer **2**. It only required the MacDonald "2+2" cyclization reaction to build two porphyrin planes by condensing compound **19** with dipyrromethane **5**. Before the synthesis of the porphyrin tweezer **2** with compound **19**, the MacDonald "2+2" cyclization reaction was tested with a model compound **17**.

As shown in Scheme 6-18, the diketone **17** was reduced with $NaBH_4$ to a diol, affording the starting material for MacDonald "2+2" porphyrin synthesis.[10] Since the diol intermediate was unstable, it had to be used immediately for the following "2+2" cyclization. The coupling of the diol and dipyrromethane **5** was achieved with TFA as acidic catalyst to yield porphyrin products in 40% yield.

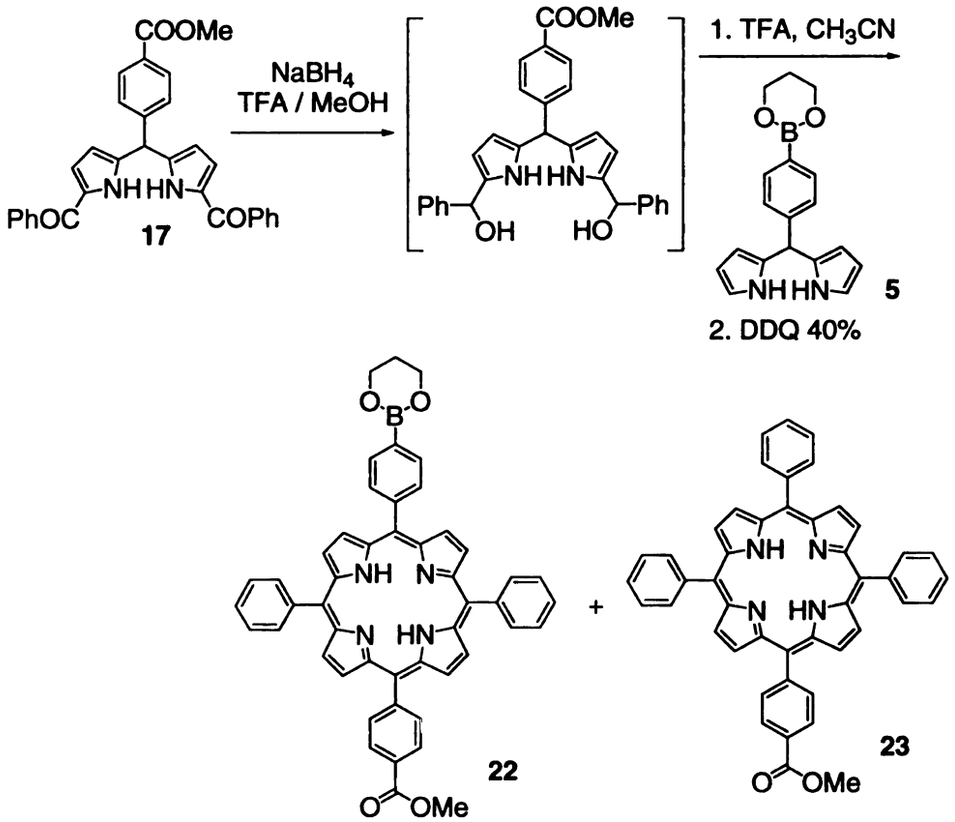

Scheme 6-18. The MacDonald "2+2" cyclization of compound **5** and **17**.

The purple color of the isolated product suggested that the desired porphyrin compound was generated in this cyclization reaction. From NMR spectrum, we could clearly observe the proton peaks characteristic of porphyrins, however, there were no signals belonging to the boronic acid protecting group. It was shown from NMR and MS studies that what we separated was a mixture of desired porphyrin **22** and the reduced

porphyrin **23**, which suggested that the boronic acid functionality was removed and lost during the reaction.

To better understand the fate of the boron, the reaction shown in Scheme 6-18 was repeated and the crude product was analyzed by MS and ^{11}B-NMR. The MS analysis revealed the presence of the molecular ion peaks for both the desired boronated porphyrin **22** and the de-boronated porphyrin **23**, with a ratio of about 2.5:1. ^{11}B-NMR of the reaction mixture exhibited a small boron peak. A small portion of the reaction mixture was subjected to a quick column to isolate some porphyrin product. MS analysis of the isolated porphyrin indicated the presence of both the desired boronated porphyrin **22** and the de-boronated porphyrin **23**, however, the ratio of the boronated porphyrin **22** to the de-boronated porphyrin **23** decreased from 2.5:1 before column to 1:2 after column. The rest of crude mixture was stored in the freezer overnight, and MS was measured. This time, the ratio of the boronated porphyrin **22** and the de-boronated porphyrin **23** decreased from 2.5:1 to 1: 1.

The comparison of these MS data makes it obvious that the 1,3-propanediol protected boronic functionality is unstable, and the C_{aryl}-B bond in porphyrins is cleaved during the acidic MacDonald "2+2" cyclization reaction conditions and on silica column. In order to improve its stability, the boronic acid should be protected with a bulkier diol, such as 2,2-dimethyl-1,3-propanediol.

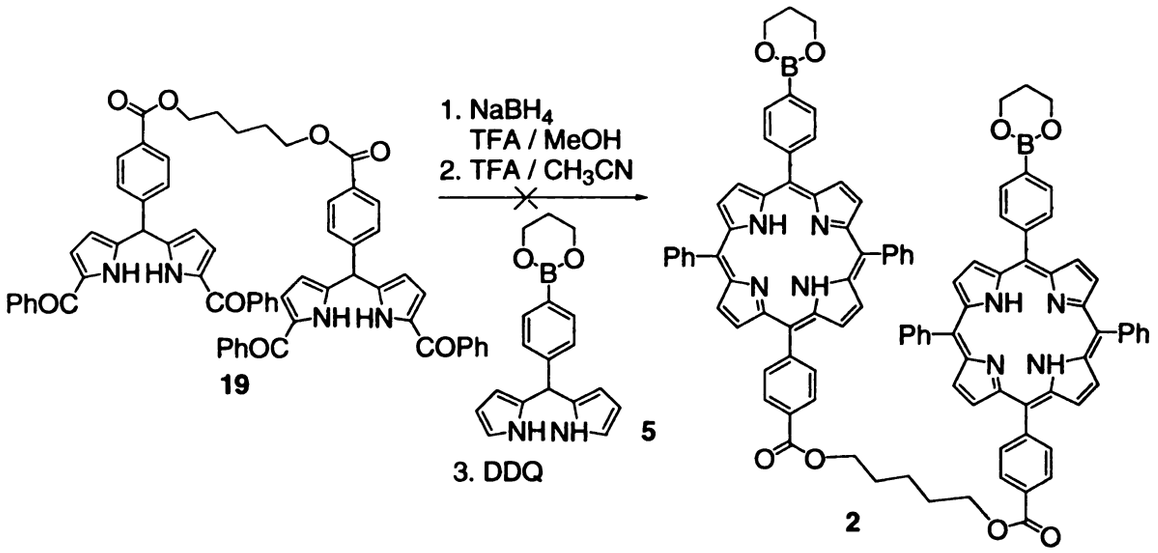

Scheme 6-19. The attempted synthesis of boronic porphyrin tweezer **2**.

The same reaction was attempted with dimer **19** as shown in Scheme 6-19. The MacDonald "2+2" cyclization reaction of the diester **19** was not as clean as that with methyl ester **17**, and provided at least three separable porphyrin products. Since the three compounds had very similar NMR spectra, it was hard to analyze the products. When submitted for FAB-MS, however, none of them were found to have the right molecular weight of the desired porphyrin tweezer **2**. The biggest problem with the MacDonald "2+2" cyclization reaction of diester **19** was that there were many porphyrin byproducts generated in the process, the separation of which was tedious.

From the unsuccessful attempt of synthesizing porphyrin tweezer **2** from dipyrromethane diester **19** (Scheme 6-19), it was quite clear that it was not an efficient method to build two porphyrin rings in one reaction. So for the synthesis of porphyrin tweezer **2**, we investigated pathway **I**, shown in Scheme 6-10, to synthesize the boronic porphyrin acid **4** first, and then couple it with 1,5-pentanediol to yield porphyrin tweezer **2** by EDC coupling reaction. As stated above, the 1,3-pentanediol was too labile, so we chose a bulkier group, 2,2-dimethyl-1,3-propanediol, to protect the boronic acid.

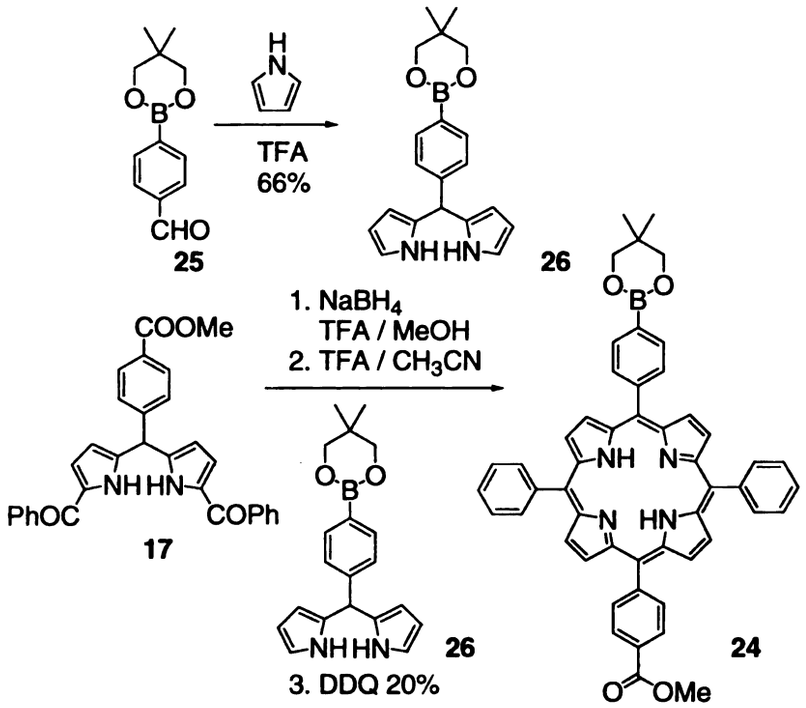

Scheme 6-20. The synthesis of boronic porphyrin methyl ester **24**.

Scheme 6-20 shows the synthesis of 2,2-dimethyl-1,3-propanediol protected porphyrin methyl ester **24**. With the newly protected boronic benzaldehyde **25** in hand, it was condensed with pyrrole to synthesize the dipyrromethane **26**, which subsequently underwent a MacDonald "2+2" cyclization with dipyrromethane-dicarbinol **17** to form the porphyrin methyl ester **24**. This time, the desired boronic porphyrin methyl ester **24** was isolated from the reaction mixture by column chromatography, and was observed by MS.

In order to synthesize the porphyrin tweezer, the porphyrin methyl ester **24** needs to be converted to its corresponding carboxylic acid **27**. However, the porphyrin methyl ester could not be converted to the carboxylic acid by standard reaction conditions, such as refluxing in the mixture of NaOH aqueous solution and THF or acidic hydrolysis, since the boron protecting group could not survive. As shown in Scheme 6-21, LiI and DMF could be used as mild conditions specifically for the removal of methyl esters.[22, 23]

The porphyrin methyl ester **24** was refluxed in a mixture of LiI and DMF for two hours, and NMR of the reaction mixture was taken. Based on NMR, the deboronated product was once again observed.

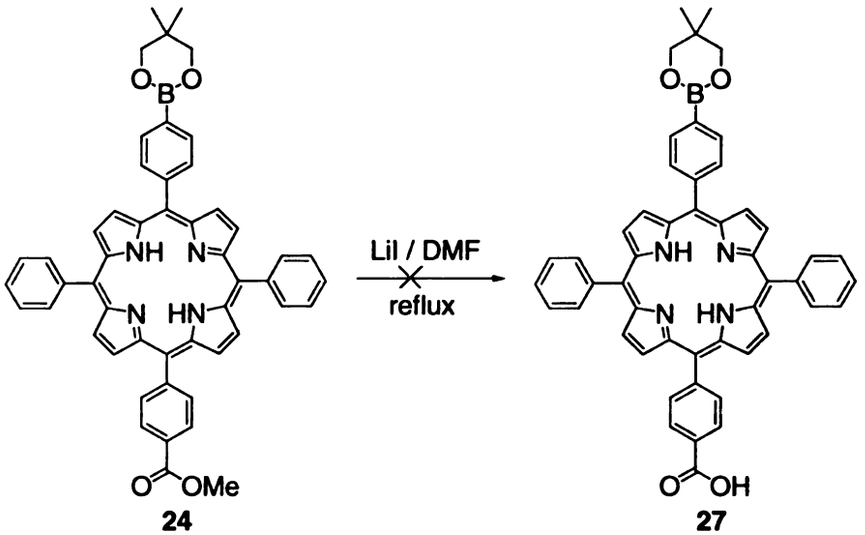

24 **27**

Scheme 6-21. The unsuccessful removal of methyl ester of compound **24**.

Since the attempt to transform the porphyrin methyl ester **24** to carboxylic acid **27** failed, the porphyrin tweezer **2** had to be synthesized from the methyl ester **24** directly instead of by transesterification. A transesterification reaction had been used in Scheme 6-17 to transfer a methyl ester **17** to a diester **19**.[21] The same condition was used to synthesize porphyrin tweezer **2** from methyl ester **24**, as shown in Scheme 6-22. However, after the reaction mixture was heated for a day, most the starting material **24** still remained in the reaction. Although a product was isolated by column chromatography, from NMR analysis, it was not the desired porphyrin tweezer **2**.

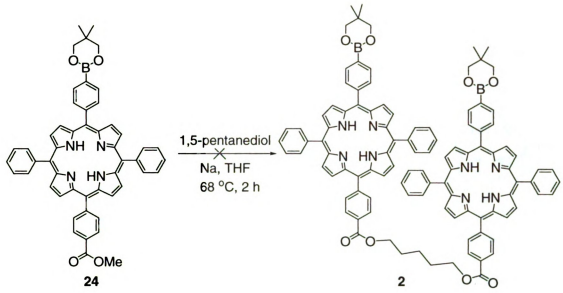

Scheme 6-22. The attempted synthesis of porphyrin tweezer **2**.

6-2.2. Synthesis of boronic porphyrin tweezer 2 by Pd catalyzed coupling reaction

We have tried to synthesize boronic porphyrin tweezer by MacDonald "2+2" cyclization method; however, the boronic functionality is too labile to be carried through in the porphyrin tweezer synthesis. Although in most cases, the carbon-boron bond is not very unstable, in our porphyrin system, the C_{aryl}-B bond becomes very unstable. Therefore, it is best to introduce the boronic functionality at the end of the synthesis. As shown in Scheme 6-23, the boronic functionality can be introduced by palladium coupling of boronic compounds, such as pinacolborane, with aryl bromide, iodide and triflates.[24, 25]

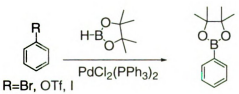

Scheme 6-23. Pd catalyzed coupling of pinacolborane with aryl halides.

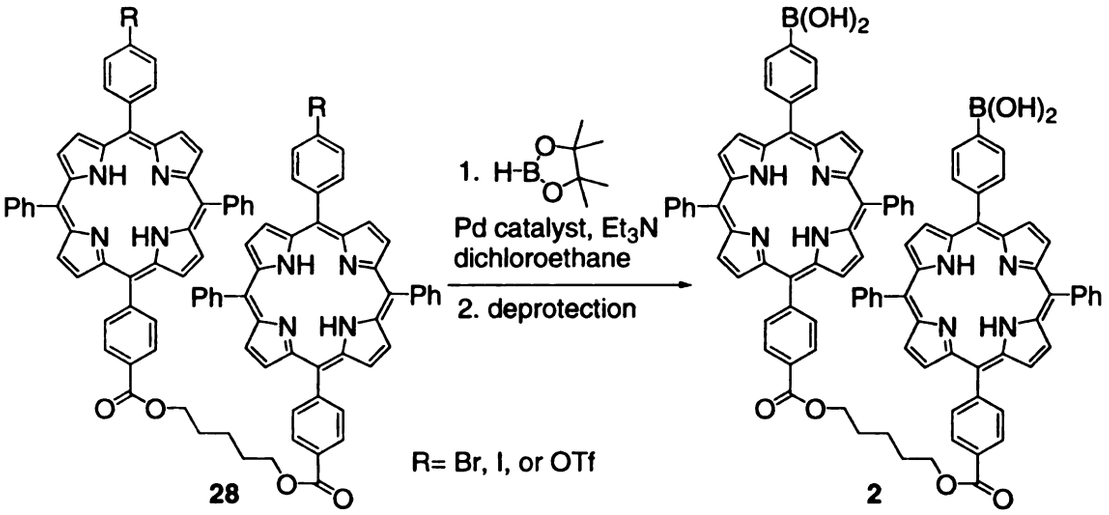

Scheme 6-24. The synthesis of porphyrin tweezer **2** by Pd coupling reaction.

Scheme 6-24 depicts the strategy of introducing the boronic acid functionality at the end of the synthesis. The synthesis of bromoporphyrin tweezer **28** requires securing the *para*-substituted bromoporphyrins. As shown in Scheme 6-25, Lindsey's method was used to synthesize the *para*-substituted bromoporphyrin alcohol **29**,[26] by condensing 4-hydroxybenzaldehyde, 4-bromobenzylaldehyde, and phenyldipyrromethane **30**[27] in CH_3Cl at 1:1:2 ratio, with $BF_3{\cdot}Et_2O$ as the acidic catalyst.

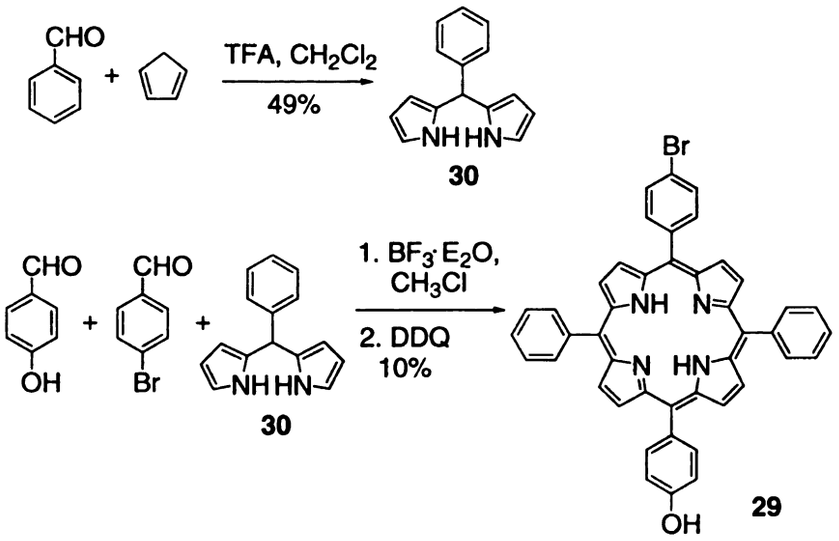

Scheme 6-25. The synthesis of *p*-bromoporphyrin alcohol **29**.

This reaction provided a mixture of di-hydroxyl, di-bromo, and the desired bromoporphyrin alcohol **29**, and correspondingly, the yield of the desired product **29** was not high. The separation of these three porphyrin products was easy enough, because the polarities of bromide and hydroxyl functionality were very different. The alcohol functionality in porphyrin **29** could be used to generate a tweezer by forming either an ether bond or an ester bond. Because of the availability of 1,3-dibromopropane, the porphyrin alcohol **29** was reacted with 1,3-dibromopropane under basic condition to form dibromo tweezer **31**. The attempted reaction between porphyrin alcohol **29** and 1,3-dibromopropane is shown in Scheme 6-26. The product of the reaction, even though a porphyrin like compound, was not analyzed further.

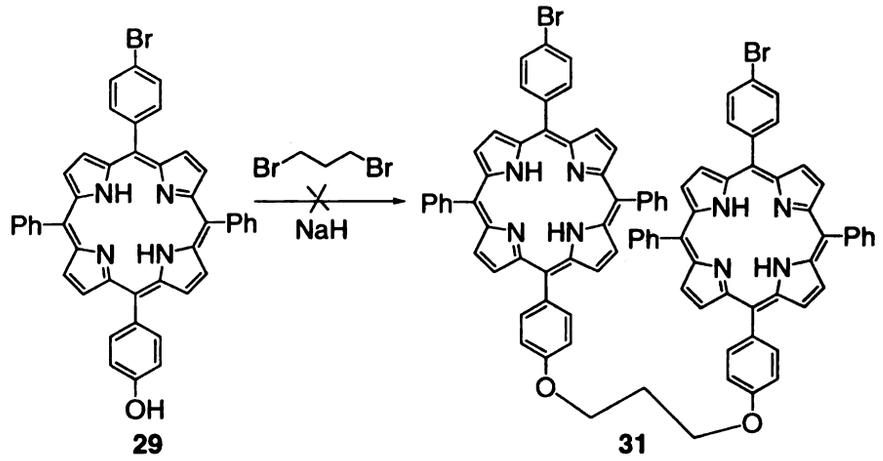

Scheme 6-26. The attempted synthesis of dibromo tweezer **31**.

Since the synthesis of bromoporphyrin tweezer via an ether bond failed, we planned to synthesize the bromoporphyrin **32**, containing a carboxylic acid functionality to react with 1,5-pentanediol by standard EDC facilitated esterification.

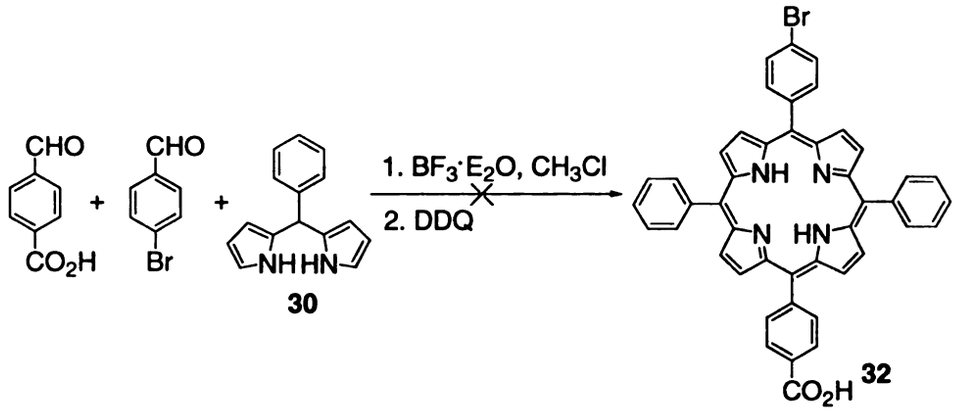

Scheme 6-27. The unsuccessful synthesis of bromoporphyrin carboxylic acid **32**.

The synthesis of bromoporphyrin carboxylic acid **32** is shown in Scheme 6-27. It was synthesized by the same method as porphyrin alcohol **29**, condensing 4-carboxybenzaldehyde, 4-bromobenzylaldehyde, and phenyldipyrromethane **30** in CH_3Cl (1:1:2 ratio) with $BF_3{\cdot}Et_2O$ as the acidic catalyst. This reaction provided a mixture with the unwanted di-bromoporphyrin as the major product. The generation of the desired porphyrin carboxylic acid **32** could be observed by TLC plate, however, it was hard to purify because of its high polarity. Since the carboxylic acid **32** was hard to synthesize directly, the corresponding methyl ester **33** was synthesized, which could be subsequently converted to the acid **32** by standard hydrolysis under basic conditions.

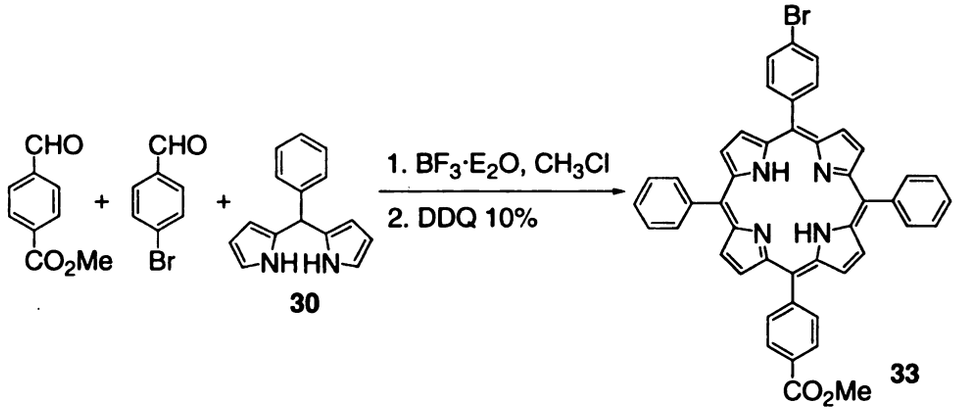

Scheme 6-28. The synthesis of porphyrin methyl ester **33**.

As shown in Scheme 6-28, porphyrin methyl ester **33** was synthesized by condensing 4-methoxycarbonylbenzaldehyde, 4-bromobenzaldehyde and 5-phenyldipyrromethane **30** in $CHCl_3$ with $BF_3{\cdot}Et_2O$ as the catalyst. This reaction provided a mixture of porphyrin products with the desired compound **33** having the medium polarity. The ratio between the dibromo porphyrin, compound **33** and diester porphyrin was about 2:4:1.

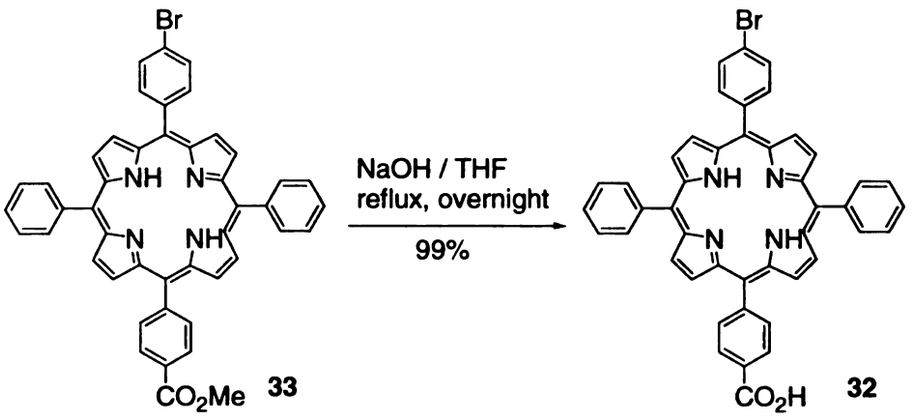

Scheme 6-29. Hydrolysis of methyl ester **33** to acid **32**.

The methyl ester **33** was then hydrolyzed under basic conditions (Scheme 6-29). The resulting carboxylic **32** dissolved quite well in organic solvents, such as CH_2Cl_2 and CH_3Cl. After carboxylic acid **31** was extracted, it was dried and used without further purification for the esterification reaction to synthesize the dibromo tweezer **34**.

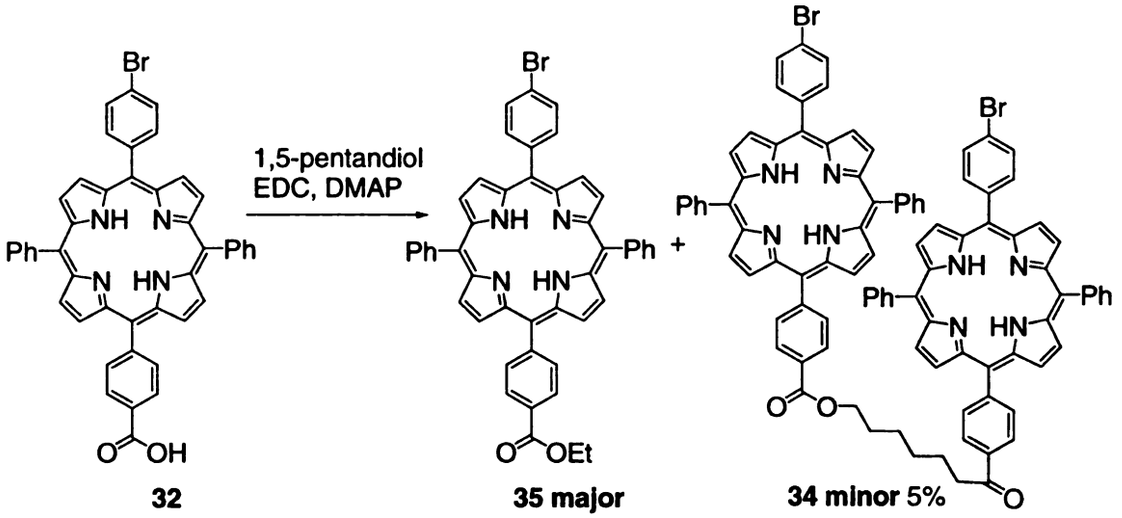

Scheme 6-30. EDC coupling of acid **32** with 1,5-pentanediol.

The esterification of the porphyrin acid **32** with 1,5-pentanediol generated the dibromo porphyrin tweezer **34**, but not as well as expected (Scheme 6-30). Surprisingly, the major product of the reaction was the porphyrin ethyl ester **35**. The only step that could have introduced a trace of ethanol into the reaction was during the synthesis of the porphyrin methyl ester **33**. In that process, chloroform was used as the solvent, which could have been contaminated with ethanol. However, the porphyrin methyl ester **33** was purified by column chromatography, and the small amount of ethanol in chloroform should have been removed by the column. So the source of ethanol still remains a mystery.

Having at hand the dibromo tweezer **34**, the palladium coupling reaction could be probed. However, before undergoing the palladium coupling reaction, the porphyrin tweezer free base **34** was converted to its corresponding zinc porphyrin tweezer, since the palladium could be inserted, if the porphyrin free base was utilized. Following established procedures, zinc ion was introduced by adding zinc acetate to compound **34**

in chloroform. The zinc porphyrin tweezer was purified by column chromatography before the palladium coupling reaction.

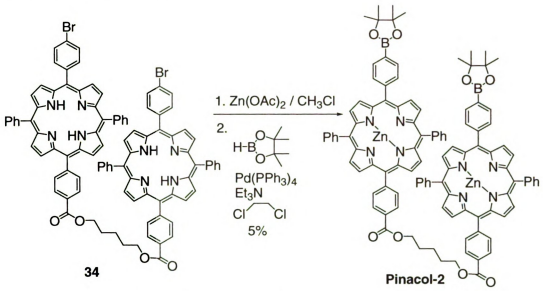

Scheme 6-31. The Pd catalyzed coupling of dibromo tweezer.

As shown in Scheme 6-31, the palladium catalyzed coupling reaction between **34** and pinacolborane[28] completed in four hours as monitored by TLC. It provided at least four different kinds of porphyrin products, which were separated by column chromatography. These porphyrin products were analyzed by FAB-MS, and one of the four products seemed to be the desired porphyrin tweezer **Pinacol-2**. Therefore, the palladium catalyzed coupling reaction is a reasonable method to synthesize boronic porphyrin tweezer. In order to optimize the reaction condition to improve the yield of the desired coupled product, modeling studies were performed with the bromoporphyrin methyl ester **33**.

Bromoporphyrin methyl ester free acid **33** was converted to its zinc porphyrin, and then coupled with pinacolborane by using $PdCl_2(PPh_3)_2$ as the catalyst. The addition of all the starting material to the Schlenk reaction flask was conducted in a dry box, since

the palladium catalyst is very sensitive to moisture and oxygen. The reaction mixture was heated to 90 °C overnight before all of the starting material **33** was consumed.

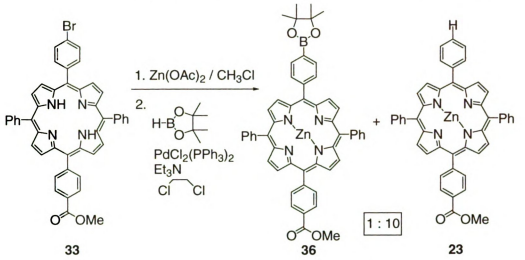

Scheme 6-32. The coupling reaction of porphyrin methyl ester **33**.

As shown in Scheme 6-32, this coupling reaction provided two products, with the major one having very similar polarity as the starting porphyrin methyl ester **33**. The two products were separated by column chromatography, and based on MS, the major product was suggested to be the reduced product **23**, and the minor product as the desired product **36**. The ratio between these two products was 10:1, and increasing the amount of triethylamine did not affect the ratio. According to known mechanism, the new hydrogen in the reduced product **23**, was transferred from pinacolborane. The formation of the reduced product could potentially be eliminated if the hydrogen was removed from the boron species.[24]

Bis(pinacolato)diboron is another commonly used coupling reagent for palladium coupling reaction. Several reaction conditions were tried to couple this boron compound to bromoporphyrin **33**,[29, 30] but unfortunately, porphyrin **36** was not isolated (Scheme 6-33).

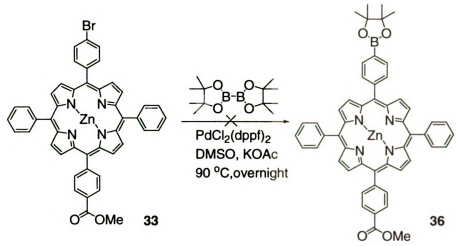

Scheme 6-33. The unsuccessful coupling with bis(pinacolato)diboron.

It is understood that for the palladium catalyzed coupling reactions, electron rich aryl halides systems proceed more smoothly than electron poor system.[31] In our porphyrin synthesis, the presence of Zn(II) makes this systems more electron deficient as compared to the porphyrin free base. Zinc was introduced to hinder any insertion of palladium into the porphyrin. However, as it turns out palladium insertion was not observed in the coupling step, and thus the conversion of porphyrin free base to zinc porphyrin was not necessary. Therefore, for the rest of the coupling reactions, porphyrins were used as porphyrin free bases instead of metalloporphyrins.

The studies with bromoporphyrins show that the bromoporphyrin system is not a good coupling partner for the palladium catalyzed reaction. Since aryl triflates and aryl iodides are better coupling reagents than aryl bromides, they become our next targets.[32, 33] The reactions of aryl triflates and iodides require lower reaction temperature, the rate of the reaction is faster, while the ratio between the desired coupling product and the reduced by-product is expected to improve.

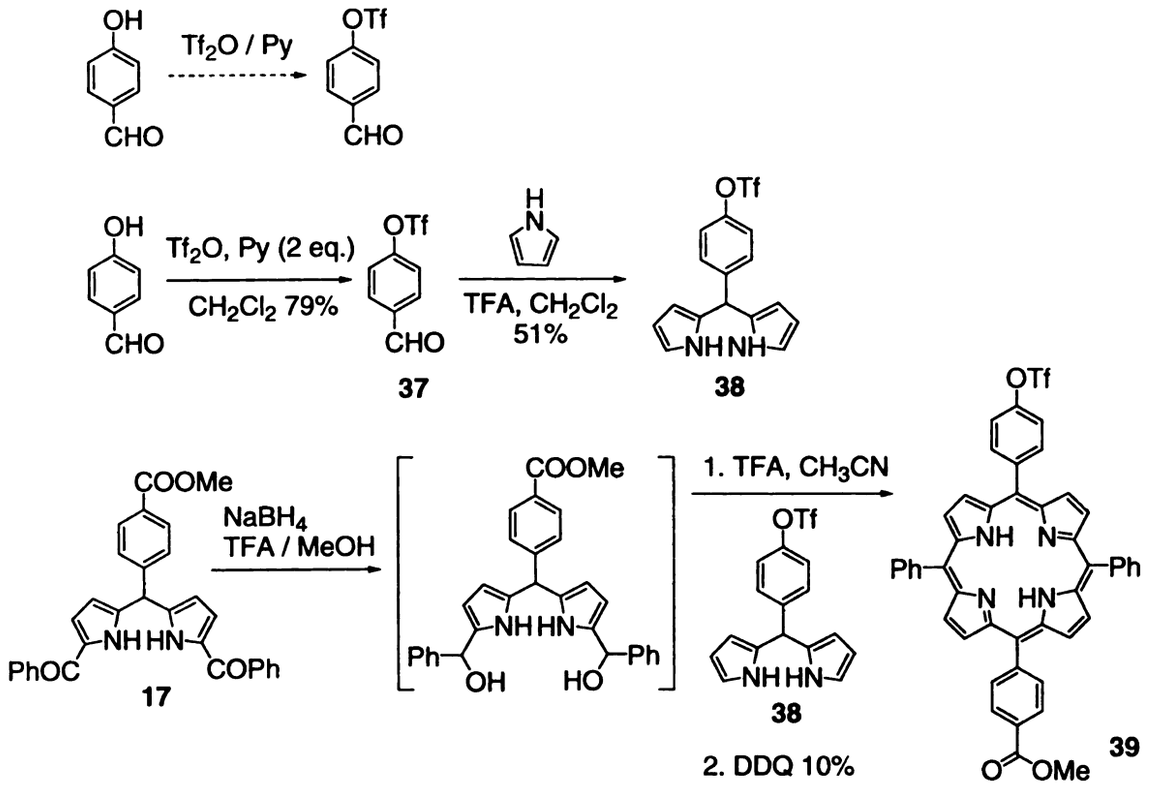

Scheme 6-34. Synthesis of triflate porphyrin methyl ester **39**.

As shown in Scheme 6-34, the synthesis of the triflate porphyrin methyl ester **39** started with the conversion of the hydroxyl group to the aryl triflate **37**. When pyridine was used as solvent, no product was generated.[34] When less amount of pyridine was applied (2 equivalents) and dichloromethane was used as the solvent,[34] this reaction yielded the aryl triflate **37** as the sole product after 30 h. The aryl triflate **37** was condensed with excess pyrrole in acidic condition to yield the dipyrrolemethane **38**, which was reacted with dipyrromethane-dicarbinol **17** by MacDonald "2+2" cyclization to synthesize the triflate porphyrin methyl ester **39**. At the same time, the de-triflated porphyrin was also isolated from the MacDonald "2+2" cyclization. Triflate porphyrin methyl ester **39** was then coupled with pinacolborane under routine palladium conditions (Scheme 6-35). After heating at 90 °C in a Schlenk flask overnight, the formation of the desired product **36** was not observed, and only the starting material **39** was recovered.

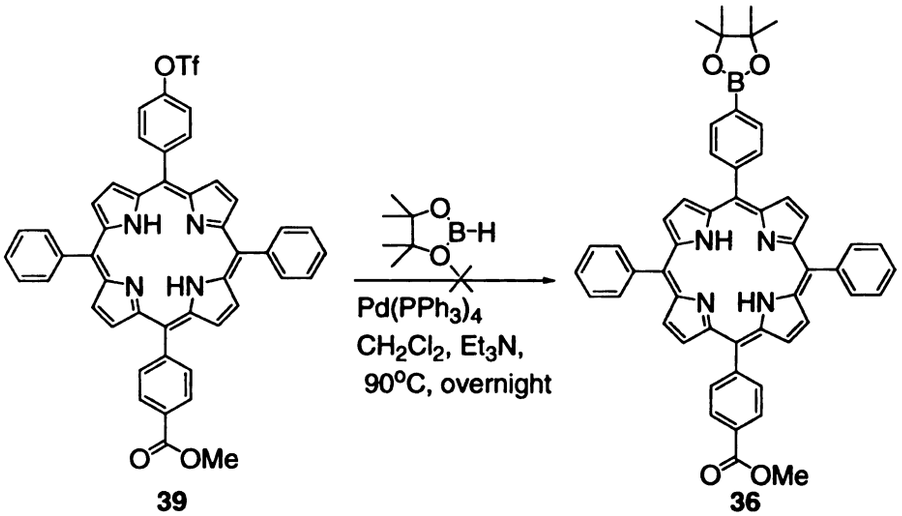

Scheme 6-35. The attempted Pd coupling of triflate **39**.

Since the triflate porphyrin methyl ester **39** failed to couple with pinacolborane under the palladium coupling condition, iodoporphyrins **41** was synthesized. The synthesis of iodoporphyrin methyl ester **41** was very similar to the synthesis of bromoporphyrin methyl ester **33** (Scheme 6-36). It started with the conversion of 4-formylphenylboronic acid to 4-iodobenzaldehyde **40**.[35] The boronic acid functionality was converted to iodide by refluxing with NIS in dry acetonitrile, and the 4-iodobenzaldhyde **40** was then condensed with methyl 4-formylbenzoate and 5-phenyldipyrromethane **30** by using $BF_3 \cdot Et_2O$ as catalyst to synthesize the iodoporphyrin methyl ester **41**.

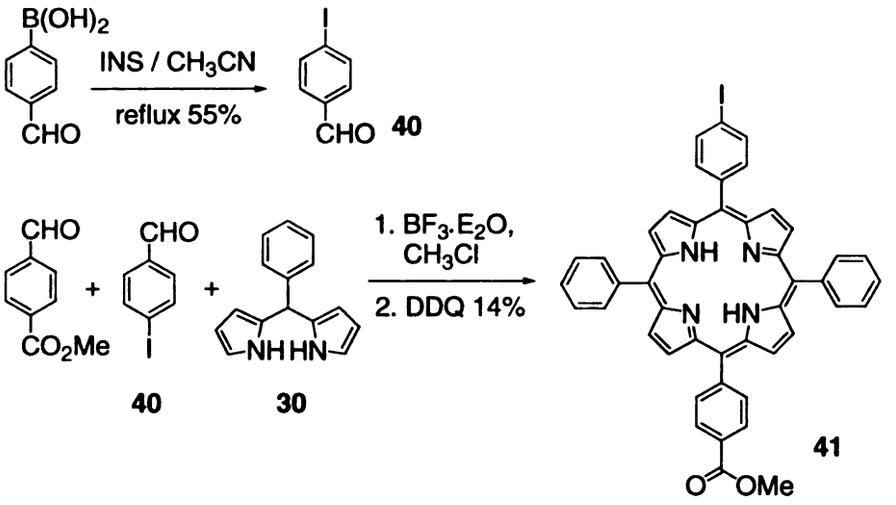

Scheme 6-36. Synthesis of iodoporphyrin methyl ester **41**.

Several reactions were tested to find the optimal palladium catalyzed reaction conditions for coupling iodoporphyrin methyl ester **41** with pinacolborane. The results are shown in Table 6-1.

Table 6-1. The palladium catalyzed coupling of iodoporphyrin **41** with pinacolborane.

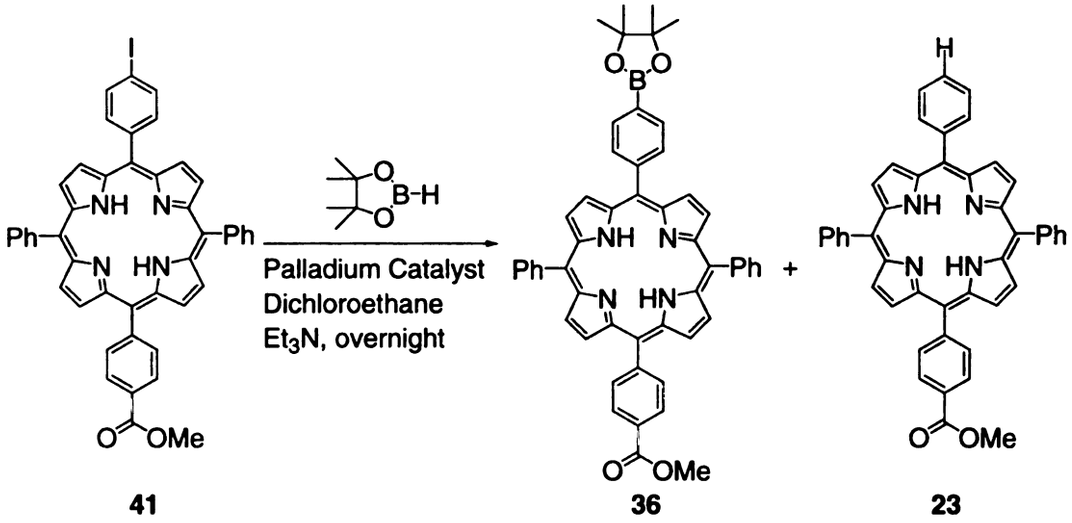

Palladium Catalyst	Temperature (°C)	Ratio (**36**:**23**)
$PdCl_2(PPh_3)_2$	140	1:1
$PdCl_2(PPh_3)_2$	90	1:8
$Pd(PPh_3)_4$	140	1:7

As shown in Table 6-1, the highest yield and the best ratio between the desired coupling product **36** and the reduced product **23** was achieved by using $PdCl_2(PPh_3)_2$ as the catalyst, and the reaction temperature at 140 °C. In this optimal condition, the yield of the desired boronic porphyrin **36** was 30%, and the ratio between the desired porphyrin **36** and the reduced porphyrin **23** was nearly 1:1. With $PdCl_2(PPh_3)_2$ as the catalyst, lowering the temperature from 140 °C to 90 °C, drastically reduced the yield, and the ratio between the desired porphyrin **36** and the reduced product **23** was 1:8. When $Pd(PPh_3)_4$ was used as the catalyst, the yield of the desired product **36** decreased, and the ratio between the desired porphyrin **36** and reduce product **23** was roughly 1:7. It is hard to discriminate between the iodoporphyrin **41**, the boronic porphyrin **36** and the reduced porphyrin **23** based on NMR, since they have very similar NMR spectra. Mass Spectrum is a better way to determine the formation of the products. The porphyrin compounds have strong molecular ion peaks, and the formation of the product can be confirmed by comparing the molecular ion mass with the calculated molecular weight.

After optimization of the palladium catalyzed coupling reaction between iodoporphyrins and pinacolborane, two things were left before the synthesis of the final boronic porphyrin tweezer **2** could be achieved. The first thing was the synthesis of the iodoporphyrin tweezer **42**. Since, the C_{aryl}-B bond was very easy to break, it was better to form the diiodoporphyrin tweezer **42** first, and then couple with pinacolborane to afford the boron protected tweezer **Pinacol-2**. The second thing was to find a mild and efficient way to deprotect the boronic acid. The challenge lied in finding reaction conditions to selectively deprotect the boronic acid functionality in the presence of another ester moiety.

The first task of synthesizing the diiodoporphyrin tweezer **42** was straightforward. As shown in 6-37, after the iodoporphyrin methyl ester **41** was hydrolyzed by refluxing in the mixture of THF and aqueous sodium hydroxide solution, the resulting pure porphyrin acid **43** was then esterfied with 1,5-pentanediol by EDC coupling reaction to provide the diiodoporphyrin tweezer **42**.

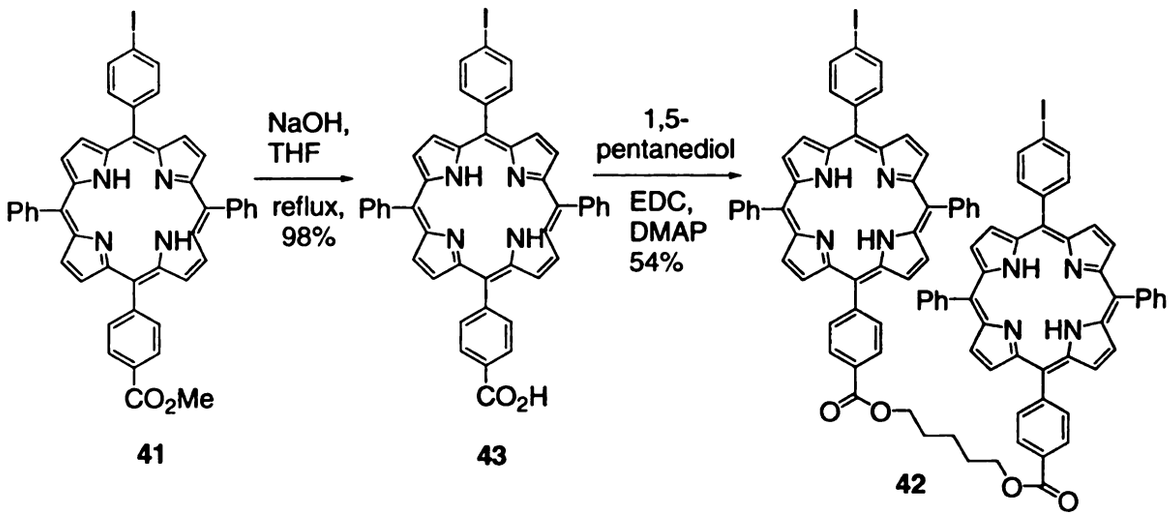

Scheme 6-37. The synthesis of diiodoporphyrin tweezer **42**.

As shown in Scheme 6-38, the diiodoporphyrin tweezer was coupled to pinacolborane by palladium catalyzed coupling reaction. Coupling the diiodoporphyrin tweezer **42** and pinacolborane, with $PdCl_2(PPh_3)_2$ as the catalyst at 140 °C, provided the fully reduced porphyrin, half reduced porphyrin and the desired diboron porphyrin tweezer **Pinacol-2**. The separation of these three products was not hard, with the desired porphyrin tweezer **Pinacol-2** being the least polar on TLC. From NMR, there was no difference between these compounds in the aromatic region, and only by FAB-MS, the formation of the desired compound could be confirmed. Coupling porphyrin tweezer **42** and pinacolborane with $PdCl_2(PPh_3)_2$ as the catalyst successfully provided the desired boronic porphyrin tweezer **pinacol-2**, but the yield was quite poor. However, in our

study, since only very small amount of boronic porphyrin tweezer is needed, the poor yield was acceptable.

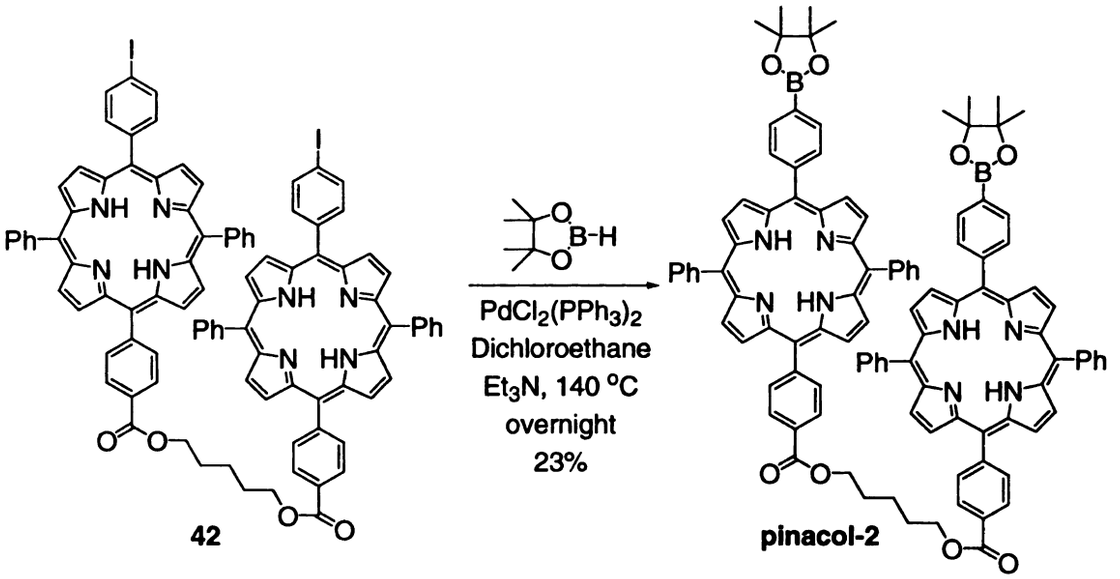

Scheme 6-38. The Pd coupling of diiodoporphyrin tweezer **42** to synthesize porphyrin tweezer **pinacol-2**.

After the synthesis of protected boronic porphyrin tweezer **pinacol-2**, the only task left was to free the boronic acid from its protection. Some studies were performed to search for the conditions that were strong enough to remove the pinacol protecting group but mild to preserve the labile C_{aryl}-B bond.

6-2.3. Hydrolysis of Pinacolborane

Most of the boronic esters are quite susceptible to hydrolysis. In aqueous solution, the ester could easily fall off at a wide range of pH values. Some boronates can even fall off on silica gel column because of its acidity. However, as the steric demands of the protecting diol increase, the rate of hydrolysis decreases. Pinacole, which is a bulky protecting group, is rather difficult to hydrolyze. Generally, there are three ways to hydrolyze pinacol boronate. Stirring the boronates in acidic or basic aqueous solution is

the most common way to hydrolyze any boronic ester, including pinacol boronate. The second is reducing the boronates with lithium aluminum hydride in THF, and the third is oxidizing the boronates with sodium periodate in a mixture of acetone and water.

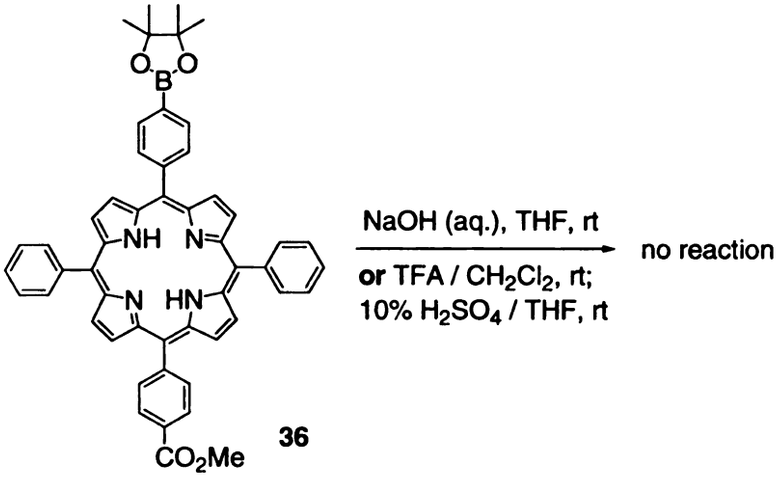

36

Scheme 6-39. The unsuccessful hydrolysis of boronic porphyrin **36**.

The first attempt to deprotect the pinacol boronate was by hydrolysis, as shown in Scheme 6-39, in both basic and acidic condition. After the pinacol boronate porphyrin methyl ester **36** was stirred in the mixture of 2 N sodium hydroxide aqueous solution and THF (1:2) for 2 days, there was no sign of the free boronic acid product. The formation of porphyrin boronic acid could be easily monitored by TLC, since the product should be more polar than the starting pinacol boronate, and the lack of purple spot at baseline excluded the formation of porphyrin boronic acid in the reaction. The hydrolysis was also tried in a variety of acidic conditions, including trifluoroacetic acid in dichloromethane, and 10% aqueous sulfuric acid in THF.[36] The reactions were kept at room temperature for 2 days; however, no free boronic acid product was observed for either reaction. Refluxing is very common for hydrolysis of boronates in aqueous media; however, the porphyrin boronate **36** could not be heated under acidic or basic aqueous

conditions, due to the presence of a methyl ester, which would have been readily hydrolyzed.

Coutts and coworkers have published on cleaving pinanediol boronate esters to yield the free boronic acids.[37] Pinanediol is a very bulky group, and the cleavage of the pinanediol group from boronate esters is known to be difficult. As shown in Scheme 6-40, they have developed two mild techniques to successfully remove pinanediol from the boronate. When comparing the structures of pinanediol and pinacol, it is quite obvious that the pinanediol is even bulkier than pinacol, and correspondingly, it should be harder to cleave.

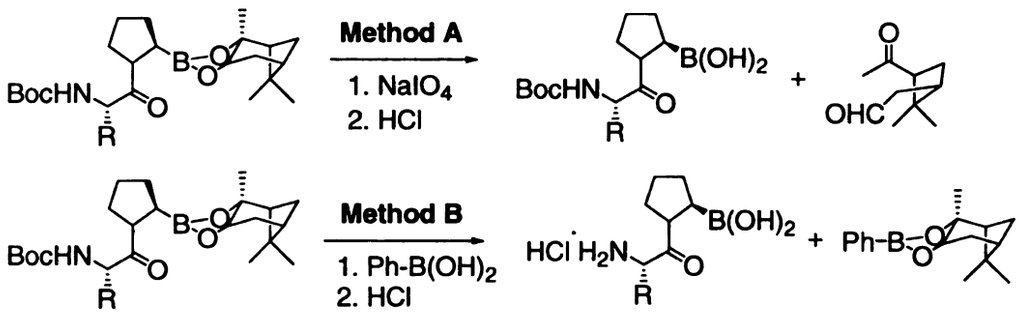

Scheme 6-40. The cleavage of pinanediol boronate to boronic acids.

As shown in Scheme 6-40, there are two methods to get free boronic acids from of pinanediol boronate esters. Method **A** relies on the oxidative cleavage of the pinanediol by using sodium periodate. Although boronic acids could be oxidized by nucleophilic oxidants, such as alkaline hydrogen peroxide, periodate is an eletrophilic oxidant, and it could not oxidize free boronic acid. This method is compatible even with Boc protected dipeptides, and it should be compatible with the methyl ester functionality as well.

Method **B** is based on the transesterification with phenylboronic acid and the removal of the pinanediol as the phenylboronate ester. It is particularly applicable to

water soluble boronates. In this process, a biphasic system is used, and the starting pinanediol ester and the free boronic acids, both the starting phenylboronic acid and the resulting boronic acid product, are dissolved in the aqueous phase with the pinanediol phenylboronate ester in the organic phase. This procedure allows for the easy recovery of the valuable pinanediols from the organic layer. However, our target molecule, the boronic porphyrin methyl ester **36**, is not water soluble, and Method **B** was not applicable to this system. Method **A** was used for the deprotection of compound **36** to form the free porphyrin boronic acid.

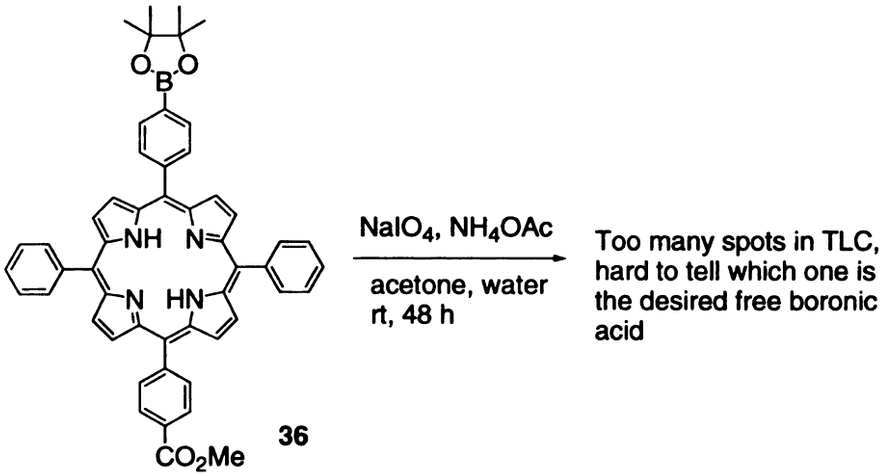

Scheme 6-41. The attempted oxidation of porphyrin methyl ester **36**.

According to the reference,[37] the solvent for this oxidation reaction is a mixture of acetone and water at 1:1 ratio, but since porphyrins do not dissolve in this mixture, the amount of acetone used in the solvent was increased. As shown in Scheme 6-41, after this mixture was stirred at room temperature for 48 h, three bands could be observed from TLC plates. The first band was the unreacted porphyrin pinacol boronate **36**. The second and the third band each contained two bands, and these two bands were very close to each other. Since pure product could not be isolated from these two bands, it was

impossible to identify them. This reaction was repeated several times, and the results were the same.

Since the porphyrin methyl ester **36** is a quite complex molecule, a simpler pinacol boronate **44** was chosen as the model compound to find the best reaction condition for the removal of pinacol from the protected boronates. As shown in Scheme 6-42, different reaction conditions were applied to this model compound **44**. When sodium peroidate served as the oxidant and NH_4OAc as the base, after two days of stirring in room temperature, the desired boronic acid product was generated with some unreacted starting material **44**. When NH_4OAc was not used in the reaction, the reaction rate significantly slowed down, and there was more starting material **44** left unreacted. When other oxidants were used, such as oxone and hydrogen peroxide, the carbon boron bond was cleaved, and the boronate **44** was oxidized to 3,5-dimethylphenol.

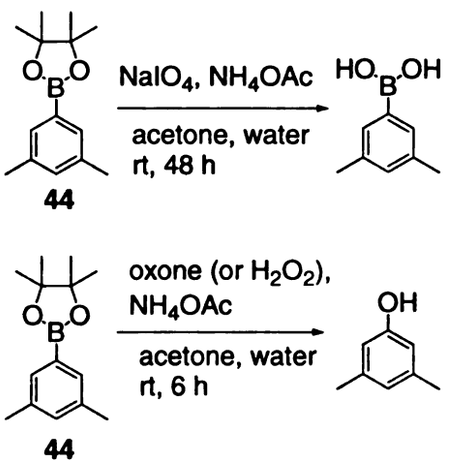

Scheme 6-42. The oxidation studies on model molecule **44**.

The studies with 3,5-dimethylphenyl pinacolboronate **44** (Scheme 6-42) showed that the oxidation with sodium periodate could afford free boronic acid from pinacolboronate. However, this method did not work for the porphyrin pinacolboronates. Then the only method left to deprotect the pinacol boronates and form free boronic acid

was by hydrolysis. The hydrolysis of boronates often occurs in refluxing acidic or basic aqueous solution, however, the methyl ester in porphyrin **35** could not survive these conditions. Therefore, it was planned to reduce the methyl ester **36** to ether first, and then hydrolyze the new compound in refluxing acidic or basic aqueous condition to afford free boronic acid compound.

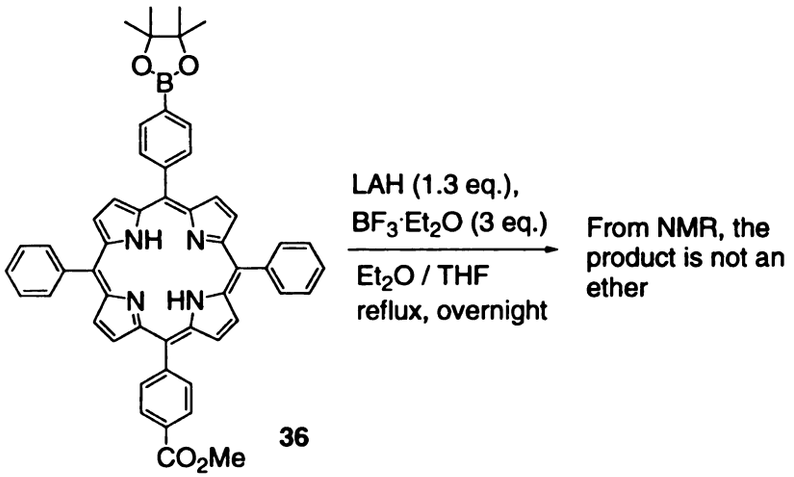

Scheme 6-43. The attempted reduction of methyl ester **36**.

A mixture of lithium aluminum hydride and BF_3 etherate can be used to reduce esters to ethers directly.[38] As shown in Scheme 6-43, pinacol boronate porphyrin **36**, 1.3 equivalent of lithium aluminum hydride, and 3 equivalents of $BF_3{\cdot}Et_2O$ were added to a solution of ether and THF. This reduction is typically performed in pure ether, but since porphyrins do not dissolve in ether very well, minimum amount of THF was used to improve the solubility of the porphyrin. When this mixture was stirred at room temperature, no reaction occurred. After this mixture was refluxed overnight, the starting material **36** decomposed.

So far, all the attempts to deprotect the pinacol borates had failed. Although, we had successful synthesized the pinacol protected boronic porphyrin tweezer **pinacol-2**, we could not find a way to remove the protecting group.

6-3. Transmetallation to introduce boronic acid

Transmetallation of aryl halides and reaction of the lithiated species with borates could be an alternative method for the introduction of boronic acid.[39] As shown in Scheme 6-44, boronic acids could be transformed from the corresponding aryl halides by transmetallation. Grignards, which are easily accessible from aryl halides, readily react with $B(OMe)_3$, and the subsequent treatment under acidic aqueous condition generates the boronic acid.

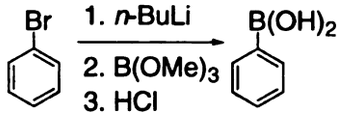

Scheme 6-44. The transmetallation with bromobenzene.

As shown in Scheme 6-45, the same transmetallation reaction condition was applied to the bromoporphyrin methyl ester **33**. However, MS analysis did not indicate a peak having the same molecular weight as the expected porphyrin boronic acid, and in fact most of the starting bromoporphyrin **33** remained unreacted. Although the same transmetallation reaction worked well for simple bromobenzene, it did not work for the bromoporphyrin **33**. The reason could be that the porphyrin stabilizes the negative charge better than a simple benzene ring. After transmetallation with *n*-BuLi, the carbon anion is too stable to attack $B(OMe)_3$.

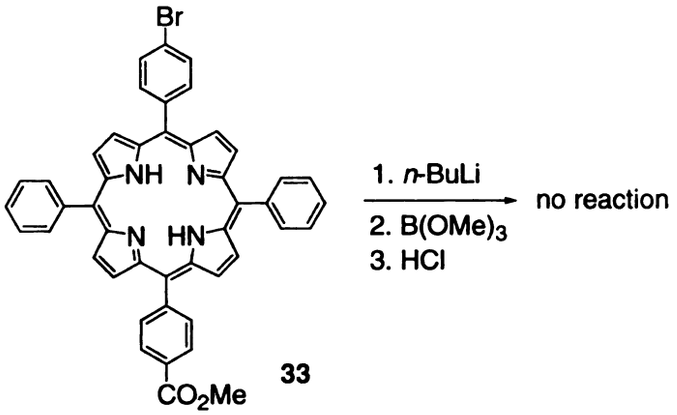

33

Scheme 6-45. The attempted transmetallation with bromoporphyrin **33**.

So far, three different methods were tried to synthesize the boronic porphyrin tweezer **2**: the MacDonald's "2+2" cyclization, the palladium catalyzed coupling reaction and the transmetallation of bromoporphyrins. However, none of them provided the desired boronic porphyrin tweezer **2**.

6-4. Synthesis of water soluble boron containing porphyrin 45

There is very limited number of papers on the synthesis of *para*-substituted boronic porphyrin, and our experience with this porphyrin suggested that the boronic porphyrin tweezer **2** was a more difficult target to synthesize than we had anticipated. We decided to change the structure, and make a more accessible boronic porphyrin tweezer **45**; the structure of which is shown in Figure 6-4.

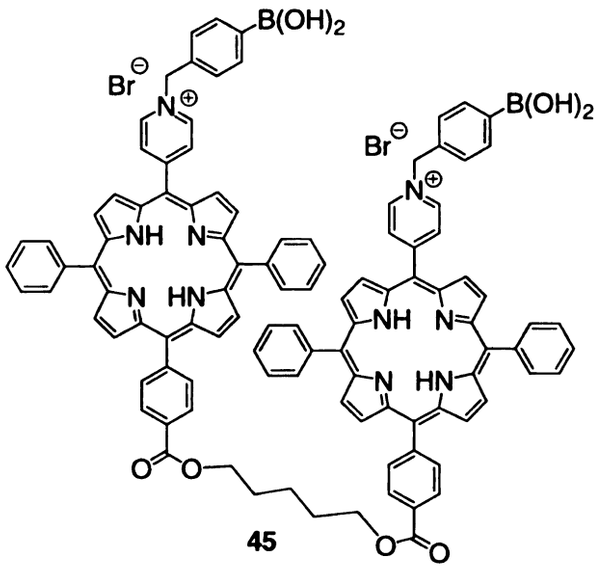

Figure 6-4. The structure of a new porphyrin tweezer **45**.

Porphyrin tweezer **45**, shown in Figure 6-4, is a water-soluble salt, and can be synthesized from the porphyrin methyl ester **46**. Shinkai in Kyushu University has synthesized a very similar molecule, which was used in binding with oligocarbohydrates.[40] As illustrated in Scheme 6-46, the phenylboronic part of molecule **46** is introduced by the pyridine porphyrin **47** reacting with the primary bromide **48**.

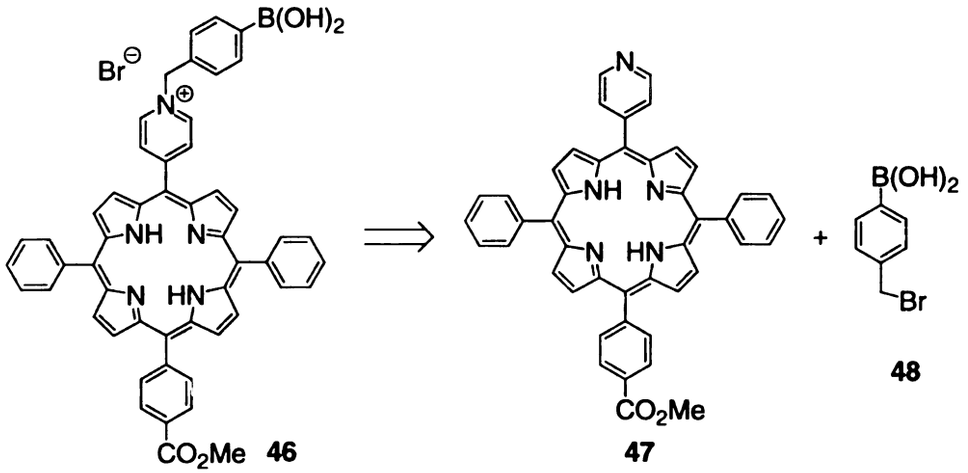

Scheme 6-46. The synthesis of boronic porphyrin methyl ester **46**.

The synthesis of the pyridine porphyrin **47** was routine, and is shown in Scheme 6-47. Porphyrin **47** was synthesized by condensing one equivalent of 4-formylpyridine

with one equivalent of methyl 4-formybenzoate and two equivalents of dipyrrolemethane **30**, using $BF_3 \cdot Et_2O$ or TFA as the acidic catalyst.

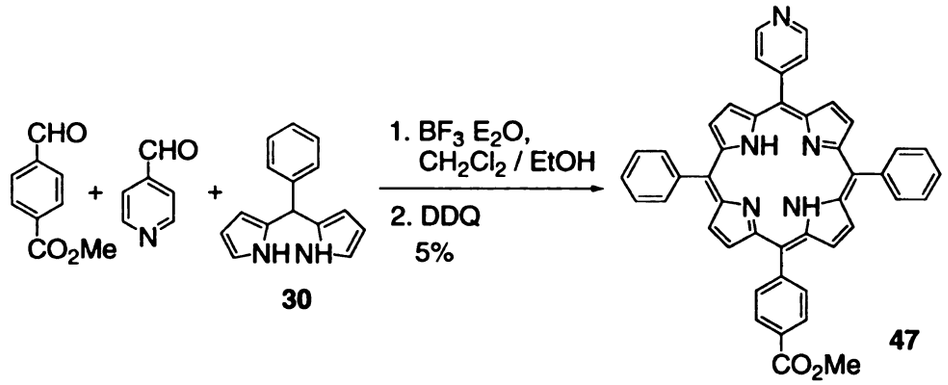

Scheme 6-47. The synthesis of pyridine porphyrin **47**.

The only difference in the synthesis of the pyridine porphyrin **47** and all the other porphyrins was the much longer reaction time it required.[41] The reaction took 24 h, while it only required one or two hours for the synthesis of the other porphyrins. Because the nitrogen atom of the starting material, 4-formylpyridine, was able to coordinate with the catalyst, either $BF_3 \cdot Et_2O$ or TFA, the reaction rate was slowed down. The separation of this reaction mixture was hard, because of the generation of many byproducts, and the yield was worse compared to the other porphyrins synthesized before.

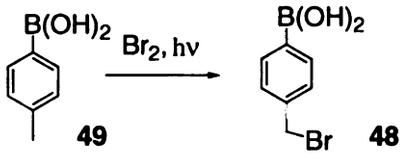

Scheme 6-48. The bromination of compound **48**.

The primary bromide **48** could either be synthesized or be purchased, however, since it is expensive ($130 per gram), the compound was synthesized. As shown in Scheme 6-48, it could be transformed from 4-methlyphenylboronic acid **49** by simple bromination with bromine under light.[42] The reaction worked smoothly when the scale of

this reaction was small, and the desired product **48** precipitated out of the mixture at the end of the reaction and was therefore, easily purified. But the same reaction did not work as well for larger amounts of starting material. In the reaction mixture, two products were observed, the desired mono-brominated product **48** together with the unwanted dibrominated product. The mixture was applied to column chromatography several times, but we were unable to separate them due to their close polarity. The compound **48** used in the reaction was purchased from herein.

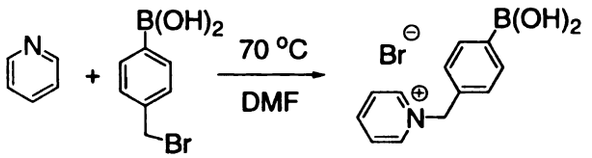

48 **50**

Scheme 6-49. The reaction between pyridine and primary bromide **48**.

As previously reported, the free boronic acid of compound **48** is first protected by 1,3-pentanediol, and then reaction with pyridine porphyrin **47** leads to the boronic containing porphyrin **46**.[40, 43] We wanted to investigate the possibility of using this reaction, without protecting the free boronic acid in compound **48**. The reaction was first checked with pyridine, as shown in Scheme 6-49. Pyridine was mixed with boronic acid **48**, and dissolved in DMF. This reaction was stirred at 70 °C for one day, and the solvent was removed with residue being washed with ether and acetone. The white precipitate left in the flask was the desired coupling product **50**. Because it was a salt, it did not dissolve in organic solvent, and was easy to separate and purify from the reaction mixture.

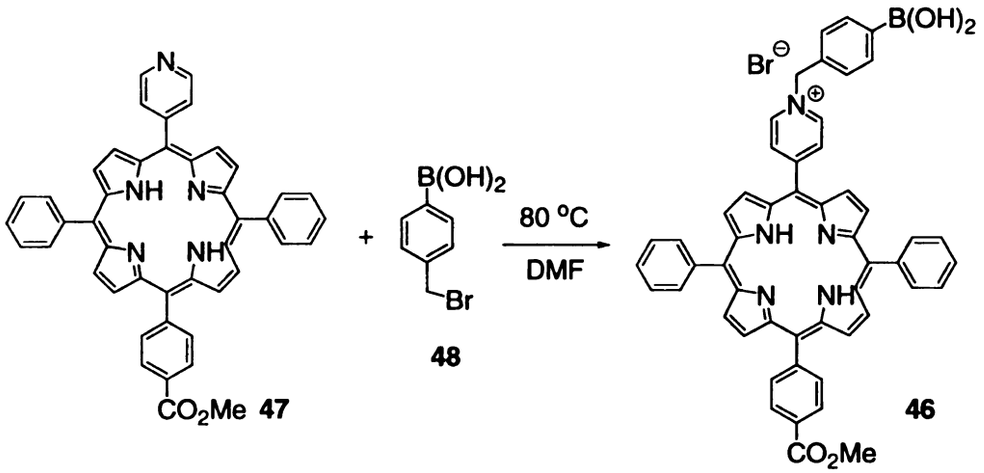

Scheme 6-50. The synthesis of water soluble porphyrin methyl ester **46**.

Since the model reaction proceeded very well, the same method was applied to the synthesis of pyridine porphyrin **46** (Scheme 6-50). After stirring at 80 °C for one day, some of the product **46** had formed, but there was still unreacted starting pyridine porphyrin **47** present. The reaction temperature was increased to 100 °C in order to convert all the starting material to the product. However, after heating this solution at 100 °C for one day, there was no formation of the desired product observed. Prolonging the reaction time at 100 °C resulted in the decomposition of the starting pyridine porphyrin **47**. We needed to optimize the reaction between the pyridine porphyrin **47** and the primary bromide **48**. After the synthesis of the pyridine porphyrin tweezer, the same condition would be applied to achieve the synthesis of the boronic porphyrin tweezer **45**.

However, we have not finished the synthesis of the boronic porphyrin tweezer **45**. After a year of working on the synthesis of the phenyl boronic acid porphyrin tweezer, I moved on to another project.

Experimental materials and general procedures:

Anhydrous CH_2Cl_2 was dried over CaH_2 and distilled. Unless otherwise noted, materials were obtained from commercial suppliers and were used without further purification. All reactions were performed in dried glassware under nitrogen. Column chromatography was performed using SiliCycle silica gel (230-400 mesh). ^{1}H-NMR spectra were obtained on Varian Inova 300 MHz instrument and are reported in parts per million (ppm) relative to the solvent resonances (δ), with coupling constants (*J*) in Hertz (Hz).

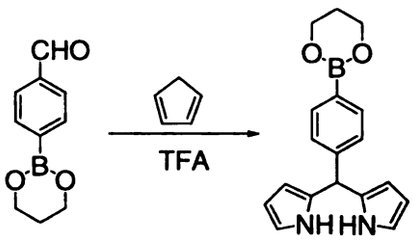

5

5-(4-Boronated)-phenyldipyrromethane 5:

A mixture of pyrrole (7 mL, 100 mmol) and 4-boronated-benzaldehyde (0.38 g, 2 mmol) was flushed with N_2 for 5 min and treated with TFA (15 μl, 2 mmol). This mixture was stirred vigorously for 5 min. 0.1 N NaOH and ethyl acetate were added, and the layers were separated. The aqueous layer was acidified and extracted with ethyl acetate twice. Organic layers were combined and dried with anhydrous Na_2SO_4. The solution was concentrated under reduced pressure. Column chromatography afforded a pale yellow solid **5** (35%). ^{1}H NMR (300 MHz, $CDCl_3$): δ 7.74 (d, *J*=8.1 Hz, 2H), 7.22 (d, *J*=8.1 Hz, 2H), 6.70 (m, 2H), 6.17 (m, 2H), 5.93 (m, 2H), 5.50 (s, 1H), 4.19 (q, *J*=5.4 Hz, 4H), 2.09 (t, *J*=5.4 Hz, 2H).

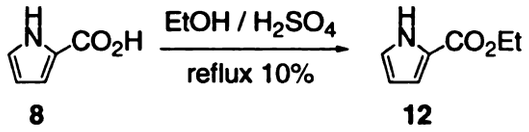

8 12

Ethyl ester of 2-pyrrol-carboxylic acid 12:

2-Pyrrol-carboxylic acid (100 mg) **8** was dissolved in 5 mL of ethanol, containing 1 mL concentrated H_2SO_4. This solution was refluxed for 24 h, and the reaction mixture was extracted with $CHCl_3$ and water. The organic layer was separated and dried over anhydrous Na_2SO_4. The solvent was removed under reduced pressure. The product was purified by column chromatography, and the product was isolated as a solid in 10% yield. ^1H NMR (300 MHz, $CDCl_3$): δ 9.20 (br, 1H), 6.96 (m, 2H), 6.28 (m, 1H), 4.34 (q, J=6.9 Hz, 2H), 1.38 (t, J=6.9 Hz, 3H).

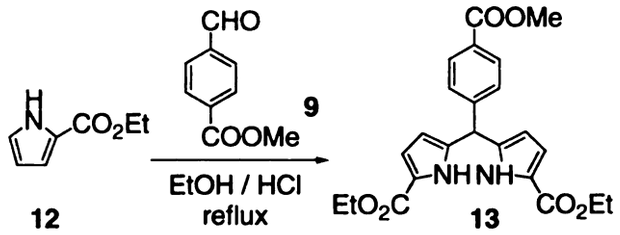

12 13

1,9-Bis(ethyloxycarbonyl)-5-(4-carboxy)-phenyldipyrromethane 13:

The ethyl ester **12** (70 mg, 0.5 mmol) and 4-carboxymethylbenzaldehyde **9** (33 mg, 0.25 mmol) was dissolved in absolute ethanol (4 mL), containing concentrated HCl (1 mL). The reaction mixture was refluxed under nitrogen for 4 h and cooled in an ice-bath. The precipitate was filtered and washed with cold methanol to afford the title compound **13** as a solid.

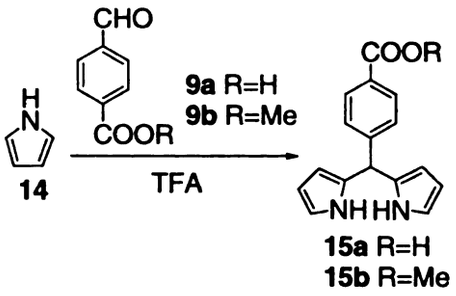

5-(4-Carboxy)-phenyldipyrromethane 15a:

A mixture of pyrrole **14** (14 mL, 200 mmol) and 4-carboxybenzaldehyde **9a** (0.6 g, 4 mmol) was flushed with N_2 for 5 min and treated with TFA (30 µl, 4 mmol). This mixture was stirred vigorously for 5 min. 0.1 N NaOH and ethyl acetate were added, and the layers were separated. The aqueous layer was acidified and extracted with ethyl acetate twice. Organic layers were combined and dried with anhydrous Na_2SO_4. The solution was concentrated under reduced pressure. Column chromatography afforded a pale brown solid **15a** (51%). ^{1}H NMR (300 MHz, $CDCl_3$): δ 9.76 (br, 1H), 7.94 (d, *J*=8.1 Hz, 2H), 7.32 (d, *J*=8.1 Hz, 2H), 6.69 (m, 2H), 5.98 (m, 2H), 5.74 (m, 2H), 5.54 (s, 1H).

5-(4-Methoxycarbonyl)-phenyldipyrromethane 15b:

A mixture of pyrrole (14 mL, 200 mmol) and 4-methoxycarbonylbenzaldehyde **12b** (1 g, 6 mmol) was flushed with N_2 for 5 min and treated with TFA (45 µl, 6 mmol). This mixture was stirred vigorously for 5 min. 0.1 N NaOH and ethyl acetate were added, and the layers were separated. The aqueous layer was acidified and extracted with ethyl acetate twice. Organic layers were combined and dried with anhydrous Na_2SO_4. The solution was concentrated under reduced pressure. Column chromatography afforded a pale brown solid **15b** (50%). ^{1}H NMR (300 MHz, $CDCl_3$): δ 7.99 (d, *J*=8.1 Hz, 2H), 7.29 (d, *J*=8.1 Hz, 2H), 6.73 (m, 2H), 6.18 (m, 2H), 5.91 (m, 2H), 5.54 (s, 1H), 3.92 (s, 3H).

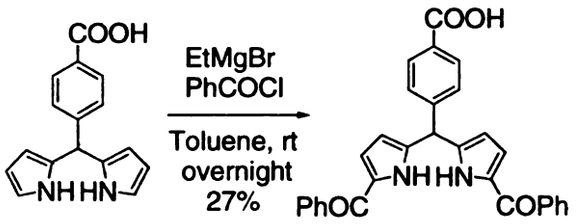

15a **16**

1,9-Bisbenzoyl-5- (4-carboxy)-phenyldipyrromethane 16:

A solution of EtMgBr in Et_2O (5 mL, 5 mmol) was slowly added to a stirred, ice-water bath cooled flask containing a solution of 5-(4-carboxy)-phenyldipyrromethane **15a** (133 mg, 0.5 mmol) in toluene (10 mL) under nitrogen atmosphere. This solution was stirred in room temperature for 30 min, and then a solution of benzoyl chloride (300 mg, 2.1 mmol) in toluene (2 mL) was added slowly. The reaction was stirred overnight. It was then quenched with saturated aq. NH_4Cl, and extracted with ethyl acetate (3 × 20 mL). The organic layers were combined and washed with brine, and dried with anhydrous Na_2SO_4. Solvent was remove under reduced pressure, and the residue was purified by column chromatography. The fraction contained the product was concentrated and dissolved with CH_2Cl_2. Precipitation with hexane to afforded a white solid **16** (27%). ^1H NMR (300 MHz, $CDCl_3$): δ 11.12 (br, 1H), 7.93 (m, 4H), 7.84 (m, 4H), 6.89 (m, 2H), 6.26 (m, 2H), 5.76 (s, 1H).

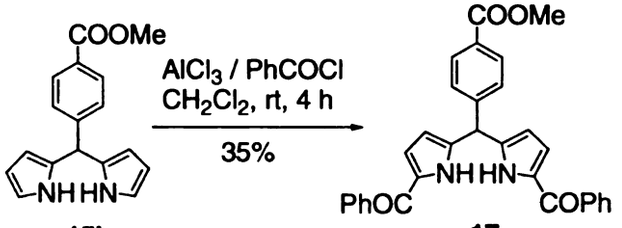

15b **17**

1,9-Bisbenzoyl-5- (4-methoxycarbonyl)-phenyldipyrromethane 17:

A solution of 5-(4-methoxycarbonyl)-phenyldipyrromethane **15b** (140 mg, 0.5 mmol) in CH_2Cl_2 (1.4 mL) was added to ice-cold solution of benzoyl chloride (210 mg,

1.5 mmol) and $AlCl_3$ (0.25 g, 1.8 mmol) in CH_2Cl_2 (14 mL) under nitrogen. The reaction was stirred in room temperature for 4 h, and quenched with saturated aq. $NaHCO_3$ (5 mL). The mixture was filtered through Celite to remove the insoluble salt, and the organic layer was separated and washed with NaOH and water. The organic layer was dried with anhydrous Na_2SO_4, and removed under the reduced pressure. The product was purified by column chromatography as a solid in 35% yield. ^1H NMR (300 MHz, $CDCl_3$): δ 11.95 (br, 2H), 8.04 (d, *J*=8.1 Hz, 2H), 7.72 (d, J=7.5 Hz, 4H), 7.63 (d, *J*=8.1 Hz, 2H), 7.46 (d, *J*=7.2 Hz, 2H), 7.37 (m, 4H), 6.51 (m, 2H), 5.93 (m, 2H), 5.77 (s, 1H), 3.91 (s, 3H).

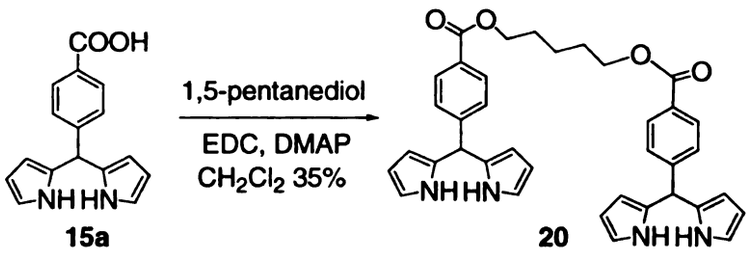

1,5-Bis (5'-*p*-carboxyphenyldipyrromethanyl) pentanoate 20:

5-(4-Carboxy)-phenyldipyrromethane **15a** (130 mg, 0.5 mmol), 1,5-pentanediol (20.8 mg, 0.2 mmol), EDC (100 mg, 0.5 mmol) and DMAP (72 mg, 0.6 mmol) was dissolved in CH_2Cl_2 (3mL), and the mixture was stirred in room temperature overnight. From TLC, there was no starting material left. The reaction mixture was directly applied to column chromatography, and the product was isolated as a solid in 35% yield. ^1H NMR (300 MHz, $CDCl_3$): δ 7.94 (d, *J*=8.1 Hz, 4H), 7.24 (d, *J*=8.1 Hz, 4H), 6.69 (m, 4H), 6.14 (m, 4H), 5.87 (s, 4H), 5.48 (s, 2H), 4.30 (t, *J*=6.6Hz, 4H), 1.82 (m, 4H), 1.55 (m, 2H).

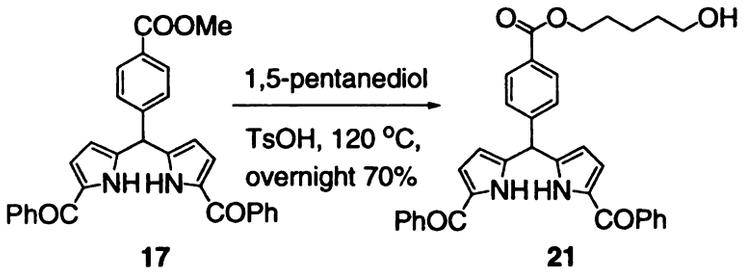

1- (1',9'-Bisbenzoyl-5'-*p*-carboxyphenyldipyrromethanyl) pentanoate 21:

1,9-Bisbenzoyl-5-(4-methoxycarbonyl)-phenyldipyrromethane **17** and catalytic amount of TsOH was dissolved in 1,5-pentanediol (4 mL). Heating this mixture at 120 °C overnight and the mixture turned black. The reaction mixture was extracted with water and chloroform (3 × 20 mL). The organic layers were combined and dried over anhydrous Na_2SO_4. The solvent was removed under reduced pressure, and the product was purified by column chromatography as a solid in 70% yield. ^{1}H NMR (300 MHz, $CDCl_3$): δ 11.59 (br, 2H), 8.07 (d, *J*=8.1 Hz, 2H), 7.76 (d, *J*=7.5 Hz, 4H), 7.64 (d, *J*=8.1 Hz, 2H), 7.51 (d, *J*=7.2 Hz, 2H), 7.44 (m, 4H), 6.59 (m, 2H), 5.99 (m, 2H), 5.77 (s, 1H), 4.36 (t, *J*=6.6 Hz, 2H), 3.68 (t, *J*=6.6 Hz, 2H), 1.82 (m, 4H), 1.55 (m, 2H).

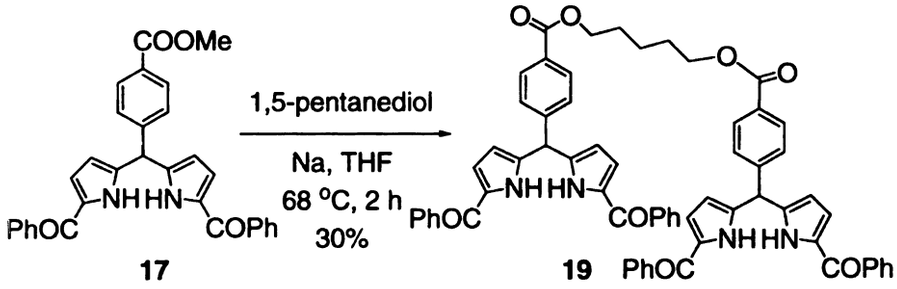

1,5-Bis (1', 9'-bisbenzoyl-5'-*p*-carboxyphenyldipyrromethanyl) pentanoate 19:

1,9-Bisbenzoyl-5-(4-methoxycarbonyl)-phenyldipyrromethane **17** (120 mg, 0.25 mmol), 1,5-pentanediol (14 mg, 0.13 mmol) and sodium (3 mg, 0.13 mmol) were dissolved in THF (1.5 mL). The reaction was heated at 68 °C for 2 h, and the solvent was removed under reduced pressure. HCl (6 N) was added to neutralize the sodium, and it

was extracted with dichloromethane (3 × 20 mL). The organic layers were combined, and dried over anhydrous Na_2SO_4. The solvent was removed under reduced pressure, and the product was isolated by column chromatography as solid in 30% yield. ^{1}H NMR (300 MHz, $CDCl_3$): δ 11.88 (br, 2H), 8.01 (d, *J*=8.1 Hz, 2H), 7.75 (d, *J*=7.5 Hz, 4H), 7.64 (d, *J*=8.1 Hz, 2H), 7.49 (d, *J*=7.2 Hz, 2H), 7.39 (m, 4H), 6.54 (m, 2H), 5.95 (m, 2H), 5.80 (s, 1H), 4.36 (t, *J*=6.6 Hz, 2H), 1.82 (m, 4H), 1.55 (m, 2H).

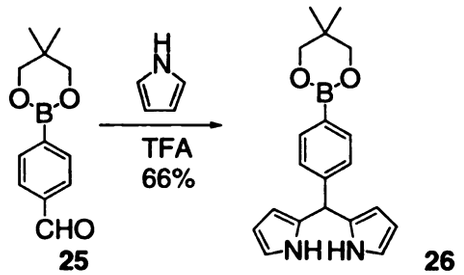

25 **26**

5-(4-Boronated)-phenyldipyrromethane 26:

A mixture of pyrrole (11.5 mL, 165 mmol) and 4-boronated-benzaldehyde **25** (0.72 g, 3.3 mmol) was flushed with N_2 for 5 min and treated with TFA (25 µl, 3.3 mmol). This mixture was stirred vigorously for 5 min. 0.1 N NaOH and ethyl acetate were added, and the layers were separated. The aqueous layer was acidified and extracted with ethyl acetate (2 × 20 mL). Organic layers were combined and dried with anhydrous Na_2SO_4. The solution was concentrated under reduced pressure. Column chromatography afforded a pale yellow solid **26** (66%). ^{1}H NMR (300 MHz, $CDCl_3$): δ 7.84 (d, *J*=8.1 Hz, 2H), 7.23 (d, *J*=8.1 Hz, 2H), 6.65 (m, 2H), 6.20 (m, 2H), 5.93 (m, 2H), 5.42 (s, 1H), 3.92 (s, 4H), 1.10 (s, 6H).

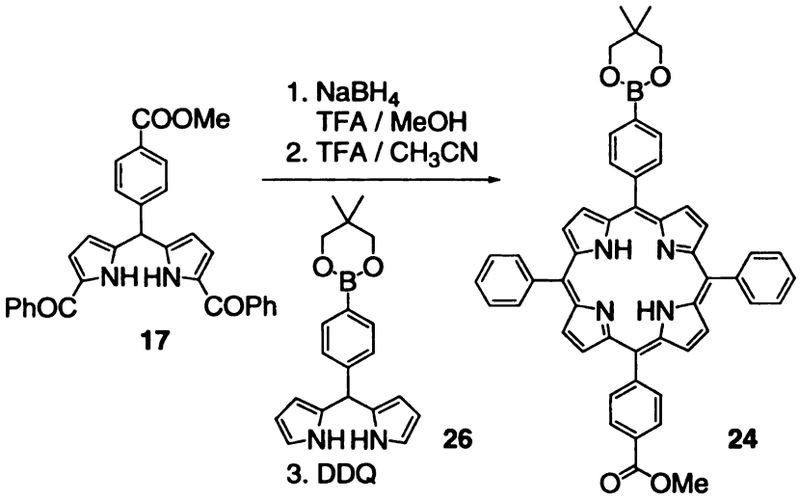

Boronic porphyrin methyl ester 24:

$NaBH_4$ (100 mg, 2.6 mmol) was added to the solution of dipyrromethane **17** (24.4 mg, 0.05 mmol) in MeOH/THF (1:3, 4 mL) at small portions. This mixture was stirred at room temperature for an hour, and quenched with saturated aq. ammonium chloride. The mixture was extracted with dichloromethane (3 × 20 mL), and the organic layers were washed with water (1 × 20 mL). The organic layer was dried over anhydrous Na_2SO_4, and was removed under reduced pressure. The residue was dissolved with dry acetonitrile (20 mL), and 5-(4-boronated)-phenyldipyrromethane **26** (16 mg, 0.05 mmol) was added into this solution. Purged N_2 into the mixture for 10 min, and TFA (0.05 mL, 0.65 mmol) was added into the reaction mixture. The deep red solution was stirred at room temperature for 1 h, and DDQ (0.35 g, 0.15 mmol) was added. The reaction mixture was stirred at room temperature for another hour, and all the solvent was removed under reducing pressure. The product was purified by column chromatography as purple solid in 20% yield. ^{1}H NMR (300 MHz, $CDCl_3$): δ 8.98 (m, 8H), 8.46 (d, *J*=8.1 Hz, 2H), 8.32 (d, *J*=8.1 Hz, 2H), 8.24 (m, 6H), 7.80 (m, 9H), 4.13 (s, 3H), 3.92 (s, 4H), 1.11 (s, 6H); -2.79 (s, 2H); MS: *m/z* 784.

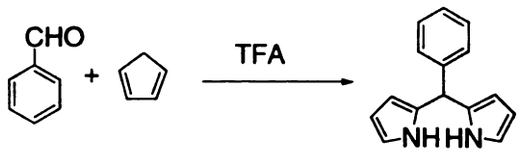

30

5-Phenyldipyrromethane 30:

A mixture of pyrrole (21 mL, 300 mmol) and benzaldehyde (5.3 g, 50 mmol) was flushed with N_2 for 5 min and treated with TFA (0.45 mL, 50 mmol). This mixture was stirred vigorously for 5 min. 0.1 N NaOH and ethyl acetate were added, and the layers were separated. The aqueous layer was acidified and extracted with ethyl acetate (2 × 100 mL). Organic layers were combined and dried with anhydrous Na_2SO_4. The solution was concentrated under reduced pressure. Column chromatography afforded a pale yellow solid **26** (49%). ^{1}H NMR (300 MHz, $CDCl_3$): δ 7.90 (br, 2H), 7.26 (m, 5H), 6.69 (br, 2H), 6.15 (d, *J*=2.8 Hz, 2H), 5.92 (br, 2H), 5.47 (s, 1H).

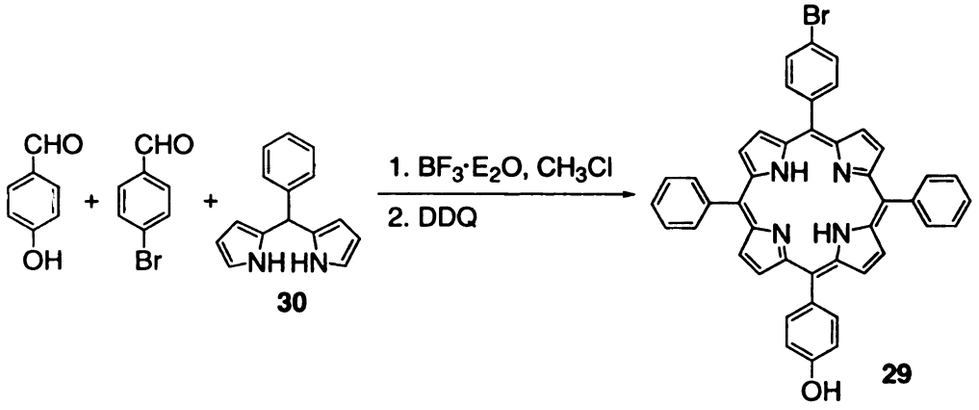

30 **29**

Monohydroxyl-monobromo porphyrin 29:

4-Hydroxybenzaldehyde (30.5 mg, 0.25 mmol), 4-bromobenzaldehyde (46 mg, 0.25 mmol) and 5-phenyldipyrromethane **30** (111 mg, 0.5 mmol) were dissolved in $CHCl_3$ (50 mL). The solution was purged with N_2 for 10 minutes, and BF_3·Et_2O (20 μl) was added. The reaction was stirred for an hour, and DDQ (0.20 g, 0.09 mmol) was

added. The reaction mixture was stirred for another hour, and subjected directly to column chromatography. The product was isolated as purple solid in 10% yield. ^{1}H NMR (300 MHz, $CDCl_3$): δ 8.89 (m, 8H), 8.22 (m, 4H), 8.04 (m, 4H), 7.90 (d, 2H), 7.75 (m, 6H), 7.13 (d, 2H), -2.81 (s, 2H).

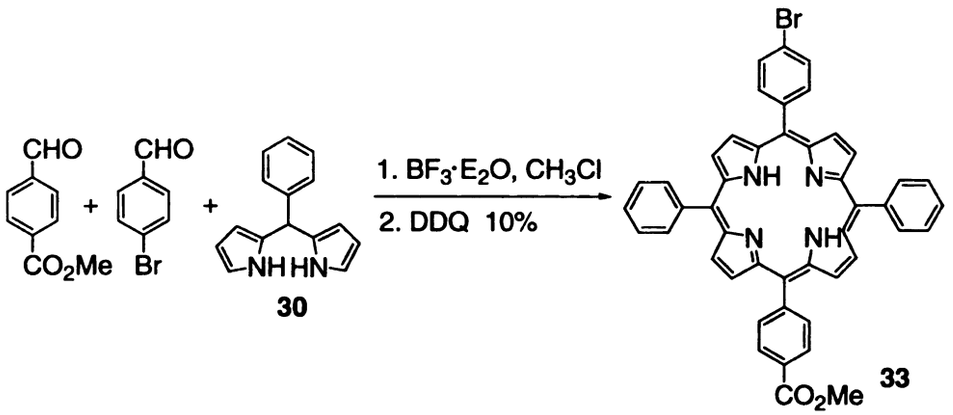

Porphyrin methyl ester 33:

4-Methoxycarbonyl-benzaldehyde (41 mg, 0.25 mmol), 4-bromobenzaldehyde (46 mg, 0.25 mmol) and 5-phenyldipyrromethane **30** (111 mg, 0.5 mmol) were dissolved in $CHCl_3$ (50 mL). The solution was purged with N_2 for 10 minutes, and $BF_3{\cdot}Et_2O$ (20 μl) was added. The reaction was stirred for an hour, and DDQ (0.20 g, 0.09 mmol) was added. The reaction mixture was stirred for another hour, and was subjected directly to column chromatography. The product was isolated as purple solid in 10% yield. The ratio between di-bromo, **33**, and di-ester is 2:4:1. ^{1}H NMR (300 MHz, $CDCl_3$): δ 8.91(m, 8H), 8.49 (d, *J*=8.1 Hz, 2H), 8.35 (d, *J*=8.1 Hz, 2H), 8.25 (m, 4H), 8.11 (d, *J*=8.1 Hz, 2H), 7.91 (d, *J*=8.1 Hz, 2H), 7.80 (m, 6H), 4.35 (s, 3H), -2.81 (s, 2H).

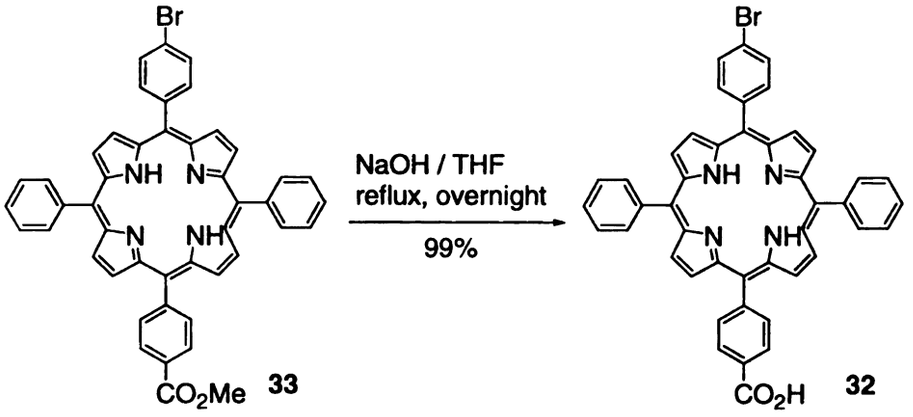

Porphyrin acid 32:

Porphyrin methyl ester **33** (35 mg) was added into NaOH (2 N, 1.5 mL) and THF (5 mL), and the reaction mixture was refluxed for 12 h. The solution was acidified with 2 N HCl to pH of 4. The reaction mixture was extracted with CH_2Cl_2 until the aqueous layer became colorless. The organic layers were combined and washed with water (2 × 20 mL). The organic layer was dried over anhydrous Na_2SO_4, and the removal of the solvent under reduced pressure provided the title compound as purple solid in 99% yield. ^{1}H NMR (300 MHz, $CDCl_3$): δ 8.91 (m, 8H), 8.56 (d, *J*=8.1 Hz, 2H), 8.39 (d, *J*=8.1 Hz, 2H), 8.23 (m, 4H), 8.10 (d, *J*=8.1 Hz, 2H), 7.92 (d, *J*=8.1 Hz, 2H), 7.81 (m, 6H).

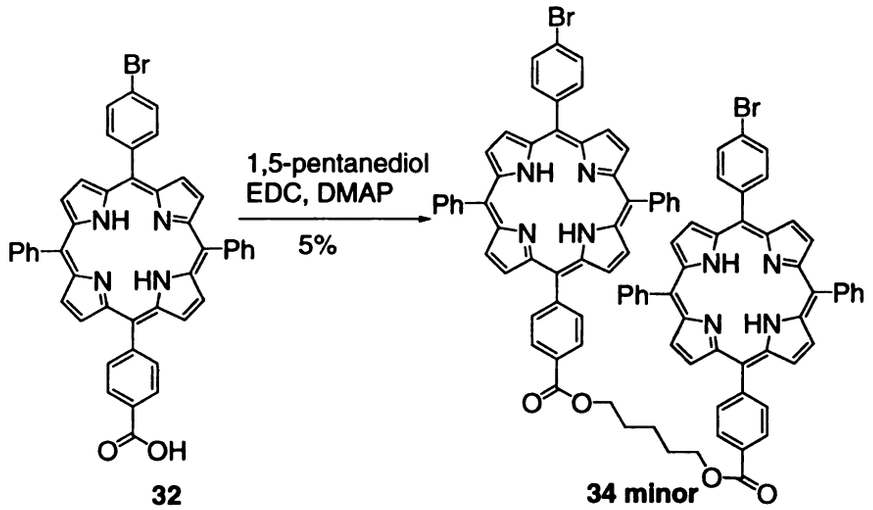

32 34 minor

Dibromo porphyrin tweezer 34:

Porphyrin acid **32** (30 mg, 0.04 mmol), 1,5-pentanediol (2.12 mg, 0.02 mmol), EDC (10 mg, 0.05 mmol) and DMAP (7.2 mg, 0.06 mmol) were dissolved in CH_2Cl_2 (5 mL). The mixture was stirred in room temperature overnight, and applied directly to column chromatography. The product was isolated as a purple solid in 5% yield. ^1H NMR (300 MHz, $CDCl_3$): δ 8.85 (m, 16H); 8.52 (d, J=8.1 Hz, 4H), 8.35 (d, *J*=8.1 Hz, 4H), 8.14 (m, 12H), 7.78 (m, 16H), 4.68 (t, *J*=6.6 Hz 4H) 1.65 (m, 4H), 1.48 (m, 2H), -2.81 (s, 2H).

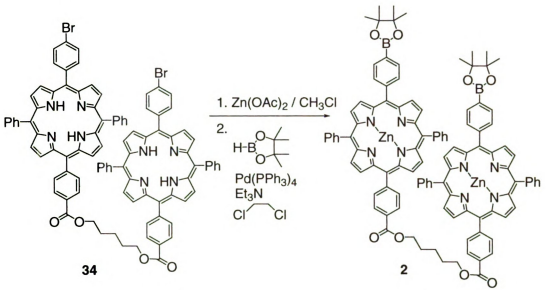

Boronate porphyrin tweezer 34:

Porphyrin tweezer free base **34** (6 mg) was dissolved in 1.5 mL of chloroform, and zinc acetate (10 mg) was added. This mixture was stirred in room temperature for 2 h, and applied to column chromatography to isolate the pure zinc porphyrin tweezer. A 50 mL Schlenk flask was charged with zinc porphyrin tweezer (6 mg), pinacolborane (20 µl, 0.14 mmol), triethylamine (30 µl, 0.22 mmol), tetraphenylphosphinepalladium (1 mg), and 2 mL of 1,2-dichloroethane in dry box. This mixture was stirred at 90 °C for 4 h, and it was then quenched with saturated aq. KCl (1 mL). The mixture was separated and the organic layer was washed with water and dried over anhydrous Mg_2SO_4. The solvent was removed under reduced pressure, and the product was isolated as a purple solid in 5% yield. MS: *m/z* 1764.

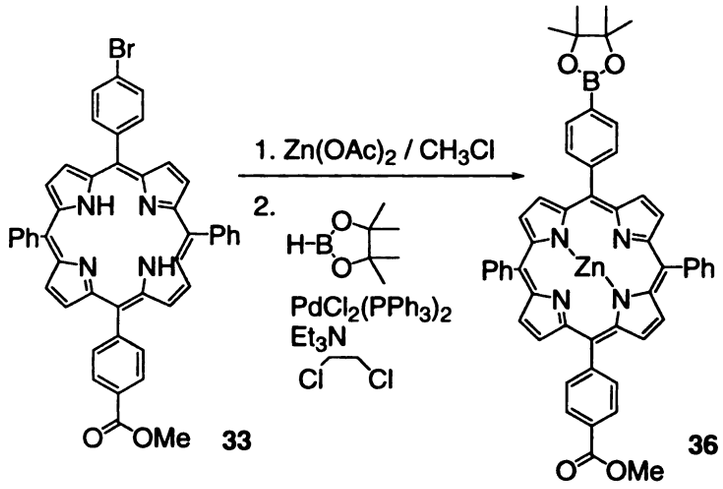

Coupling of bromoporphyrin 33 with pinacolborane:

Bromoporphyrin methyl ester free base **33** (15 mg) was dissolved in 1.5 mL of chloroform, and zinc acetate (20 mg) was added. This mixture was stirred at room temperature for 2 h, and applied to column chromatography to isolate the pure zinc porphyrin tweezer. A 50mL Schlenk flask was charged with zinc porphyrin (15 mg), pinacolborane (20 μl, 0.14 mmol), triethylamine (30 μl, 0.22 mmol), $PdCl_2(PPh_3)_2$ (1 mg), and 3 mL of 1,2-dichloroethane in dry box. This mixture was stirred at 90 °C overnight before it was quenched with saturated aq. KCl (1 mL). The mixture was separated and the organic layer was washed with water and dried over anhydrous Mg_2SO_4. The solvent was removed under reduced pressure, and the product was isolated as a purple solid in 6% yield. ^{1}H NMR (300 MHz, $CDCl_3$): δ 8.87 (m, 8H), 8.46 (d, *J*=8.2 Hz, 2H), 8.33 (d, *J*=8.2 Hz, 2H), 8.25 (m, 8H), 7.79 (m, 8H), 4.13 (s, 3H), 1.28 (s, 9H); MS: *m/z* 862.

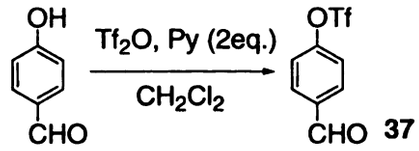

37

4-Formylphenyl trifloromethanesulfonate 37:

Suspended 4-hydroxylbenzaldehyde (1.22 g, 10 mmol) and pyridine (0.9 mL) in CH_2Cl_2 (20 mL), the mixture was slowly added to ice-bath colded Tf_2O (2 mL, 12 mmole) in CH_2Cl_2 (15 mL). This mixture was stirred at 0 °C for 10 minutes, and then warmed up to room temperature, and stirred for 30 h. The solvent was removed, and the residue was purified by column chromatography to yield the title compound **37** (79%). The spectrum matches the reported literature.[34] ^1H NMR (300 MHz, $CDCl_3$): δ 10.1 (s, 1H), 8.01 (d, *J*=8.7 Hz, 2H), 7.47 (d, *J*=8.7 Hz, 2H).

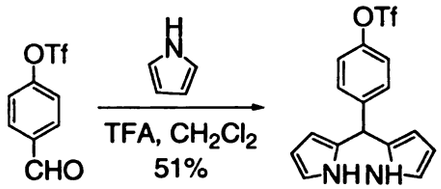

37 **38**

5-(4-Triflate)-phenyldipyrromethane 38:

A mixture of pyrrole (2.5 mL, 31 mmol) and aldehyde **37** (0.12 g, 0.55 mmol) was flushed with N_2 for 5 min and treated with TFA (5 μl, 0.66 mmol). This mixture was stirred vigorously for 5 min. 0.1 N NaOH and ethyl acetate were added, and the layers were separated. The aqueous layer was acidified and extracted with ethyl acetate (2 × 30 mL). Organic layers were combined and dried with anhydrous Na_2SO_4. The solution was concentrated under reduced pressure. Column chromatography afforded a pale yellow solid **38** (51%). ^1H NMR (300 MHz, $CDCl_3$) δ 7.99 (br, 2H), 7.27 (m, 4H), 6.72 (m, 2H), 6.21 (m, 2H), 5.90 (m, 2H), 5.50 (s, 1H).

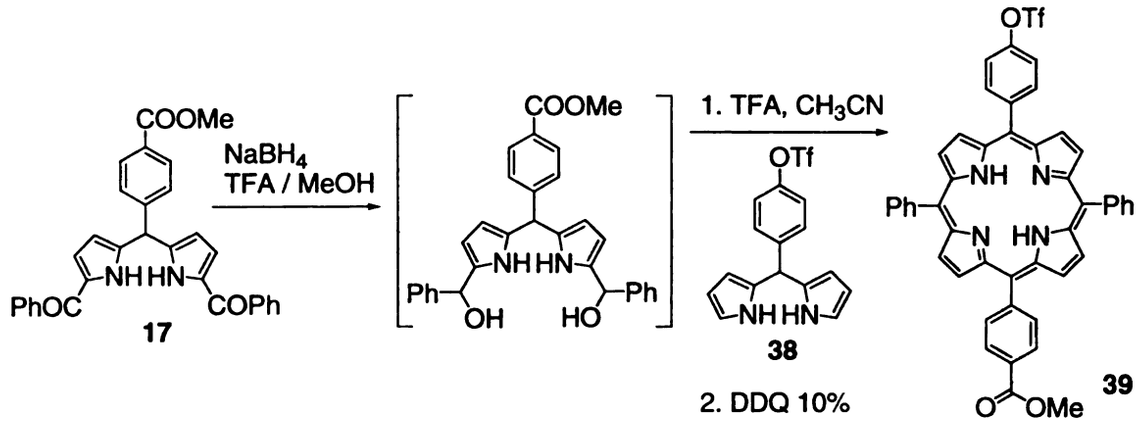

Triflate porphryin methyl ester 39:

$NaBH_4$ (200 mg, 5 mmol) was added to the solution of phenyldipyrromethane **17** (48.8 mg, 0.1 mmol) in MeOH/THF (1:3, 4 mL) at small portions. This mixture was stirred at room temperature for an hour, and quenched with saturated aq. ammonium chloride. The mixture was extracted with dichloromethane (3 × 20 mL), and the organic layer was washed with water (1 × 20 mL). The organic layer was dried over anhydrous Na_2SO_4, and was removed under reduced pressure. The residue was dissolved with dry acetonitrile (20 mL), and 5-(4-triflate)-phenyldipyrromethane **38** (37 mg, 0.1 mmole) was added into this solution. Purged N_2 into the mixture for 10 min, and TFA (0.05 mL, 0.65 mmol) was added into the reaction mixture. The deep red solution was stirred at room temperature for 1 h, and DDQ (0.35 g, 0.15 mmol) was added. The reaction mixture was stirred at room temperature for another hour, and all the solvent was removed under reducing pressure. The product was purified by column chromatography as purple solid in 10% yield. MS: *m/z* 820.

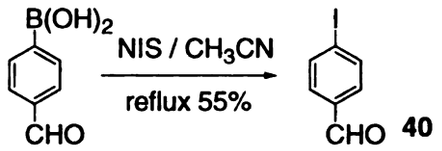

Synthesis of 4-iodobenzaldehyde 40:

4-Formylphenylboronic acid (300 mg, 2 mmol) and NIS (612 mg, 2.4 mmol) was dissolved in 10 mL of dry MeCN, and this mixture was refluxed for 16 h. The solvent was then removed reduced pressure, and the product was separated by column chromatography as a solid in 55% yield. The NMR spectrum matches the reported literature.[35] ^{1}H NMR (300 MHz, $CDCl_3$): δ 10.1 (s, 1H), 8.06 (d, *J*=8.7 Hz, 2H), 7.52 (d, *J*=8.7 Hz, 2H).

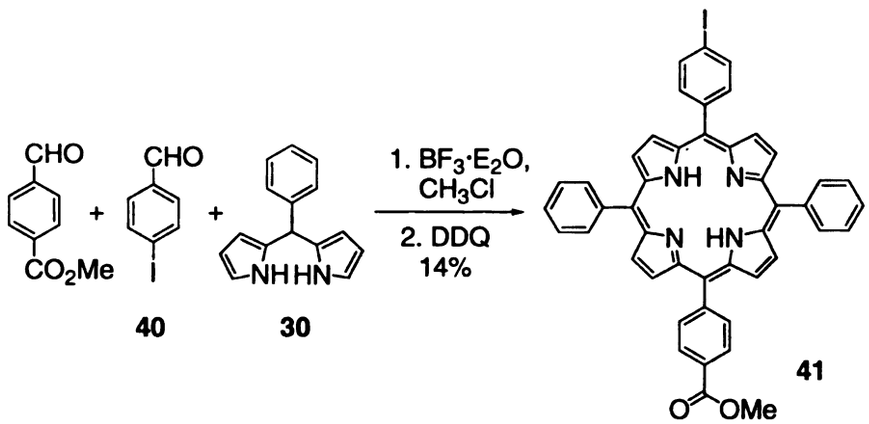

Synthesis of iodoporphyrin methyl ester 41:

4-Methoxycarbonylbenzaldehyde (73 mg, 0.5 mmol), 4-iodobenzaldehyde **40** (115 mg, 0.5 mmol) and 5-phenyldipyrromethane **30** (222 mg, 1 mmol) were dissolved in CH_2Cl_2 (100 mL). The solution was purged with N_2 for 10 minutes, and $BF_3{\cdot}Et_2O$ (40 μl) was added. The reaction was stirred for an hour, and DDQ (0.20 g, 0.09 mmol) was added. The reaction mixture was stirred for another hour, and subjected directly to column chromatography. The product was isolated as purple solid in 14% yield. ^{1}H

NMR (300 MHz, $CDCl_3$): δ 8.91 (m, 8H), 8.48 (d, *J*=8.2 Hz, 2H), 8.35(m, 2H), 8.25 (m, 4H), 8.11 (d, *J*=8.2 Hz, 2H), 7.95 (m, 2H), 7.81 (m, 6H), 4.15 (s, 3H), -2.81 (s, 2H).

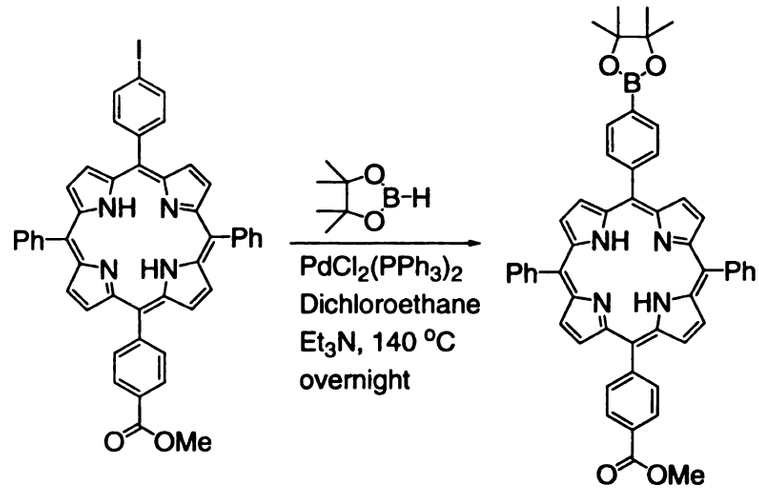

41 **36**

Coupling of iodoporphyrin with pinacolborane by $PdCl_2(PPh_3)_2$:

A 50 mL Schlenk flask was charged with iodoporphyrin methyl ester free base **41** (20 mg), pinacolborane (50 μl, 0.35 mmol), triethylamine (100 μl, 0.7 mmol), $PdCl_2(PPh_3)_2$ dichlorodi(triphenyl)phosphinepalladium (1 mg), and 2 mL of 1,2-dichloroethane in dry box. This mixture was stirred at 140 °C overnight before it was quenched with aq. KCl (1 mL). The mixture was separated and the organic layer was washed with water and dried over anhydrous Mg_2SO_4. The solvent was removed under reduced pressure, and the product was isolated as a purple solid in 30% yield. ^1H NMR (300 MHz, $CDCl_3$): δ 8.87 (m, 8H), 8.46 (d, *J*=8.2 Hz, 2H), 8.33 (d, *J*=8.2 Hz, 2H), 8.25 (m, 8H), 7.79 (m, 8H), 4.13 (s, 3H), 1.28 (s, 9H); MS: *m/z* 862.

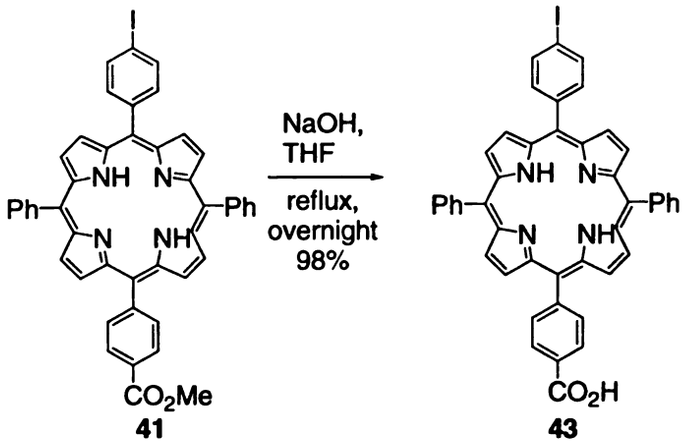

Synthesis of iodoporphyrin acid 43:

Iodoporphyrin methyl ester **41** (65 mg) was added into NaOH (2 N, 1.5 mL) and THF (5 mL), and refluxed for 12 h. The solution was acidified with 2 N HCl to pH of 4. The reaction mixture was extracted with CH_2Cl_2 until the aqueous layer became colorless. The organic layers were combined and washed with water (2 × 20 mL). The organic layer was dried over anhydrous Na_2SO_4, and the removal of the solvent under reduced pressure provided the title compound as purple solid in 98% yield. ^{1}H NMR (300 MHz, $CDCl_3$): δ 8.88 (m, 8H), 8.58 (d, *J*=8.2 Hz, 2H), 8.38 (d, *J*=7.7 Hz, 2H), 8.24 (m, 4H), 8.13 (d, J=7.7 Hz, 2H), 7.97 (d, *J*=8.2 Hz, 2H), 7.80 (m, 6H), -2.74 (s, 2H).

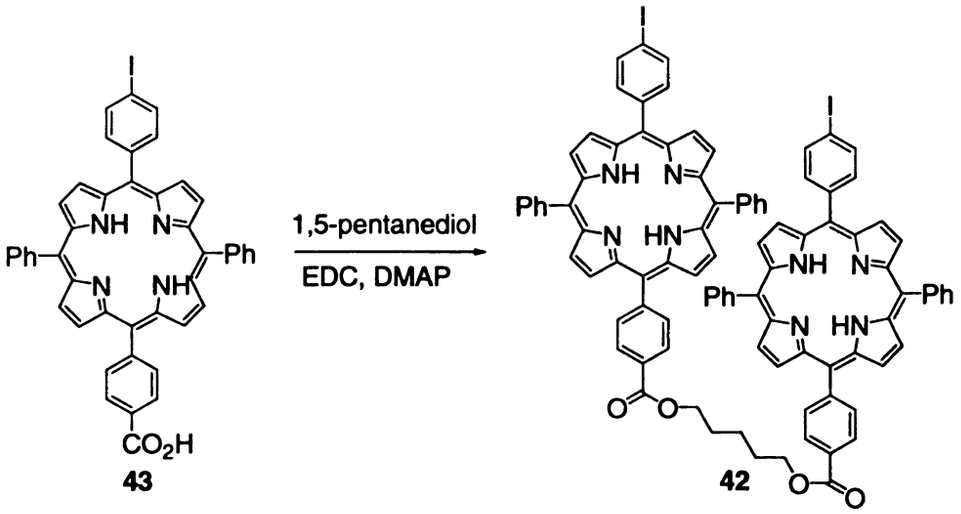

Synthesis of diiodoporphyrin tweezer 42:

Porphyrin acid **43** (57 mg, 0.07 mmol), 1,5-pentanediol (3.78 mg, 0.036mmole), EDC (19.1 mg, 0.1 mmole) and DMAP (13.5 mg, 0.11 mmole) were dissolved in CH_2Cl_2, and the mixture was stirred in room temperature overnight. From TLC, there was no starting material left. The product was purified by column chromatography as a purple solid (54%). ^{1}H NMR (300 MHz, CDCl3): δ 8.88 (m, 16H), 8.58 (d, *J*=8.2 Hz, 2H), 8.38 (d, *J*=7.7 Hz, 4H), 8.24-8.13 (m, 16H), 7.97-7.80 (m, 18H), 4.28 (t, *J*=6.6 Hz, 4H), 1.65 (m, 4H), 1.48 (m, 2H), -2.81 (s, 2H).

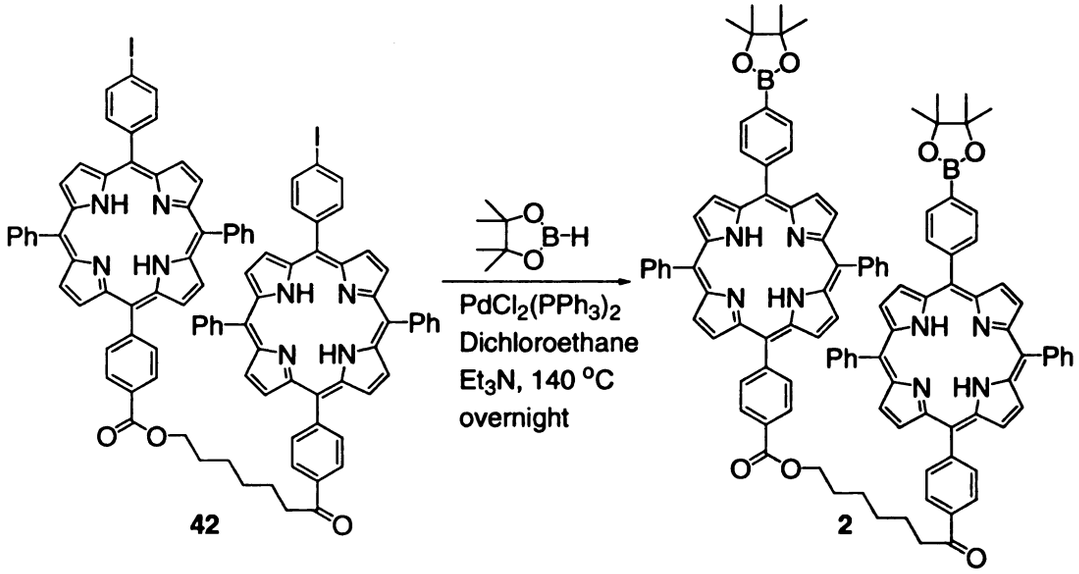

Synthesis of Boron porphyrin tweezer:

A 50 mL Schlenk flask was charged with diiodoporphyrin tweezer free base **40** (20 mg), pinacolborane (50 μl, 0.35 mmol), triethylamine (100 μl, 0.7 mmol), $PdCl_2(PPh3)_2$ (1 mg), and 2 mL of 1,2-dichloroethane in dry box. This mixture was stirred at 140 °C overnight before it was quenched with aq. KCl (1 mL). The mixture was separated and the organic layer was washed with water and dried over anhydrous Mg_2SO_4. The solvent was removed under reduced pressure, and the product was isolated as a purple solid in 23% yield. ^{1}H NMR (300 MHz, $CDCl_3$): δ 8.87 (m, 16H), 8.46 (d, *J*=8.2 Hz, 4H), 8.33-8.25 (m, 16H), 7.79-8.24 (m, 18H), 4.28 (t, *J*=6.6 Hz, 4H), 1.65 (m, 4H), 1.48 (m, 2H), -2.81 (s, 2H); MS: *m/z* 1636.7.

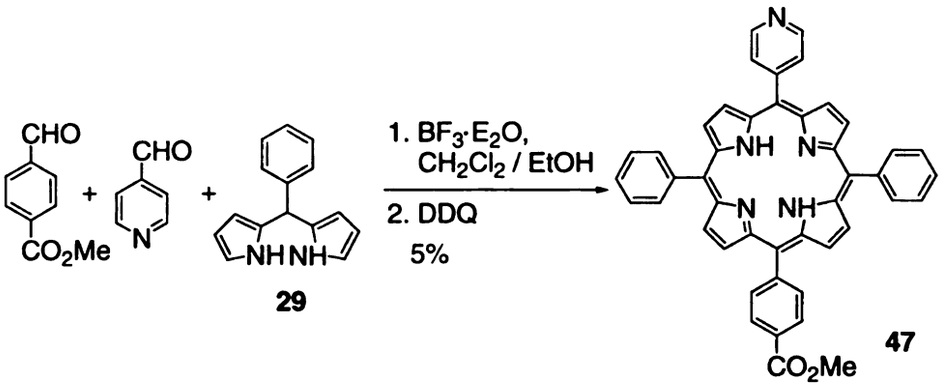

Synthesis of pyridine porphyrin 47:

To a degassed solution of dipyrrolmethane **29** (444 mg, 2 mmol) in CH_2Cl_2/EtOH (100 mL, 95:5) was successively added methyl 4-formylbenzoate (146 mg, 1 mmol), $BF_3{\cdot}Et_2O$ (231 μl) and 4-pyridinecarboxaldehyde (107 mg, 1 mmol). This solution was protected from light and stirred under N_2 for 36 hours. Then DDQ (340 mg, 1.5 mmol) was added and the stirring was continued for another 2 hours. The solvent was removed under reduced pressure, and the product was separated by column chromatography as a purple solid in 5% yield. Mass Spectrum: *m/z* 873.

Reference:

1. Lorand, J. P.; Edward, J. O. *J. Org. Chem.* **1959**, *24*, 769.

2. Sugashi, A.; Ikeda, M.; Takeuchi, M.; Shinkai, S. *Angew. Chem. Int. Ed.* **2000**, *39*, 3839.

3. Yang, W.; He, H.; Drueckhammer, D. G. *Angew. Chem. Int. Ed.* **2001**, *40*, 1714.

4. Cooper, C. R.; James, T. D. *Chem. Lett.* **1998**, 883.

5. McNichols, R. J.; Cote, G. L. *J. Biomed. Opt.* **2000**, *5*, 15.

6. Gardiner, S. J.; Smith, B. D.; Duggan, P. J.; Karpa, M. J.; Griffin, G. J. *Tetrahedron* **1999**, *55*, 2857.

7. Arimori, S.; Takeuchi, M.; Shinkai, S. *J. Am. Chem. Soc.* **1996**, *118*, 245.

8. Bartlett, P. A.; SHea, G. T.; Telfer, S. J.; Waterman, S. *Molecular Recognition: Chemical and Biological Problems*; Royal Society of Chemistry: London, **1989**.

9. Bartlett, P. A.; Lauri, G. *J. Comput. Aided Mol. Des.* **1994**, *8*, 51.

10. Arsenault, G. P.; Bullock, E.; MacDonald, S. F. *J. Chem. Soc.* **1960**, *82*, 4384.

11. Boyle, R. W.; Clarke, O. J. *Tetrahedron Lett.* **1998**, *39*, 7167.

12. Hughes, M. P.; Shang, M.; Smith, B. D. *J. Org. Chem.* **1996**, *61*, 4510.

13. Valasinas, A.; Hurst, J.; Frydman, B. *J. Org. Chem.* **1998**, *63*, 1239.

14. Chang, C. J.; Deng, Y. Q.; Heyduk, A. F.; Chang, C. K.; Nocera, D. G. *Inorg. Chem.* **2000**, *39*, 959.

15. Soufiaoui, C. *Tetrahedron* **1989**, *45*, 3351.

16. Rao, P. D.; Dhanalekshmi, S.; Linsey, J. S. *J. Org. Chem.* **2000**, *65*, 7323.

17. Sessler, J. L.; Hugdahl, J.; Johnson, M. R. *J. Org. Chem.* **1986**, *51*, 2838.

18. Khoury, R. G.; Jaquinod, L.; Smith, K. M. *Chem. Commun.* **1997**, 1057.

19. Cho, W.; Kim, H.; Littler, B. J.; Miller, M. A.; Lee, C. -H.; Lindsey, J. S. *J. Org. Chem.* **1999**, *64*, 7890.

20. Chen, Q.; Lightner, D. A. *J. Org. Chem.* **1998**, *63*, 2265.

21. Djurendic, A.; Suranyi, T. M.; Milikovic, D. A. *Chzech. Chem. Commun.* **1990**, *55*, 1763.

22. Martinez, A. G.; Barcina, J. O.; Veccio, H. D.; Hanack, M.; Subramanian, L. R. *Tetrahedron Lett.* **1991**, *32*, 5931.

23. Zieglar, T.; Lemanski, G.; Hurttlen, J. *Tetrahedron Lett.* **2001**, *42*, 569.

24. Miyaura, N.; Ishiyama, T.; Sasaki, H.; Ishikawa, M.; Satoh, M.; Suzuki, A. *J. Am. Chem. Soc.* **1989**, *111*, 314.

25. Ohe, T.; Ohe, K.; Uemura, S.; Sugita, N. *J. Organomet. Chem.* **1988**, *344*, C5.

26. Littler, B. J.; Miller, M. A.; Hung, C. -H.; Lindsey, J. S. *J. Org. Chem.* **1999**, *64*, 1391.

27. Boyle, R. W.; Bruckner, C.; Posakony, J.; James, B. R.; Dolphin, D. *Org. Synt.* **1999**, *76*, 287.

28. Hyslop, A. G.; Kellett, M. A.; Iovine, P. M.; Therien, M. J. *J. Am. Chem. Soc.* **1998**, *120*, 12676.

29. Ishiyama, T.; Ishida, K.; Miyaura, N. *Tetrahedron* **2001**, *57*, 9813.

30. Ishiyama, T.; Murata, M.; Miyaura, N. *J. Org. Chem.* **1995**, *60*, 7508.

31. Murata, M.; Oyama, T.; Watanabe, S.; Masuda, Y. *J. Org. Chem.* **2000**, *65*, 164.

32. Ishiyama, T.; Itoh, Y.; Kinato, T.; Miyaura, N. *Tetrahedron Lett.* **1997**, *38*, 3447.

33. Nakamura, H.; Fujiwara, M.; Yamamoto, U. *Bull. Chem. Soc. Jpn.* **2000**, *73*, 231.

34. Echavarren, A. M.; Stille, J. K. *J. Am. Chem. Soc.* **1987**, *109*, 5478.

35. Thiebes, C.; Prakash, G. K. S.; Petasis, N.; Olah, G. A. *Syn. Lett.* **1998**, 141.

36. Takeuchi, M.; Chin, Y.; Imada, T.; Shinkai, S. *Chem. Commun.* **1996**, 1867.

37. Coutts, S. J.; Adams, J.; Drolikowski, D.; Snow, R. J. *Tetrahedron Lett.* **1994**, *35*, 5109.

38. Pettit, G. R.; Kasturi, T. R. *J. Org. Chem.* **1960**, *25*, 875.

39. Boisnard, A.; Carbonnelle, A. -C.; Zhu, J. *Org. Lett.* **2001**, *3*, 2061.

40. Sugasaki, A.; Ikeda, M.; Takeuchi, M.; Koumoto, K.; Shinkai, S. *Tetrahedron* **2000**, *56*, 4717.

41. Rucareanu, S.; Mongin, O.; Schuwey, A.; Hoyler, N.; Gossauer, A. *J. Org. Chem.* **2001**, *66*, 4973.

42. Thomas, A. P.; Robert, D. A.; Thomason, D. A. *Bioorg. Med. Chem. Lett.* **1994**, *4*, 2615.

43. Arimori, S.; Murakami, H.; Takeuchi, M.; Shinkai, S. *J. Chem. Soc., Chem. Commun.* **1995**, 961.

APPENDIX

Change in proton chemical of compound **21** upon addition to ZnTPP

a) Compound **21**
b) Compound **21** with ZnTPP

21

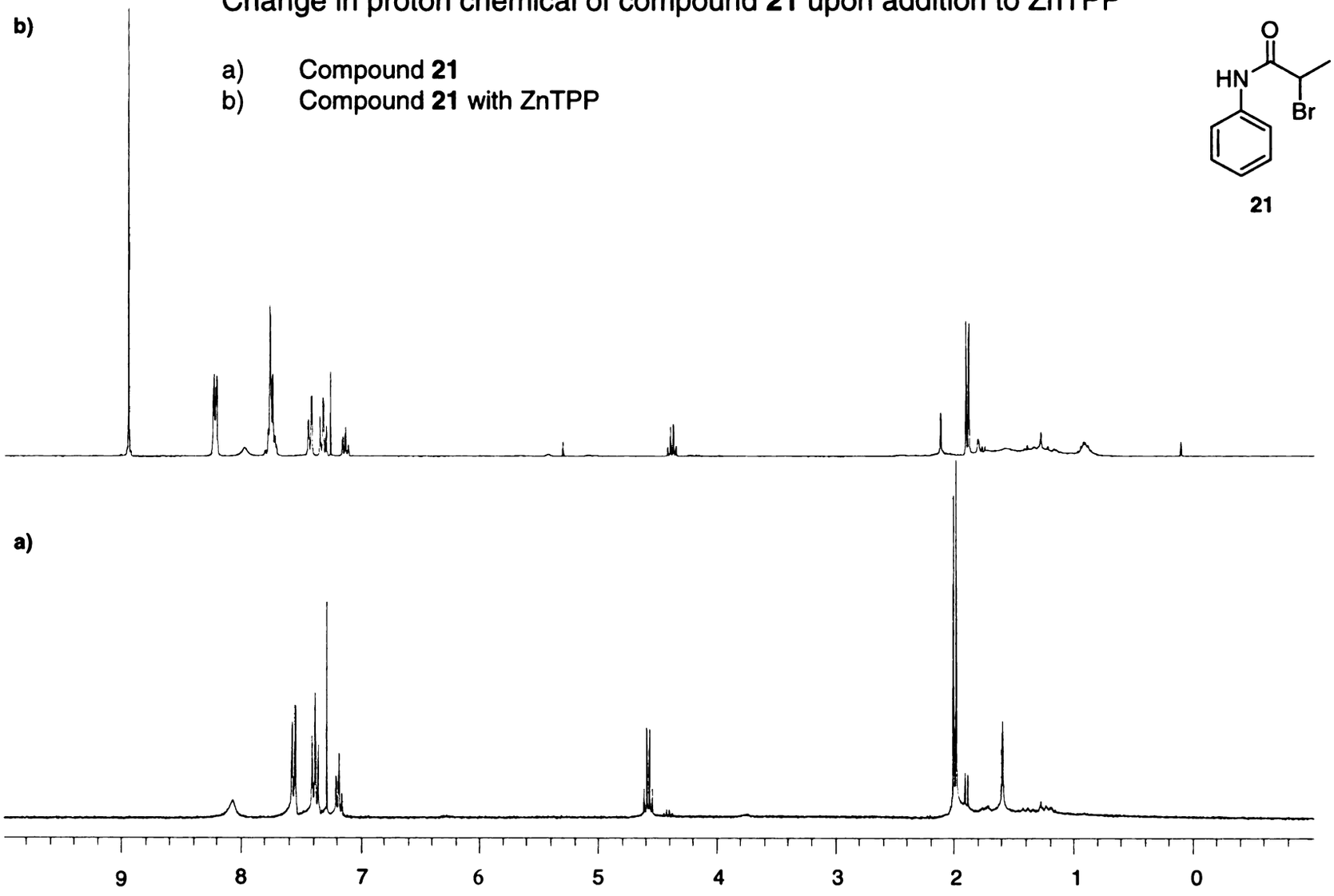

Change in proton chemical of compound **26** upon addition to ZnTPP

a) Compound **26**

b) Compound **26** with ZnTPP

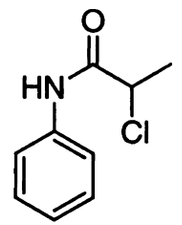

26

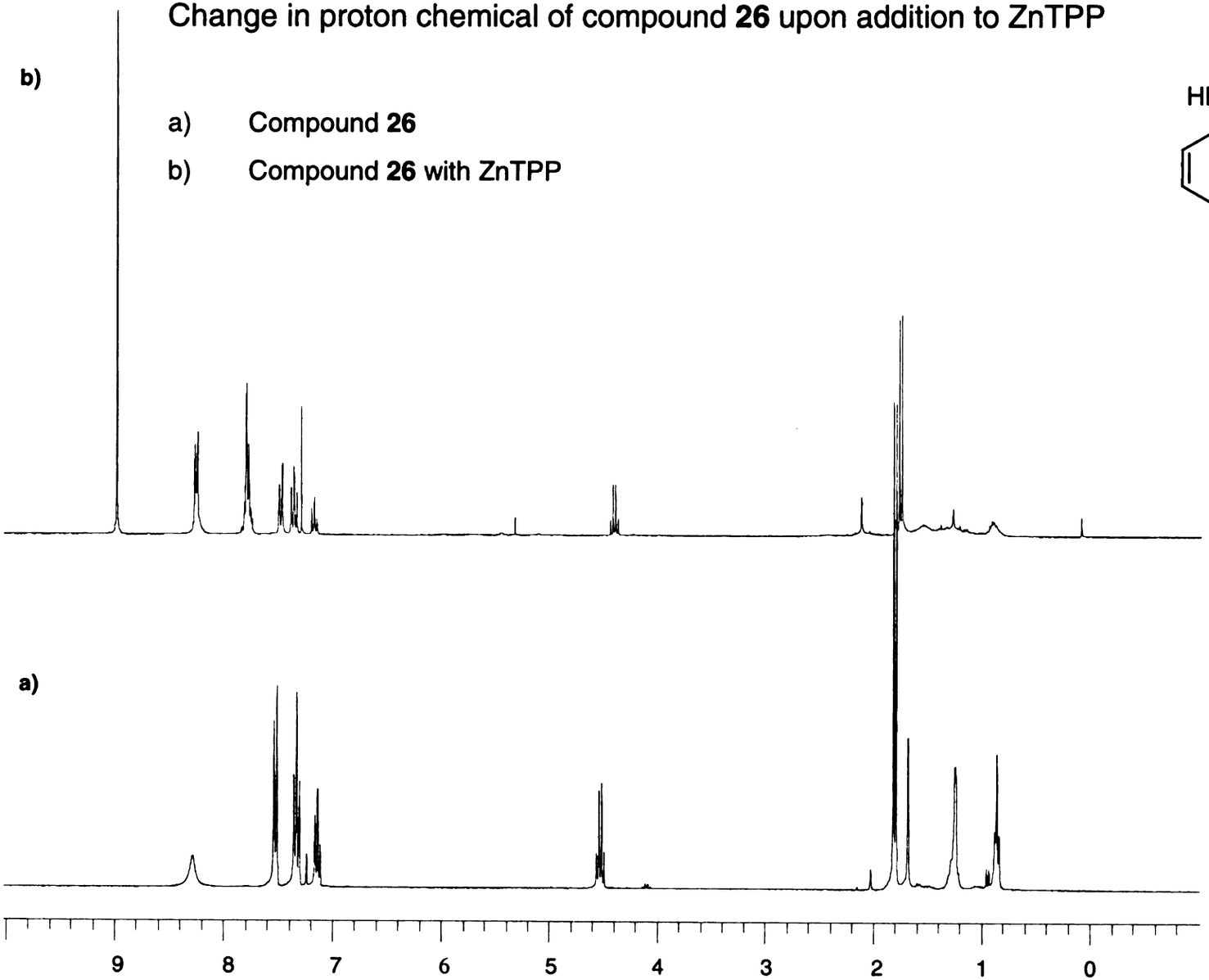

Change in proton chemical of compound **27** upon addition to ZnTPP

a) Compound **27**

b) Compound **27** with ZnTPP

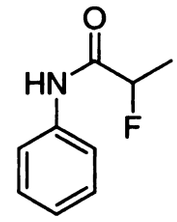

27

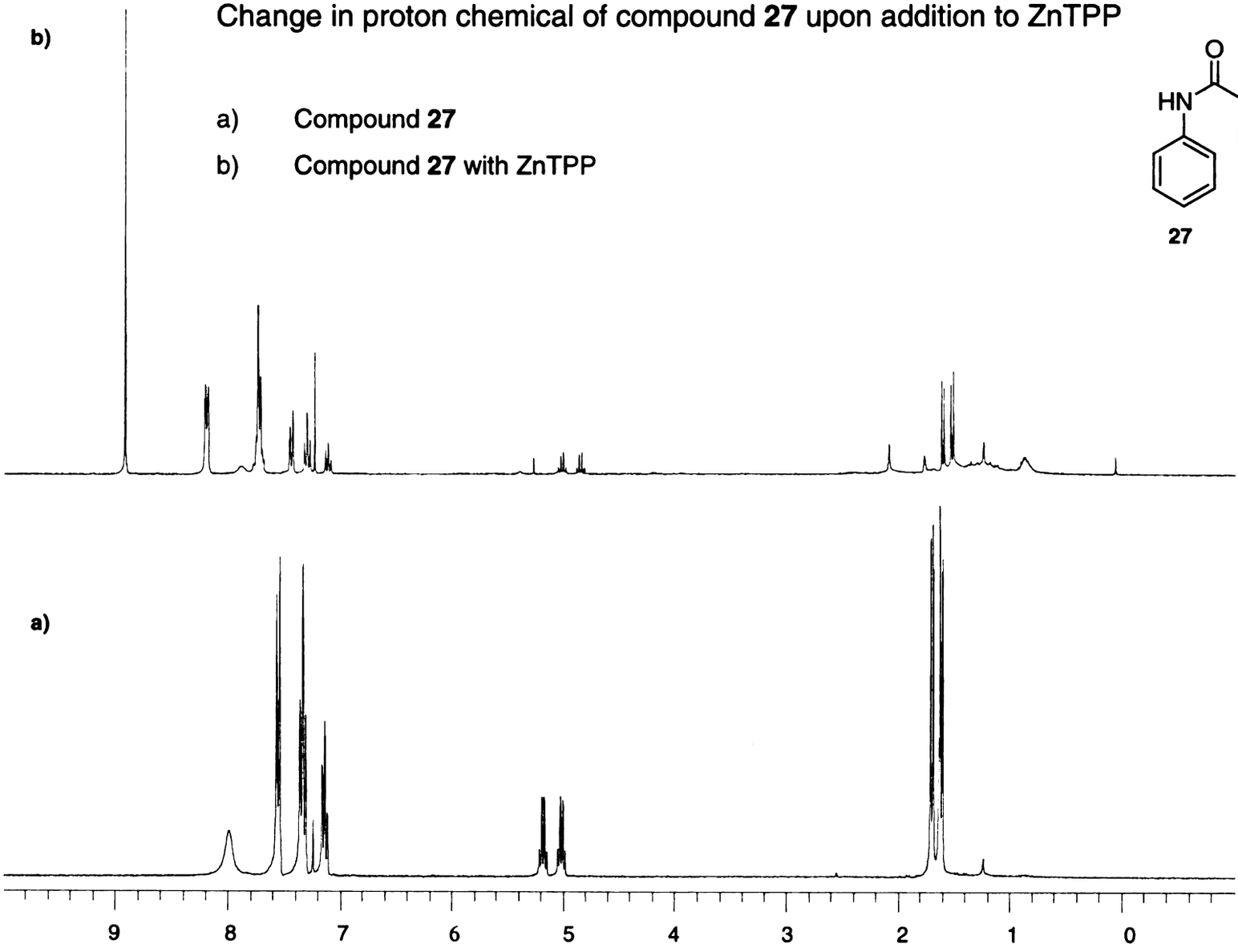

Change in proton chemical of compound **28** upon addition to ZnTPP

a) Compound **28**

b) Compound **28** with ZnTPP

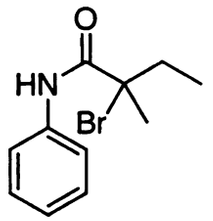

28

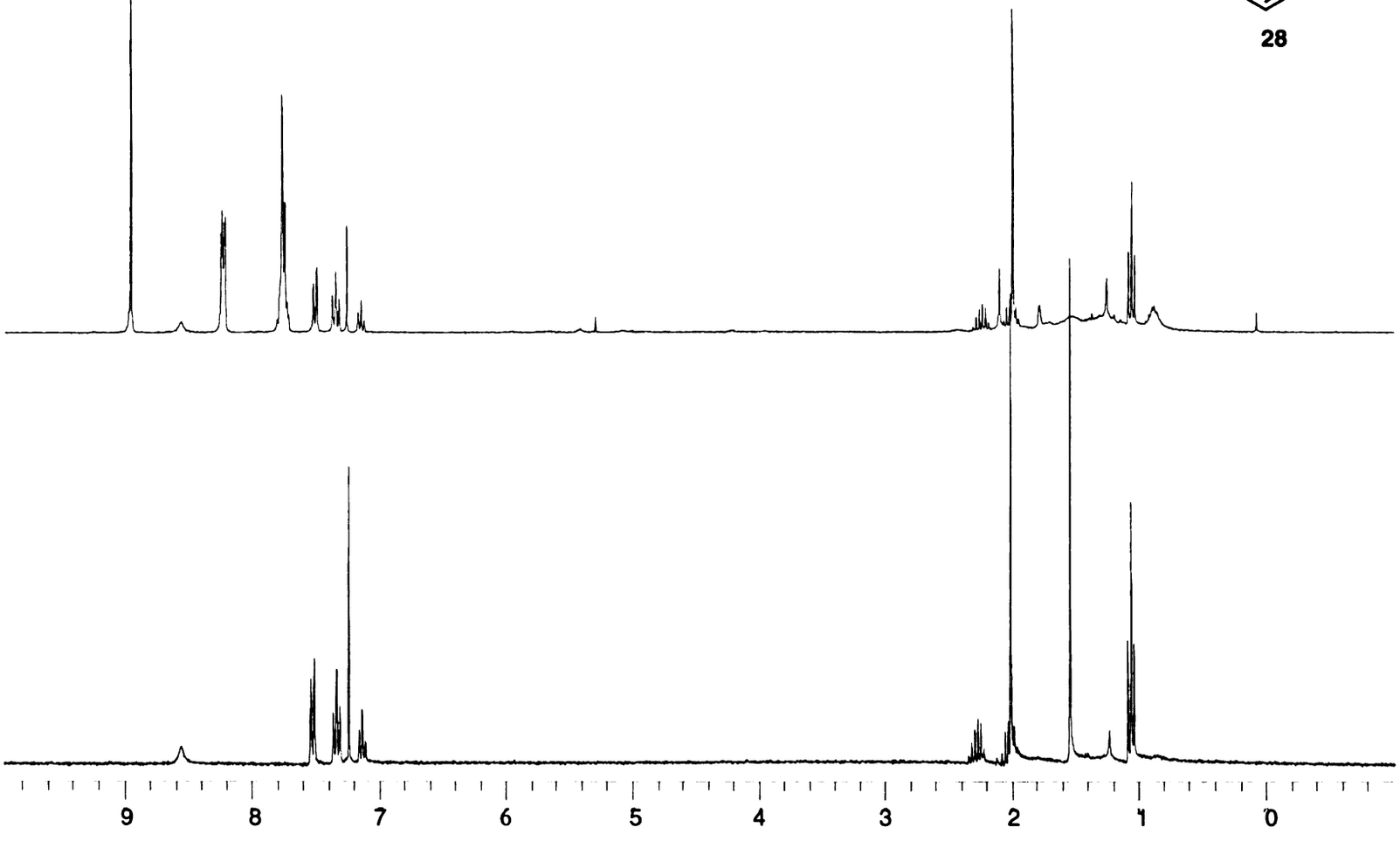

ECCD spectrum of compound **B-1-Br**

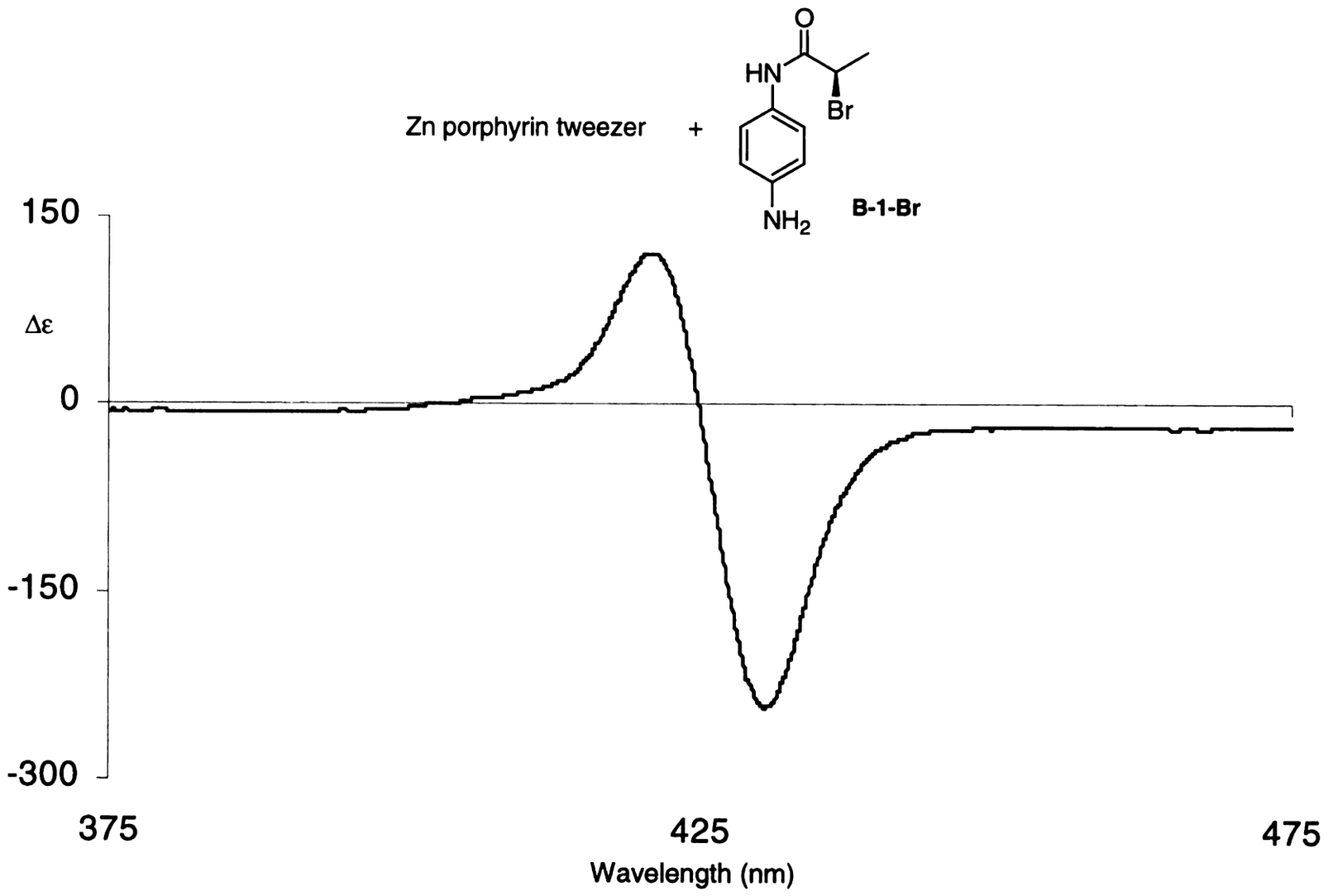

ECCD spectrum of compound **B-2-Br**

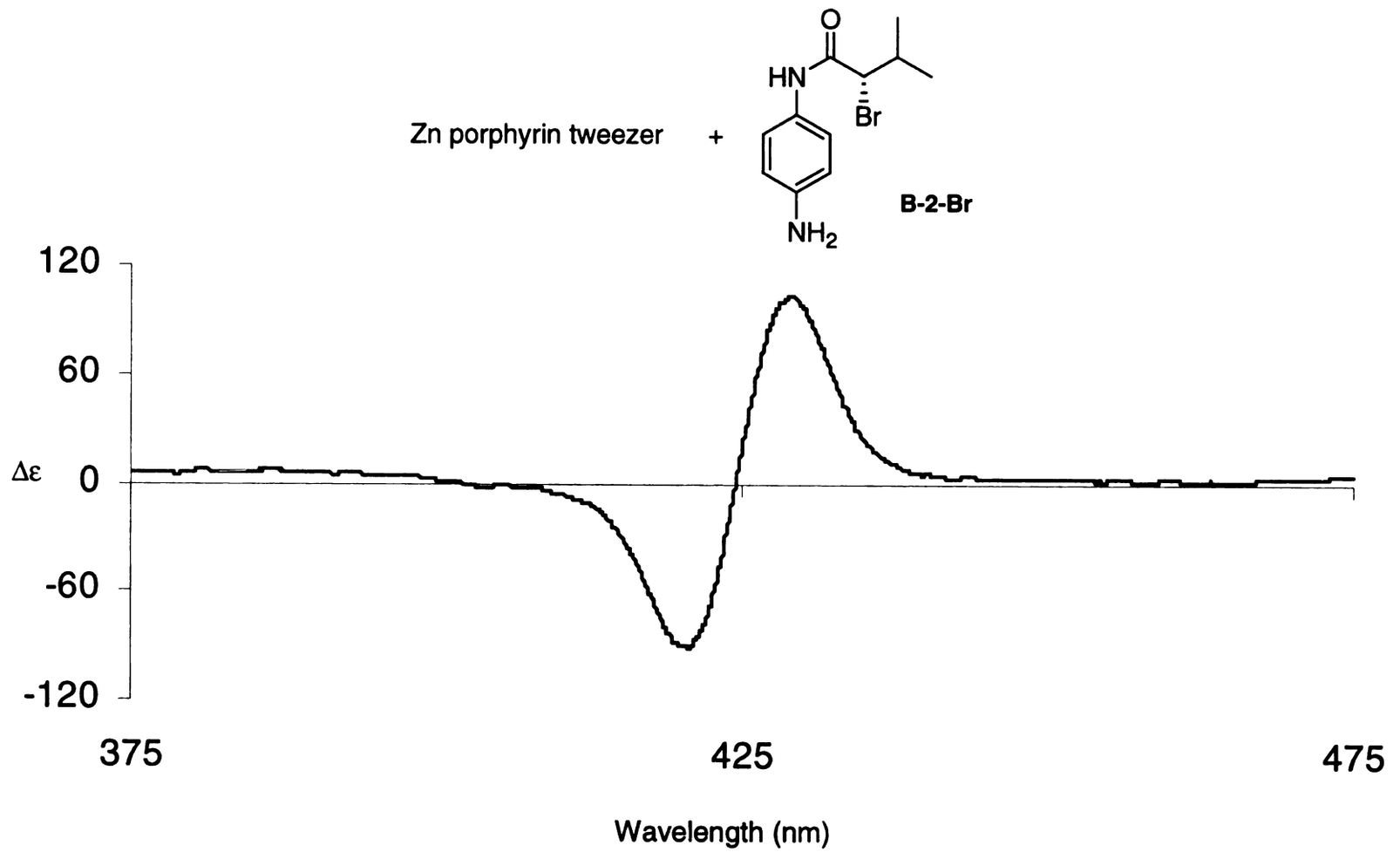

ECCD spectrum of compound **B-3-Br**

Zn porphyrin tweezer + 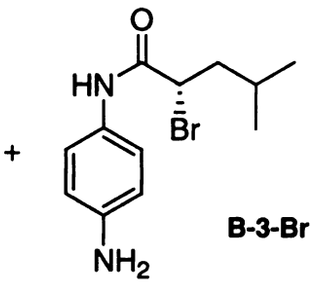

B-3-Br

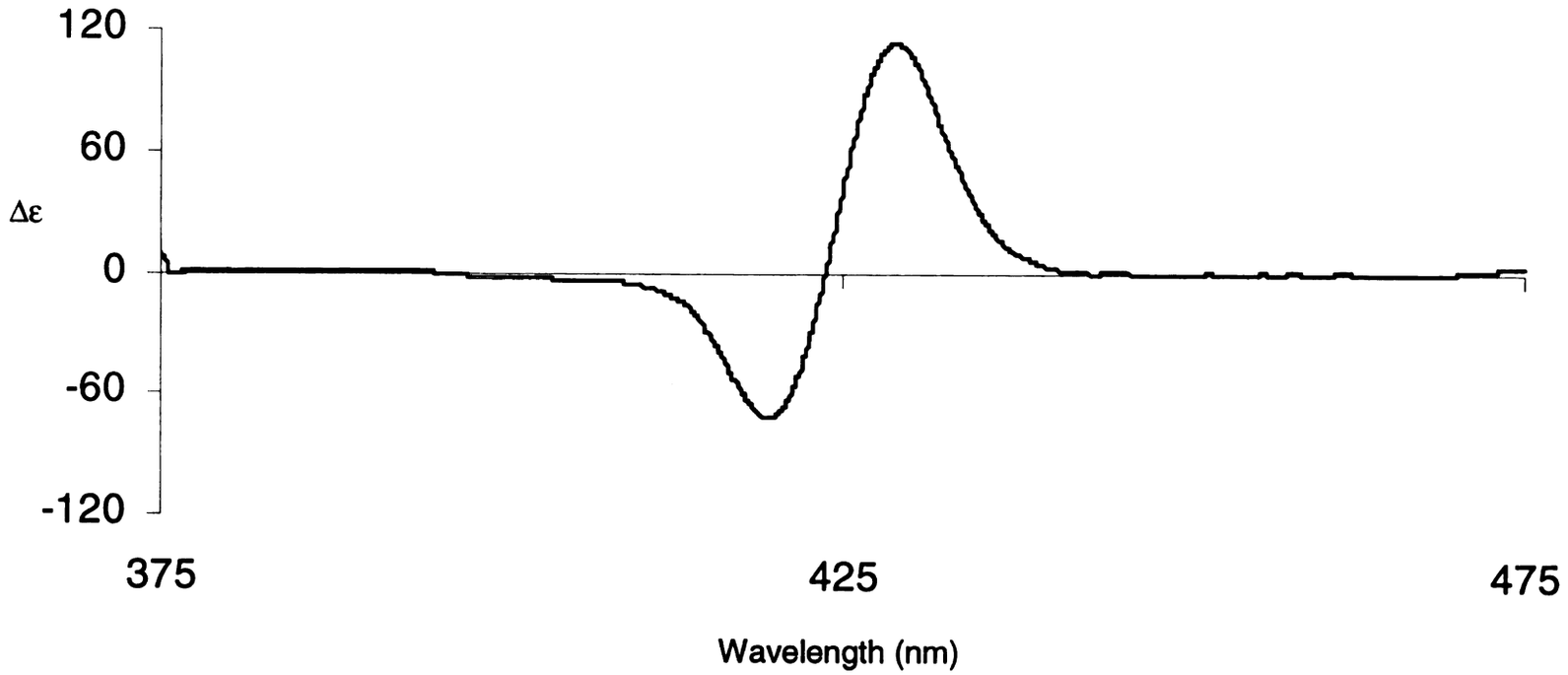

ECCD spectrum of compound **B-4-Br**

Zn porphyrin tweezer +

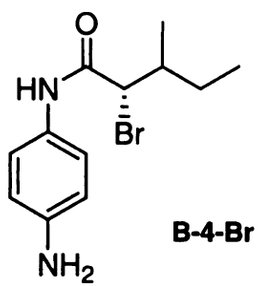

B-4-Br

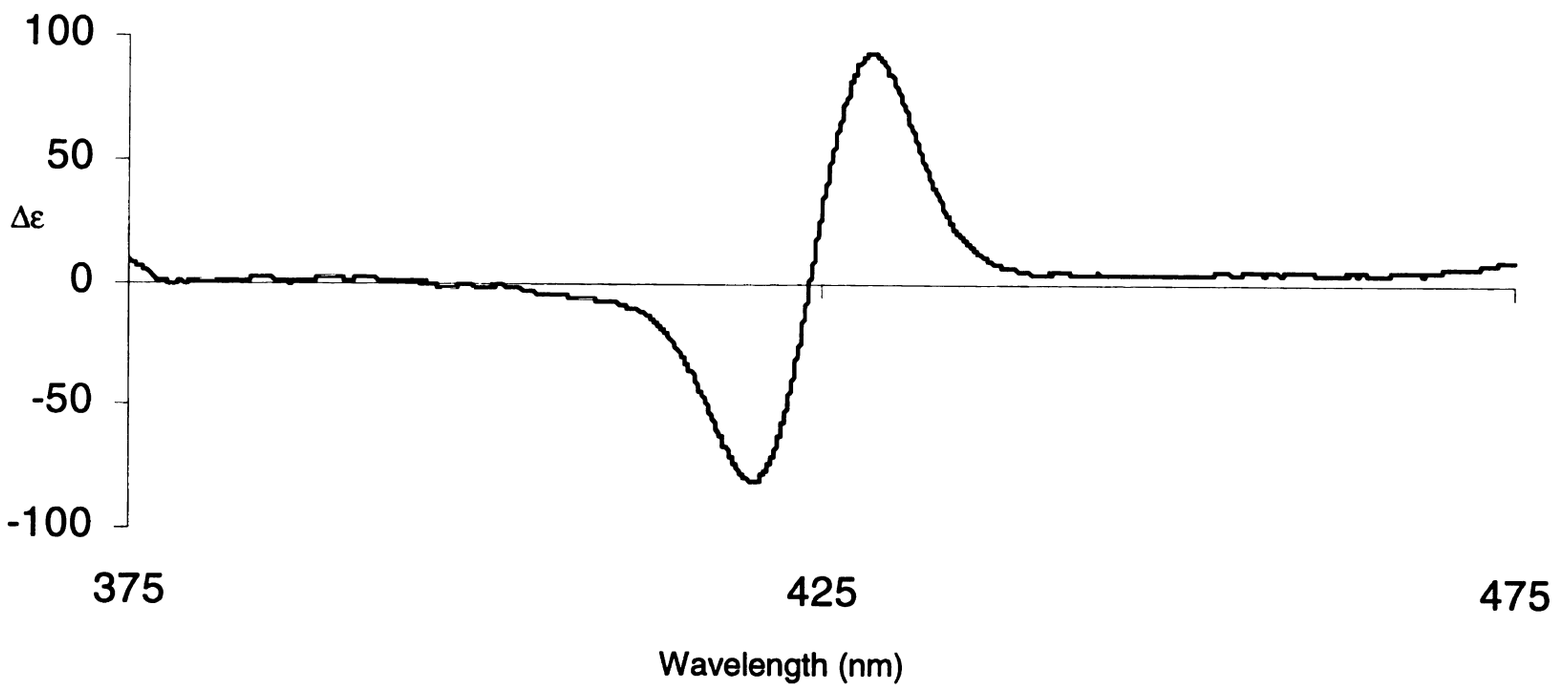

ECCD spectrum of compound **B-5-Br**

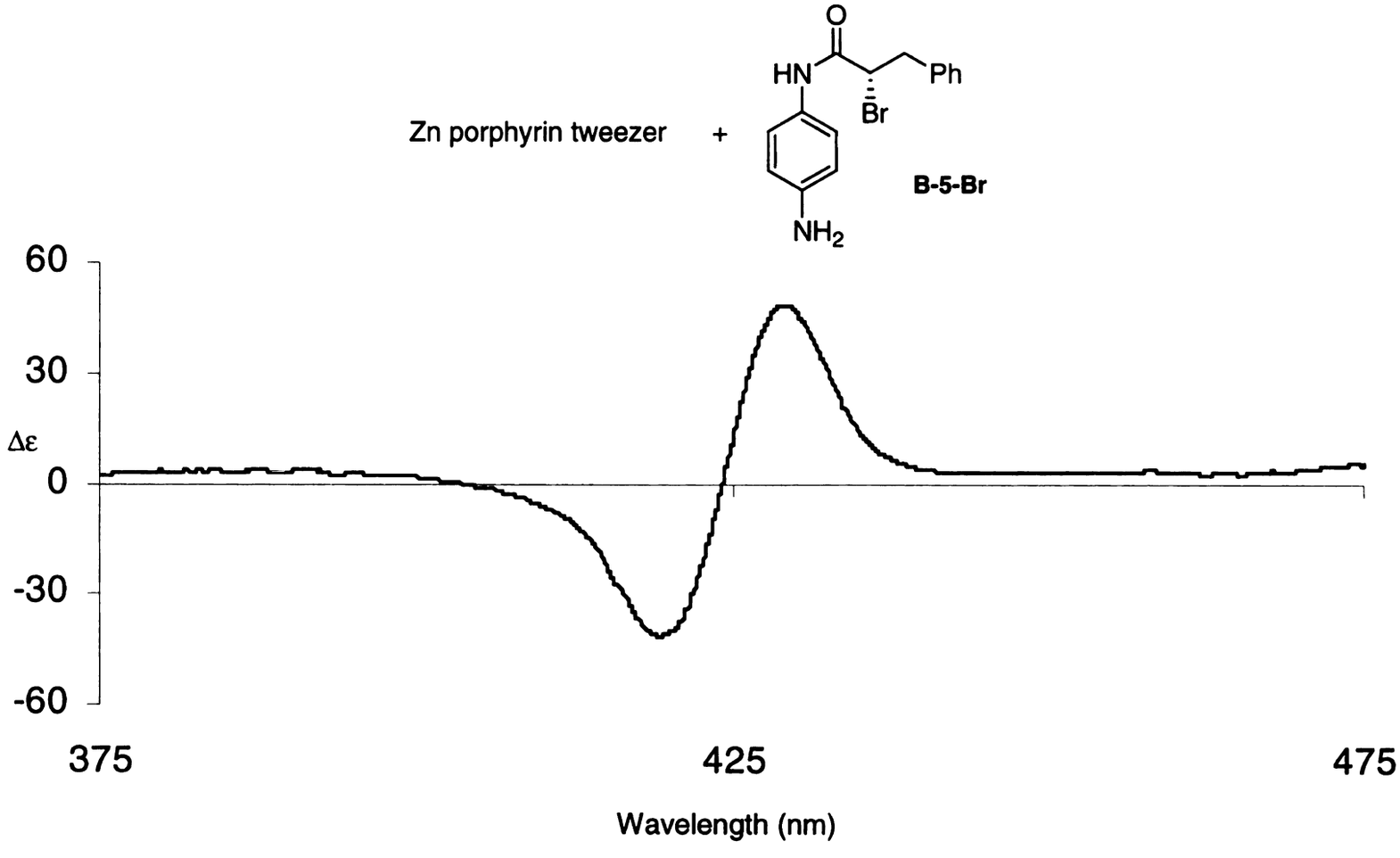

ECCD spectrum of compound **B-1-Cl**

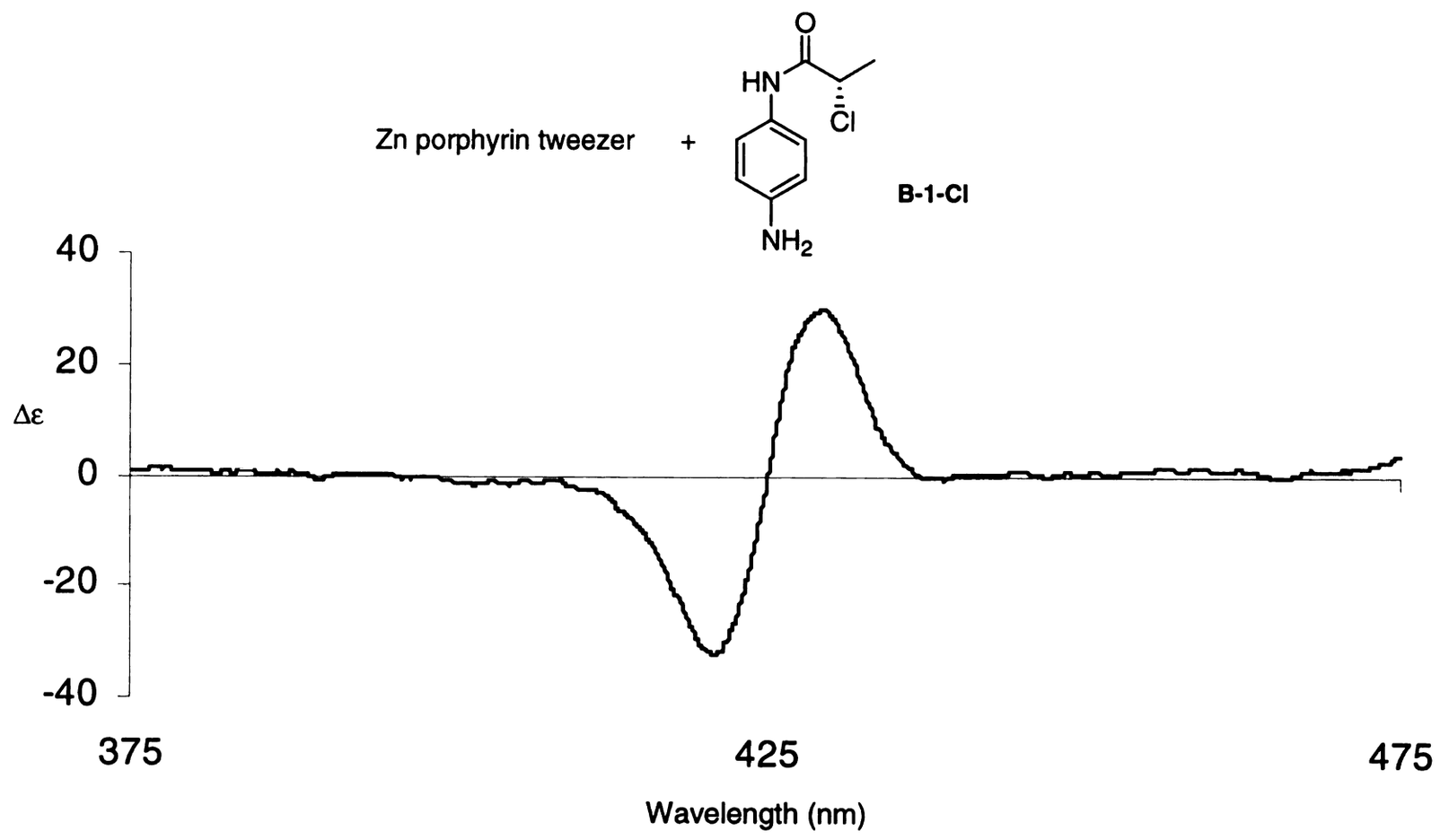

ECCD spectrum of compound **B-2-Cl**

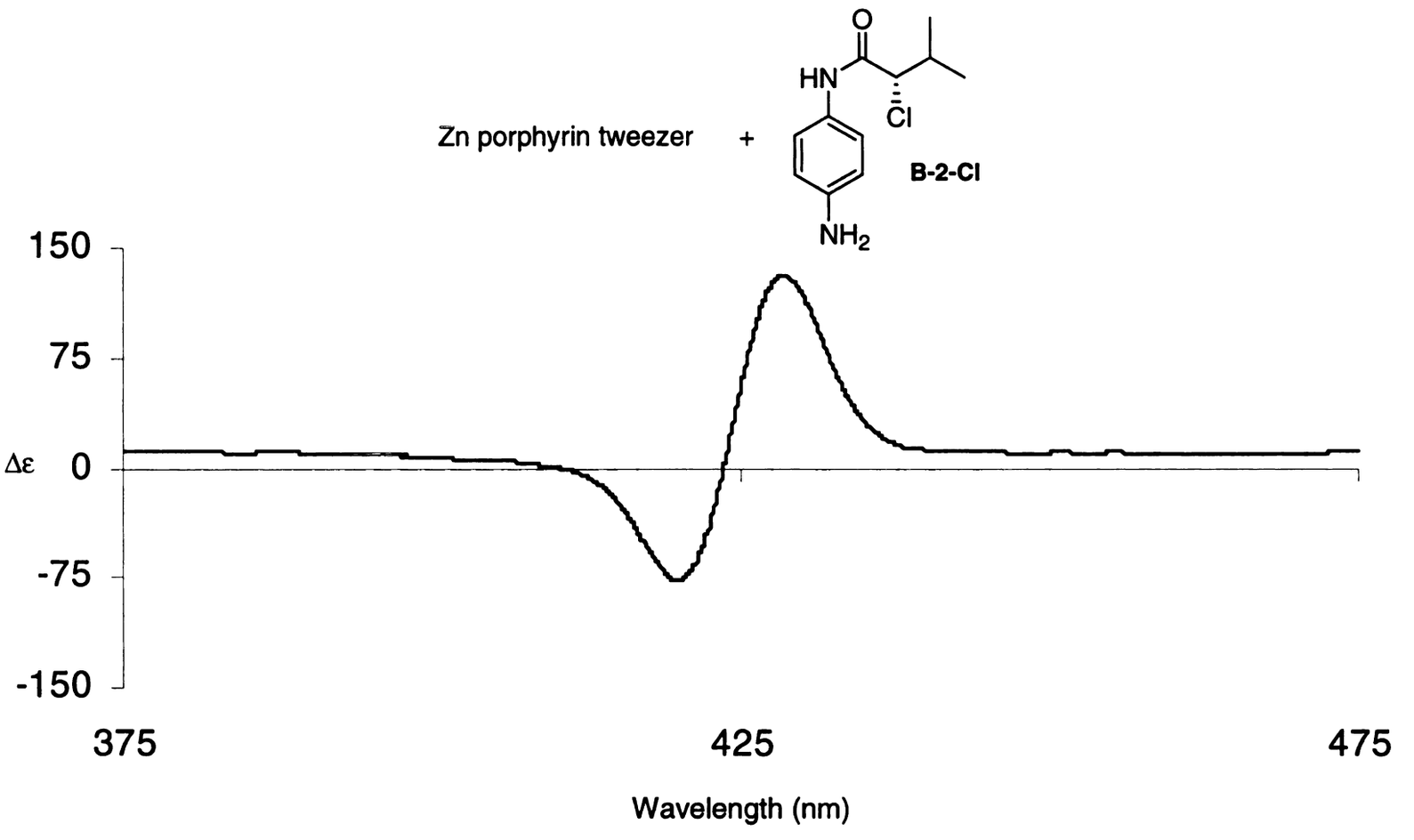

ECCD spectrum of compound **B-3-Cl**

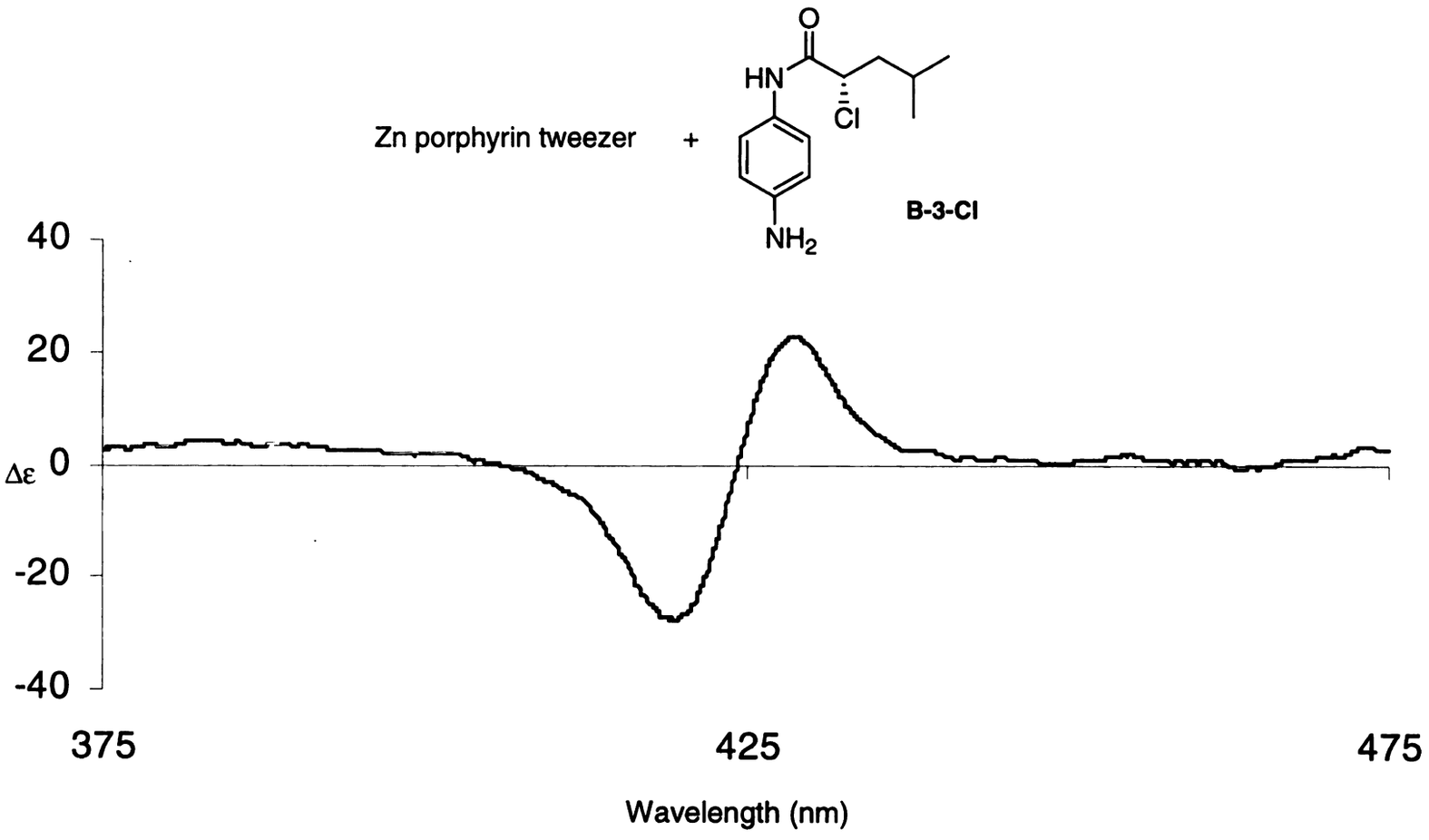

ECCD spectrum of compound **B-4-Cl**

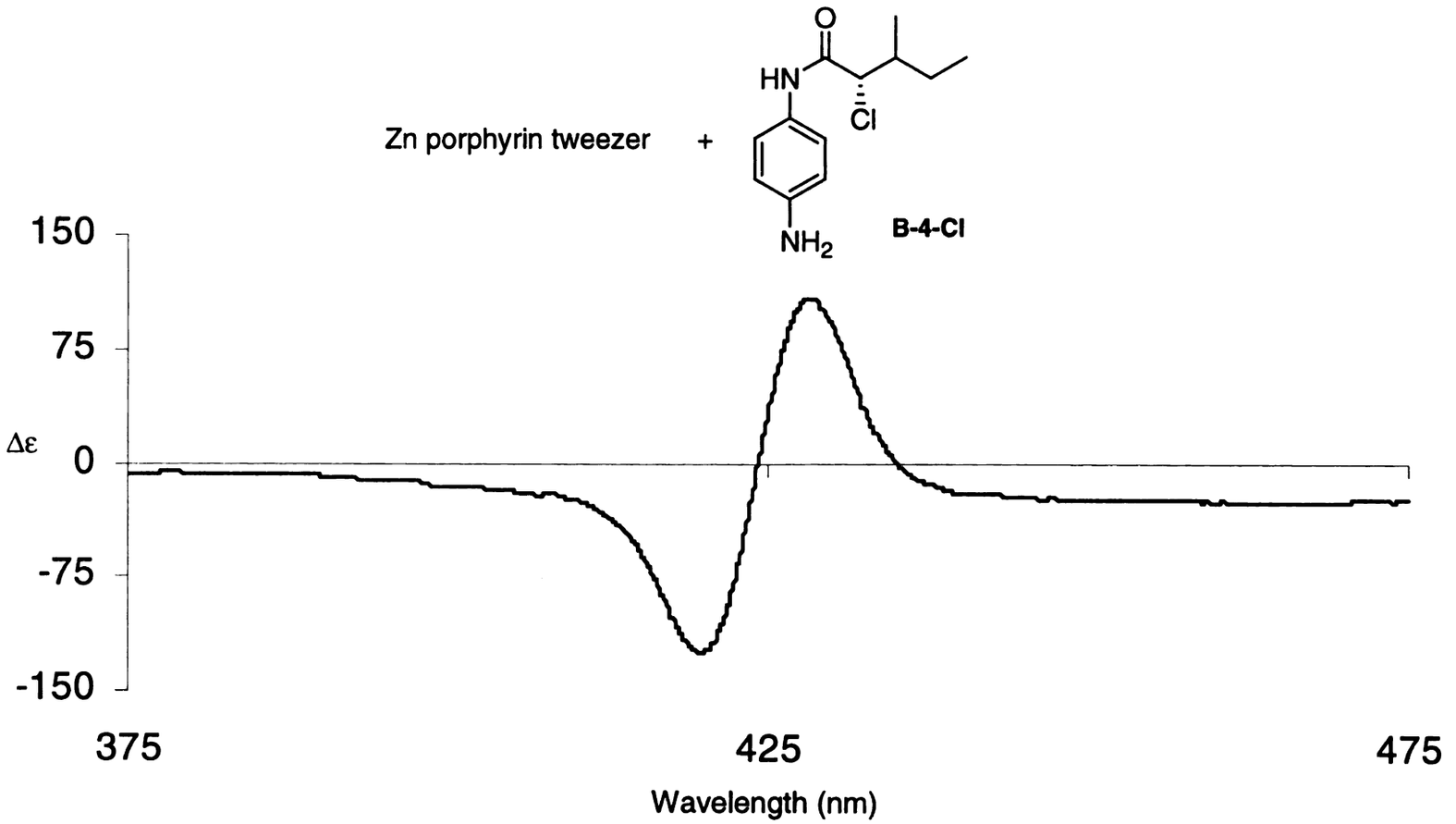

ECCD spectrum of compound **B-5-Cl**

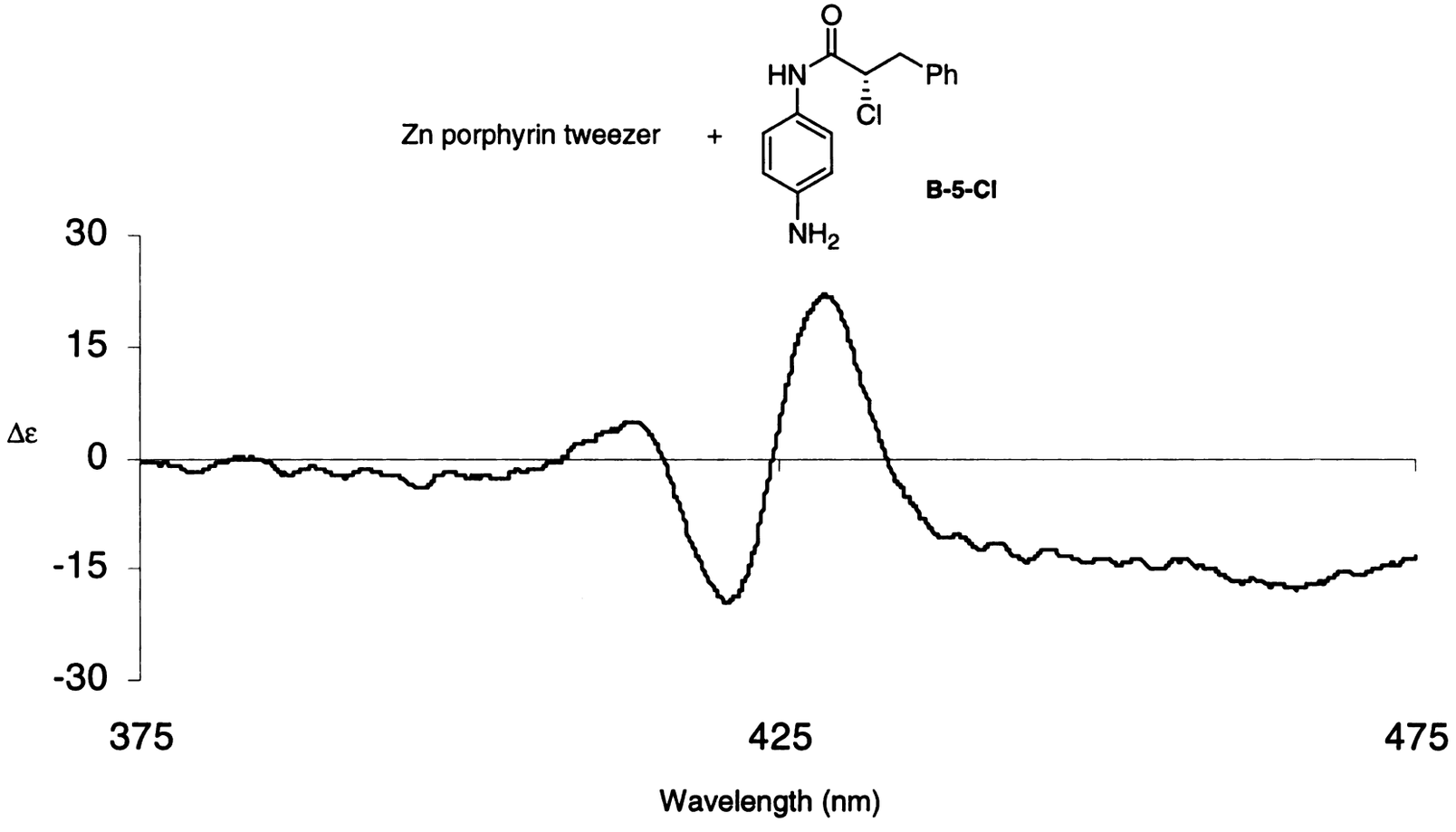

ECCD spectrum of compound **B-1-F**

Zn porphyrin tweezer + 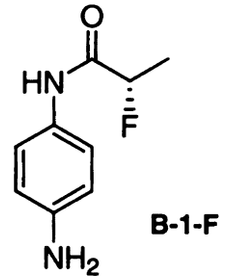

B-1-F

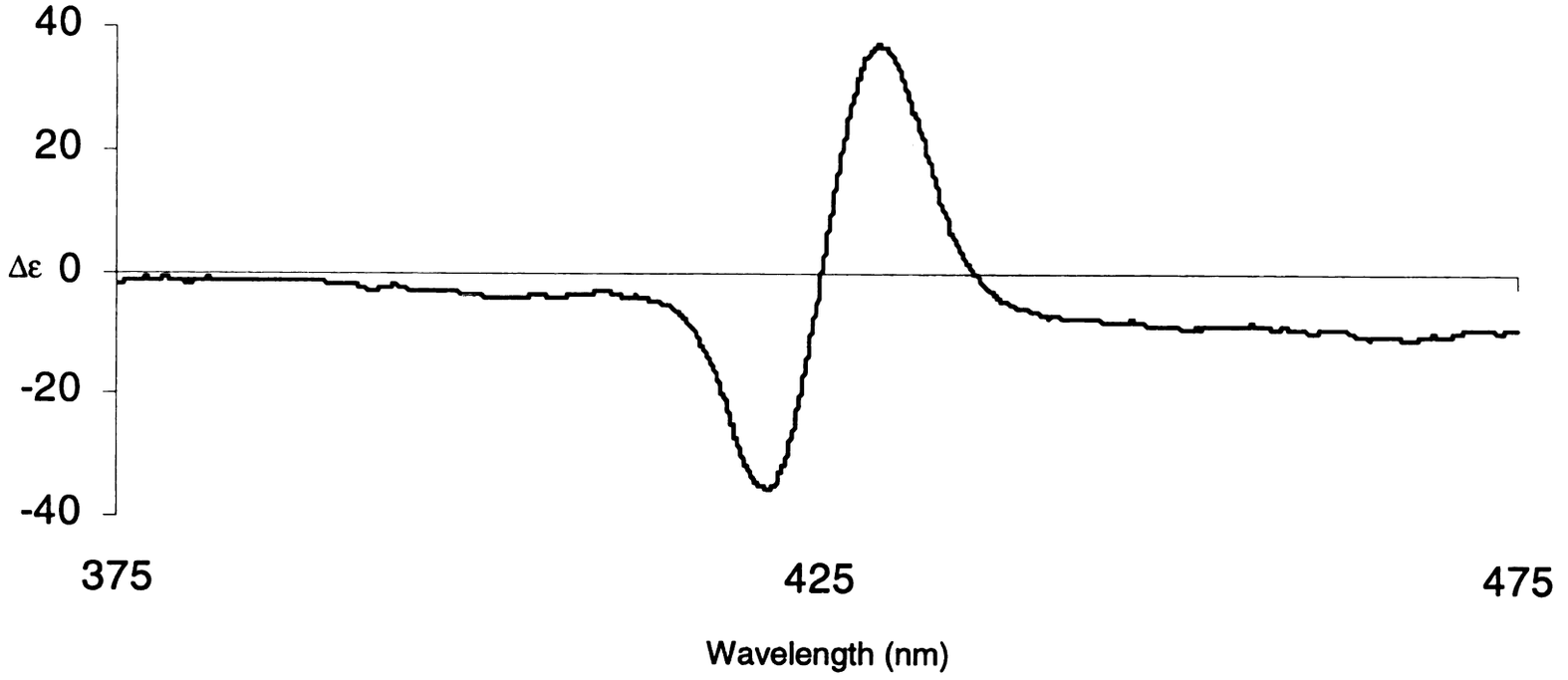

ECCD spectrum of compound **B-2-F**

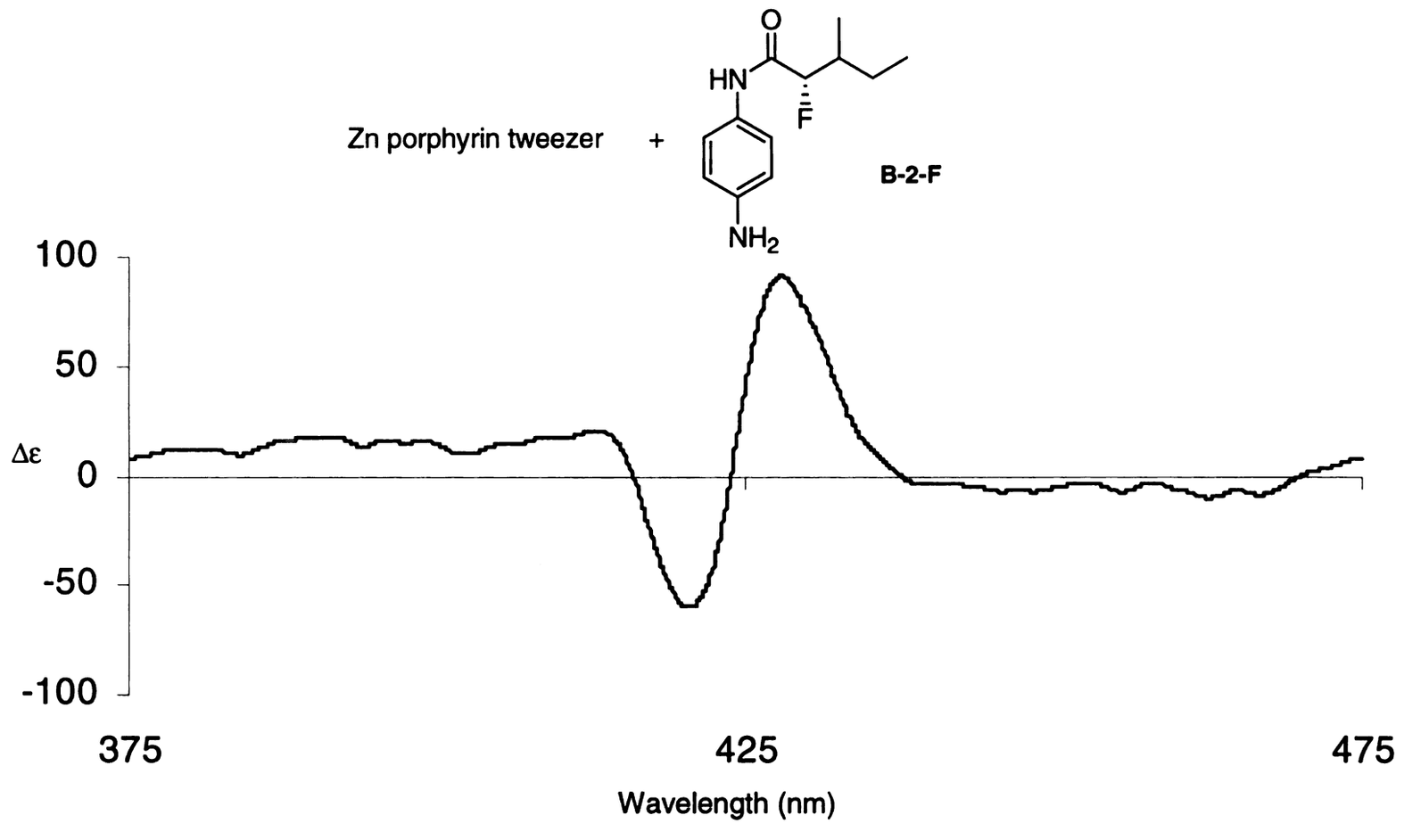

ECCD spectrum of compound **B-3-F**

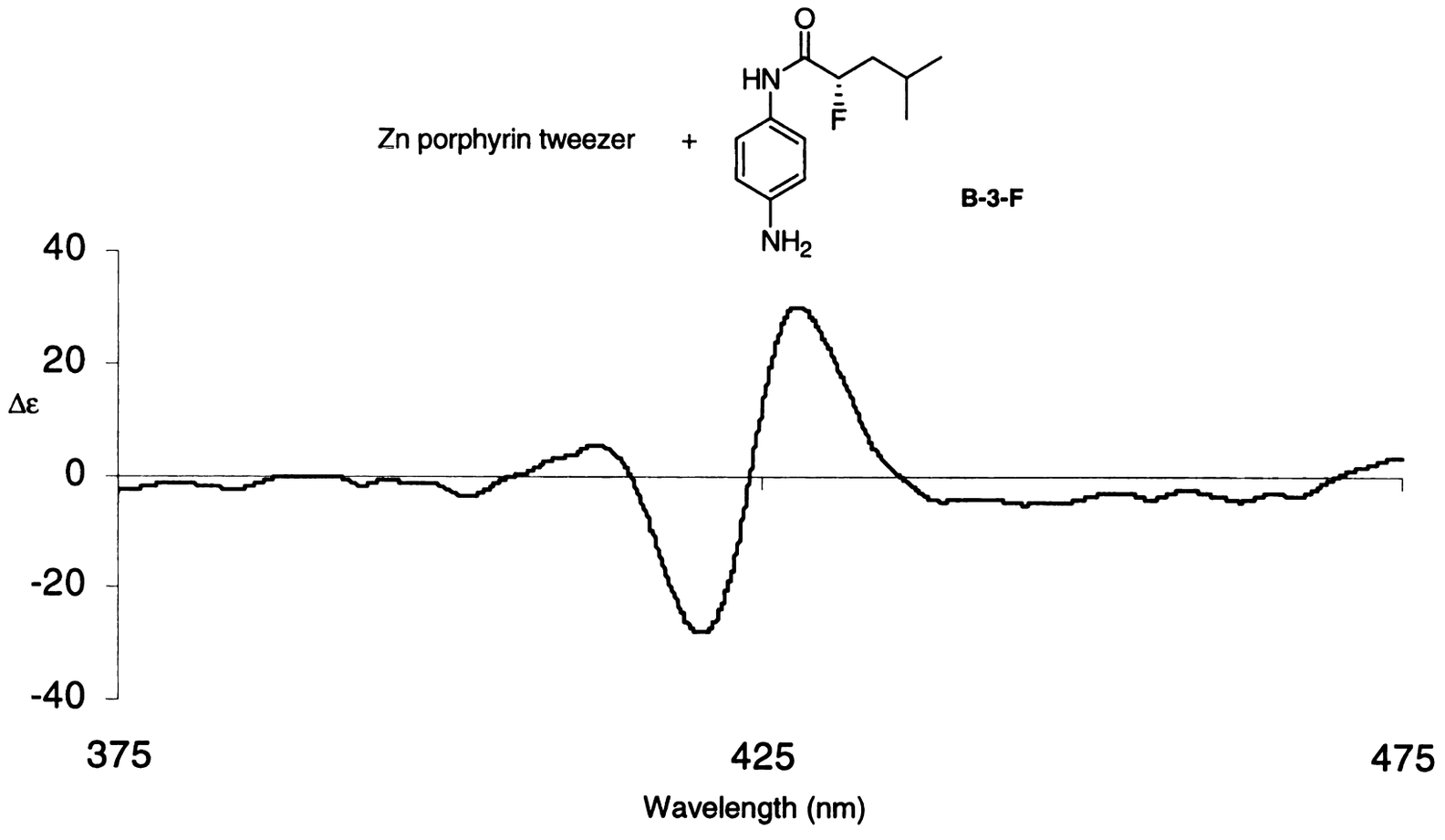

ECCD spectrum of compound **B-4-F**

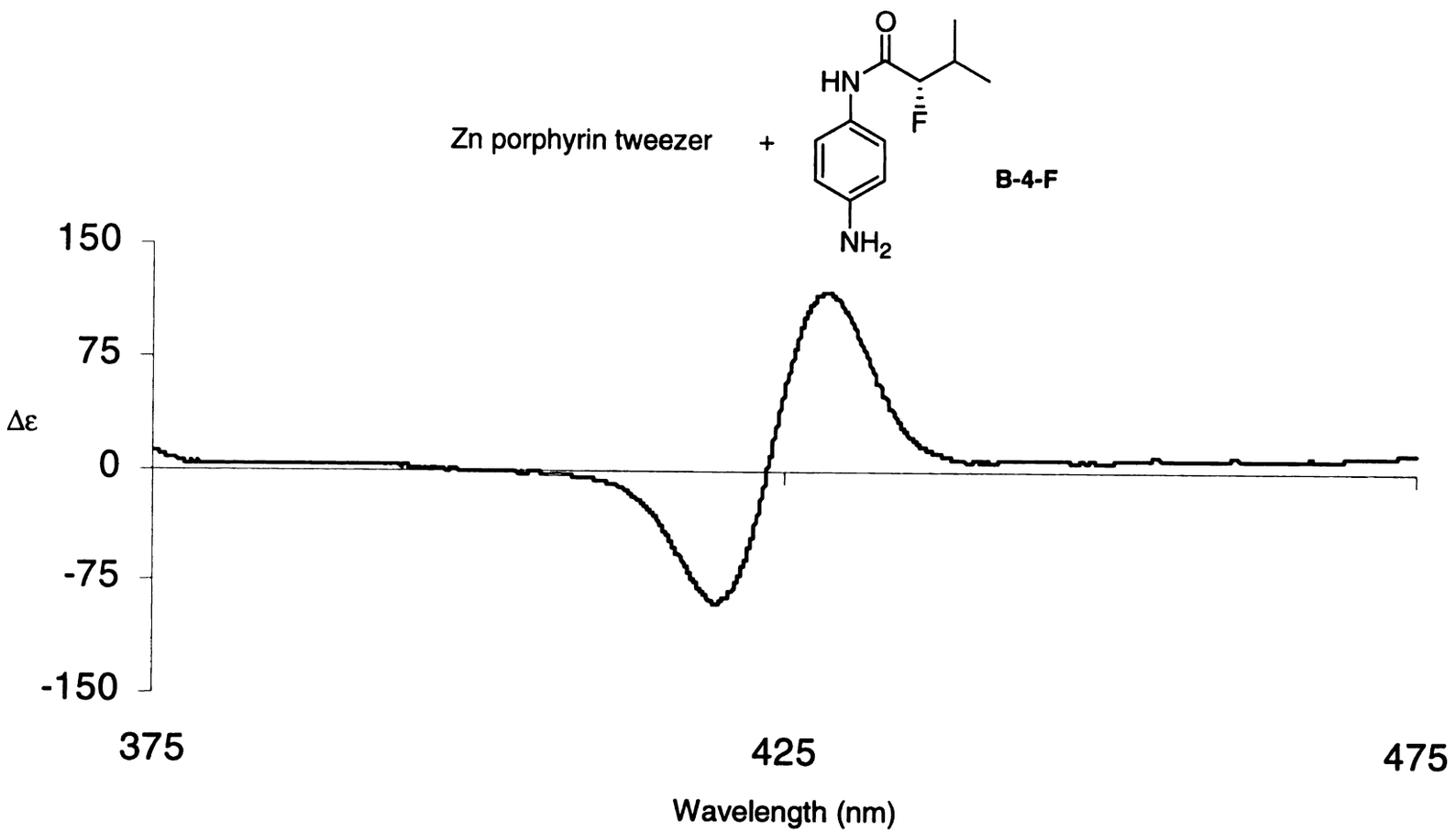

ECCD spectrum of compound **B-5-F**

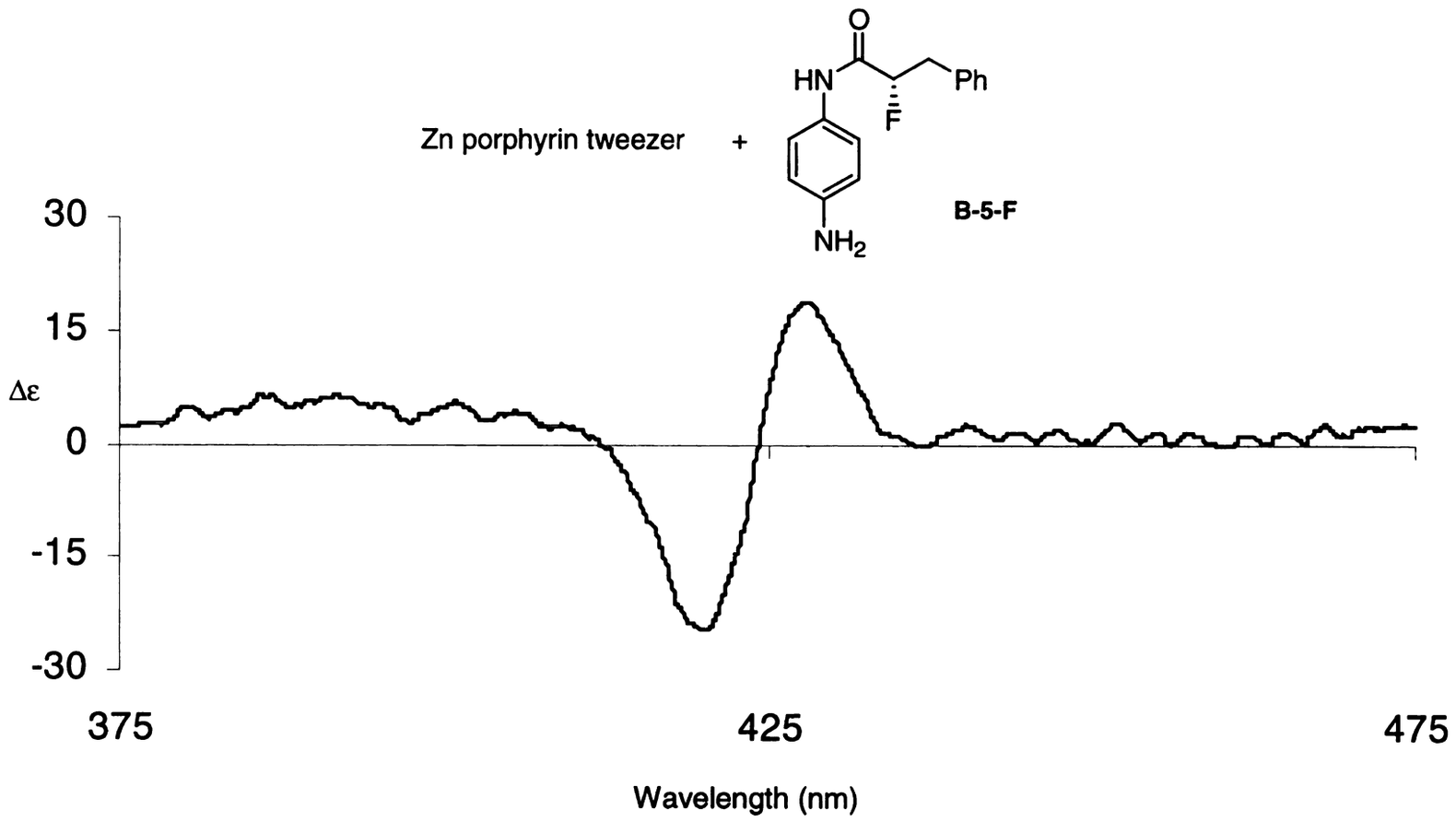

ECCD spectrum of compound **B-1-I**

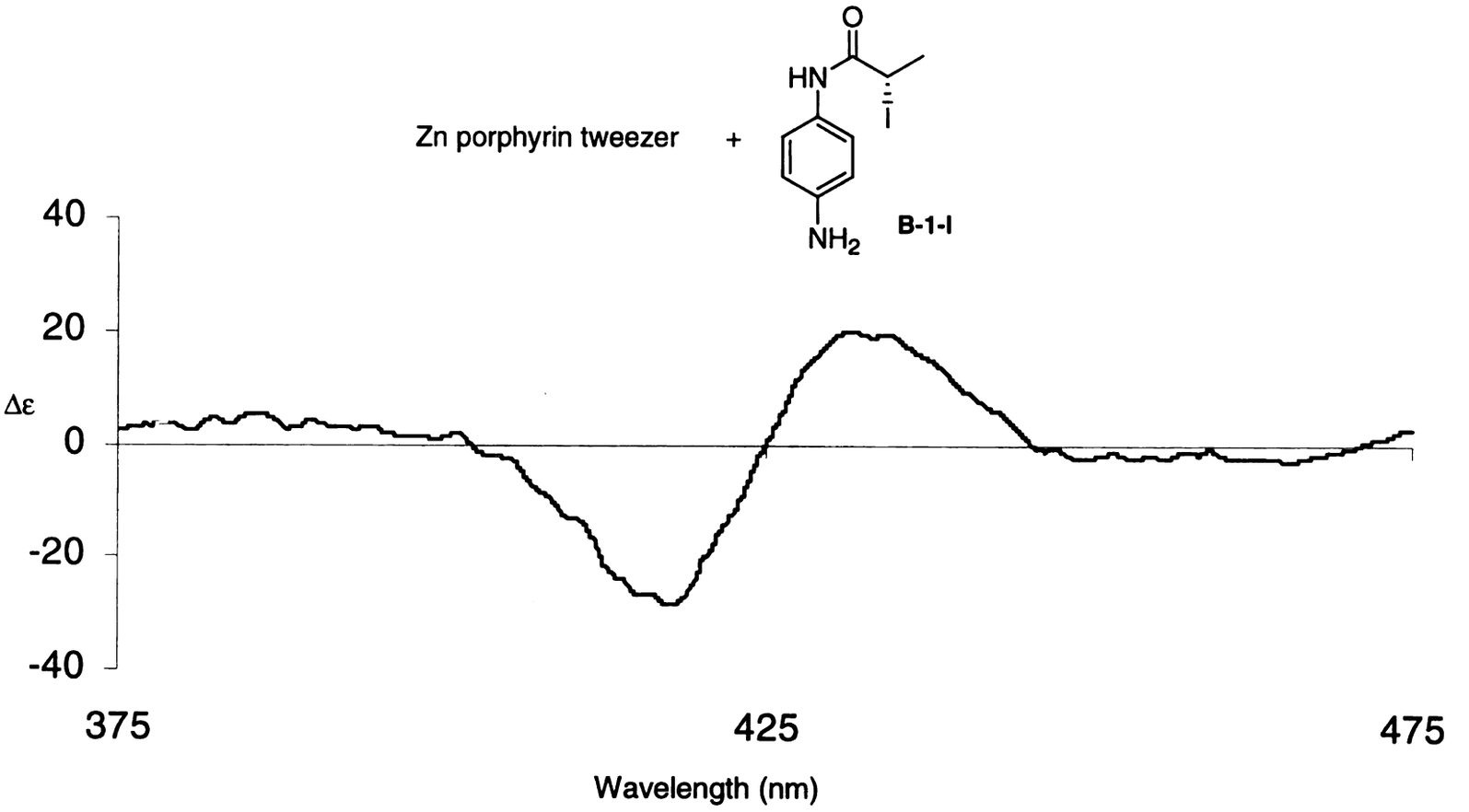

ECCD spectrum of compound **37**

Zn porphyrin tweezer +

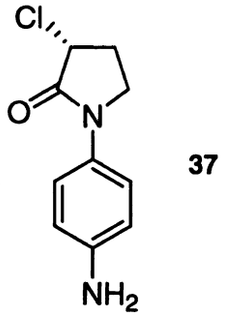

37

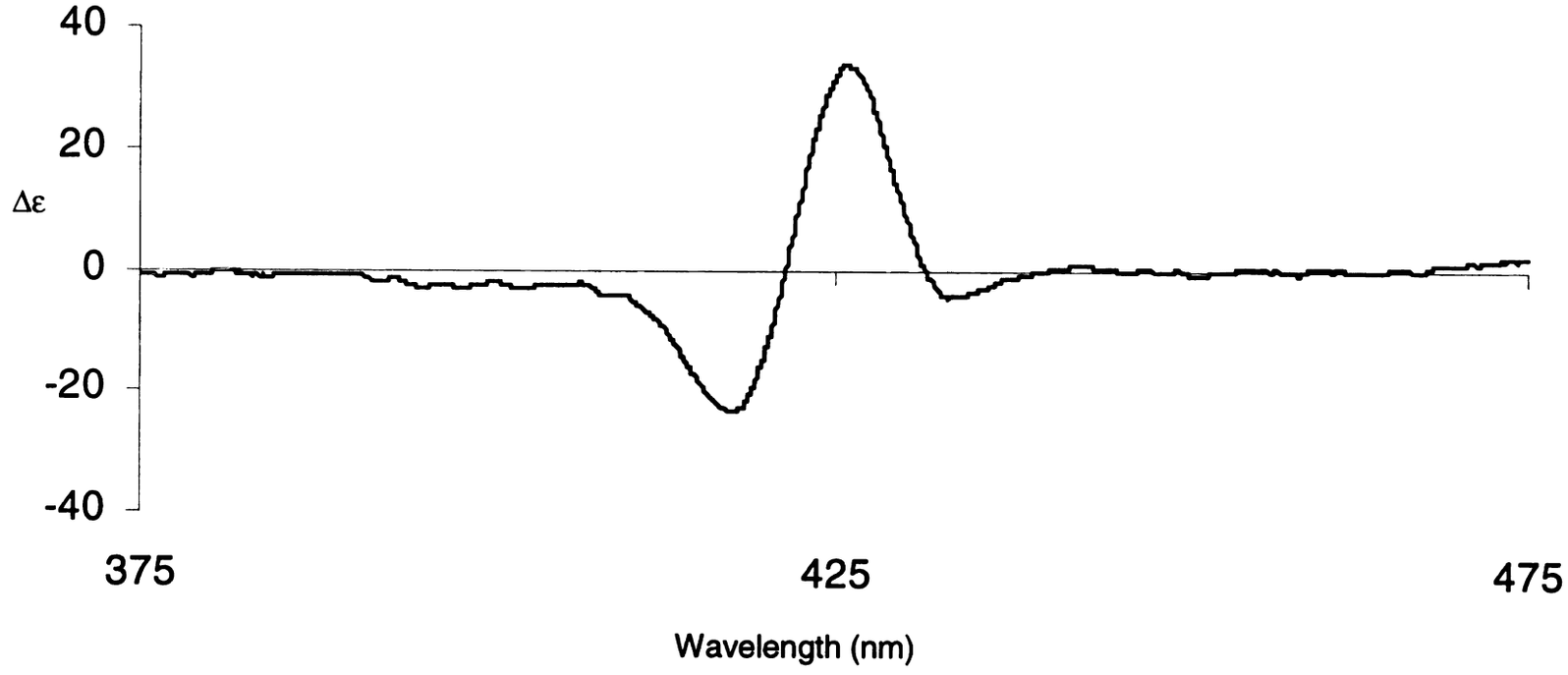

ECCD spectrum of compound **38**

Zn porphyrin tweezer +

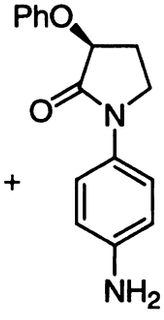

38

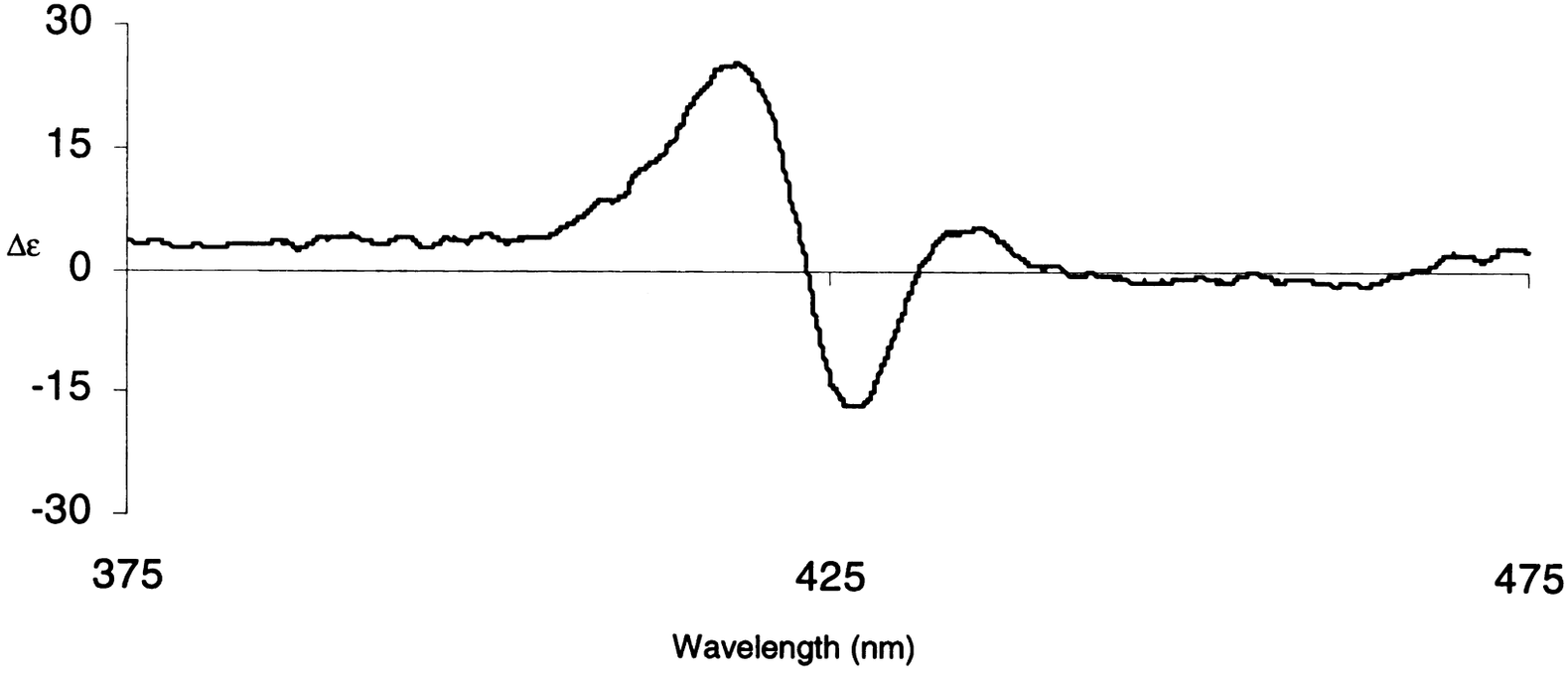

ECCD spectrum of compound **50**

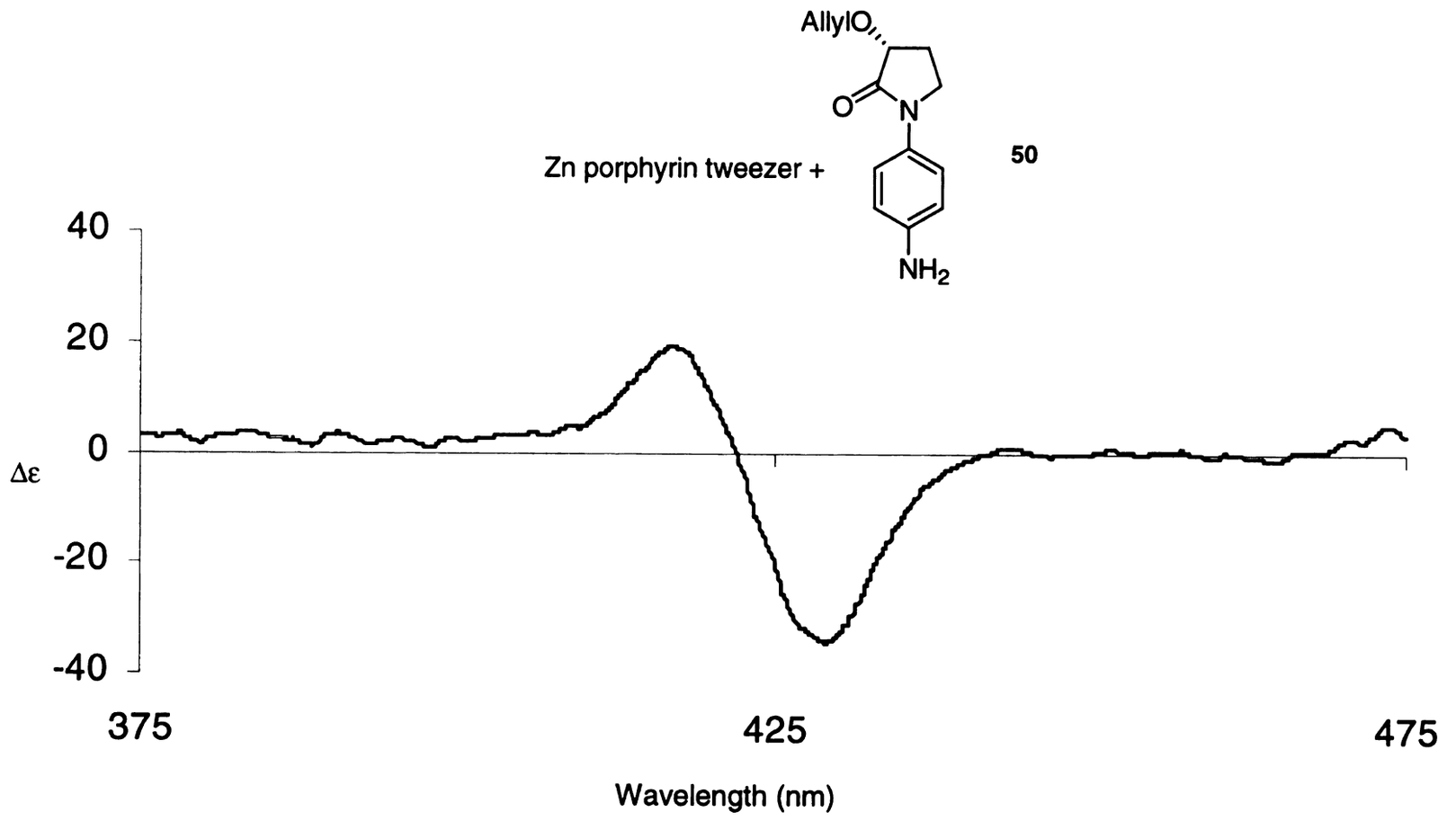

ECCD spectrum of compound **51**

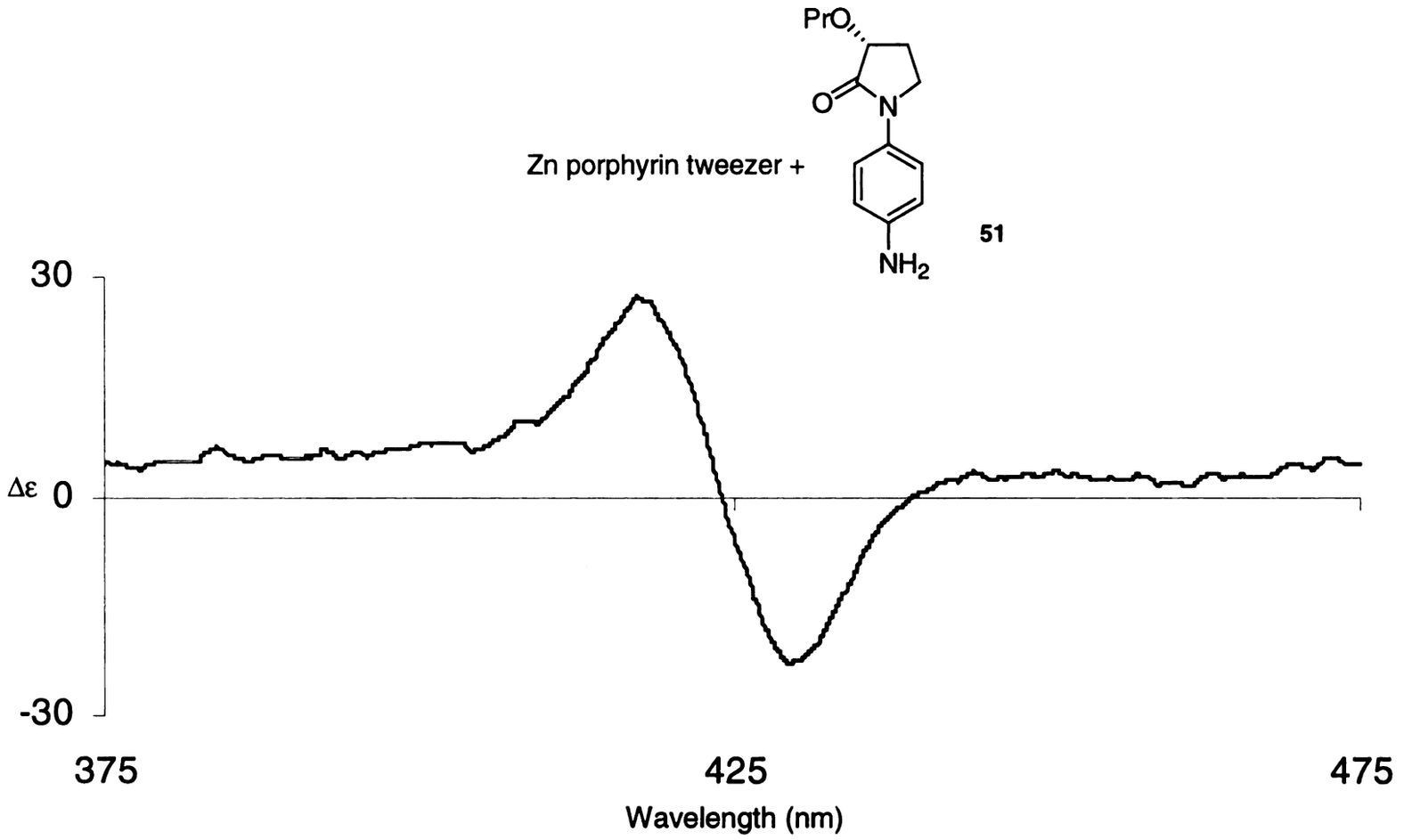

ECCD spectrum of compound **52**

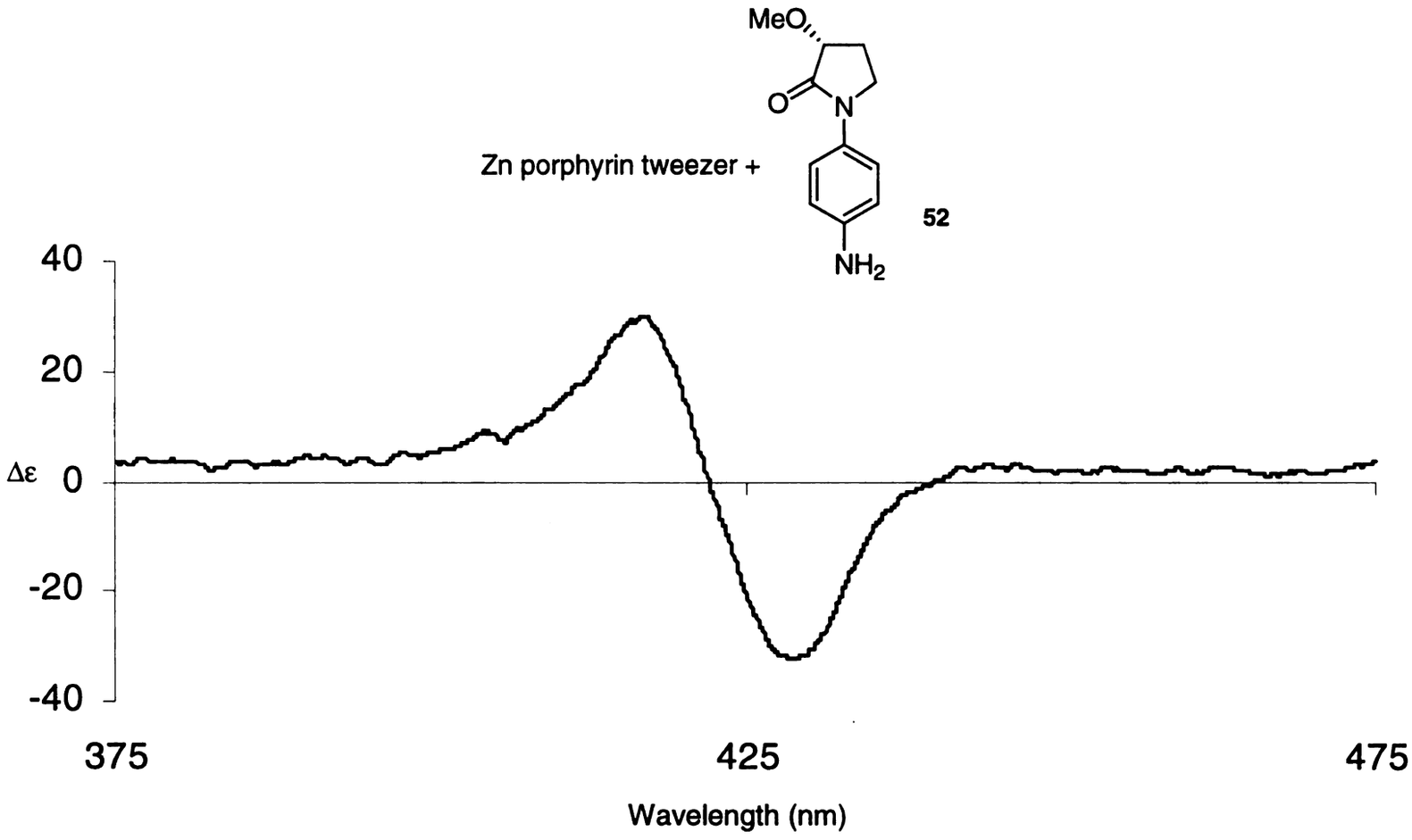

ECCD spectrum of compound **53**

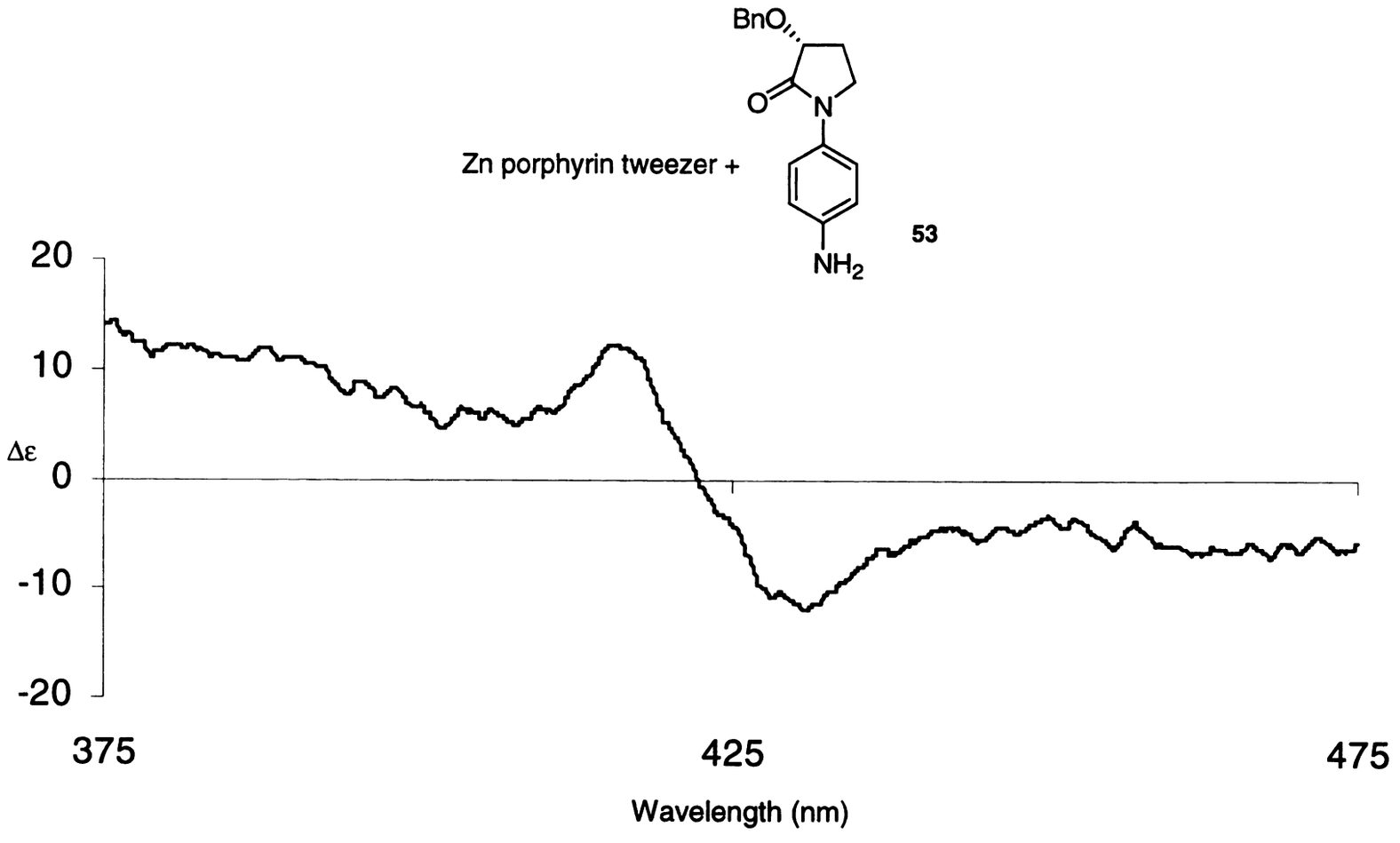

ECCD spectrum of compound **54**

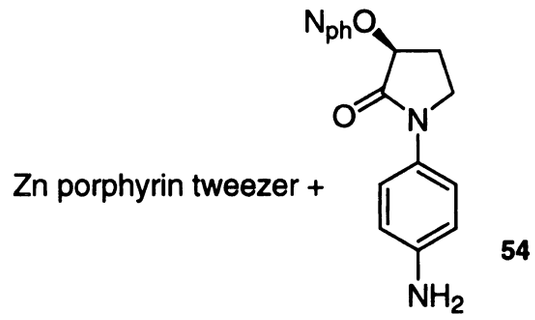

Zn porphyrin tweezer +

54

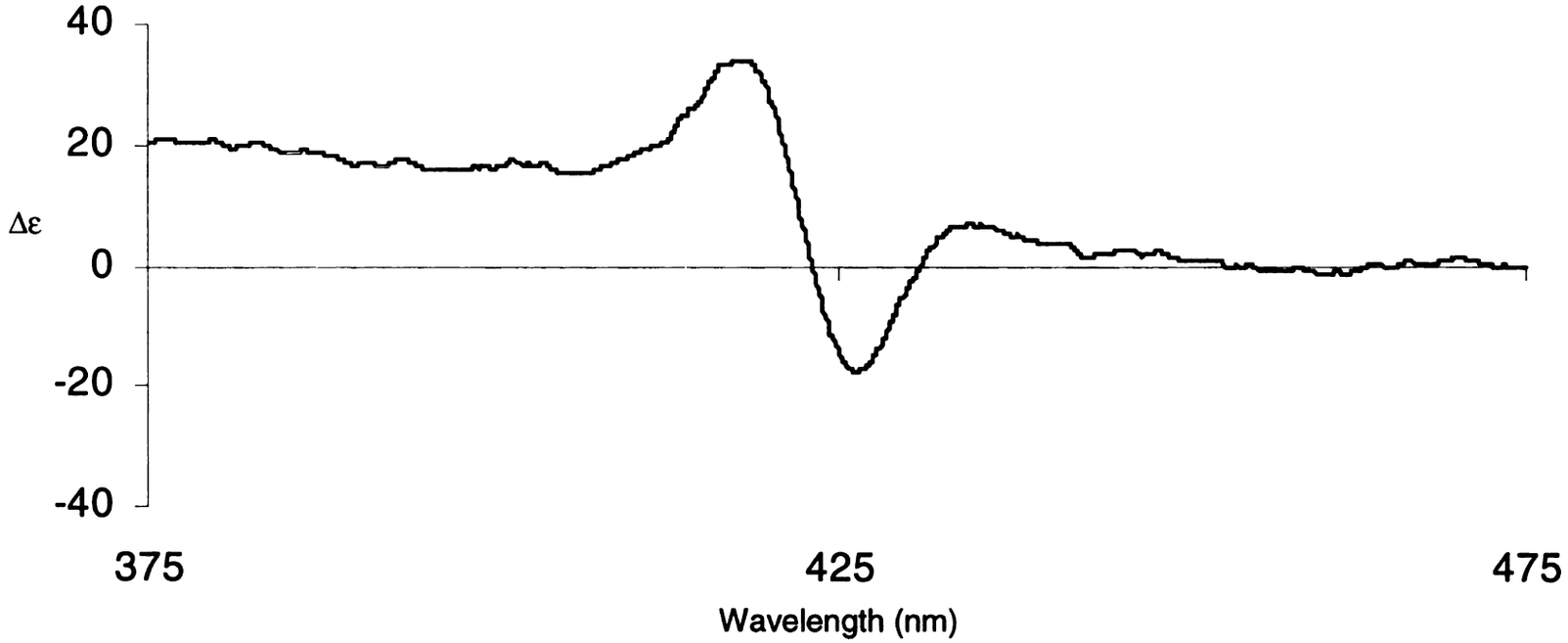

ECCD spectrum of compound **55**

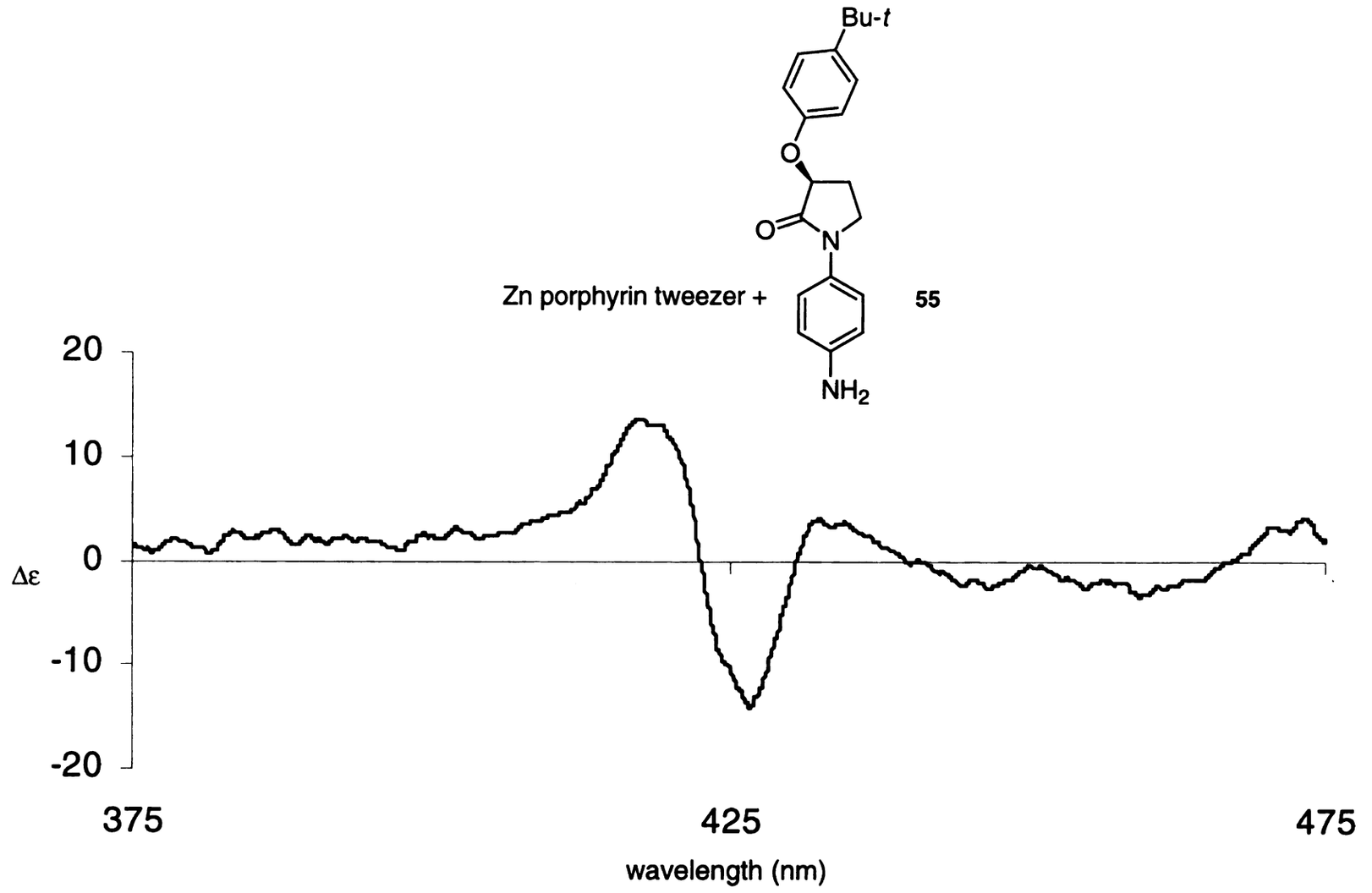

ECCD spectrum of compound **75**

Zn porphyrin tweezer +

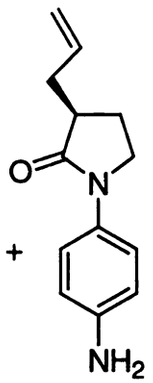

75

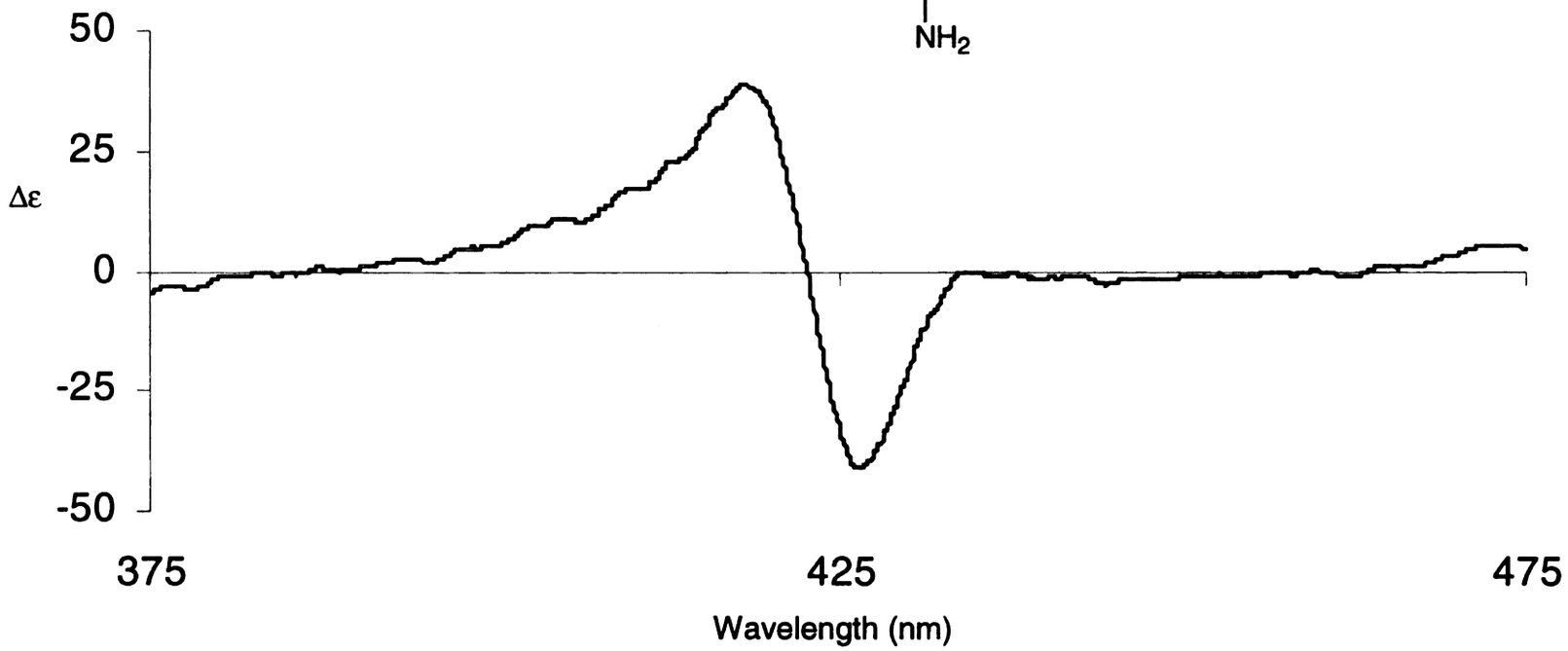

ECCD spectrum of compound **77**

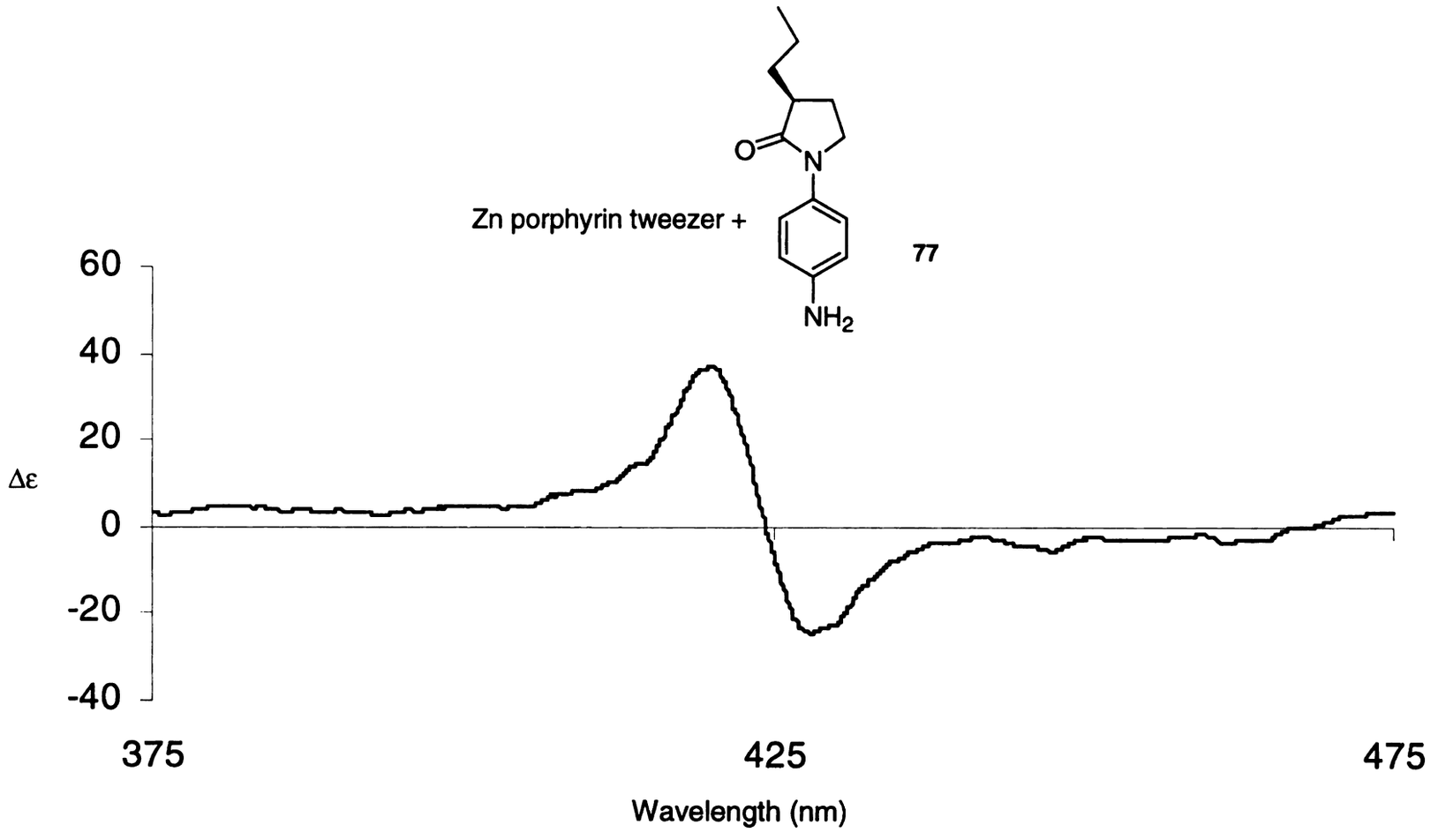

ECCD spectrum of compound **78**

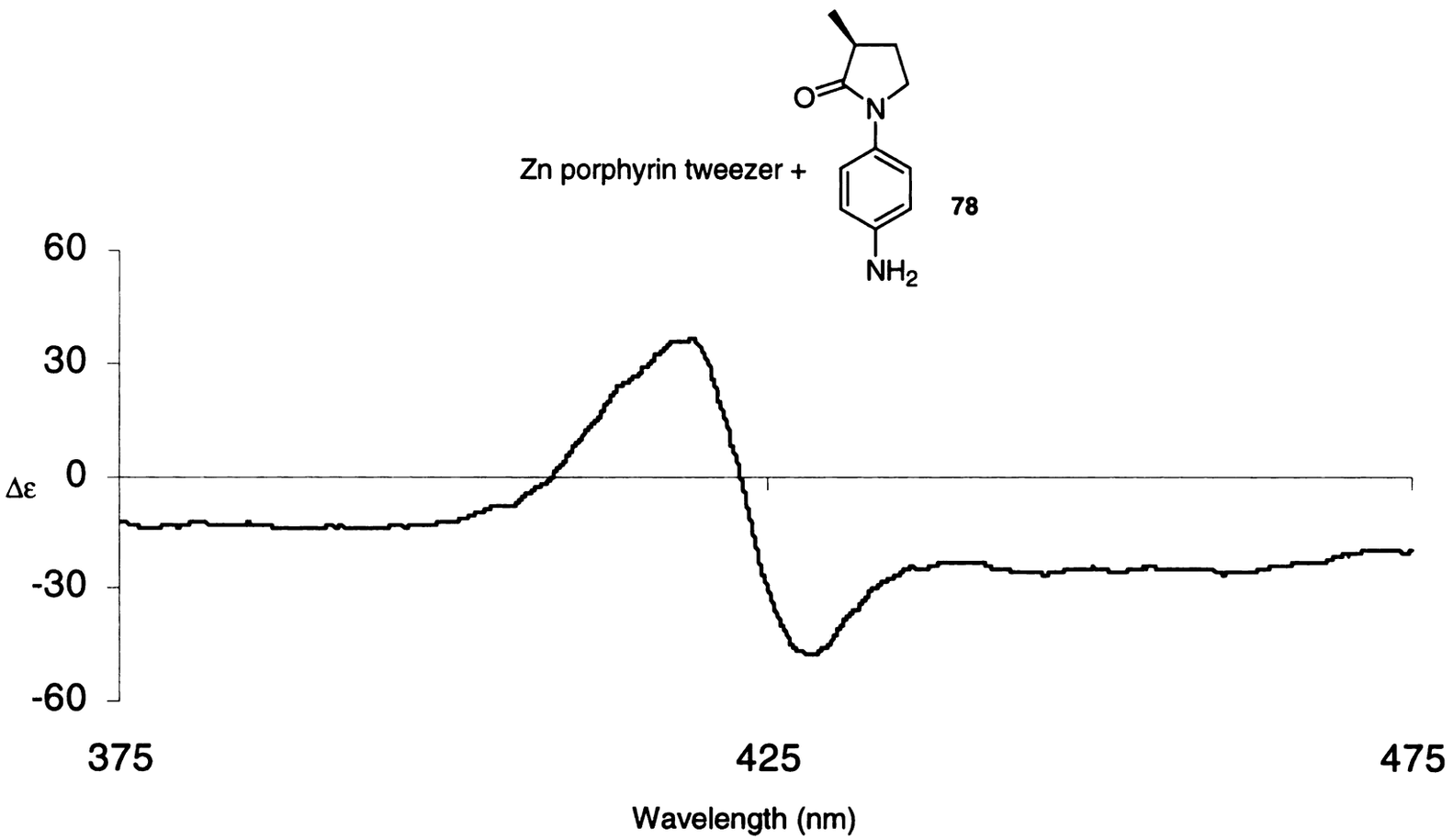

Addition of L-lysine to zinc porphyrin alcohol **2**

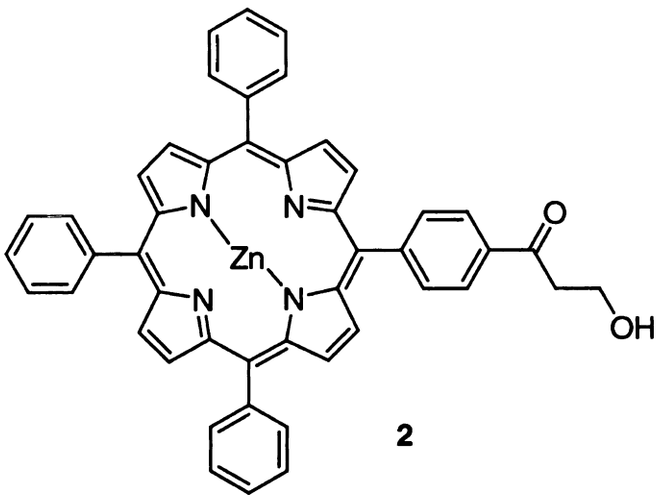

+ L-lysine
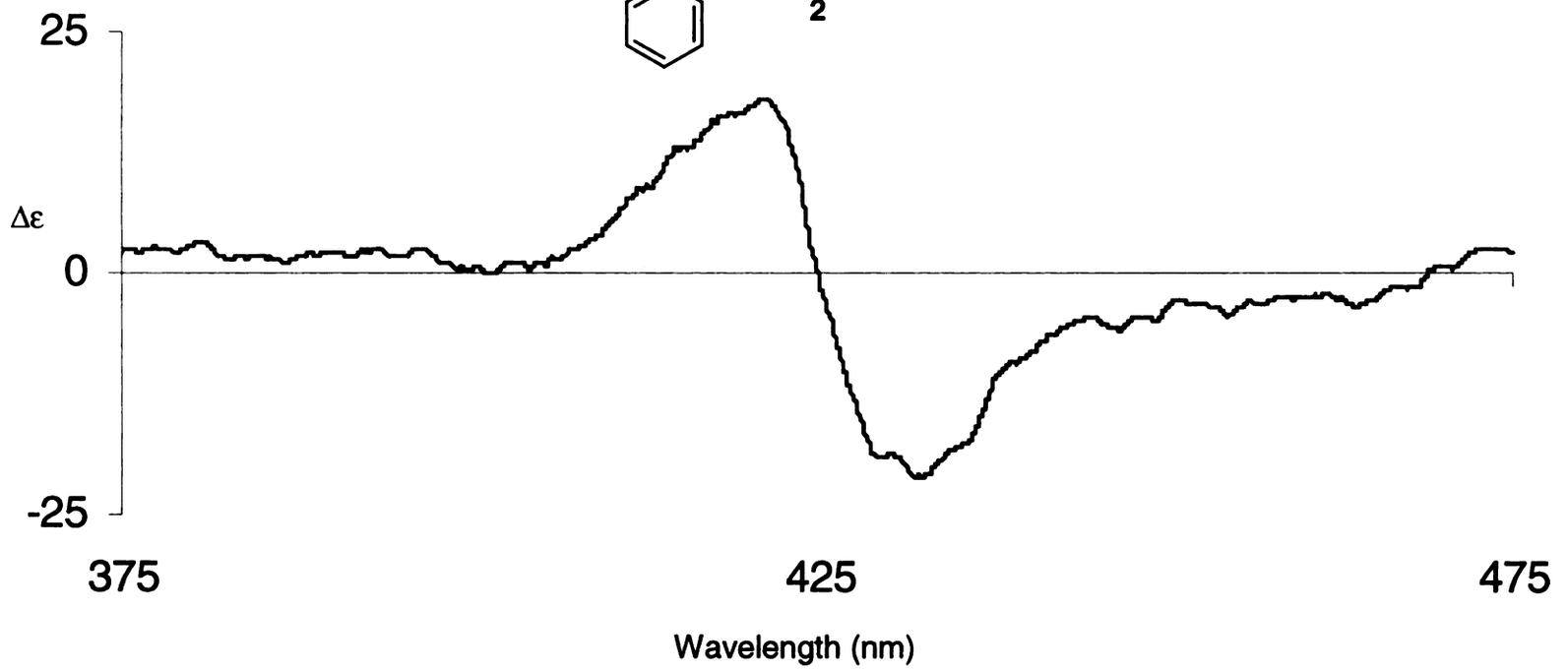
2